frontiers | Research Topics

Effects of endogenous and exogenous factors on reproductive system development

Edited by
Shunfeng Cheng, Juan P. Arrebola and Changyin Zhou

Published in
Frontiers in Endocrinology

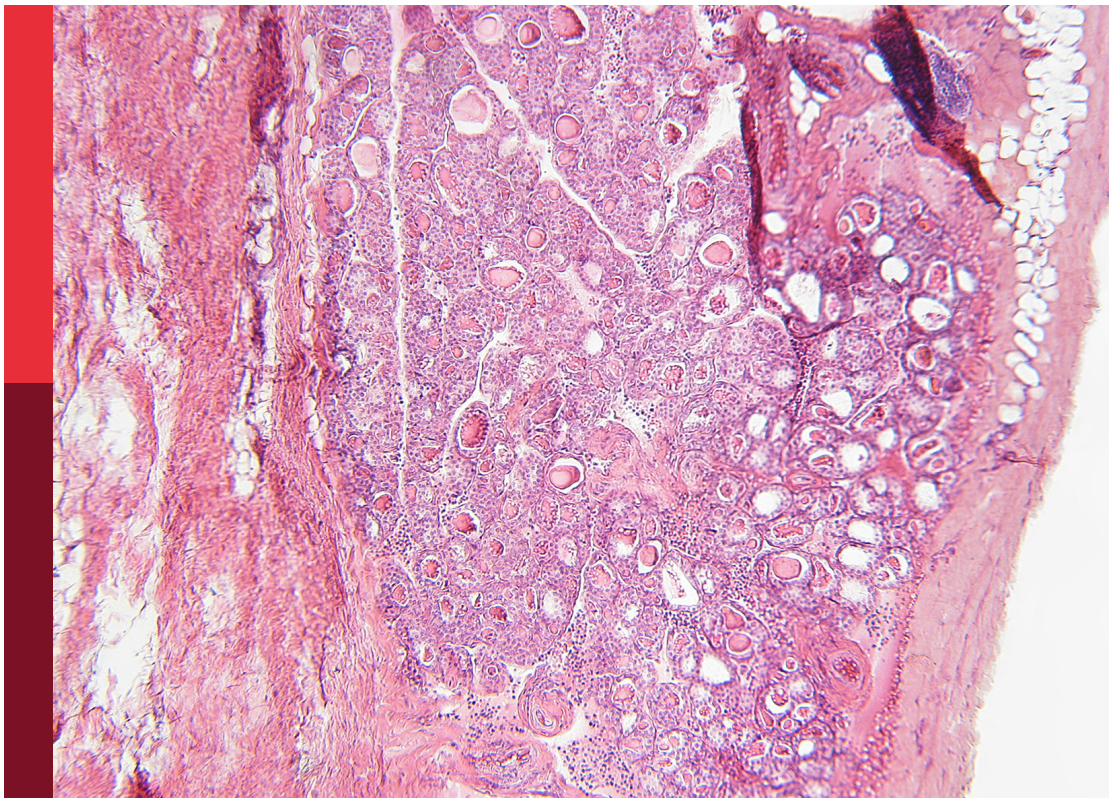

ISSN 1664-8714
ISBN 978-2-8325-3915-6
DOI 10.3389/978-2-8325-3915-6

About Frontiers

Frontiers is more than just an open access publisher of scholarly articles: it is a pioneering approach to the world of academia, radically improving the way scholarly research is managed. The grand vision of Frontiers is a world where all people have an equal opportunity to seek, share and generate knowledge. Frontiers provides immediate and permanent online open access to all its publications, but this alone is not enough to realize our grand goals.

Frontiers journal series

The Frontiers journal series is a multi-tier and interdisciplinary set of open-access, online journals, promising a paradigm shift from the current review, selection and dissemination processes in academic publishing. All Frontiers journals are driven by researchers for researchers; therefore, they constitute a service to the scholarly community. At the same time, the *Frontiers journal series* operates on a revolutionary invention, the tiered publishing system, initially addressing specific communities of scholars, and gradually climbing up to broader public understanding, thus serving the interests of the lay society, too.

Dedication to quality

Each Frontiers article is a landmark of the highest quality, thanks to genuinely collaborative interactions between authors and review editors, who include some of the world's best academicians. Research must be certified by peers before entering a stream of knowledge that may eventually reach the public - and shape society; therefore, Frontiers only applies the most rigorous and unbiased reviews. Frontiers revolutionizes research publishing by freely delivering the most outstanding research, evaluated with no bias from both the academic and social point of view. By applying the most advanced information technologies, Frontiers is catapulting scholarly publishing into a new generation.

What are Frontiers Research Topics?

Frontiers Research Topics are very popular trademarks of the *Frontiers journals series*: they are collections of at least ten articles, all centered on a particular subject. With their unique mix of varied contributions from Original Research to Review Articles, Frontiers Research Topics unify the most influential researchers, the latest key findings and historical advances in a hot research area.

Find out more on how to host your own Frontiers Research Topic or contribute to one as an author by contacting the Frontiers editorial office: frontiersin.org/about/contact

Effects of endogenous and exogenous factors on reproductive system development

Topic editors

Shunfeng Cheng — Qingdao Agricultural University, China

Juan P. Arrebola — University of Granada, Spain

Changyin Zhou — Guangdong Second Provincial General Hospital, China

Citation

Cheng, S., Arrebola, J. P., Zhou, C., eds. (2023). *Effects of endogenous and exogenous factors on reproductive system development*.

Lausanne: Frontiers Media SA. doi: 10.3389/978-2-8325-3915-6

Table of contents

frontiers | Frontiers in Endocrinology

TYPE Original Research
PUBLISHED 06 February 2023
DOI 10.3389/fendo.2023.1122709

OPEN ACCESS

EDITED BY
Shunfeng Cheng,
Qingdao Agricultural University, China

REVIEWED BY
Wen-Xiang Liu,
Inner Mongolia University, China
Guruswami Gurusubramanian,
Mizoram University, India

*CORRESPONDENCE
Li-Juan Fu
fulijuan@cqmu.edu.cn
Qian Feng
469280497@qq.com

†These authors have contributed equally to this work and share first authorship

SPECIALTY SECTION
This article was submitted to Reproduction, a section of the journal Frontiers in Endocrinology

RECEIVED 13 December 2022
ACCEPTED 24 January 2023
PUBLISHED 06 February 2023

CITATION
Su Y-N, Wang M-J, Yang J-P, Wu X-L, Xia M, Bao M-H, Ding Y-B, Feng Q and Fu L-J (2023) Effects of Yulin Tong Bu formula on modulating gut microbiota and fecal metabolite interactions in mice with polycystic ovary syndrome.
Front. Endocrinol. 14:1122709.
doi: 10.3389/fendo.2023.1122709

Effects of Yulin Tong Bu formula on modulating gut microbiota and fecal metabolite interactions in mice with polycystic ovary syndrome

Ya-Nan Su[1,2†], Mei-Jiao Wang[2,3†], Jun-Pu Yang[2], Xiang-Lu Wu[2], Min Xia[4], Mei-Hua Bao[5], Yu-Bin Ding[2], Qian Feng[2,4,6*] and Li-Juan Fu[1,2,5*]

[1]Department of Herbal Medicine, Chongqing Key Laboratory of Traditional Chinese Medicine for Prevention and Cure of Metabolic Diseases, School of traditional Chinese Medicine, Chongqing Medical University, Chongqing, China, [2]Joint International Research Laboratory of Reproduction and Development of the Ministry of Education of China, School of Public Health, Chongqing Medical University, Chongqing, China, [3]Department of Physiology, School of Basic Medicine, Chongqing Medical University, Chongqing, China, [4]Department of Gynecology, Chongqing Hospital of Traditional Chinese Medicine, Chongqing, China, [5]Department of Pharmacology, Academician Workstation, Changsha Medical University, Changsha, China, [6]Department of Obstetrics and Gynecology, Chongqing General Hospital, University of Chinese Academy of Sciences, Chongqing, China

Background: Polycystic ovarian syndrome (PCOS) is a common endocrine disorder characterized by hyperandrogenism, ovarian dysfunction and polycystic ovarian morphology. Gut microbiota dysbiosis and metabolite are associated with PCOS clinical parameters. Yulin Tong Bu formula (YLTB), a traditional Chinese medicine formula, has been recently indicated to be capable of ameliorating polycystic ovary symptoms and correcting abnormal glucose metabolism. However, the therapeutic mechanism of YLTB on PCOS has not been fully elucidated.

Methods: A pseudo sterile mouse model was established during this four-day acclimatization phase by giving the animals an antibiotic cocktail to remove the gut microbiota. Here, the therapeutic effects of YLTB on PCOS were investigated using dehydroepiandrosterone plus high-fat diet-induced PCOS mice model. Female prepuberal mice were randomly divided into three groups; namely, the control group, PCOS group and YLTB (38.68 $g \cdot kg^{-1} \cdot day^{-1}$) group. To test whether this effect is associated with the gut microbiota, we performed 16S rRNA sequencing studies to analyze the fecal microbiota of mice. The relationships among metabolites, gut microbiota, and PCOS phenotypes were further explored by using Spearman correlation analysis. Then, the effect of metabolite ferulic acid was then validated in PCOS mice.

Results: Our results showed that YLTB treatment ameliorated PCOS features (ovarian dysfunction, delayed glucose clearance, decreased insulin sensitivity, deregulation of glucolipid metabolism and hormones, etc.) and significantly attenuated PCOS gut microbiota dysbiosis. Spearman correlation analysis showed that metabolites such as ferulic acid and folic acid are negatively correlated with PCOS clinical parameters. The effect of ferulic acid was similar to

10.3389/fendo.2023.1122709

that of YLTB. In addition, the bacterial species such as *Bacteroides dorei* and *Bacteroides fragilis* were found to be positively related to PCOS clinical parameters, using the association study analysis.

Conclusion: These results suggest that YLTB treatment systematically regulates the interaction between the gut microbiota and the associated metabolites to ameliorate PCOS, providing a solid theoretical basis for further validation of YLTB effect on human PCOS trials.

KEYWORDS

polycystic ovary syndrome, YLTB formula, gut microbiota, metabolites, ferulic acid

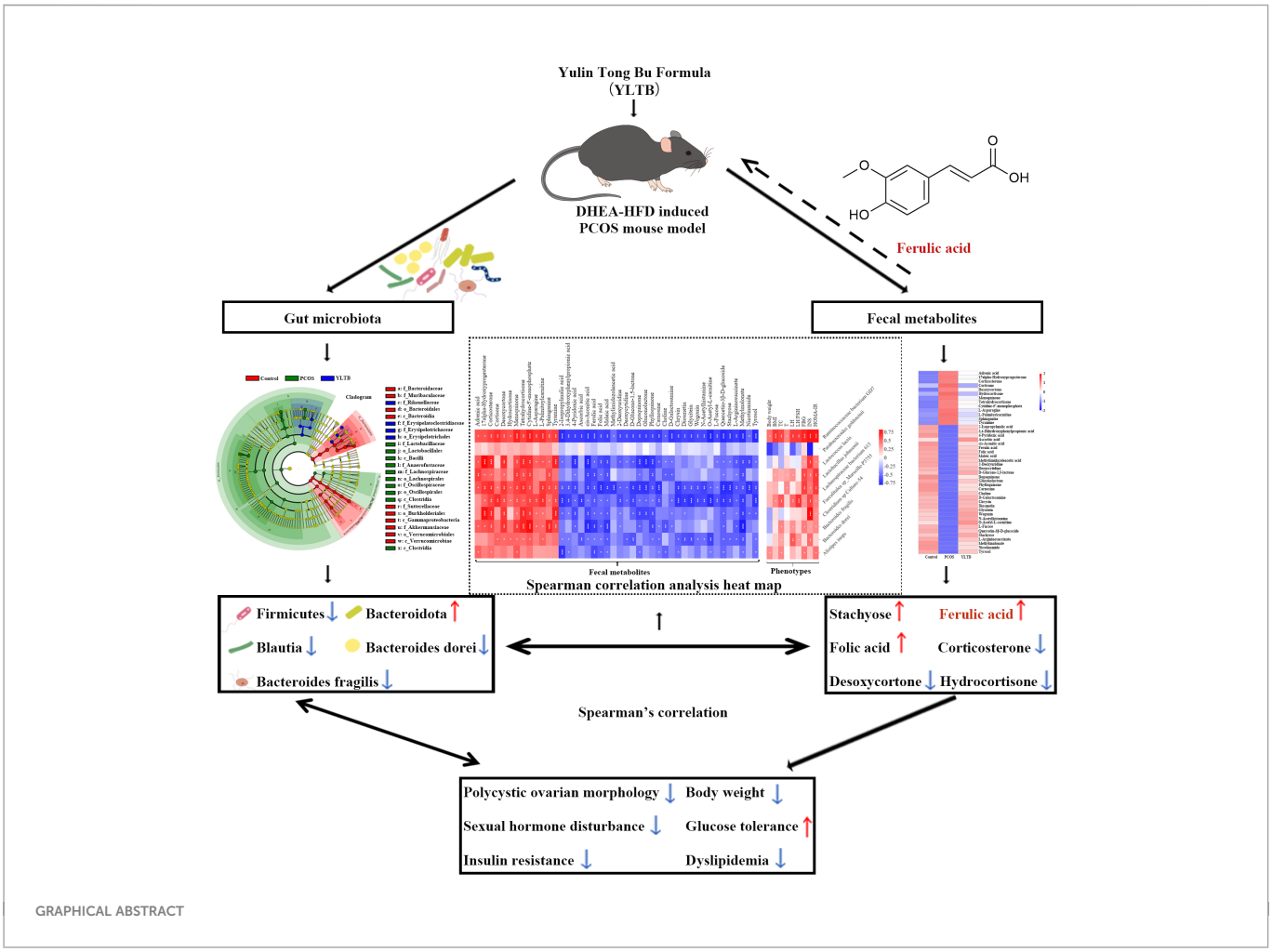

GRAPHICAL ABSTRACT

1 Introduction

Polycystic ovarian syndrome (PCOS) is a common endocrine disorder, from which 6-10% of reproductive females suffer severely (1, 2). The features of PCOS include hyperandrogenism, ovarian dysfunction and polycystic ovarian morphology (1–3). Usually, the disease is accompanied with insulin resistance (IR), obesity and metabolic disorders (4). Among metabolic disorders, dyslipidemia is characterized by increased levels of total cholesterol (TC), triglycerides (TG) and low-density lipoprotein cholesterol (LDL-C), but decreased levels of high-density lipoprotein cholesterol (HDL-C) (5).

The changes in those metabolites are often induced in human PCOS with high testosterone (T) levels (1) and obese (4) as well as gut microbiota disorder (6, 7). The gut microbiota is a complex ecosystem involved in host metabolic homeostasis, energy balance and immune modulation (8), which includes bacteria, fungi, viruses and protozoa (9). The diversity of gut microbiota can be divided into α or β diversity. The former refers to the species diversity within a community, and β diversity depicts the clustering of gut microbiota communities, mainly focusing the differences among different communities (10). The 16S rRNA sequencing studies have shown that disruption of the diversity and relative abundance of gut microbiota occurs during PCOS

development (11). Gut microbiota dysbiosis is correlated with clinical parameters of PCOS women such as T, luteinizing hormone/follicle stimulating hormone (LH/FSH), LH, IR, fasting blood glucose (FBG), body mass index (BMI) and TG (12, 13). Fecal microbiota transplantation (FMT) of PCOS women into the germ-free mice led to variations in the levels of serum glucose, insulin (INS) and sex hormones (14). Consistently, increased Bacteroides vulgatus abundance resulted in ovarian dysfunction and metabolic disorders in the same germ-free mice (14).

In addition to those metabolites mentioned above, more have been reported to be associated with the gut microbiota of PCOS patients or rodent animals (14–16). For example, stachyose has a significantly negative correlation with *Ruminococcus 2* and regulates estrous cycle disorder, polycystic ovary morphology and T levels in PCOS rats (15). The levels of short-chain fatty acids (SCFAs) are decreased in PCOS rats (17), which play key functional regulatory roles in inflammation dissipation (18), IR and glucose tolerance (19). In addition, the levels of glyodeoxycholic acid (GDCA) and taurine deoxycholic acid (TUDCA) are negatively correlated with the abundance of *Bacteroides vulgatus* in the intestinal microbiota of PCOS patients (14).

The relationships among metabolites, gut microbiota, and PCOS sheds light on the development of novel treatments against PCOS. Currently, gonadotropins, clomiphene citrate and metformin have been clinically applied (20), but with many side effects such as ovarian hyperstimulation syndrome (21), drug resistance (22) and gastrointestinal distress (23, 24). Some of these could be avoided by using traditional Chinese medicine (TCM), such as FuFang ZhenZhu TiaoZhi formula (25), Bu Shen Hua Zhuo formula (26) and Liuwei Dihuang Pills (27). In TCM theory, the key pathogenesis of PCOS is based on “phlegm-dampness block and spleen-kidney deficiency”. Based on Buzhong Yiqi Decoction, which derived from Fu Qing Zhu Nv Ke and the key pathogenesis of PCOS, we created a decoction named as Yulin Tong Bu formula (YLTB). Our research team has been using the YLTB formula in the clinical treatment of PCOS for many years, and earlier clinical trials have shown that YLTB formula could improve the therapeutic effect of metformin (28). YLTB is made of 12 traditional Chinese herbs (listed in Table 1). Out of them, Astragalus mongholicus Bunge, Actaea cimicifuga L., Citrus × aurantium L. and Poria cocos (Schw.)Wolf were reported to impact metabolite levels and gut microbiota (29–33). For example, Citrus × aurantium L., mainly containing nobiletin, could improve high-fat diet (HFD)-induced obesity, deregulate intestinal lipid metabolism, and reshape gut microbiota (29, 30). Astragalus mongholicus Bunge includes soyasaponin I and formononetin, which can reshape gut microbiota (34), inhibit obesity and dyslipidemia, reduce IR and improve glucose homeostasis (35–37). Although these studies suggest the potential therapeutic effect of YLTB against PCOS, the molecular mechanism underlying it remains unclear.

In this study, we determined the therapeutic effect of YLTB on PCOS using dehydroepiandrosterone (DHEA) plus HFD-induced PCOS mice model. The mechanism could be explained by the ability of YLTB to orchestrate gut microbiota and the related metabolites. Compared with the control mice, PCOS mice presented a series of syndromes such as ovarian dysfunction, delayed glucose clearance, decreased insulin sensitivity, and metabolic deregulation of lipid as well as hormones. Those syndromes in PCOS mice can be greatly ameliorated by YLTB treatment. The 16S rRNA sequencing analysis was applied to demonstrate the landscape of gut microbial composition in PCOS mice. We found that the dysbiosis of PCOS gut microbiota was significantly attenuated by YLTB treatment. The correlation between gut microbiota and fecal metabolites in mice was further investigated by the association study analysis, combined with LC–MS (liquid chromatography-mass sectromety)-based metabolic sequencing analysis. The analysis results predicted that metabolites such as ferulic acid, folic acid, menaquinone and phylloquinone are negatively correlated with bacterial species such as *Bacteroides dorei* and *Bacteroides fragilis*. These bacteria were positively correlated with the PCOS clinical parameters such as TC, LH, FBG, and insulin resistance index in the homeostasis model (HOMA-IR). In addition, the therapeutic effect of ferulic acid was validated in PCOS mice, similar to YLTB effect. Taken together, YLTB treatment systematically regulate the interaction between gut microbiota and the associated metabolites to ameliorate PCOS.

TABLE 1 The Chinese herb drugs contained in YLTB.

Chinese name	Botanical name	Family	Genus	Part used	Weight (g)
Dangshen	Codonopsis pilosula (Franch.) Nannf.	Campanulaceae	Codonopsis Wall.	root	45
Huangqi	Astragalus mongholicus Bunge	Fabaceae	Astragalus L.	root	30
Baizhu	Atractylodes macrocephala Koidz.	Asteraceae	Atractylodes DC.	rhizome	30
Shengma	Actaea cimicifuga L.	Ranunculaceae	Cimicifuga L.	rhizome	10
Chenpi	Citrus × aurantium L.	Rutaceae	Citrus	fruit peel	10
Fuling	Poria cocos(Schw.)Wolf	Polyporaceae	Poria	sclerotium	15
Banxia	Pinellia ternata (Thunb.) Makino	Araceae	Pinellia Tenore	tuber	10
Cangzhu	Atractylodes lancea (Thunb.) DC.	Asteraceae	Atractylodes	rhizome	30
Jixueteng	Spatholobus suberectus Dunn	Fabaceae	Spatholobus Hassk.	stem	30
Xiangfu	Cyperus rotundus L.	Cyperaceae	Cyperus L.	rhizome	10
Tusizi	Cuscuta chinensis Lam.	Convolvulaceae	Subg. Grammica	ripe seed	20
Bajitian	Gynochthodes officinalis (F.C.How) Razafim. & B.Bremer	Rubiaceae	Morinda	root	15

2 Materials and methods

2.1 Preparation of Yulin Tong Bu formula

The herb details of YLTB are presented in Table 1. The clinical dose of YLTB was 255g (28), 45 g Dangshen (*Codonopsis pilosula (Franch.) Nannf.*), 30 g Huangqi (*Astragalus mongholicus Bunge*), 30 g Baizhu (*Atractylodes macrocephala Koidz.*), 10 g Shengma (*Actaea cimicifuga L.*), 10 g Chenpi (*Citrus × aurantium L.*), 15 g Fuling *(Poria Cocos (Schw.) Wolf.*), 10 g Banxia (*Pinellia ternata (Thunb.) Makino*), 30 g Cangzhu (*Atractylodes Lancea (Thunb.) Dc.*), 30 g Jixueteng (*Spatholobus Suberectus Dunn*), 10 g Xiangfu (*Cyperus rotundus L.*), 20 g Tusizi (*Cuscuta chinensis Lam.*), and 15 g Bajitian (*Gynochthodes officinalis (F.C.How) Razafim. & B.Bremer*), respectively. The Chinese herbs were purchased from Chongqing Hospital of Traditional Chinese Medicine. They were then suspended in distilled water at room temperature for one hour to soften the raw materials and facilitate the extraction of water-soluble ingredients in subsequent steps. The herbs were boiled for two hours and passed through filter paper. The process lasted two times followed by concentrating a decoction at 100°C, to obtain the extracts of YLTB containing 2.55-g raw herbs/mL. In this paper, the dosages of YLTB used in mice were converted from clinical dosage using the following equation (38, 39):

$$Dm = Dh/W \times F$$

Where Dm is the administrated dose of YLTB for mouse in the present work, Dh is the clinical dose of YLTB, W is the weight of human body, F is the dose conversion factor of mouse and human. W is set as 60 kg. Considering the dose conversion factor of 9.1 between mouse and human, the high dosage is 38.68 g/kg, the medium dosage is 19.34 g/kg, and the low dosage is 9.67 g/kg.

2.2 Liquid chromatography–mass spectrometry

ACQUITY UPLC HSS T3 (2.1 × 100 mm 1.8 m columns) was used for liquid chromatography–mass spectrometry (LC-MS) (Waters, UPLC; Thermo, Q Exactive). The following chromatographic separation conditions were used: column temperature, 40°C; flow rate, 0.30 mL/min; mobile phase A, water + 0.05 percent formic acid; mobile phase B, acetonitrile; injection volume, 2 µL; automatic injector temperature, 4°C. The MS parameters are as follow: ESI+: spray voltage, 3.0 (ESI+) or 3.2 (ESI-) kV; S-Lens RF level, 30% (ESI+) or 60% (ESI-); heater temperature, 300 °C; sheath gas flow rate, 45 arb; auxiliary gas flow rate, 15 arb; sweep gas flow rate, 1arb; capillary temperature, 350°C. Scan duration is 100 ms, interscan time is 50 ms, and the scan range is 70-1050 m/z. Data was analyzed using Compound Discoverer 3.1 software (Thermo Fisher Scientific,USA), normalized, and converted into a two-dimensional matrix using Excel 2010 software, containing retention time, compound molecular weight, observations (samples), and peak intensity (39, 40).

2.3 Animals and treatment

Female prepuberal C57BL/6 (21-d-old) mice (specific pathogen-free, Animal Qualification Certificate No.2022109) were purchased from the Animal Management Center of Chongqing Medical University. The mice were maintained under standard circumstances (22-24 °C, 50% relative humidity, 12-hour dark/light cycle) with unrestricted access to food and water. The Institutional Animal Care and Use Committee of Chongqing Medical University authorized all mouse experimental procedures (Chongqing, China). Mice were given four days to adjust to their new surroundings before being tested. A pseudo sterile mouse model was established during this four-day acclimatization phase by giving the animals an antibiotic cocktail (ABX) to remove the gut microbiota. Freshly prepared antibiotic cocktail comprised 1 mg mL^{-1} ampicillin sodium (1146GR005, Biofroxx, Einhausen, Germany), 1 mg mL^{-1} neomycin sulfate (N814740-5G, MACKUN, Shanghai, China), 1 mg mL^{-1} metronidazole (M1547-5G, Sigma–Aldrich, MO, USA), and 0.5 mg mL^{-1} vancomycin hydrochloride (#1161GR1001, Biofroxx, Einhausen, Germany) in drinking water, and the mice were given autoclaved drinking water four days later.

According to the preliminary experiment (Figure S1), 30 mice were randomly divided into six groups (n = 5) to optimize the dosage of YLTB: control group, PCOS group, high dosage YLTB group [YLTB (H), 38.68 $g{\cdot}kg^{-1}{\cdot}day^{-1}$], medium dosage YLTB group [YLTB (M), 19.34 $g{\cdot}kg^{-1}{\cdot}day^{-1}$], low dosage YLTB group [YLTB (L), 9.67 g $kg^{-1}{\cdot}day^{-1}$], and metformin group (positive control, 250 mg $kg^{-1}{\cdot}day^{-1}$, #D150959-5G, Sigma –Aldrich, MO, USA). To establish the PCOS group, mice were fed a high-fat diet (HFD, 60% kcal% fat; #D12492, Research Diets, Inc., NB, USA) and received daily subcutaneous injections of DHEA (#252805-10GM, Millipore, CA, USA; 60 mg/kg, dissolved in 0.1 ml of sesame oil) (41, 42). To determine the most effective YLTB dosage for PCOS, mice were fed an HFD, gavaged with various YLTB dosages, and injected with DHEA on the same day. The control group was fed a normal chow diet (NCD) and injected daily with sesame oil (#8008-74-0, Acros, BE, USA).

In order to verify the effects of high dose YLTB group on glucolipid metabolism, intestinal microbiota and fecal metabolism of PCOS mice, 30 mice were randomly divided into three groups (n = 10), namely, the control group, PCOS group and YLTB group (38.68 $g{\cdot}kg^{-1}{\cdot}day^{-1}$). To test the efficacy of the metabolite ferulic acid, 40 mice were randomly divided into four groups (n = 10), namely, the control group, PCOS group, FA1 group (50 $mg{\cdot}kg^{-1}{\cdot}day^{-1}$) and FA2 group (100 $mg{\cdot}kg^{-1}{\cdot}day^{-1}$) (33, 43). For FA groups, mice were fed an HFD and subcutaneously injected with DHEA daily, as well as administered ferulic acid (purity > 99.00%, #128708, Sigma–Aldrich, MO, USA, dissolved in lukewarm water) by oral gavage every day.

The mice mentioned above were all treated for 20 days. At the end of the experiment, mice were fasted over 12 hours and anesthetized by intraperitoneal injection of 10% chloral hydrate with 0.1 mL/10 g, and then weighed, measured to determine the distance from the tip of the nose to the anus, and tested for fasting blood glucose and oral glucose tolerance tests (OGTTs). The serum was collected and centrifuged for 20 minutes at 3,000 rpm to measure insulin and sex hormones. The ovaries and uteri of mice were collected, weighed, and wax-fixed or snap-frozen and stored at –80 °C for further use.

2.4 Estrous cycle determination

From the 11th to the 20th day of the gavage treatment, vaginal smears of mice were collected every day. The estrous cycle stage was determined by microscopic analysis of the predominant cell type in vaginal smears.

2.5 Measurement of serum biochemical markers

Enzyme-linked immunosorbent assay (ELISA) kits were used to determine serum testosterone, luteinizing hormone (LH), follicle stimulating hormone (FSH) and serum insulin levels (#JL25196, #JL10432, #JL10329, #JL11459, Shanghai Jianglai Biology, Shanghai, China). A glucometer was used to evaluate blood glucose. The homeostatic model assessment of IR (HOMA-IR) index was calculated using the formula: [FBG (mmol/L)] × [FINS (lU/mL)]/22.5. After an overnight fast, the oral glucose tolerance tests (OGTTs) were administered *via* oral gavage of 2 g/kg glucose. The blood glucose level of the mice was tested using blood glucose test paper at 0, 15, 30, 60, 90, and 120 minutes. At least 5 mice were used for these experiments.

2.6 Body weight, Lee's index analysis, BMI and lipid profile analysis

Every four days, the mice weight was recorded. The length from the tip of the nose to the anus of the mouse was measured after anesthesia, and the Lee's index and BMI were calculated (Lee's index = [Body mass (g) × 1000]$^{1/3}$/body length (cm), BMI=body weight (kg)/body length (m^2)). Biochemical analysis kits were used to assess serum lipid profiles, including TC, TG, HDL-C, and LDL-C (#A111-1-1, #A110-1-1, #A112-1-1, #A113-1-1; Nanjing Jiancheng Bioengineering Institute, Nanjing, China).

2.7 Tissue processing and H&E staining

Mouse ovaries were harvested, fixed with 4% paraformaldehyde (#BL539A, Biosharp) and embedded in paraffin. Hematoxylin and eosin (H&E) kits were used to stain ovary sections to observe follicle changes. Sections of 5 μm were placed on glass slides, with 40 μm discarded between each section; six sections from each ovary were collected. These tests required at least 5 mice per group (44, 45).

2.8 16S rRNA sequencing

The fecal pellets were collected in sterile cryopreservation tubes immediately after being discharged before sacrifice. Before analysis, the fecal samples were snap-frozen and stored at −80 °C. Fecal samples were sent to Novogene (Beijing, China) for 16S RNA sequencing. DNA was extracted from mouse fecal samples using a Magnetic Soil and Stool DNA Kit (#DP712, Tiangen). DNA concentration and purity were measured on 1% agarose gels. DNA was diluted to 1 ng/μL in sterile water according to the concentration.

The V3–V4 hypervariable region of the 16S rRNA gene was amplified by PCR at 98 °C for 1 minute, followed by 30 cycles of denaturation at 98 °C for 10 seconds, annealing at 50 °C for 30 seconds, elongation at 72 °C for 30 seconds, and final incubation at 72 °C for 5 minutes. The common primer pair (515F5′-CCTAYGGGRBGCASCAG-3'; 806R5′-GGACTACNN ptGGGTATCTAAT-3′) was used to amplify the bacterial 16S rRNA gene. All PCRs were carried out with 15 μL of Phusion® High-Fidelity PCR Master Mix (#M0531S, New England Biolabs, MA, USA), 2 μM primers, and 10 ng template DNA. The amplification products were isolated using a 2% agarose gel and purified with a Universal DNA Purification Kit (#DP214, Tiangen, Beijing, China). The NEB Next® Ultra DNA Library Prep Kit (#E7370L, Illumina, CA, USA) was used for library construction. The established library was detected by an Agilent Bioanalyzer 5400 system and quantified by Q-PCR. Finally, the library was sequenced on an Illumina NovaSeq platform (Illumina Novaseq6000, Illumina, CA, USA), and 250 bp paired-end reads were generated (46).

2.9 Fecal metabolic profiling

Individual mouse feces samples (100 mg) were crushed in liquid nitrogen before being resuspended in prechilled 80% methanol using a well vortex (n = 6). The samples were placed on ice for 5 minutes before being centrifuged at 15,000 g and 4 °C for 20 minutes. LC–MS grade water was used to dilute some of the supernatant to a final concentration of 53% methanol. The samples were then transferred to a new tube and centrifuged at 15,000 g and 4 °C for 20 minutes. The supernatant was then injected into the LC–MS/MS apparatus for analysis.

UHPLC–MS/MS analyses were carried out using a Vanquish UHPLC system (ThermoFisher) paired with an Orbitrap Q ExactiveTM HF mass spectrometer (Thermo Fisher) by Novogene. Using a 17-min linear gradient at a flow rate of 0.2 mL/min, samples were injected onto a Hypersil Gold column (100 × 2.1 mm, 1.9 μm). Eluent A (0.1% formic acid in water) and eluent B (methanol) served as the eluents for the positive polarity mode. Eluent A (5 mM ammonium acetate, pH 9.0) and eluent B (methanol) were the eluents for the negative polarity mode. The solvent gradient was set as follows: 2% B, 1.5 min; 2-85% B, 3 min; 100% B, 10 min; 100-2% B, 10.1 min; 2% B, 12 min. The Q ExactiveTM HF mass spectrometer was operated in positive/negative polarity mode, with a spray voltage of 3.5 kV, capillary temperature at 320°C, sheath gas flow rate at 35 arb and aux gas flow rate at 10 arb, S-lens RF level at 60 and aux gas heater temperature at 350°C.

Compound Discoverer 3.1 (CD3.1, ThermoFisher) was used to analyze the raw data files produced by UHPLC–MS/MS to perform peak alignment, peak selection, and quantification for each metabolite. The primary parameters were established: retention time tolerance, 0.2 minutes; actual mass tolerance, 5 ppm; signal intensity tolerance, 30%; signal/noise ratio, 3; and minimum intensity. Peak intensities were then normalized to reflect the total spectral intensity. Based on additive ions, molecular ion peaks, and fragment ions, the normalized data were utilized to predict the molecular formula. To obtain correct qualitative and relative quantitative

results, peaks were matched with the MassList, mzCloud (https://www.mzcloud.org/), and mzVault databases (46).

Statistical analyses were carried out using the statistical tools R (R version R-3.4.3), Python (Python 2.7.6 version) and CentOS (CentOS release 6.6). The KEGG, HMDB, and LIPIDMaps databases were used to annotate these metabolites. MetaX was used to perform partial least squares discriminant analysis (PLS-DA) and principal components analysis (PCA). Univariate analysis (t test) was used to determine statistical significance (*P* value). VIP > 1 and *P* value < 0.05, as well as fold change ≥ 2 or FC ≤ 0.5, were deemed to indicate differential metabolites. The data for clustering heatmaps were standardized using z scores of differential metabolite intensity areas and plotted using the Pheatmap package in R language.

2.10 Data and statistical analysis

GraphPad Prism version 8.3 was used to analyze all data, which were then displayed as the means ± standard error of the mean (SEM). When $P < 0.05$, the results were considered statistically significant. Each variable was tested for differences among three or more groups using one-way or two-way analysis of variance (ANOVA) followed by Tukey's multiple comparisons test to assess statistical significance. The cor.test function from the stats R package was used to perform a Spearman correlation among the levels of fecal metabolites, phenotype, and relative abundance of species. We only performed the correlation for those species ($P < 0.05$), phenotypes ($P < 0.05$) and metabolites ($P < 0.05$ VIP>1) that were statistically significant across groups.

3 Results

3.1 Chemical composition and LC-MS analysis of YLTB

LC-MS analysis data of YLTB was performed using feature extraction and preprocessing with Compound Discoverer 3.1 software, normalized, and edited into a two-dimensional matrix using Excel 2010 software, including retention time, compound molecular weight, observations (samples), peak intensity and library matching (based on mzCloud and mzVault database, the mzVault include OTCML, KEGG and Chemspider database). The aim of this method was to complete the target screening without standard products. Several ingredients in YLTB were identified (Figure 1A, Table 2 and 3). The following seven important compounds were distinguishable, as shown in Figure 1B: (I) Nobiletin, (II) Tangeritin, (III) Berberine, (IV) Quercetin, (V) Catechin, (VI) Chlorogenic acid, and (VII) Liquiritigenin.

3.2 YLTB formula attenuates ovarian dysfunction in DHEA plus HFD-induced PCOS mice

Before the effect of YLTB on PCOS was investigated, the PCOS mice were generated by a HFD and DHEA subcutaneous injections (60 mg/kg body weight) for 20 days. The YLTB group mice were additionally gavaged with YLTB (38.68 $g \cdot kg^{-1} \cdot day^{-1}$) at the same time. The usage of YLTB was optimized in our preliminary data, as shown

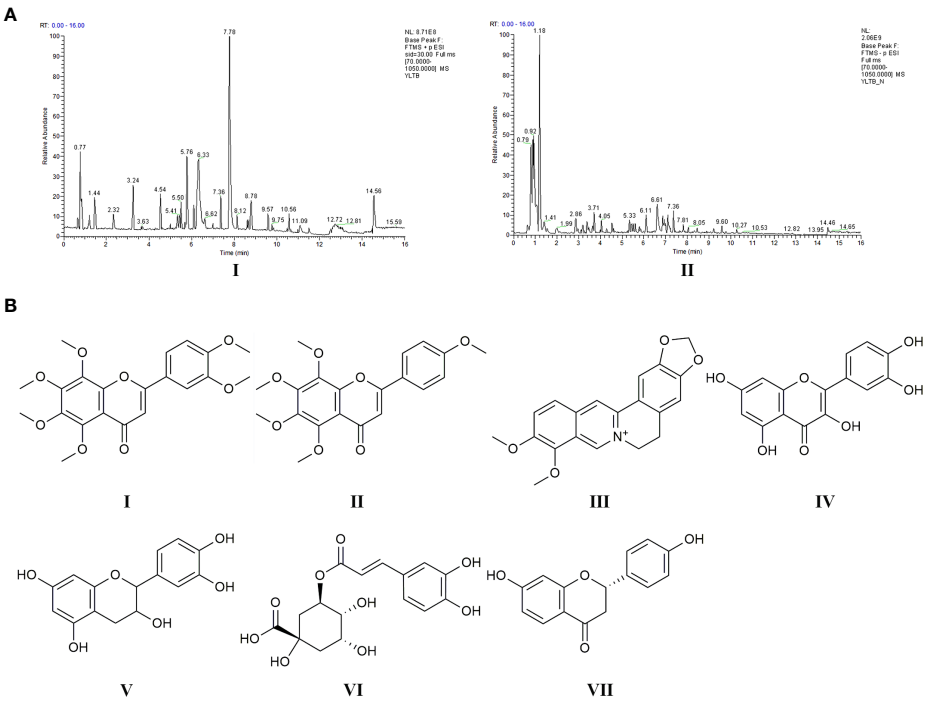

FIGURE 1
Chemical ingredients and LC-MS analysis of YLTB. **(A)** The total ion flow diagram for YLTB. I. Positive ion mode. II. Negative ion mode. **(B)** The molecular structures of seven important compounds identified in the analysis. I Nobiletin. II. Tangeritin. III. Berberine. IV. Quercetin. V;.Catechin. VI. Chlorogenic acid. VII. Liquiritigenin. RT, Run Time.

TABLE 2 LC-MS analysis data and the top 20 primary elemental composition of YLTB in positive ion mode.

NO.	Name	Formula	RT. [min]+	Molecular. Weight	Area
1	Benzothiazole	C7 H5 N S	6.302	135.01431	4452592429
2	Choline	C5 H13 N O	0.766	103.10016	1169277665
3	dimethyl(tetradecyl)amine	C16 H35 N	8.777	241.27692	1126416722
4	2-Mercaptobenzothiazole	C7 H5 N S2	6.603	166.98631	746968672
5	Creatinine	C4 H7 N3 O	0.9	113.05924	406383888.3
6	Maltol	C6 H6 O3	3.219	126.0319	380600348.2
7	1-Aminocyclopropane-1-carboxylic acid	C4 H7 N O2	0.821	101.04828	371648740.5
8	Pelargonidin	C15 H10 O5	5.422	270.05263	360361721.4
9	Nobiletin	C21 H22 O8	8.127	402.13114	352054134.2
10	DL-Stachydrine	C7 H13 N O2	0.84	143.09462	291876915.1
11	Tangeritin	C20 H20 O7	8.668	372.12019	290269427.2
12	Berberine	C20 H17 N O4	5.243	335.1147	275753582.5
13	Apocynin	C9 H10 O3	5.773	166.06301	229918577.4
14	7-Hydroxycoumarine	C9 H6 O3	3.634	162.0318	218666113.6
15	Indole	C8 H7 N	3.236	117.0582	206668891
16	3-Formylindole	C9 H7 N O	3.212	145.05278	206103311.7
17	PC (16:0/0:0)	C24 H50 N O7 P	10.111	495.3324	200782893.9
18	Pyrrole-2-carboxylic acid	C5 H5 N O2	1.2	111.03239	198819312.2
19	L-Pyroglutamic acid	C5 H7 N O3	1.195	129.04276	189601241.9
20	Quercetin	C15 H10 O7	4.597	302.04247	154436644.8

in the Supplement Figure S1. The control group was only daily injected with sesame oil. The mouse intervention process was illustrated in the Figure 2A. To address the effect of YLTB on mice ovary function, multiple parameters were evaluated, including ovarian morphology, mice weight, wet weight of uterus and ovaries, and sex hormone changes.

Ovarian H&E staining were performed to ensure a successful PCOS establishment and to determine YLTB's effect on ovarian morphology as well as follicle counts (Figure 2B). Many cystic and atretic follicles in the ovaries of the PCOS group were absent in the ovaries of the YLTB group. The PCOS group also showed fewer antral follicles and corpus luteum, while YLTB administration increased them (Figure 2C). Figure 2D illustrated that the mice body weight was significantly decreased in the YLTB group, compared to the PCOS group. There was no significant difference in mice body weight between the control group and YLTB group. The uterus and ovary weights of PCOS mice were also significantly reduced after YLTB therapy (Figure 2E). In addition, YLTB dramatically downregulated serum T and LH levels in PCOS mice. Consistently, the LH/FSH ratio was significantly lower in the YLTB group in comparison to the PCOS group (Figures 2F, G). In summary, the application of YLTB largely restored these ovarian parameters of the PCOS group to the normal levels. Although it could affect sex hormone levels, YLTB did not impact the estrus cycle of the PCOS group (Figure S2 A, B).

3.3 YLTB ameliorates the disorder of glucose and lipid metabolism in PCOS mice

To address whether YLTB ameliorates PCOS condition through alternation of glucose and lipid metabolism, the glucose levels, insulin levels, Lee's index, BMI, lipid levels, and insulin sensitivity as well as the degree of obesity among the mice groups of the control, PCOS and YLTB were compared. Firstly, OGTTs were performed in those mice administered *via* oral gavage of 2 g/kg of glucose after 12 hours of fasting. The administered mice were sampled for the blood glucose levels using the test paper at 0, 15, 30, 60, 90, and 120 minutes. The glucose levels of the PCOS group were the highest, suggesting that the delayed glucose clearance in the PCOS group was removed in the YLTB group (Figure 3A). Consistently, YLTB significantly attenuated increases in the levels of fasting glucose, serum insulin and HOMA-IR in PCOS mice (Figures 3B–D). Meanwhile, the body size of the PCOS group was larger than the control group, assayed by Lee's index and

TABLE 3 LC-MS analysis data and the top 20 primary elemental composition of YLTB in negative ion mode.

NO.	MS2.name	Formula	RT.[min]–	Molecular.Weight	Area
1	D-FRUCTOSE	C6 H12 O6	0.796	180.06215	9655427837
2	α, α-Trehalose	C12 H22 O11	0.8	342.11478	7276775260
3	Citric acid	C6 H8 O7	1.182	192.02568	6221487818
4	2-Mercaptobenzothiazole	C7 H5 N S2	6.609	166.98485	2777846346
5	Gluconic acid	C6 H12 O7	0.788	196.05702	2316575258
6	D-(-)-Quinic acid	C7 H12 O6	0.83	192.06227	1234943274
7	Piscidic Acid	C11 H12 O7	2.848	256.05742	885987564.1
8	Catechin	C15 H14 O6	3.711	290.07826	846282140.4
9	L-Iditol	C6 H14 O6	0.779	182.07755	429101979.4
10	Chlorogenic acid	C16 H18 O9	3.18	354.09404	420580341.2
11	3-Hydroxy-3-methylglutaric acid	C6 H10 O5	1.547	162.05134	383522438.1
12	(-)-Gallocatechin	C15 H14 O7	2.946	306.07313	339562782.9
13	Quercetin-3β-D-glucoside	C21 H20 O12	4.601	464.0938	319376854.6
14	Formononetin-7-O-glucoside	C22 H22 O9	5.51	430.12437	311798194.2
15	(+/-)9-HpODE	C18 H32 O4	8.444	312.22923	276336157.3
16	Liquiritigenin	C15 H12 O4	7.16	256.07265	275731693.6
17	L-Arginine	C6 H14 N4 O2	0.717	174.1104	264866724.1
18	Jasmonic acid	C12 H18 O3	7.204	210.1244	253463816.8
19	Quinic acid	C7 H12 O6	2.318	192.06208	232639631.6
20	Procyanidin B2	C30 H26 O12	3.784	578.14076	220607671.2

BMI, while the values of these two indexes were lowered down in the YLTB group (Figure 3E, F).

The lipid profiles of the three groups were characterized by determination of levels of total TC, TG, LDL-C and HDL-C. Importantly, the TC levels in the YLTB group was lower than the one in the PCOS group (Figure 3G). In contrast, there was no significant changes of TG levels between the PCOS group and the YLTB group (Figure 3H). Notably, although the HDL-C levels in the YLTB group was higher than the one in the PCOS group (Figure 3I), the levels in the PCOS group were similar to in the control group (Figure 3I). On the other hand, LDL-C levels were significantly increased in the PCOS group compared to the control group (Figure 3J). However, YLTB had no significant impact on the elevated LDL-C levels in PCOS mice. This indicates that the mechanism by which YLTB acts on TC to affect PCOS is complicated.

3.4 YLTB attenuates gut microbiota dysbiosis in PCOS mice

Given that the gut microbiota can regulate many metabolites, we next investigated whether the gut microbiota contributes to YLTB manipulation on sex hormone levels and metabolism indicators in mice with PCOS. Before that, the profile of the gut microbiota, simulated by the fecal microbiota, was described for the control, PCOS, and YLTB groups. The 16S rRNA sequencing analysis was performed with fecal samples separately collected from the groups. The rarefaction curves (Figure 4A) and rank abundance curves (Figure 4B) of the three groups growed in a similar manner, reflecting that the amount of sequencing data and the species richness were qualified for further analysis.

The α diversity indicator Simpson index scored closely for the three groups, showing no difference of species diversity across the three groups (Figure 4C). The β-diversity of the gut microbiota of the three groups were also determined using various approaches such as the UPGMA (unweighted pair group method with arithmetic mean) clustering method, principal coordinate analysis (PCoA), and nonmetric multidimensional scaling (NMDS). The weighted unifrac UPGMA clustering method classified the control and PCOS mice samples into two distinct groups (Figure 4D), implying that the gut microbial composition of the PCOS mice differed from that of the control mice. Although the YLTB group could not be completely separated from the PCOS group, it was significantly different from the PCOS group, demonstrating that YLTB administration alters the gut microbial composition of PCOS mice (Figure 4D). Based on the unweighted unifrac distance, PCoA analysis showed a clear separation among the three groups, with the principal component 1 (PC1) value of 43.61% and PC2 value of 11.03% (Figure 4E). In addition, the degree of variation among the three groups was illustrated using NMDS analysis based on

10.3389/fendo.2023.1122709

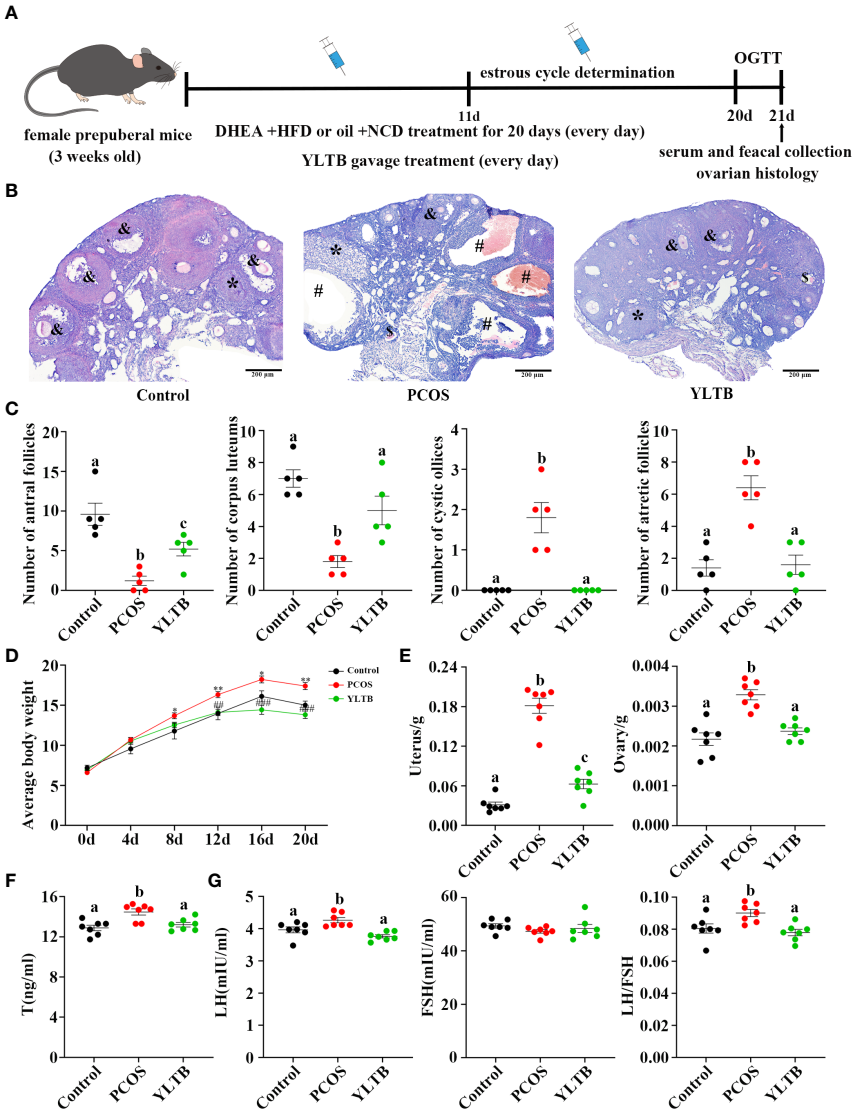

FIGURE 2
YLTB rescued ovarian dysfunction in PCOS mice. **(A)** The timeline of the experimental process. **(B)** Representative ovarian slices stained with hematoxylin and eosin (H&E). Scale bar = 200 μm; & indicates antral follicle; * indicates corpora luteum; # indicates cystic follicle; $ indicates atretic follicle. **(C)** The difference in the number of antral follicles, corpora lutea, cystic follicles, and atretic follicles among groups (n = 5/group). **(D)** Measurement of mouse body weight every four days among the three groups (n = 7/group, * P < 0.05; ** P < 0.01 compared with the control group, ## P < 0.01; ### P <0.001 compared with the PCOS group). **(E)** Measurement of the wet weight of the uterus and ovary among the three groups (n = 7/group). **(F, G)** Serum T, LH, and FSH levels were measured using an enzyme-linked immunosorbent assay kit, and the LH/FSH ratio was calculated (n = 7/group). Statistical significance was determined using one-way or two-way ANOVA with Tukey's multiple comparisons test, and data are presented as the mean ± standard error of the mean (SEM). a, b and c indicate $P < 0.05$; if 2 groups have the same letter, it indicates no statistical significance.

Bray–Curtis distance, when stress is less than 0.2 (stress = 0.158, Figure 4F). Both PCoA and NMDS analyses revealed that the intergroup distances were greater than the intragroup distances, implying that PCOS and YLTB therapy have an effect on the β-diversity of gut microbiota.

3.5 YLTB alters the taxonomic composition of gut microorganism communities at the phylum, genus and species levels

In addition to diversity details, the abundance of gut microbiota of the control, PCOS and YLTB groups was analyzed, using the linear discriminant analysis (LDA) effect size (LEfSe) method. In our studies, the cut-off threshold of LDA was set at the score 4.0. Our data showed that the *Bacteroidota* phylum was enriched in the control mice, and the *Firmicutes* phylum was enriched in PCOS mice, as well as the *Erysipelotrichales* order in YLTB mice (Figures 5A, B). This observation demonstrated a great shift of gut microbiota composition from PCOS mice to YLTB mice.

The detailed differences of the taxonomic composition of gut microbiota among the three groups were shown in the Figure 5C–H at the phylum, genus, and species levels. At the phylum levels, *Firmicutes* and *Bacteroidota* were dominant in all three groups (Figure 5C). Furthermore, the relative *Firmicutes* abundance levels

10.3389/fendo.2023.1122709

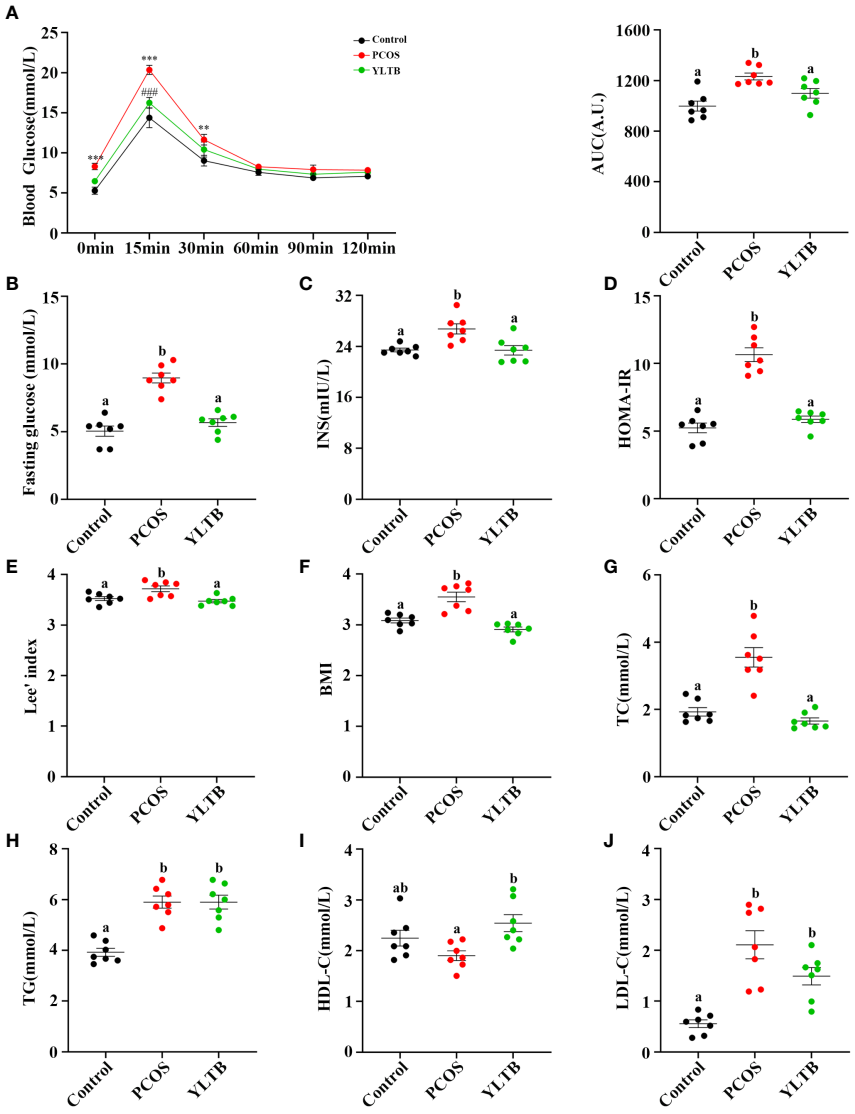

FIGURE 3
The effects of YLTB on glucose tolerance, insulin sensitivity and lipid metabolism in PCOS mice. **(A)** OGTTs in mice from the control, PCOS, and YLTB groups. The corresponding area under the curve (AUC) values of blood glucose levels in each group were calculated (** $P < 0.01$; *** $P < 0.001$ compared with the control group, ### $P < 0.001$ compared with the PCOS group). **(B, C)** Blood glucose and serum insulin level assessment after 12 h of fasting in mice from the control, PCOS, and YLTB (38.68 g·kg^{-1}·day^{-1}) groups. **(D)** The homeostasis model assessment of insulin resistance (HOMA-IR) index = [FBG (mmol/L)] × [FINS (IU/mL)]/22.5 in mice from the control, PCOS, and YLTB groups. **(E, F)** Lee's index = [Body mass (g) × 1,000]$^{1/3}$/body length (cm) and Body mass index (BMI = weight (kg)/height (m^2) calculation. **(G–J)** Detection of TC, TG, HDL-C and LDL-C to evaluate the level of serum lipid metabolism in mice from the control, PCOS, and YLTB groups. n = 7/group, statistical significance was determined using one-way or two-way ANOVA with Tukey's multiple comparisons test, and data are presented as the mean ± SEM. a and b indicate $P < 0.05$; if 2 groups have the same letter, it indicates no statistical significance.

were highest in PCOS mice, but the levels of *Bacteroidota* and *Proteobacteria* were lower than the ones in other two groups. These changes were attenuated in YLTB mice (Figure 5D). For *Bacteroidota*, the *Bacteroides* and *Parabacteroides* genus abundance levels were lower in the PCOS mice than in the control group (Figure 5E). For *Firmicutes*, the *Blautia* and *Lactobacillus* abundance levels in PCOS mice were restored to the normal levels by YLTB administration. The similar effects were observed with the abundance levels of *Parabacteroides* (Figure 5E). Besides *Blautia* and *Lactobacillus*, *Lachnospiraceae UCG-005* and *UCG-006* were greatly enriched in the PCOS group, which were also significantly reduced by YLTB (Figure 5F). *Bacteroides*, *Blautia* and *Lactobacillus* genera were further analyzed for the detailed information at the species levels (Figures 5G, H). The data showed that *Bacteroides dorei*, *Bacteroides fragilis*, *Lactobacillus johnsonii* and *Lachnospiraceae bacterium* 28-4 as well as Lachnospiraceae bacterium 615 were enriched in the PCOS group and could be reverted in the YLTB group (Figure 5H). These results suggested that YLTB can restore PCOS gut microbiota disturbances.

3.6 Association among fecal metabolites, gut microbiota and PCOS mice phenotypes

Since we have shown that YLTB administration greatly changed basal metabolism, ovary dysfunction, and the gut microbiota in

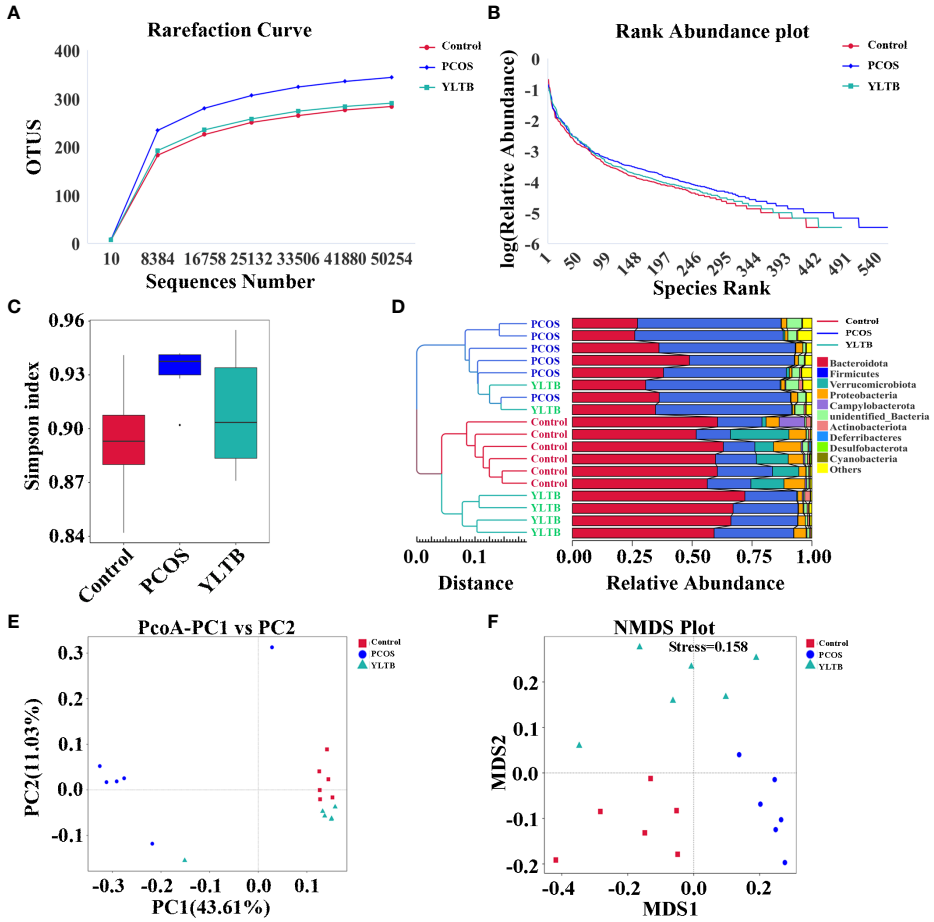

FIGURE 4
Effect of YLTB on α and β diversity of gut microbiota. **(A, B)** Analysis of gut microbial diversity was performed on the basis of 16S rRNA sequencing and was presented by rarefaction curves and rank abundance curves. **(C)** The α-diversity of gut bacterial assemblages with Simpson index in the mice receiving different treatments. **(D)** Evaluation of β-diversity with bacterial community compositional similarity using UPGMA cluster analysis, and the clustering result and the relative abundance of each sample at the phylum level were displayed. The left side is the UPGMA clustering tree structure, and the right side is the relative abundance distribution map of each sample at the phylum level. **(E, F)** Plots of unweighted UniFrac-based PCoA and nonmetric multidimensional scaling (NMDS) based on Bray-Curtis distance. Each point in the graph represents a sample, the distance between points indicates the degree of variation, and the samples of the same group are represented by the same color. n = 6 mice/group.

PCOS mice, we next seek for more association information among fecal metabolites, gut microbiota and PCOS mice phenotypes using biostatistical approaches. Firstly, the fecal metabolite profile from mice was determined by the untargeted metabolomics. Principal component analysis (PCA) and partial least squares discrimination analysis (PLS-DA) showed a distinct separation of those metabolites among the three groups, with different PC1 and PC2 values (Figure 6A, B). The detailed relationship between the metabolites and the three groups were illustrated in Figure 6C. 44 fecal metabolites demonstrated that the abundances of fecal metabolites in PCOS mice were different from those in the control mice, which were significantly manipulated by YLTB. These metabolites mainly consist of hormones, vitamins, and organic acids. For example, hormones include cortisone, hydrocortisone, menaquinone, and etc; vitamins such as ascorbic acid, folic acid and phylloquinone, whereas organic acids include cis-aconitic acid, maleic acid, ferulic acid, and etc (Figure 6C).

Spearman's correlation analysis was next used to comprehensively analyze the correlations among fecal metabolites, the gut microbiota and host phenotypes (Figure 7). In the relationship between fecal metabolites and the gut microbiota, metabolites (such as ferulic acid, folic acid and methylmalonate) were negatively correlated with 9 bacterial species. Among those metabolites, ferulic acid (FA) was strongly correlated with basal metabolism. The correlations between the gut microbiota and host phenotypes were also shown in the Figure 7. Nine bacterial strains (*Alistipes inops*, *Bacteroides dorei*, *Bacteroides fragilis*, *Clostridium sp Culture-54*, *Faecalitalea sp Marseille-P3755*, *Lachnospiraceae bacterium 615*, *Lactobacillus johnsonii*, *Lactococcus lactis*, and *Ruminococcaceae bacterium GD7*) were positively correlated with the host parameters (including body weight, BMI, TC, T, LH, LH/FSH ratio, FBG, INS and HOMA-IR). Taken together, our findings showed a tight association among fecal metabolites, the gut microbiota and host phenotypes in PCOS mice administered with YLTB.

10.3389/fendo.2023.1122709

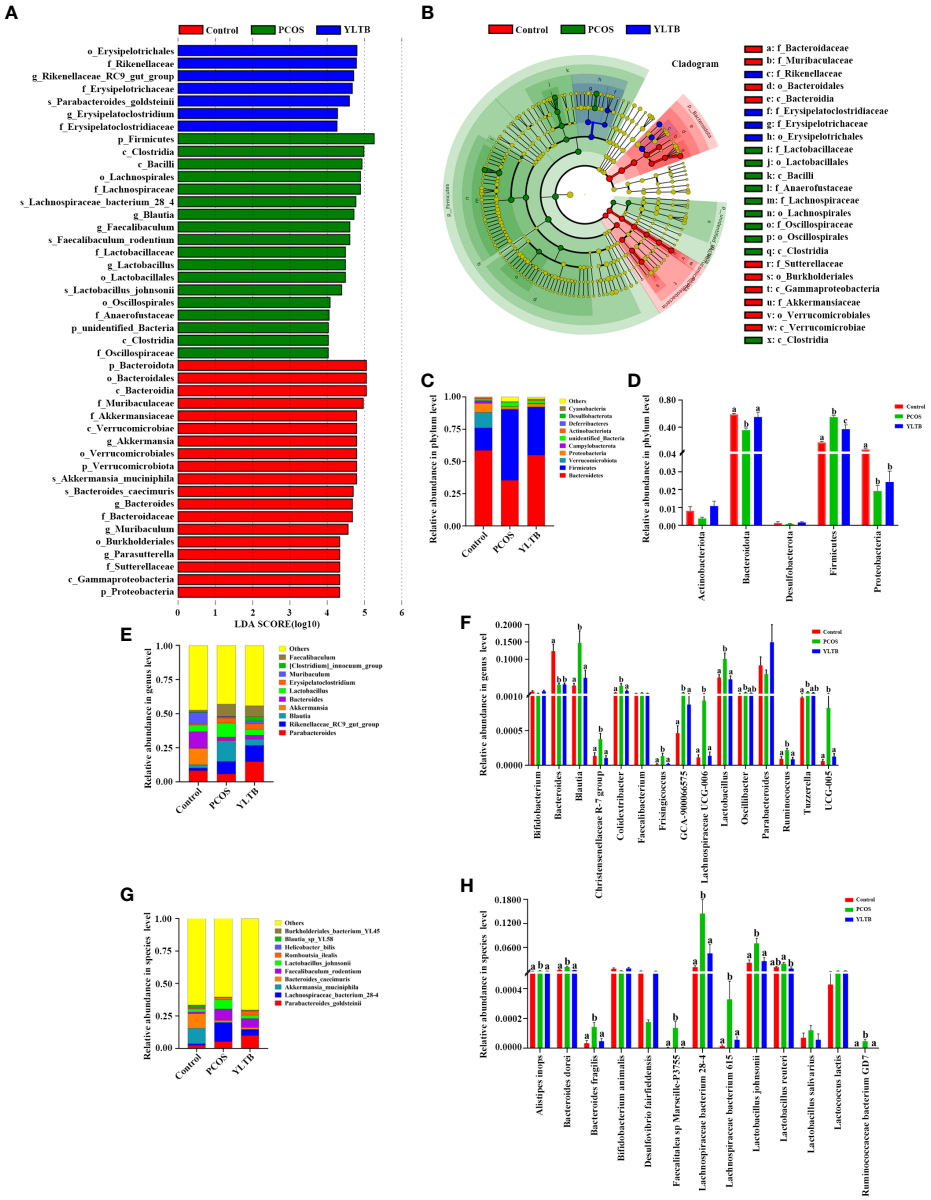

FIGURE 5
Changes in the taxonomic composition of gut microorganism communities at the phylum, genus and species levels. Statistical differences in the level of biomarkers between the control, PCOS, and YLTB groups were identified using the line discriminant analysis (LDA) effect size (LEfSe) method. **(A)** Taxa enrichment as indicated by discriminant analysis (LDA) scores in the control (red), PCOS (green), and YLTB (blue) treated groups. Only the taxa meeting an LDA significance threshold of four are displayed, and the length of the histogram represents the influence of different species. **(B)** The output of the LEfSe algorithm as visualized by cladograms. Significantly distinct taxonomic nodes are colored and the branch areas are shaded according to the effect size of each taxa. **(C, E, G)** The top ten bacteria with maximum abundance of intestinal bacteria at the phylum, genus and species levels among control, PCOS-treated and YLTB-treated mice. **(D, F, H)** Significant changes in abundance at the phylum, genus and species levels among the control, PCOS, and YLTB groups. N = 6 mice/group. For **D**, **F**, and **H**, statistical significance was determined using one-way ANOVA with Tukey's multiple comparisons test, and data are presented as the mean ± SEM. a, b and c indicate $P < 0.05$; if 2 groups have the same letter, it indicates no statistical significance.

3.7 The addition of ferulic acid attenuated ovarian dysfunction in PCOS mice

The Figure 7 showed that FA is a critical metabolite that contribute to the effect of YLTB to the PCOS mice. Therefore, FA was then tested whether it regulates ovarian functions in PCOS mice. The DHEA-treated mice were administered with low-dose FA (FA1 group, 50 mg/kg) or high-dose FA (FA2 group, 100 mg/kg) for 20 days, before they were sampled for further analysis of ovarian function changes (process illustrated as Figure 8A). Next, we tested ovarian morphology, body weight, wet weight of the uterus and ovaries and sex hormone alterations among the control, PCOS, FA1 and FA2 groups. H&E staining revealed that the FA administration reduced the number of cystic and atretic follicles, while promoting the development of antral follicles and corpus lutea in the PCOS ovaries (Figures 8B, C). The body weight, as well as wet uterine and ovary weight, was significantly reduced in both high and low FA-gavaged mice (Figures 8D, E). Consistently, the decreased serum T levels were

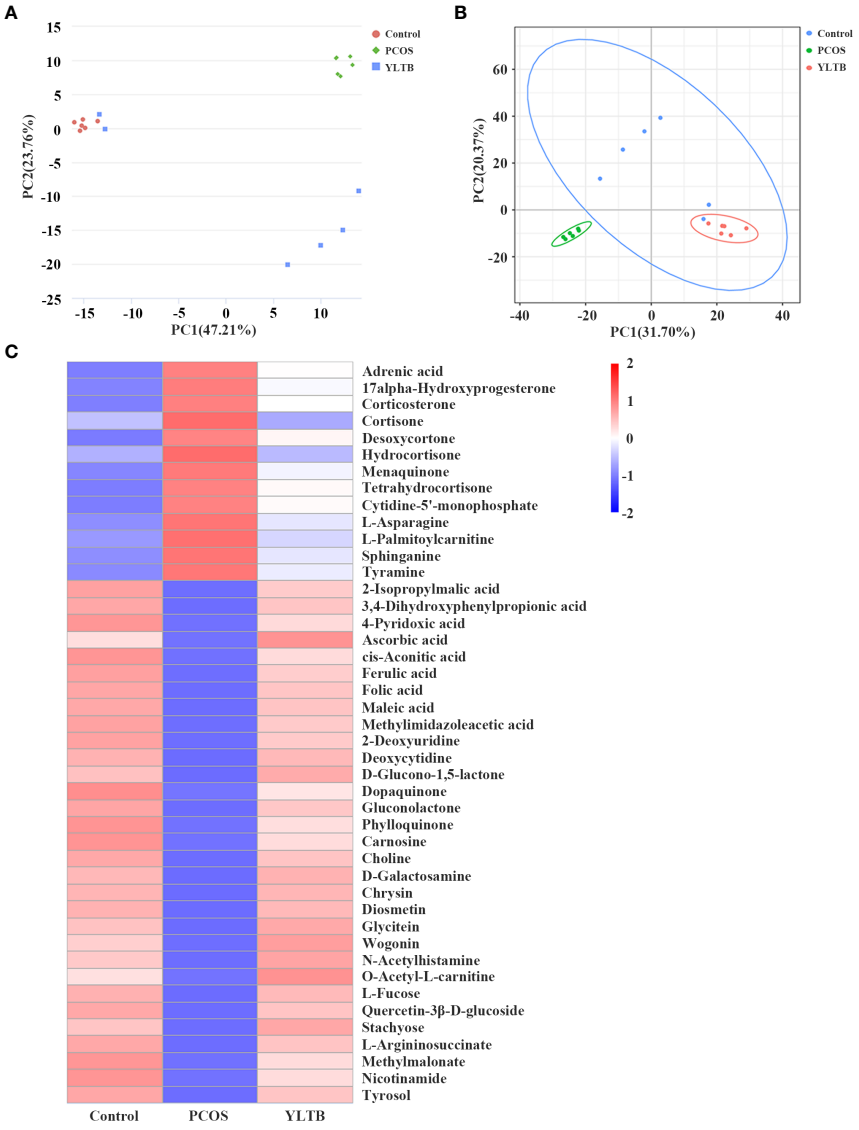

FIGURE 6
The effect of YLTB on the metabolomic profiles of mouse feces. **(A, B)** Principal component analysis (PCA) and partial least squares discrimination analysis (PLS-DA) were used to observe the overall distribution trends among the three groups of samples. The abscissa PC1 and the ordinate PC2 represent the scores of the first and second principal components, respectively. The scattered points of different colors represent samples of different experimental groups. **(C)** A heatmap of the hierarchical clustering analysis with respect to the relative abundances of 44 fecal metabolites among the three groups. Abscissas represent different experimental groups, ordinates represent different metabolites, and different colors represent the relative expression of metabolites at the corresponding position. N = 6 mice/group.

observed in FA-gavaged mice compared to PCOS mice (Figure 8F). However, FA had no impact on the estrus period (Figure S2C-D). These findings showed that FA alleviated ovarian dysfunction and reduced pathological damage to ovarian tissues in PCOS mice.

3.8 Ferulic acid ameliorates glucose and lipid metabolism disorders in PCOS mice

FA was next tested for its regulatory effect on disrupted glucose and lipid metabolism in PCOS mice. The Figure 9A illustrated that FA administration largely corrected glucose tolerance impairment and dramatically reduced fasting glucose, serum insulin, and HOMA-IR levels in PCOS mice (Figure 9B–D). Besides, FA significantly lowered the values of BMI, Lee's index, TC and LDL-C levels (Figure 9E, F, G, J). Consistently, the high FA dose significantly increased the HDL-C levels while decreased the TG levels (Figures 9H, I). Differently, the levels of TG and HDL-C in the low dose FA group were lower than the ones in the PCOS group but without statistical differences (Figures 9H, I). In general, these studies validated the effect of FA on PCOS similar to YLTB.

4 Discussion

PCOS is a common endocrine disorder, which s characterized by ovarian dysfunction, hyperandrogenism and polycystic ovarian

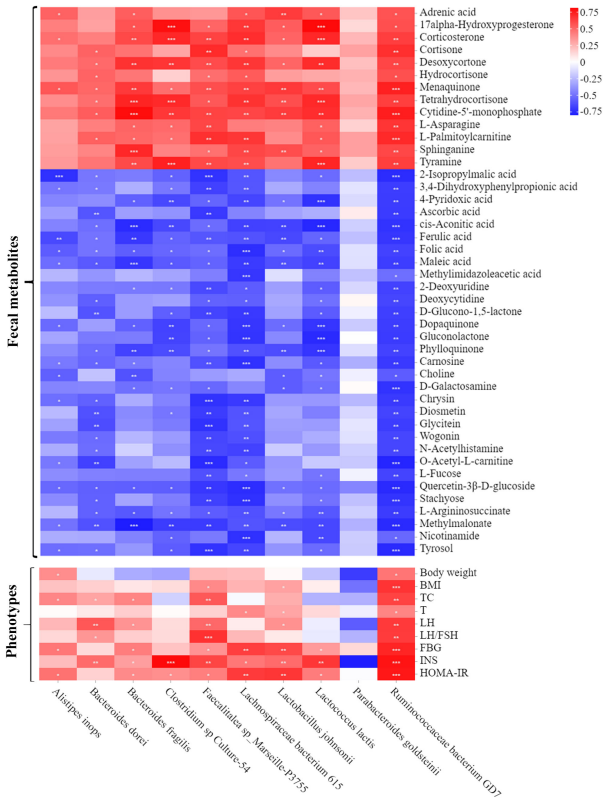

FIGURE 7
Associations among fecal microbiota, fecal metabolites and PCOS phenotypes. A heatmap of the three-tiered analyses integrating the gut microbiome, fecal metabolites and phenotypes measured by Spearman's correlation coefficient in the control, PCOS, and YLTB group mice (n = 6/mouse). Associations between the 10 gut microbial species and 44 fecal metabolites are shown in the up panel. The down panel displays associations between 10 gut microbial species and 9 phenotypes. The value range of the correlation coefficient is (-0.75, 0.75). The degree of association is indicated by the color intensity (red represents positive correlations, and blue represents negative correlations). * indicates significant correlation, * $P < 0.05$; ** $P < 0.01$; *** $P < 0.001$.

morphology. At present, TCM has been used to treat PCOS in Chinese women. The quality control of the YLTB used in this study was investigated by LC-MS (Figure 1A). The results showed that the positive and negative ion modes were respectively detected for the top 20 main compounds of YLTB detected, including nobiletin, berberine, quercetin, catechin, etc (Figure 1B, Table 2, Table 3). Numerous studies have found that the main components of YLTB (berberine, catechin, quercetin, and so on) have beneficial therapeutic effects in decreasing the levels of serum T (47, 48), TC (49), LH (48, 49), the ratio of LH/FSH (50), alleviating IR (47, 51, 52), dyslipidemia (51, 53) and other PCOS-related diseases.

With a focus on the therapeutic effects of YLTB on PCOS, our studies demonstrated the complicated association among the ovarian functions, the gut microbiota and metabolites in YLTB-gavaged PCOS mice, using 16S RNA sequencing combined with the non-targeted metabolomics. The ovarian dysfunction in PCOS mice was clearly attenuated by YLTB administration. Consistently, YLTB greatly restored the levels of fasting glucose, serum insulin and total cholesterol from PCOS condition to the normal. Other metabolites such as ferulic acid, folic acid and stachyose were regulated in a similar manner. In the PCOS group, the *Firmicutes* phylum was enriched whereas the *Bacteroidota* phylum was dominant in the YLTB group. Moreover, YLTB suppressed the abundance of the species of *Bacteroides dorei*, *Bacteroides fragilis*, and *Lactobacillus johnsonii* that were all enriched in PCOS mice. The enrichment of these bacteria species was tightly associated with metabolism of many metabolites, as well as host phenotypes in PCOS mice. Among the fecal metabolites, ferulic acid was validated to be effective against PCOS due to its capabilities of reducing ovarian dysfunction, improving disorders of glycolipid metabolism, and associating with the bacterial species.

YLTB ameliorates the host features of PCOS including glucose tolerance, insulin insensitivity, lipid metabolic disorder, and obesity. It is natural to propose that YLTB could substitute current medicines to treat PCOS patients. This idea can be supported by some other TCM studies targeting PCOS (54, 55). For instance, the formula Dang gui shao yao san treatment can significantly reduce plasma LH levels and increase estradiol levels as well as the ovulation rates in PCOS patients (54). Buzhong Yiqi prescription reduces serum androgen levels and regulates lipid metabolism in PCOS patients (55). It is not known yet whether YLTB is better than these two TCM treatments, which might be compared in future. Although ferulic acid has been identified as a critical component, it is not excluded that other possibilities might play important roles.

The therapeutic effect of YLTB on PCOS mice is also related to the amelioration of the gut microbiota dysbiosis. Transplantation with fecal

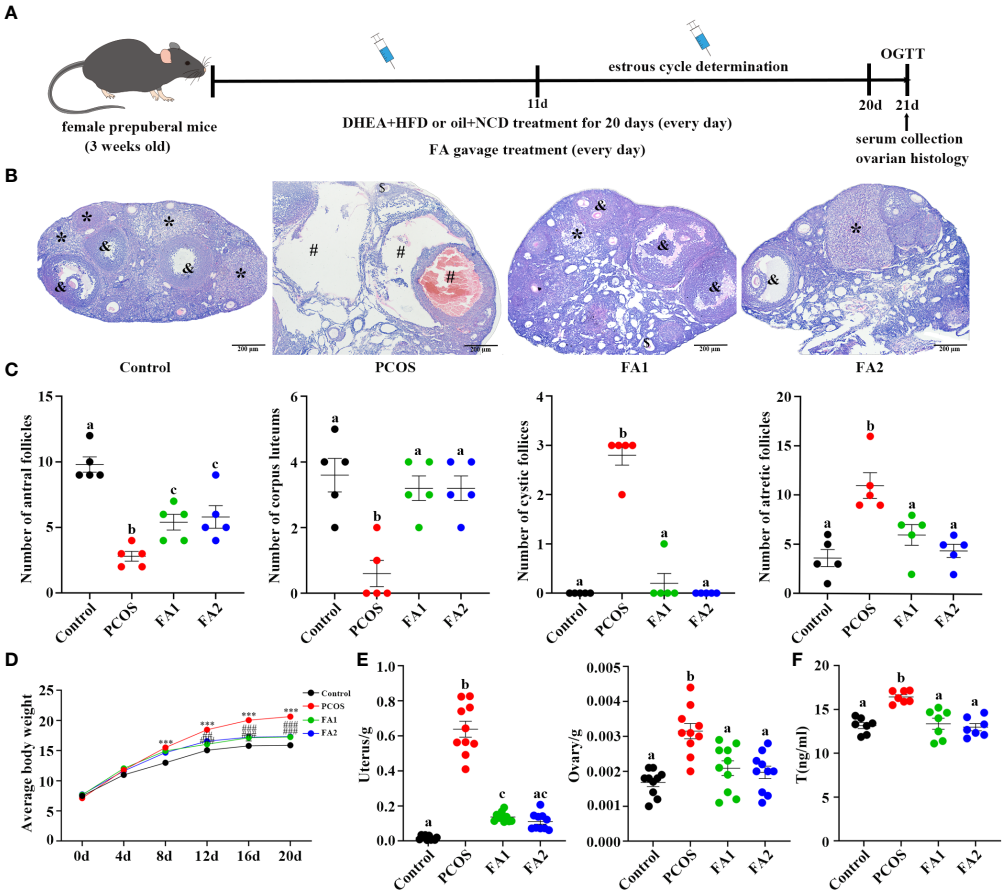

FIGURE 8
Amelioration of ovarian function in PCOS mice after ferulic acid administration. **(A)** Timeline of the experimental process. **(B)** Changes of ovary stained with Hematoxylin and eosin (H&E) (scale bar=200μm; & indicates antral follicle, * indicates corpora lutea; # indicates cystic follicles, $ indicates atretic follicle). **(C)** Changes in the numbers of antral follicles, corpora lutea, cyst-like follicles, and atretic follicles counted with H&E staining sections (n = 5/group). **(D, E)** Determination of weight of body, uterus and ovaries (n = 10/group, *** P <0.001 compared with the control group, ## P < 0.01; ### P < 0.001 compared with the PCOS group). **(F)** The levels of testosterone in the serum were determined using an enzyme-linked immunosorbent assay kit (n = 7/group). Statistical significance was determined using one-way or two-way ANOVA with Tukey's multiple comparisons test and data are presented as the mean ± SEM, a, b and c indicate $P < 0.05$, if 2 groups have the same letter, it indicates no statistical significance.

microbiota of healthy control women has been shown to improve PCOS conditions via restoration of gut microbiota dysbiosis. (56). Our data demonstrated that the genus of Blautia, and species of *Bacteroides dorei*, *Bacteroides fragilis* were all enriched in PCOS mice and that YLTB administration attenuated the enrichment of these bacteria species. Consistent with our findings, others reported that *Blautia* was significantly increased in PCOS animals (57) and positively correlated with testosterone concentration, cysts in the ovaries, bodyweight and serum lipids (57, 58). *Bacteroides fragilis* was enriched in PCOS patients, and that clinical indicators such as BMI, T, and LH were positively correlated with it (59–61). In addition, enriched in the intestinal microbiota of PCOS patients, *Bacteroides vulgatus* caused ovarian dysfunction and metabolic disorders in mice (14). Therefore, the present study indicated that YLTB might ameliorate several PCOS disorders in mice by reversing disturbances in the gut microbiota.

Our analysis demonstrated a strong correlation among the fecal metabolites, the host phenotypes and the gut microbiota in PCOS or YLTB mice. FA was prioritized to be investigated for its association with the gut microbiota and PCOS. In our studies, PCOS resulted in a decrease in FA abundance, whereas YLTB reverted it significantly. FA improved disorders of glucose or lipid metabolism in PCOS mice. This is consistent with others' observations that FA ameliorates lipid profiles and insulin sensitivity (62). Furthermore, our data demonstrated that FA is negatively correlated with 9 bacteria species, all of which were positively correlated with the host phenotypes, such as body weight, BMI, TC,T, LH, FBG, INS and HOMA-IR. Consistently, previous studies shown that FA improves a variety of disorders through modulating gut microbiota (31, 32, 63, 64). Our untargeted metabolomics predicted the roles of some metabolites, and we showed that ferulic acid and the other metabolites (such as folic acid, stachyose, etc.) may have crucial roles, which we will investigate deeply in our in our future studies.

5 Conclusion

The current study focuses on the therapeutic effects of YLTB administration on PCOS *via* modulating the gut microbiota and the associated metabolites. YLTB administration clearly attenuated ovarian dysfunction, restored glucose and lipid metabolism, and suppressed the abundance of several bacteria species such as

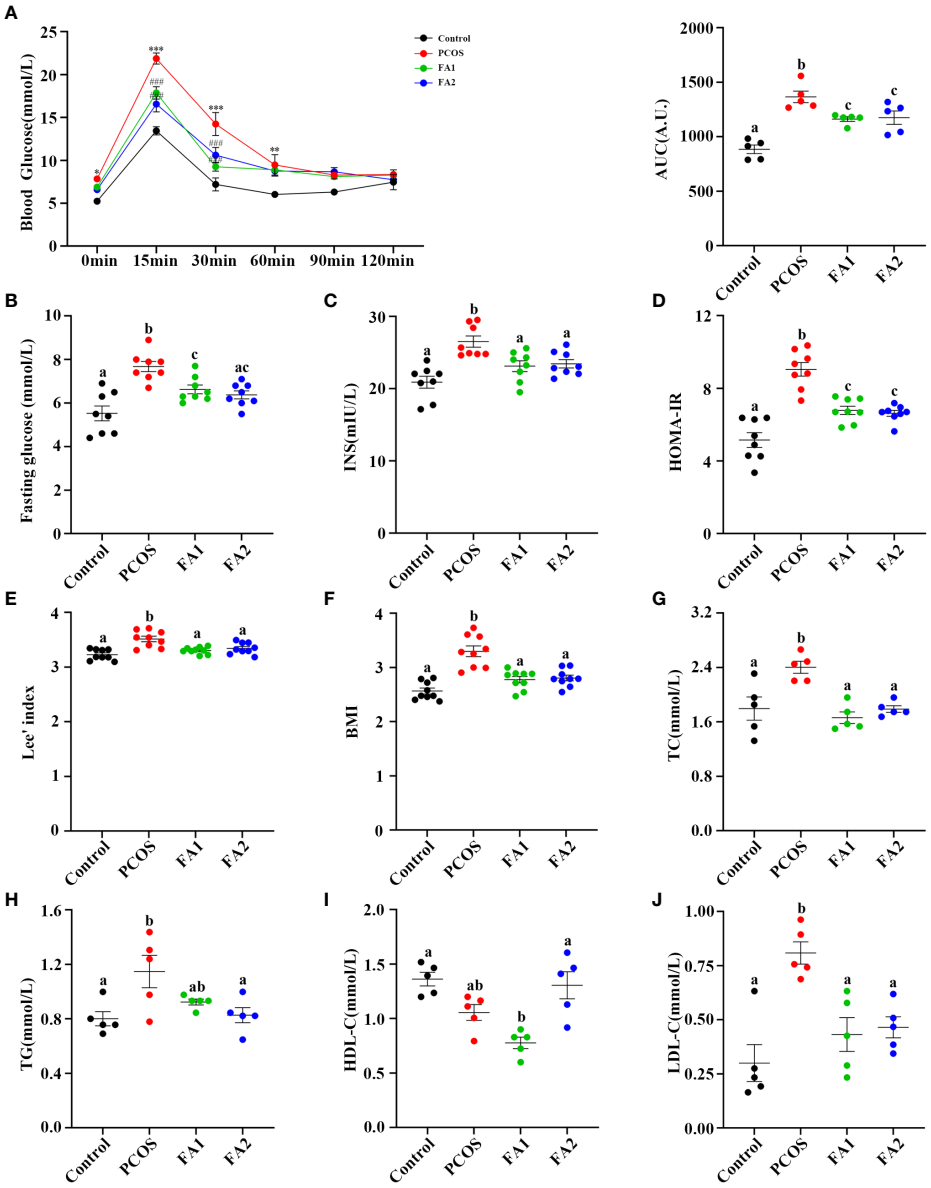

FIGURE 9
Ferulic acid ameliorated glucose and lipid metabolism disorders of PCOS mice. **(A)** Oral glucose tolerance tests (n = 5/group, ** P < 0.01; *** P < 0.001 compared with the control group, ### P < 0.001 compared with the PCOS group). **(B, C)** Blood glucose and serum insulin (n = 8/group) detection after a 12-hour fast in mice from the control, PCOS, and FA groups. **(D)** Changes of HOMA-IR index. HOMA-IR index = [FBG (mmol/L)] × [FINS (IU/mL)]/22.5 (n = 8/group). **(E)** Lee's index and BMI calculation (n = 9/group). **(G, H, I and J)** Detection of plasma lipid metabolic indicators, TC, TG, HDL-C, and LDL-C in mice (n = 5/group). Statistical significance was determined using one-way or two-way ANOVA with Tukey's multiple comparisons test and data are presented as the mean ± SEM, a, b and c indicate *P* < 0.05, if 2 groups have the same letter, it indicates no statistical significance.

Bacteroides dorei, *Bacteroides fragilis*, and *Lactobacillus johnsonii* of PCOS mice. These bacteria were strongly associated with many metabolites. Among the fecal metabolites, the effect of FA against PCOS was similar to that of YLTB.

Data availability statement

The datasets presented in this study can be found in online repositories. The names of the repository/repositories and accession number(s) can be found below: http://www.ncbi.nlm.nih.gov/bioproject/914098 (accession number PRJNA914098), http://www.ebi.ac.uk/metabolights/MTBLS6736 (identifier MTBLS6736).

Ethics statement

The animal study was reviewed and approved by Institutional Animal Care and Use Committee of Chongqing Medical University (Animal Qualification Certificate No.2022109).

Author contributions

L-JF, QF designed and edited the experiments. Y-NS wrote the manuscript. Y-NS performed the experiments of PCOS model and M-JW conducted data analysis. Y-BD finalized the manuscript. J-PY and X-LW assisted the study. MX and M-HB contributed to experimental design. All authors have read, discussed and approved the final manuscript.

Funding

This work was funded by grants from National Natural Science of Foundation of China (Nos. 82104923, 82171624), Natural Science of Foundation of Chongqing (Nos. cstc2021jcyj-msxmX0236, cstc2021jcyj-msxmX0900, cstc2019jxjl130030) and Chongqing medical scientific research project (Joint project of Chongqing Health Commission and Science and Technology) (No.2022QNXM042), Chongqing Municipal Health Bureau Chinese Medicine Technology Project (serial number: ZY201802044).

Conflict of interest

The authors declare that the research was conducted in the absence of any commercial or financial relationships that could be construed as a potential conflict of interest.

Publisher's note

Supplementary material

The Supplementary Material for this article can be found online at: https://www.frontiersin.org/articles/10.3389/fendo.2023.1122709/full#supplementary-material

References

1. Norman RJ, Dewailly D, Legro RS, Hickey TE. Polycystic ovary syndrome. *Lancet* (2007) 370:685–97. doi: 10.1016/S0140-6736(07)61345-2

2. March WA, Moore VM, Willson KJ, Phillips DI, Norman RJ, Davies MJ. The prevalence of polycystic ovary syndrome in a community sample assessed under contrasting diagnostic criteria. *Hum Reprod* (2010) 25:544–51. doi: 10.1093/humrep/dep399

3. Han Q, Wang J, Li W, Chen ZJ, Du Y. Androgen-induced gut dysbiosis disrupts glucolipid metabolism and endocrinal functions in polycystic ovary syndrome. *Microbiome* (2021) 9:101. doi: 10.1186/s40168-021-01046-5

4. Escobar-Morreale HF. Polycystic ovary syndrome: Definition, aetiology, diagnosis and treatment. *Nat Rev Endocrinol* (2018) 14:270–84. doi: 10.1038/nrendo.2018.24

5. Schmidt TH, Khanijow K, Cedars MI, Huddleston H, Pasch L, Wang ET, et al. Cutaneous findings and systemic associations in women with polycystic ovary syndrome. *JAMA Dermatol* (2016) 152:391–98. doi: 10.1001/jamadermatol.2015.4498

6. Insenser M, Murri M, Del CR, Martinez-Garcia MA, Fernandez-Duran E, Escobar-Morreale HF. Gut microbiota and the polycystic ovary syndrome: Influence of sex, sex hormones, and obesity. *J Clin Endocrinol Metab* (2018) 103:2552–62. doi: 10.1210/jc.2017-02799

7. He FF, Li YM. Role of gut microbiota in the development of insulin resistance and the mechanism underlying polycystic ovary syndrome: A review. *J Ovarian Res* (2020) 13:73. doi: 10.1186/s13048-020-00670-3

8. Janssen AW, Kersten S. The role of the gut microbiota in metabolic health. *FASEB J* (2015) 29:3111–23. doi: 10.1096/fj.14-269514

9. Martinez LE, Segura CM. Effect of ultra-processed diet on gut microbiota and thus its role in neurodegenerative diseases. *Nutrition* (2020) 71:110609. doi: 10.1016/j.nut.2019.110609

10. Xia WJ, Xu ML, Yu XJ, Du MM, Li XH, Yang T, et al. Antihypertensive effects of exercise involve reshaping of gut microbiota and improvement of gut-brain axis in spontaneously hypertensive rat. *Gut Microbes* (2021) 13:1–24. doi: 10.1080/19490976.2020.1854642

11. Thackray VG. Sex, microbes, and polycystic ovary syndrome. *Trends Endocrinol Metab* (2019) 30:54–65. doi: 10.1016/j.tem.2018.11.001

12. Liu R, Zhang C, Shi Y, Zhang F, Li L, Wang X, et al. Dysbiosis of gut microbiota associated with clinical parameters in polycystic ovary syndrome. *Front Microbiol* (2017) 8:324. doi: 10.3389/fmicb.2017.00324

13. Torres PJ, Siakowska M, Banaszewska B, Pawelczyk L, Duleba AJ, Kelley ST, et al. Gut microbial diversity in women with polycystic ovary syndrome correlates with hyperandrogenism. *J Clin Endocrinol Metab* (2018) 103:1502–11. doi: 10.1210/jc.2017-02153

14. Qi X, Yun C, Sun L, Xia J, Wu Q, Wang Y, et al. Gut microbiota-bile acid-interleukin-22 axis orchestrates polycystic ovary syndrome. *Nat Med* (2019) 25:1225–33. doi: 10.1038/s41591-019-0509-0

15. Li T, Zhang T, Gao H, Liu R, Gu M, Yang Y, et al. Tempol ameliorates polycystic ovary syndrome through attenuating intestinal oxidative stress and modulating of gut microbiota composition-serum metabolites interaction. *Redox Biol* (2021) 41:101886. doi: 10.1016/j.redox.2021.101886

16. Zhang J, Sun Z, Jiang S, Bai X, Ma C, Peng Q, et al. Probiotic bifidobacterium lactis V9 regulates the secretion of sex hormones in polycystic ovary syndrome patients through the gut-brain axis. *Msystems* (2019) 4:e17–19. doi: 10.1128/mSystems.00017-19

17. Wang T, Sha L, Li Y, Zhu L, Wang Z, Li K, et al. Dietary alpha-linolenic acid-rich flaxseed oil exerts beneficial effects on polycystic ovary syndrome through sex steroid hormones-Microbiota-Inflammation axis in rats. *Front Endocrinol (Lausanne)* (2020) 11:284. doi: 10.3389/fendo.2020.00284

18. Richards JL, Yap YA, McLeod KH, Mackay CR, Marino E. Dietary metabolites and the gut microbiota: an alternative approach to control inflammatory and autoimmune diseases. *Clin Transl Immunol* (2016) 5:e82. doi: 10.1038/cti.2016.29

19. De Vadder F, Kovatcheva-Datchary P, Goncalves D, Vinera J, Zitoun C, Duchampt A, et al. Microbiota-generated metabolites promote metabolic benefits *via* gut-brain neural circuits. *Cell* (2014) 156:84–96. doi: 10.1016/j.cell.2013.12.016

20. Wang R, Kim BV, van Wely M, Johnson NP, Costello MF, Zhang H, et al. Treatment strategies for women with WHO group II anovulation: systematic review and network meta-analysis. *Bmj* (2017) 356:j138. doi: 10.1136/bmj.j138

21. Weiss NS, Kostova E, Nahuis M, Mol B, van der Veen F, van Wely M. Gonadotrophins for ovulation induction in women with polycystic ovary syndrome. *Cochrane Database Syst Rev* (2019) 1:D10290. doi: 10.1002/14651858.CD010290.pub3

22. Mitwally M, Casper RF. Reprint of: Use of an aromatase inhibitor for induction of ovulation in patients with an inadequate response to clomiphene citrate. *Fertil Steril* (2019) 112:e178–82. doi: 10.1016/j.fertnstert.2019.08.087

23. Morley LC, Tang T, Yasmin E, Norman RJ, Balen AH. Insulin-sensitising drugs (metformin, rosiglitazone, pioglitazone, d-chiro-inositol) for women with polycystic ovary syndrome, oligo amenorrhoea and subfertility. *Cochrane Database Syst Rev* (2017) 11:D3053. doi: 10.1002/14651858.CD003053.pub6

24. Penzias A, Bendikson K, Butts S, Coutifaris C, Falcone T, Fossum G, et al. Role of metformin for ovulation induction in infertile patients with polycystic ovary syndrome (PCOS): a guideline. *Fertil Steril* (2017) 108:426–41. doi: 10.1016/j.fertnstert.2017.06.026

25. Xu Y, Tang J, Guo Q, Xu Y, Yan K, Wu L, et al. Traditional Chinese medicine formula FTZ protects against polycystic ovary syndrome through modulating adiponectin-mediated fat-ovary crosstalk in mice. *J Ethnopharmacol* (2021) 268:113587. doi: 10.1016/j.jep.2020.113587

26. Wang Y, Xiao H, Liu Y, Tong Q, Yu Y, Qi B, et al. Effects of bu shen hua zhuo formula on the LPS/TLR4 pathway and gut microbiota in rats with letrozole-induced polycystic ovary syndrome. *Front Endocrinol (Lausanne)* (2022) 13:891297. doi: 10.3389/fendo.2022.891297

27. Qiu Z, Dong J, Xue C, Li X, Liu K, Liu B, et al. Liuwei dihuang pills alleviate the polycystic ovary syndrome with improved insulin sensitivity through PI3K/Akt signaling pathway. *J Ethnopharmacol* (2020) 250:111965. doi: 10.1016/j.jep.2019.111965

28. Chen J, Feng Q, Fu LJ, Xia M. Yulin tongbu decoction in the treatment of spleen and kidney deficiency, phlegm-dampness block type therapeutic effect analysis of PCOS. *Asia-Pacific Traditional Med* (2022) 18:129–32. doi: 10.11954/ytctyy.202206027

29. Kou G, Li P, Hu Y, Chen H, Nyantakyiwaa AA, Seydou TS, et al. Nobiletin activates thermogenesis of brown and white adipose tissue in high-fat diet-fed C57BL/6 mice by shaping the gut microbiota. *FASEB J* (2021) 35:e21267. doi: 10.1096/fj.202002197R

30. Morrow NM, Trzaskalski NA, Hanson AA, Fadzeyeva E, Telford DE, Chhoker SS, et al. Nobiletin prevents high-fat diet-induced dysregulation of intestinal lipid metabolism and attenuates postprandial lipemia. *Arterioscler Thromb Vasc Biol* (2022) 42:127–44. doi: 10.1161/ATVBAHA.121.316896

31. Tian B, Geng Y, Wang P, Cai M, Neng J, Hu J, et al. Ferulic acid improves intestinal barrier function through altering gut microbiota composition in high-fat diet-induced mice. *Eur J Nutr* (2022) 61:3767–83. doi: 10.1007/s00394-022-02927-7

32. Gu Y, Zhang Y, Li M, Huang Z, Jiang J, Chen Y, et al. Ferulic acid ameliorates atherosclerotic injury by modulating gut microbiota and lipid metabolism. *Front Pharmacol* (2021) 12:621339. doi: 10.3389/fphar.2021.621339

33. Ghosh S, Chowdhury S, Sarkar P, Sil PC. Ameliorative role of ferulic acid against diabetes associated oxidative stress induced spleen damage. *Food Chem Toxicol* (2018) 118:272–86. doi: 10.1016/j.fct.2018.05.029

34. Naudhani M, Thakur K, Ni ZJ, Zhang JG, Wei ZJ. Formononetin reshapes the gut microbiota, prevents progression of obesity and improves host metabolism. *Food Funct* (2021) 12:12303–24. doi: 10.1039/d1fo02942h

35. Ma C, Xia R, Yang S, Liu L, Zhang J, Feng K, et al. Formononetin attenuates atherosclerosis *via* regulating interaction between KLF4 and SRA in apoE(-/-) mice. *Theranostics* (2020) 10:1090–106. doi: 10.7150/thno.38115

36. Oza MJ, Kulkarni YA. Formononetin treatment in type 2 diabetic rats reduces insulin resistance and hyperglycemia. *Front Pharmacol* (2018) 9:739. doi: 10.3389/fphar.2018.00739

37. Xie Q, Gu X, Chen J, Liu M, Xiong F, Wu X, et al. Soyasaponins reduce inflammation and improve serum lipid profiles and glucose homeostasis in high fat diet-induced obese mice. *Mol Nutr Food Res* (2018) 62:e1800205. doi: 10.1002/mnfr.201800205

38. Ren Y, Chen X, Li P, Zhang H, Su C, Zeng Z, et al. Si-Miao-Yong-An decoction ameliorates cardiac function through restoring the equilibrium of SOD and NOX2 in heart failure mice. *Pharmacol Res* (2019) 146:104318. doi: 10.1016/j.phrs.2019.104318

39. Ye Y, Zhang B, Li Y, Xu HD, Liu XM, Huang SM, et al. Yin huo tang, a traditional Chinese herbal formula, relives ovariectomy and empty bottle stimulation-induced menopause-like symptoms in mice. *Front Endocrinol (Lausanne)* (2022) 13:994642. doi: 10.3389/fendo.2022.994642

40. Pan X, Liu Y, Liu L, Pang B, Sun Z, Guan S, et al. Bushen jieyu tiaochong formula reduces apoptosis of granulosa cells *via* the PERK-ATF4-CHOP signaling pathway in a rat model of polycystic ovary syndrome with chronic stress. *J Ethnopharmacol* (2022) 292:114923. doi: 10.1016/j.jep.2021.114923

41. Wang M, Zhao D, Xu L, Guo W, Nie L, Lei Y, et al. Role of PCSK9 in lipid metabolic disorders and ovarian dysfunction in polycystic ovary syndrome. *Metabolism* (2019) 94:47–58. doi: 10.1016/j.metabol.2019.02.002

42. Lai H, Jia X, Yu Q, Zhang C, Qiao J, Guan Y, et al. High-fat diet induces significant metabolic disorders in a mouse model of polycystic ovary syndrome. *Biol Reprod* (2014) 91:127. doi: 10.1095/biolreprod.114.120063

43. Vashistha B, Sharma A, Jain V. Ameliorative potential of ferulic acid in vincristine-induced painful neuropathy in rats: An evidence of behavioral and biochemical examination. *Nutr Neurosci* (2017) 20:60–70. doi: 10.1179/1476830514Y.0000000165

44. Benrick A, Chanclon B, Micallef P, Wu Y, Hadi L, Shelton JM, et al. Adiponectin protects against development of metabolic disturbances in a PCOS mouse model. *Proc Natl Acad Sci U S* (2017) 114:E7187–96. doi: 10.1073/pnas.1708854114

45. Kyei G, Sobhani A, Nekonam S, Shabani M, Ebrahimi F, Qasemi M, et al. Assessing the effect of MitoQ(10) and vitamin D3 on ovarian oxidative stress, steroidogenesis and histomorphology in DHEA induced PCOS mouse model. *Heliyon* (2020) 6:e4279. doi: 10.1016/j.heliyon.2020.e04279

46. Xiao HW, Cui M, Li Y, Dong JL, Zhang SQ, Zhu CC, et al. Gut microbiota-derived indole 3-propionic acid protects against radiation toxicity *via* retaining acyl-CoA-binding protein. *Microbiome* (2020) 8:69. doi: 10.1186/s40168-020-00845-6

47. Zhang SW, Zhou J, Gober HJ, Leung WT, Wang L. Effect and mechanism of berberine against polycystic ovary syndrome. *BioMed Pharmacother* (2021) 138:111468. doi: 10.1016/j.biopha.2021.111468

48. Khorshidi M, Moini A, Alipoor E, Rezvan N, Gorgani-Firuzjaee S, Yaseri M, et al. The effects of quercetin supplementation on metabolic and hormonal parameters as well as plasma concentration and gene expression of resistin in overweight or obese women with polycystic ovary syndrome. *Phytother Res* (2018) 32:2282–89. doi: 10.1002/ptr.6166

49. Wang Z, Nie K, Su H, Tang Y, Wang H, Xu X, et al. Berberine improves ovulation and endometrial receptivity in polycystic ovary syndrome. *Phytomedicine* (2021) 91:153654. doi: 10.1016/j.phymed.2021.153654

50. Hong G, Wu H, Ma ST, Su Z. Catechins from oolong tea improve uterine defects by inhibiting STAT3 signaling in polycystic ovary syndrome mice. *Chin Med* (2020) 15:125. doi: 10.1186/s13020-020-00405-y

51. Mulvihill EE, Assini JM, Lee JK, Allister EM, Sutherland BG, Koppes JB, et al. Nobiletin attenuates VLDL overproduction, dyslipidemia, and atherosclerosis in mice with diet-induced insulin resistance. *Diabetes* (2011) 60:1446–57. doi: 10.2337/db10-0589

52. Gandhi GR, Vasconcelos A, Wu DT, Li HB, Antony PJ, Li H, et al. Citrus flavonoids as promising phytochemicals targeting diabetes and related complications: A systematic review of *In vitro* and *In vivo* studies. *Nutrients* (2020) 12:2907. doi: 10.3390/nu12102907

53. Mulvihill EE, Burke AC, Huff MW. Citrus flavonoids as regulators of lipoprotein metabolism and atherosclerosis. *Annu Rev Nutr* (2016) 36:275–99. doi: 10.1146/annurev-nutr-071715-050718

54. Ushiroyama T, Hosotani T, Mori K, Yamashita Y, Ikeda A, Ueki M. Effects of switching to wen-jing-tang (unkei-to) from preceding herbal preparations selected by eight-principle pattern identification on endocrinological status and ovulatory induction in women with polycystic ovary syndrome. *Am J Chin Med* (2006) 34:177–87. doi: 10.1142/S0192415X06003746

55. Ni Z, Cheng W, Ding J, Yao R, Zhang D, Zhai D, et al. Impact of buzhong yiqi prescription on the gut microbiota of patients with obesity manifesting polycystic ovarian syndrome. *Evid Based Complement Alternat Med* (2021) 2021:6671367. doi: 10.1155/2021/6671367

56. Quaranta G, Sanguinetti M, Masucci L. Fecal microbiota transplantation: A potential tool for treatment of human female reproductive tract diseases. *Front Immunol* (2019) 10:2653. doi: 10.3389/fimmu.2019.02653

57. Liyanage G, Inoue R, Fujitani M, Ishijima T, Shibutani T, Abe K, et al. Effects of soy isoflavones, resistant starch and antibiotics on polycystic ovary syndrome (PCOS)-like features in letrozole-treated rats. *Nutrients* (2021) 13:3759. doi: 10.3390/nu13113759

58. Zeng Q, Li D, He Y, Li Y, Yang Z, Zhao X, et al. Discrepant gut microbiota markers for the classification of obesity-related metabolic abnormalities. *Sci Rep* (2019) 9:13424. doi: 10.1038/s41598-019-49462-w

59. Chu W, Han Q, Xu J, Wang J, Sun Y, Li W, et al. Metagenomic analysis identified microbiome alterations and pathological association between intestinal microbiota and polycystic ovary syndrome. *Fertil Steril* (2020) 113:1286–98. doi: 10.1016/j.fertnstert.2020.01.027

60. Liang Z, Di N, Li L, Yang D. Gut microbiota alterations reveal potential gut-brain axis changes in polycystic ovary syndrome. *J Endocrinol Invest* (2021) 44:1727–37. doi: 10.1007/s40618-020-01481-5

61. Dong S, Jiao J, Jia S, Li G, Zhang W, Yang K, et al. 16S rDNA full-length assembly sequencing technology analysis of intestinal microbiome in polycystic ovary syndrome. *Front Cell Infect Microbiol* (2021) 11:634981. doi: 10.3389/fcimb.2021.634981

62. Senaphan K, Kukongviriyapan U, Sangartit W, Pakdeechote P, Pannangpetch P, Prachaney P, et al. Ferulic acid alleviates changes in a rat model of metabolic syndrome induced by high-carbohydrate, high-fat diet. *Nutrients* (2015) 7:6446–64. doi: 10.3390/nu7085283

63. Song Y, Wu MS, Tao G, Lu MW, Lin J, Huang JQ. Feruloylated oligosaccharides and ferulic acid alter gut microbiome to alleviate diabetic syndrome. *Food Res Int* (2020) 137:109410. doi: 10.1016/j.foodres.2020.109410

64. Ma Y, Chen K, Lv L, Wu S, Guo Z. Ferulic acid ameliorates nonalcoholic fatty liver disease and modulates the gut microbiota composition in high-fat diet fed ApoE(-/-) mice. *BioMed Pharmacother* (2019) 113:108753. doi: 10.1016/j.biopha.2019.108753

Glossary

ANOVA	One-way analysis of variance
BMI	Body mass index
CL	Corpora lutea
DHEA	Dehydroepiandrosterone
FA	Ferulic acid
FBG	Fasting blood glucose
FINS	Fasting insulin
FSH	Follicle stimulating hormone
HDL-C	High densitylipoprotein
HFD	High-fat diet
HOMA-IR	Insulin resistance index in the homeostasis model
IR	Insulin resistance
LC-MS	Liquid chromatography–mass spectrometry
LDA	Linear Discriminant Analysis
LDL-C	Low densitylipoprotein
LEfSe	LDA Effect Size
LH	Luteinizing hormone
NCD	Normal chow diet
NMDS	Non-Metric Multi-Dimensional Scaling
OGTTs	Oral glucose tolerance tests
PCA	Principal Component Analysis
PCoA	Unweighted principal coordinate analysis
PCOS	Polycystic ovary syndrome
PLS-DA	Partial least squares discriminant analysis
T	Testosterone
TC	Total cholesterol
TG	Triglycerides
UPGMA	Unweighted Pair-group Method with Arithmetic Mean
YLTB	Yulin Tong Bu Decoction

frontiers | Frontiers in Endocrinology

TYPE Correction
PUBLISHED 14 April 2023
DOI 10.3389/fendo.2023.1184616

OPEN ACCESS

EDITED BY
Shunfeng Cheng,
Qingdao Agricultural University, China

REVIEWED BY
Wen-Xiang Liu,
Inner Mongolia University, China

*CORRESPONDENCE
Li-Juan Fu
fulijuan@cqmu.edu.cn
Qian Feng
469280497@qq.com

†These authors have contributed equally to this work and share first authorship

SPECIALTY SECTION
This article was submitted to Reproduction, a section of the journal Frontiers in Endocrinology

RECEIVED 12 March 2023
ACCEPTED 04 April 2023
PUBLISHED 14 April 2023

CITATION
Su Y-N, Wang M-J, Yang J-P, Wu X-L, Xia M, Bao M-H, Ding Y-B, Feng Q and Fu L-J (2023) Corrigendum: Effects of Yulin Tong Bu formula on modulating gut microbiota and fecal metabolite interactions in mice with polycystic ovary syndrome.
Front. Endocrinol. 14:1184616.
doi: 10.3389/fendo.2023.1184616

Corrigendum: Effects of Yulin Tong Bu formula on modulating gut microbiota and fecal metabolite interactions in mice with polycystic ovary syndrome

Ya-Nan Su[1,2†], Mei-Jiao Wang[2,3†], Jun-Pu Yang[2], Xiang-Lu Wu[2], Min Xia[4], Mei-Hua Bao[5], Yu-Bin Ding[2], Qian Feng[2,4,6*] and Li-Juan Fu[1,2,5*]

[1]Department of Herbal Medicine, Chongqing Key Laboratory of Traditional Chinese Medicine for Prevention and Cure of Metabolic Diseases, School of traditional Chinese Medicine, Chongqing Medical University, Chongqing, China, [2]Joint International Research Laboratory of Reproduction and Development of the Ministry of Education of China, School of Public Health, Chongqing Medical University, Chongqing, China, [3]Department of Physiology, School of Basic Medicine, Chongqing Medical University, Chongqing, China, [4]Department of Gynecology, Chongqing Hospital of Traditional Chinese Medicine, Chongqing, China, [5]Department of Pharmacology, Academician Workstation, Changsha Medical University, Changsha, China, [6]Department of Obstetrics and Gynecology, Chongqing General Hospital, University of Chinese Academy of Sciences, Chongqing, China

KEYWORDS

polycystic ovary syndrome, YLTB formula, gut microbiota, metabolites, ferulic acid

A Corrigendum on

Effects of Yulin Tong Bu formula on modulating gut microbiota and fecal metabolite interactions in mice with polycystic ovary syndrome

By Su Y-N, Wang M-J, Yang J-P, Wu X-L, Xia M, Bao M-H, Ding Y-B, Feng Q, Fu L-J (2023). *Front. Endocrinol.* 14: 1122709. doi: 10.3389/fendo.2023.1122709

Error in Figure/Table

In the published article, there was an error in Figure 3 as published. We recently found by ourselves that the picture 3-J was misplaced. The corrected Figure 3 and its caption: "The effects of YLTB on glucose tolerance, insulin sensitivity and lipid metabolism in PCOS mice." appear below.

The authors apologize for this error and state that this does not change the scientific conclusions of the article in any way. The original article has been updated.

Text Correction

In the published article, there were three errors. There were two unit errors in the **Materials and methods** section and one spelling error in the **Results** section.

A correction has been made to **2 Materials and methods**, 2.2 Liquid chromatography–mass spectrometry, paragraph three. This sentence previously stated:

"injection volume, 2 ml"

The corrected sentence appears below:

"injection volume, 2 μL"

10.3389/fendo.2023.1184616

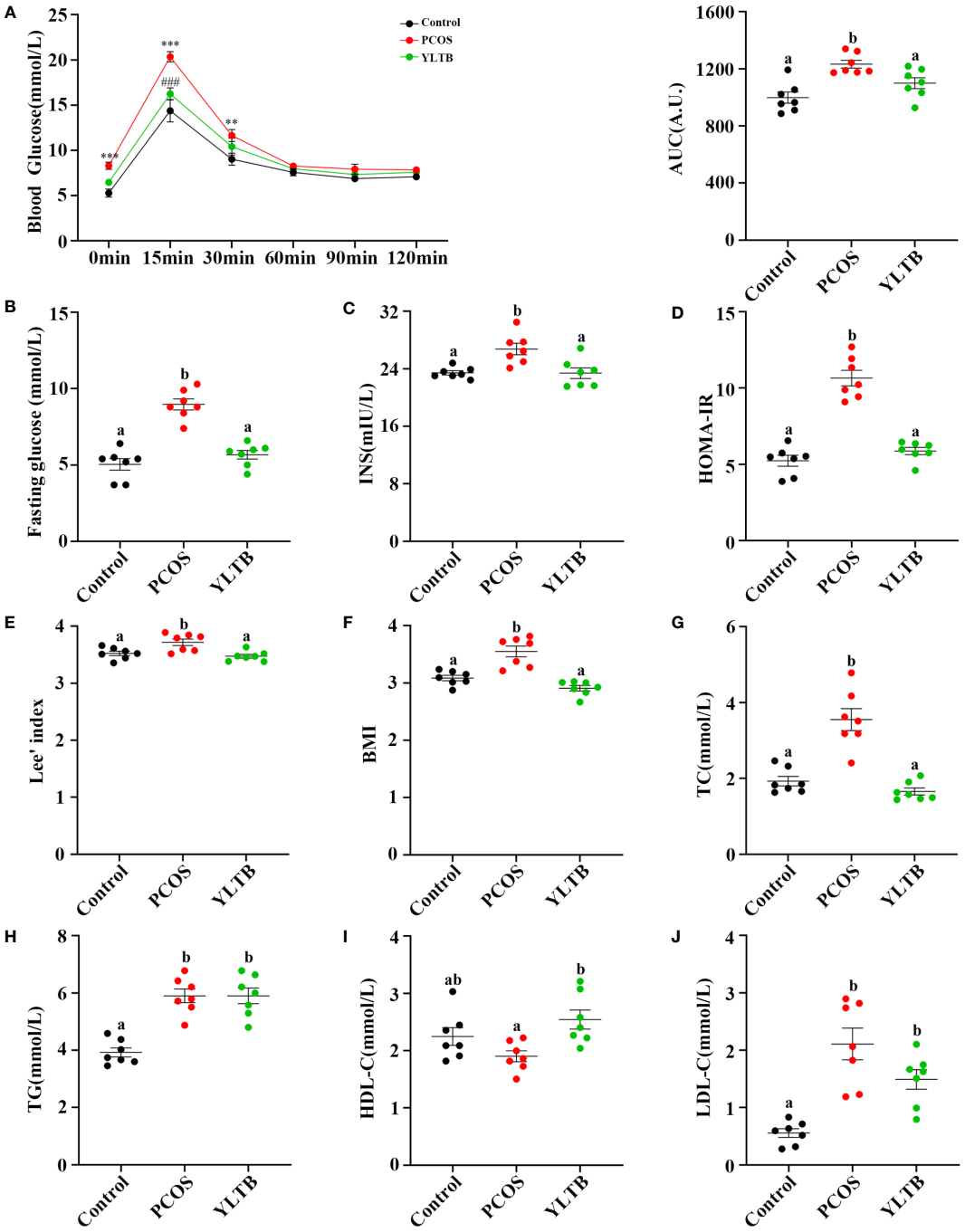

FIGURE 3
The effects of YLTB on glucose tolerance, insulin sensitivity and lipid metabolism in PCOS mice. **(A)** OGTTs in mice from the control, PCOS, and YLTB groups. The corresponding area under the curve (AUC) values of blood glucose levels in each group were calculated (** $P < 0.01$; *** $P < 0.001$ compared with the control group, ### $P < 0.001$ compared with the PCOS group). **(B, C)** Blood glucose and serum insulin level assessment after 12 h of fasting in mice from the control, PCOS, and YLTB (38.68 g·kg^{-1}·day^{-1}) groups. **(D)** The homeostasis model assessment of insulin resistance (HOMA-IR) index = [FBG (mmol/L)] × [FINS (IU/mL)]/22.5 in mice from the control, PCOS, and YLTB groups. **(E, F)** Lee's index = [Body mass (g) × 1,000]$^{1/3}$/body length (cm) and Body mass index (BMI = weight (kg)/height (m^2) calculation. **(G–J)** Detection of TC, TG, HDL-C and LDL-C to evaluate the level of serum lipid metabolism in mice from the control, PCOS, and YLTB groups. n = 7/group, statistical significance was determined using one-way or two-way ANOVA with Tukey's multiple comparisons test, and data are presented as the mean ± SEM. a and b indicate $P < 0.05$; if 2 groups have the same letter, it indicates no statistical significance.

A correction has been made to **2 Materials and methods**, 2.8 16S rRNA sequencing, paragraph four. This sentence previously stated:

"DNA was diluted to 1 ng/L in sterile water according to the concentration."

The corrected sentence appears below:

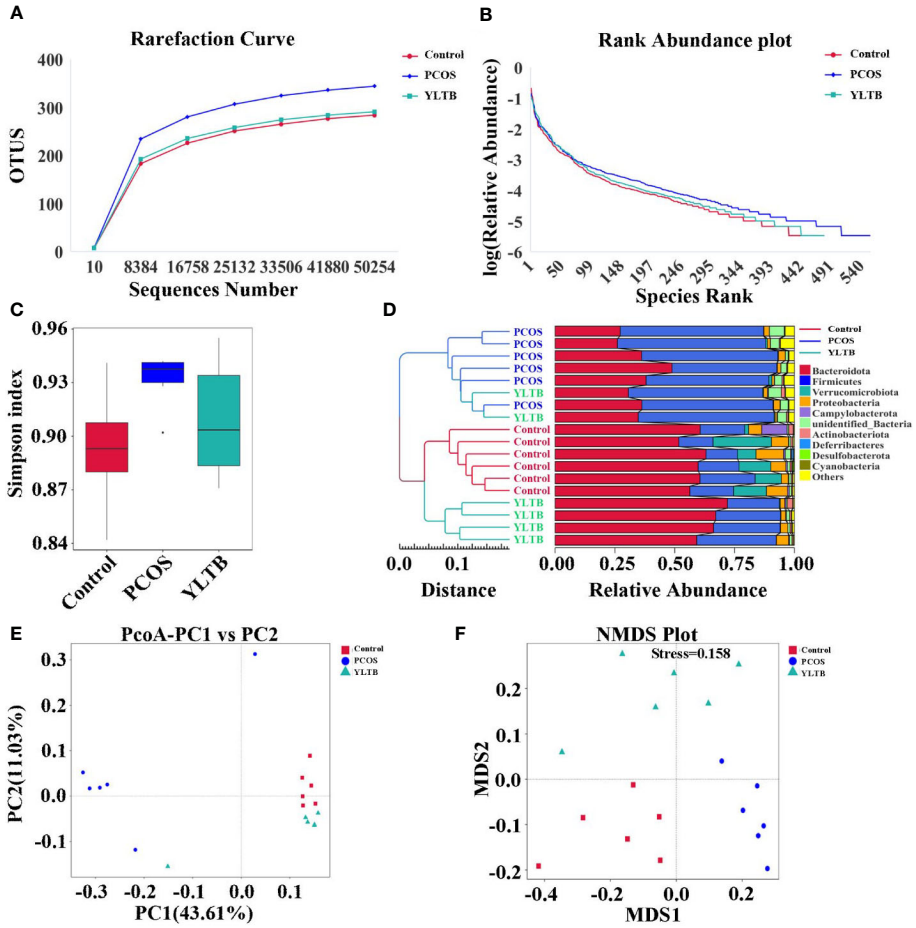

FIGURE 4
Effect of YLTB on α and β diversity of gut microbiota. **(A, B)** Analysis of gut microbial diversity was performed on the basis of 16S rRNA sequencing and was presented by rarefaction curves and rank abundance curves. **(C)** The α-diversity of gut bacterial assemblages with Simpson index in the mice receiving different treatments. **(D)** Evaluation of β-diversity with bacterial community compositional similarity using UPGMA cluster analysis, and the clustering result and the relative abundance of each sample at the phylum level were displayed. The left side is the UPGMA clustering tree structure, and the right side is the relative abundance distribution map of each sample at the phylum level. **(E, F)** Plots of unweighted UniFrac-based PCoA and nonmetric multidimensional scaling (NMDS) based on Bray-Curtis distance. Each point in the graph represents a sample, the distance between points indicates the degree of variation, and the samples of the same group are represented by the same color. n = 6 mice/group.

"DNA was diluted to 1 ng/μL in sterile water according to the concentration."

A correction has been made to **3 Results**, 3.8 Ferulic acid ameliorates glucose and lipid metabolism disorders in PCOS mice, paragraph two. This sentence previously stated:

"the high FA dose significantly increased the HDL-C levels while decreased the TC levels."

The corrected sentence appears below:

"the high FA dose significantly increased the HDL-C levels while decreased the TG levels."

The authors apologize for this error and state that this does not change the scientific conclusions of the article in any way. The original article has been updated.

Error in Figure/Table Legend

In the published article, there was an error in the legend for Figure 4 as published. 16S rRNA was misspelled as 16S rDNA. The corrected legend appears below.

"(A, B) Analysis of gut microbial diversity was performed on the basis of 16S rRNA sequencing and was presented by rarefaction curves and rank abundance curves."

The authors apologize for this error and state that this does not change the scientific conclusions of the article in any way. The original article has been updated.

Incorrect Supplementary Material

In the published article, there were two errors in Supplementary Figure legend. Figure 1 legend, "20 days instead of 21 days." The correct material statement appears below.

"(B, C) DHEA or sesame oil were given to female mice for 20 days."

Figure 2 legend, "FA instead of FC days." The correct material statement appears below.

"(C, D) Estrus cycles of the control, PCOS and FA groups (n = 5/group)."

The authors apologize for this error and state that this does not change the scientific conclusions of the article in any way. The original article has been updated.

Publisher's note

Supplementary material

The Supplementary Material for this article can be found online at: https://www.frontiersin.org/articles/10.3389/fendo.2023.1184616/full#supplementary-material

frontiers | Frontiers in Endocrinology

TYPE Original Research
PUBLISHED 31 March 2023
DOI 10.3389/fendo.2023.1077590

OPEN ACCESS

EDITED BY
Shunfeng Cheng,
Qingdao Agricultural University, China

REVIEWED BY
Saba Tariq,
University of Faisalabad, Pakistan
Jiexue Pan,
Fudan University, China

*CORRESPONDENCE
Ye Tian
tianyesdu@126.com
Xueru Song
tjsongxr@126.com

†These authors have contributed equally to this work

SPECIALTY SECTION
This article was submitted to Reproduction, a section of the journal Frontiers in Endocrinology

RECEIVED 11 November 2022
ACCEPTED 10 March 2023
PUBLISHED 31 March 2023

CITATION
Tian Y, Zhang J, Li M, Shang J, Bai X, Zhang H, Wang Y, Chen H and Song X (2023) Serum fatty acid profiles associated with metabolic risk in women with polycystic ovary syndrome. *Front. Endocrinol.* 14:1077590. doi: 10.3389/fendo.2023.1077590

Serum fatty acid profiles associated with metabolic risk in women with polycystic ovary syndrome

Ye Tian[1,2*†], Jingjing Zhang[3,4†], Mingyue Li[1,2], Jie Shang[1,2], Xiaohong Bai[1,2], Huijuan Zhang[1,2], Yanxia Wang[1,2], Haitao Chen[3,4] and Xueru Song[1,2*]

[1]Department of Gynecology and Obstetrics, Tianjin Medical University General Hospital, Tianjin, China, [2]Tianjin Key Laboratory of Female Reproductive Health and Eugenics, Tianjin Medical University General Hospital, Tianjin, China, [3]School of Public Health (Shenzhen), Sun Yat-sen University, Guangzhou, China, [4]School of Public Health (Shenzhen), Sun Yat-sen University, Shenzhen, China

Purpose: Dyslipidemia is a feature of polycystic ovary syndrome (PCOS) that may augment metabolic disturbances. Serum fatty acids are important biomedical indicators of dyslipidemia. The aim of this study was to determine the distinct serum fatty acids in various PCOS subtypes and their association with metabolic risk in women with PCOS.

Methods: Fatty acids in the serum of 202 women with PCOS were measured using gas chromatography-mass spectrometry. Fatty acids were compared between PCOS subtypes and correlated with glycemic parameters, adipokines, homocysteine, sex hormones, and sex hormone-binding globulin (SHBG).

Results: The levels of total monounsaturated fatty acids (MUFAs) and polyunsaturated fatty acids (PUFAs) in the reproductive subtype of PCOS were lower than those in the metabolic subtype. Docosahexaenoic acid, a PUFA, was associated with higher SHBG after correction for multiple comparisons. Eighteen species of fatty acids emerged as potential biomarkers associated with the metabolic risk factors measured, independent of body mass index (BMI). Among them, myristic acid (C14:0), palmitoleic acid (C16:1), oleic acid (C18:1n-9C), cis-vaccenic acid (C18:1n-7), and homo-gamma-linolenic acid (C20:3n-6) were the strongest lipid species that were consistently associated with metabolic risk factors, particularly insulin-related parameters in women with PCOS. As for adipokines, 16 fatty acids were positively associated with serum leptin. Among them, C16:1 and C20:3n-6were significantly associated with leptin levels.

Conclusion: Our data demonstrated that a distinct fatty acid profile comprising high C14:0, C16:1, C18:1n-9C, C18:1n-7, and C20:3n-6levels is associated with metabolic risk in women with PCOS, independent of BMI.

KEYWORDS

pcos, fatty acid, metabolic risk, PUFA, GC-MS

1 Introduction

Polycystic ovary syndrome (PCOS) is a complex disorder affecting 5%–20% of women of reproductive age worldwide (1). It is characterized by hyperandrogenism (HA; hirsutism, persistent acne, and/or biochemical hyperandrogenemia), ovulatory dysfunction (oligo/anovulation, menstrual irregularity, and infertility), and polycystic ovarian morphology (an excessive number of preantral follicles in the ovaries).PCOS is associated with metabolic abnormalities and possibly with an increased risk of metabolic syndrome, type II diabetes mellitus, and cardiovascular diseases (2).

Dyslipidemia is an increasingly common feature, reported in 41%–70% of women with PCOS (3–5). Increased triglyceride and low-density lipoprotein cholesterol levels and decreased high-density lipoprotein cholesterol(HDL-C) levels are common lipid abnormalities in women with PCOS (6). Dyslipidemia plays an important role in metabolic and endocrine pathways in women with PCOS. Drugs used to reduce the level of cholesterol in PCOS cases could cause a reduction in the levels of total testosterone, free androgen index(FAI)and dehydroepiandrosterone sulfate; however, the certainty of the evidence is low (7).Beyond known risk factors for cardiovascular disease, decreased HDL-C levels and elevated triglyceride levels are also reportedly associated with a lower maturation rate in women with PCOS undergoing *in vitro* maturation (8).

Apart from conventional lipid profiling, including for triglycerides, total cholesterol, low-density lipoprotein cholesterol, and HDL-C, free fatty acids are also important biomedical indicators of dyslipidemia. Fatty acids are efficient substrates for energy production and may directly affect the metabolism of various lipid and glycemic molecules (9, 10). However, the association between fatty acid profiles and metabolic risk in PCOS cases has not been comprehensively explored (11).

The signs and symptoms of PCOS are heterogeneous and can be categorized into several subtypes. Dyslipidemia may differ among subsets of women with PCOS. Lower HDL-C levels may also be related to hyperandrogenemia in lean PCOS patients (12). However, the fatty acid levels in PCOS patients with or without hyperandrogenemia have not been well defined. In addition, Dapas et al. recently performed a clustering analysis in women with PCOS and identified two distinct subtypes: reproductive and metabolic (13). It remains unclear whether these two subtypes have distinct fatty acid profiles.

As a branch of targeted metabolomics, absolute quantification of fatty acids is used to systematically investigate many fatty acids rather than focusing on a single specific fatty acid. In this study, we carried out systematic fatty acid profiling of PCOS cases of various subtypes using gas chromatography-mass spectrometry. We aimed to investigate the distinct fatty acid profiles of different PCOS subtypes and define the associations between fatty acids and metabolic risk factors.

2 Methods

2.1 Patients

This cohort consisted of 202 Han Chinese women with PCOS and 34 women without PCOS, recruited from the Reproductive Center, Tianjin Medical University General Hospital. PCOS was defined using the 2003 Rotterdam PCOS consensus criteria (14), and other related diseases with similar presentations (congenital adrenal hyperplasia, androgen-secreting tumors, Cushing's syndrome, thyroid disease, and hyperprolactinemia) were excluded. PCOS diagnosis requires two of the following criteria: oligo/anovulation (menstrual cycle length >35 days), clinical or biochemical HA(Ferriman-Gallwey score ≥6, severe acne, or total testosterone≥57ng/dL), and polycystic ovarian morphology (at least 12 follicles measuring 2–9 mm in diameter in one ovary and/or increased ovarian volume >10 mL on ultrasound). The inclusion criteria for the control group were as follows: normal menstrual cycles, and neither HA nor polycystic ovaries under ultrasound. Individuals taking medications, such as oral contraceptives and metformin, during the previous 3 months were also excluded. The study was approved by the Ethics Committee of Tianjin Medical University General Hospital, and written informed consent was obtained from all the participants.

2.2 Clinical and biochemical measurement

All participants were assessed for age, height, and weight. Body mass index (BMI) was calculated as weight (kg)/height $(m)^2$. Fasting blood samples were obtained on days 2–4 of the menstrual cycle to examine circulating serum levels of hormones, including follicle-stimulating hormone (FSH), luteinizing hormone (LH), and total testosterone. Serum sex hormone-binding globulin (SHBG)and dehydroepiandrosterone sulfate were measured using a chemiluminescence immunoassay (IMMULITE1000, USA). Insulin levels were also measured using a chemiluminescence immunoassay (ARCHITECT i2000SR, USA), and fasting glucose (Glu0) was measured using the glucose oxidase method (VITROS 5600, USA).The FAI was calculated as follows: testosterone (nmol/L)/ SHBG (nmol/L) × 100. The homeostasis model assessment for insulin resistance (HOMA-IR) was calculated as Glu0 (mmol/L) × fasting insulin (mIU/L)/22.5.

2.3 Enzyme-linked immunosorbent assay

Adiponectin and leptin concentrations were determined using an enzyme-linked immunosorbent assay with specific commercial kits designed for humans (CUSABIO, China). All procedures were performed according to the manufacturer's instructions.

2.4 Metabolite extraction

The serum was pipetted into a 15-mLcentrifuge tube, and 2 mL of 1% sulfuric acid methanol solution was added. Thereafter, esterification was performed in an 80°C water bath for 30 min.After the mixture was removed from the water and cooled,1 mL of n-hexane was added for extraction.The mixture was shaken and mixedfor 30 sand incubated upright at room temperaturefor 5 min.Subsequently,5 mL of H_2O (4°C) was added for washing, and the mixture was centrifuged at 3500 rpm at 4°C for 10 min.The supernatant (700 µL) was carefully transferred to a 2-ml centrifuge tube, and 100 mg of anhydrous sodium sulfate powder was added to remove excess water. The mixture was shaken and mixed for 30 s and centrifuged at 12000 rpm for 5 min. The supernatant (200 µL) was carefully transferred to a 2-mL centrifuge tube, and 200 mL of n-hexane was added. Further, 300µL of the diluent was carefully transferred to a 2-mL centrifuge tube and 15 ml of 500 ppm methyl salicylate was added as an internal standard. The mixture was shaken and mixed for 10s, and 200 µL supernatant was accurately absorbed in the detection bottle.

2.5 Gas chromatography-mass spectrometry method

A gas chromatograph coupled to a mass spectrometry system (Thermo Trace 1310 GC-Thermo ISQ 7000, Thermo-Fisher Scientific Corp., FairLawn, NJ, USA) was used to quantify fatty acids at Novogene Co., Ltd. (Beijing, China). The system utilized a Thermo TG-Fame capillary column (50 m×0.25 mm, internal diameter = 0.20 µm). A 1 µL aliquot of the sample was injected into the system. Helium was used as the carrier gas, and the gas flow rate through the column was 0.63 mL/min. The initial temperature was maintained at 80°C for 1min, raised to 160°C at a rate of 20°C/min, and maintained for 1.5 min. Thereafter, it was increased to 196°C at a rate of 3°C/min and maintained for 8.5 min. Finally, it was raised to 250°C at a rate of 20°C/min and maintained for 1.5 min. The mass spectrometer was operated in the single-ion monitoring mode. The energy in the electron impact ion source was 70 eV.

2.6 Clustering

Clustering was performed for 202 PCOS cases on eight quantitative traits: BMI, total testosterone, dehydroepiandrosterone sulfate, fasting insulin (Ins0), Glu0, SHBG, LH, and FSH, according to a previous publication (13). Briefly, quantitative trait values were normalized and clustered using unsupervised, agglomerative, and hierarchical clustering according to Ward's minimum variance method on Manhattan distances between trait values. The Complex Heatmap software package was used to visualize the distributions of clustering of PCOS cases with different quantitative trait levels.

2.7 Statistical analysis

Quantitative variables of clinical characteristics of PCOS subjects are displayed as the mean ± standard error. Values for each fatty acid were $\log_{10}$ transformed because most had a naturally skewed distribution. Fatty acid classes, including saturated fatty acids (SFAs), monounsaturated fatty acids (MUFAs), polyunsaturated fatty acids (PUFAs), and trans fatty acids (TFAs), were generated by summing the individual fatty acid concentrations that make up each class. Statistical analysis was performed using IBM SPSS version22.0 for Windows (IBM Corp., Armonk, NY, USA) or R software (4.0.5). Normality was assessed using the Kolmogorov–Smirnov test. Differences between the PCOS and control groups or two PCOS subgroups were assessed using individual sample t-tests for normal distributions or Mann–Whitney U tests for non-normal distributions. Univariate and multivariable linear regressions were used to determine associations between fatty acids and the outcomes of interest, and age and BMI were used as covariates in the analysis. We corrected for the false discovery rate (FDR) by using the Benjamini–Hochberg method, and statistical significance was set at $P<0.05$.

3 Results

3.1 Characteristics of the patients

The anthropometric, clinical, and biochemical characteristics of the 202 PCOS patients are shown in Table 1. The mean age of the PCOS subjects was 30.78years, and the mean BMI was 25.08 kg/m^2. For PCOS-related endocrine parameters, the cases had a significantly higher total testosterone level, LH level, FAI, and anti-Müllerian hormone level(all $P<0.01$) than controls. Except for higher leptin levels in women with PCOS, there were no differences in other metabolic characteristics between BMI-matched women with and without PCOS, including fasting blood glucose, fasting serum insulin, HOMA-IR, and adiponectin levels (all $P>0.05$). Fatty acid components significantly differed between women with and without PCOS after adjusting for age. The levels of total MUFAs and PUFAs in the PCOS group were markedly lower, whereas those of SFAs and TFAs were significantly higher in the PCOS group than those in the control group (Table 1).

3.2 Serum fatty acids in PCOS subtypes

In women with PCOS with or without the HA subtype, the levels of serum fatty acids were similar after adjusting for age and BMI (Table 2). Clustering was performed for the 202 PCOS cases (Figure 1). Clustering revealed two distinct phenotypic subtypes: the

10.3389/fendo.2023.1077590

TABLE 1 Characteristics of PCOS cases and controls.

	PCOS (n=202)	Controls (n=34)	*P*
Age (years)	30.78 ± 3.66	31.94 ± 3.56	0.042
BMI (kg/m^2)	25.08 ± 4.66	23.73 ± 4.26	0.117
Follicle-stimulating hormone (IU/L)	5.22 ± 1.45	6.14 ± 2.29	0.055
Luteinizing hormone (IU/L)	7.12 ± 4.49	3.97 ± 2.16	<0.001
Total testosterone (ng/dL)	46.86 ± 17.95	24.18 ± 8.03	<0.001
Sex hormone-binding globulin(nmol/L)	57.46 ± 60.56	44.67 ± 28.89	0.811
Free androgen index	5.40 ± 4.73	2.69 ± 1.98	0.002
Anti-Müllerian hormone (ng/mL)	8.25 ± 5.34	2.13 ± 0.87	<0.001
Fasting glucose (mmol/L)	5.26 ± 1.34	4.94 ± 0.59	0.086
Fasting insulin(mIU/L)	13.69 ± 8.82	12.04 ± 7.27	0.327
HOMA-IR	3.32 ± 2.64	2.73 ± 1.89	0.187
Leptin (ng/mL)	34.88 ± 14.06	22.41 ± 14.57	<0.001
Adiponectin (μg/mL)	33.79 ± 15.40	38.96 ± 13.53	0.082
Log_{10}total SFAs (μg/mL)	3.17 ± 0.10	3.06 ± 0.12	<0.001
Log_{10}total MUFAs (μg/mL)	2.48 ± 0.18	2.68 ± 0.17	<0.001
Log_{10}total TFAs (μg/mL)	1.77 ± 0.26	1.70 ± 0.13	0.008
Log_{10}total PUFAs (μg/mL)	2.57 ± 0.16	2.71 ± 0.19	<0.001

PCOS, polycystic ovary syndrome; BMI, body mass index; HOMA-IR, homeostasis model assessment for insulin resistance; SFAs, saturated fatty acids; MUFAs, monounsaturated fatty acids; PUFAs, polyunsaturated fatty acids; TFAs, trans fatty acids.

reproductive subtype (n=55, higher LH and SHBG levels with relatively low BMI and Ins0 levels) and the metabolic subtype (n=65, higher BMI and Glu0 and Ins0 levels with relatively low SHBG and LH levels).The remaining cases showed no distinguishable patterns after clustering. The levels of total MUFAs and PUFAs in the reproductive subtype of PCOS were lower than those in the metabolic subtype (Table 2).

3.3 Associations between serum fatty acid and sex hormone concentrations

The associations of fatty acids with FSH, LH, total testosterone, FAI, SHBG, and anti-Müllerian hormone are shown in Supplementary Table 1. Docosahexaenoic acid (DHA, C22:6N3), which belongs to the PUFA class, was associated with higher SHBG

TABLE 2 Distributions of serum fatty acids in various PCOS subtypes.

	HA subtype (n=50)	Non-HA subtype (n=144)	*P*	*P*-adj[a]	Reproductive subtypes (n=55)	Metabolic subtypes (n=65)	*P*	*P*-adj[b]
Age (years)	30.32 ± 4.2	30.89 ± 3.4	0.343	–	30.65 ± 3.5	30.42 ± 3.9	0.726	–
BMI (kg/m^2)	26.24 ± 5.7	24.69 ± 4.2	0.043	–	23.46 ± 3.7	24.35 ± 4.2	0.277	–
Log_{10}total SFAs (μg/mL)	3.19 ± 0.11	3.16 ± 0.10	0.074	0.087	3.16 ± 0.10	3.17 ± 0.11	0.713	0.715
Log_{10}total MUFAs (μg/mL)	2.51 ± 0.18	2.47 ± 0.17	0.099	0.154	2.42 ± 0.14	2.49 ± 0.15	0.016	0.018
Log_{10}total TFAs (μg/mL)	1.78 ± 0.25	1.78 ± 0.30	0.997	0.924	1.74 ± 0.23	1.79 ± 0.21	0.282	0.287
Log_{10}total PUFAs (μg/mL)	2.60 ± 0.15	2.56 ± 0.16	0.143	0.166	2.52 ± 0.15	2.59 ± 0.15	0.009	0.012
Log_{10}n-3 PUFA (μg/mL)	1.61 ± 0.15	1.57 ± 0.17	0.152	0.139	1.54 ± 0.16	1.60 ± 0.16	0.027	0.029
Log_{10}n-6 PUFA (μg/mL)	2.51 ± 0.16	2.55 ± 0.15	0.146	0.174	2.47 ± 0.16	2.55 ± 0.15	0.009	0.012

PCOS, polycystic ovary syndrome; HA, hyperandrogenism; P-adj[a], Padjusted by age and BMI; P-adj[b], Padjusted by age; SFAs, saturated fatty acids; MUFAs, monounsaturated fatty acids; PUFAs, polyunsaturated fatty acids; TFAs, trans fatty acids.

levels after FDR correction (P<0.05). Mild correlations were observed between some fatty acids and FSH or FAI; however, none of these correlations were significant after correction for multiple comparisons. In addition, no significant associations were detected between a single fatty acid and LH, total testosterone, or anti-Müllerian hormone levels.

3.4 Associations between serum fatty acids and metabolic parameters

Associations of fatty acids with Glu0, 2-h glucose,Ins0, HOMA-IR, leptin, adiponectin, and homocysteine are shown in Supplementary Table 2 and Figure 2. No significant associations were observed with Glu0, but 2-hour glucose after the 75-g oral glucose tolerance test was positively associated with myristic acid (C14:0),palmitoleic acid (C16:1),oleic acid (C18:1n-9C),cis-vaccenic acid (C18:1n-7), and homo-gamma-linolenic acid (C20:3n-6), all of which was significant after FDR correction(P<0.05).After adjustment for age and BMI, the associations between the five types of fatty acid and 2-hour glucose were still significant. In total, 18 fatty acid species were significantly associated with Ins0 levels (FDR-corrected P<0.05). Most notably, six fatty acids, that is, myristic acid (C14:0), hexadecanoic acid (C16:0), palmitoleic acid(C16:1),oleic acid (C18:1n-9C), cis-vaccenic acid (C18:1n-7), and homo-gamma-linolenic acid (C20:3n-6),emerged as the lipid biomarkers most strongly associated with Ins0 (FDR-corrected P<0.001).Consistently, 12 species of fatty acids were significantly associated with HOMA-IR; the strongest associations were with myristic acid (C14:0), palmitoleic acid(C16:1), oleic acid (C18:1n-9C), cis-vaccenic acid(C18:1n-7), and homo-gamma-linolenic acid(C20:3n-6)after adjustment for age and BMI (FDR-corrected P<0.001).

As for adipokines, 16 fatty acids were positively associated with serum leptin using multiple longitudinal models, even after adjustment for age (FDR-corrected P<0.05). Among them, palmitoleic acid (C16:1) and homo-gamma-linolenic acid (C20:3n-6) were most significantly associated with the level of leptin (FDR-corrected P<0.001). However, no significant correlations were detected between fatty acids and adiponectin or homocysteine levels after correction for multiple comparisons (FDR-corrected P>0.05).

4 Discussion

In the present study, we performed absolute quantification of 51 fatty acids in the serum and found that the reproductive subtype of PCOS cases has a distinct fatty acid profile compared to the metabolic subtype. Specific fatty acids, including myristic acid (C14:0),palmitoleic acid (C16:1),oleic acid (C18:1n-9C),cis-vaccenic acid (C18:1n-7), and homo-gamma-linolenic acid (C20:3n-6) were associated with metabolic risk factors, including 2-hour glucose, Ins0, and HOMA-IR, in PCOS patients, independent of BMI.

In a previous study, lipidomic analysis of plasma samples identified differences in lipidomic profiles in women with PCOS at different stages of the menstrual cycle (15); however, the results were inconsistent with those of other studies (16, 17), partly owing to the recruited PCOS populations and characteristics. In this study, we found that the levels of total MUFAs and PUFAs in the PCOS group were lower than those in the control group, whereas the levels of SFAs and TFAs were higher in the PCOS group. Consistent with our study, Li et al. and Lu et al. found that PCOS patients had decreased PUFA levels and increased levels of SFAs in serum compared to lean controls (18, 19). In the subcutaneous adipose tissue of pregnant women with PCOS, the level of total PUFAs was lower, while that of total MUFAs was higher than that in non-PCOS women.

The lipid profile was significantly more disordered in the full-blown PCOS group (oligo/anovulation+HA+ polycystic ovaries) with

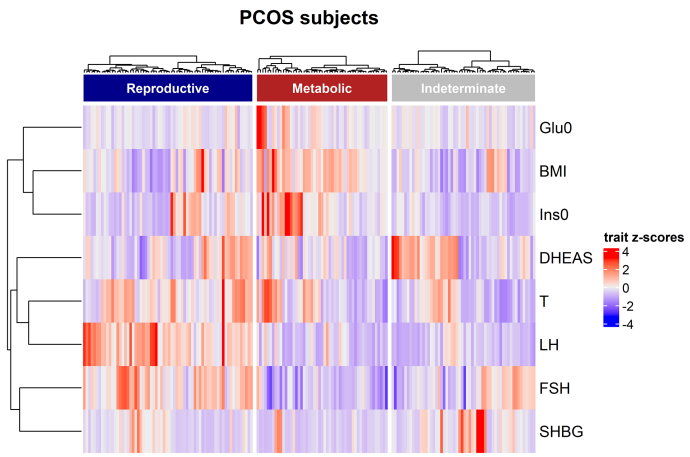

FIGURE 1
Hierarchical clustering of genotyped PCOS clustering cohort. The three clusters are shown as dark blue, dark red, and grey color bars. Heatmap colors correspond with the trait Z-scores, as shown to the right side, in which red implies high values and blue indicates low values for each trait. The trait-based dendrogram represents relative distances between the trait distributions and was calculated using the same approach as that for the subject-based clustering.

10.3389/fendo.2023.1077590

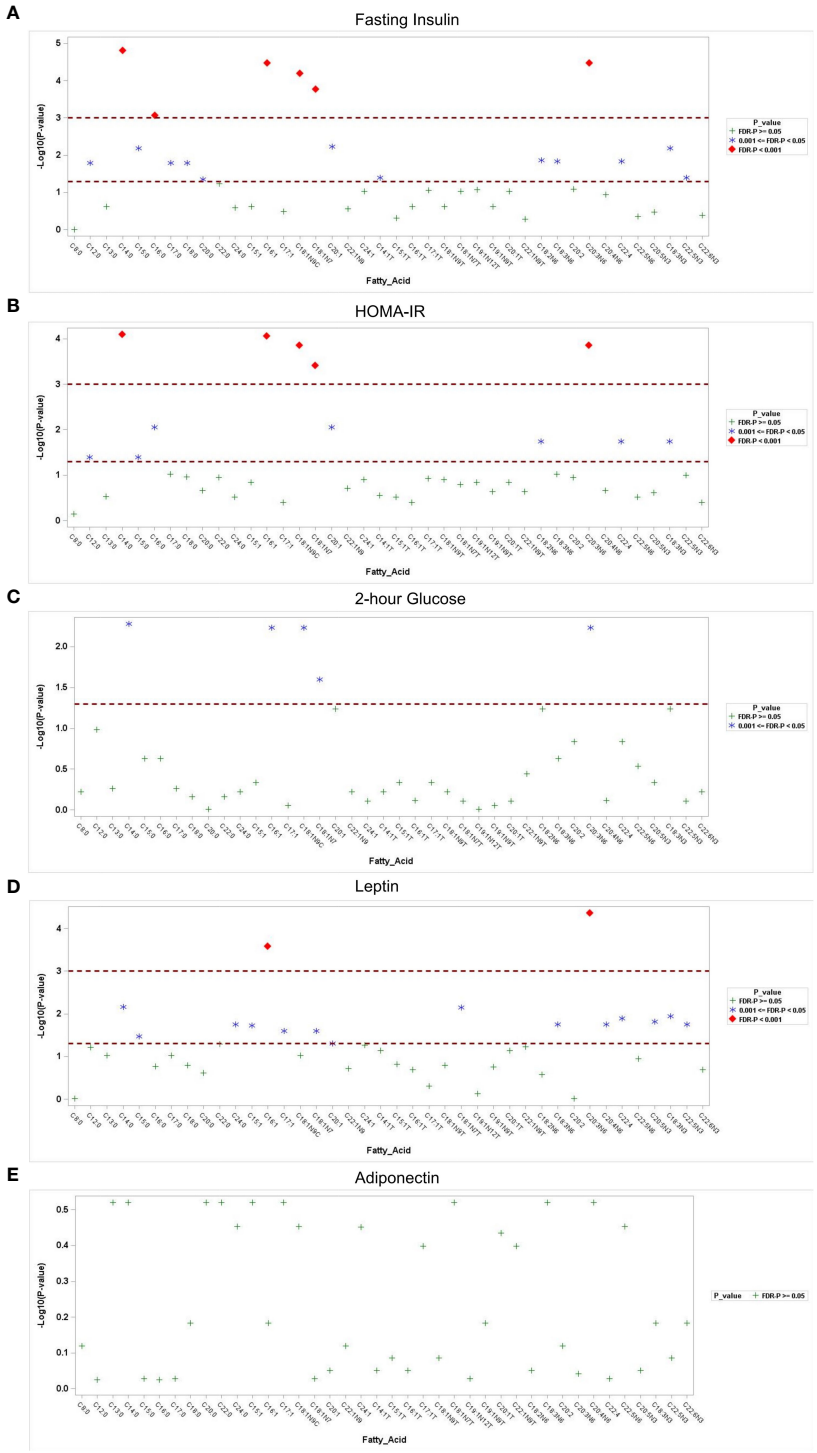

FIGURE 2
Association of fatty acids with metabolic parameters. Manhattan plots of the -log$_{10}$p-value for the fasting insulin **(A)**, HOMA-IR **(B)**, 2-hour glucose **(C)**, serum leptin **(D)** and adiponectin **(E)** regressed on log-transformed fatty acids. Each y-axis represents the-log$_{10}$p-value for each respective model, and each x-axis represents the serum fatty acid. Serumfatty acids with Benjamini–Hochberg false discovery rate-corrected *p*-values <0.05 and *p*-values <0.001 are separated.

higher low-density lipoprotein cholesterol and total cholesterol and lower HDL values than the non-HA PCOS group (oligo/anovulation +polycystic ovaries) (20). However, the fatty acid profiles of women with HA and non-HA PCOS remain unclear. In the present study, no significant differences in the levels of SFAs, TFAs, MUFAs, or PUFAs were found between women with PCOS with and without HA after adjustment for age and BMI. Recently, two distinct subtypes (reproductive and metabolic) have been identified in women with PCOS (13). We found that the total MUFAs and PUFAs in the reproductive subtype of PCOS cases were even lower than those in

the metabolic subtype, indicating that a unique fatty acid profile was associated with each of the PCOS subtypes. The subtypes of PCOS were generated by cluster analysis of eight quantitative hormonal and glycemic parameters, and it is possible that the addition of lipid parameters may optimize clustering.

Lower SHBG levels are usually used as an indicator of HA in women with PCOS, considering its binding to androgens. In addition, a low serum SHBG level is related to insulin resistance (IR) and, hence, is considered an indicator of abnormal metabolism (21). Here, we report a positive association between SHBG and DHA in women with PCOS. However, other fatty acids were not significantly associated with SHBG after correction for multiple comparisons. Consistent with our study, Mousa et al. found that lower DHA concentrations were associated with lower SHBG and higher adiposity, IR, Ins0, and FAI (17). Lu et al. found that serum DHA levels were positively correlated with FSH and SHBG but negatively correlated with Ins0andtotal testosterone (19). In addition, DHA is one of the most well-known omega-3 PUFAs (n-3 PUFAs), and several studies have evaluated the changes in hormones in women with PCOS after supplementation with n-3PUFA; however, the results have been mixed. Increased dietary PUFA intake can exert positive metabolic and endocrine effects in women with PCOS; however, there is no change in SHBG level (22). Conversely, according to a meta-analysis, PCOS patients with n-3 PUFA supplementation had an increase in serum SHBG (0.68 mg/dL; 95% confidence interval:0.06 to 1.31 mg/dL) (23). The functional mechanism by which DHA regulates SHBG levels is unclear. PUFAs are ligands of peroxisome proliferator-activated receptors (PPARs), and the human SHBG promoter contains a PPAR-response element. Thus, DHA may regulate SHBG levels through PPARs (24). Importantly, administration of the PPAR agonist, rosiglitazone, to women with PCOS increases their serum SHBG levels (25).

IR is a key pathophysiological feature of PCOS and is likely to contribute to dyslipidemia. Lipolysis mainly occurs in the adipose tissue and an enlarged adipose tissue mass can release more free fatty acids. In patients with IR, the rate of lipolysis is higher, leading to an increase in fatty acid delivery to the liver and muscle, and the oxidation of fatty acids is compromised (26). Increased levels of free fatty acids have deleterious effects and further contribute to IR, considering that ectopic triglyceride accumulation in the liver and skeletal muscle triggers pathways that impair insulin signaling (27). The underlying mechanisms of free fatty acid-induced IR are as follows: activation of serine/threonine kinases, reduced tyrosine phosphorylation of the insulin receptor substrate (IRS1/2), and impairment of the IRS/PI3K pathway (28). Free fatty acids can lead to the generation of reactive oxygen species and act as modulators of the NLRP3 inflammasome, which may play an important role in IR (29, 30). In our study, the serum fatty acid profiles indicated dramatically increased levels of 12 fatty acids in PCOS patients in the IR group compared to those in the non-IR group, irrespective of obesity. Most notably, five fatty acids were strongly related to IR (FDR-corrected $P<0.001$), including myristic acid, palmitoleic acid, oleic acid, cis-vaccenic acid, and homo-gamma-linolenic acid. Moreover, we also found that these five fatty acids were significantly correlated with 2-hour glucose and Ins0 levels, which indicated that they were potential lipid biomarkers for metabolic risk in PCOS patients. Our findings are similar to those of Holte et al., who found that the concentrations of total free fatty acids were closely associated with lower insulin sensitivity and lower glucose tolerance in women with PCOS (31); however, they only focused on the total rather than each specific fatty acid. Niu et al. also studied the total free fatty acid content and found a weak correlation between total fatty acid levels in follicular fluid and IR in lean PCOS patients (32).

Previous studies have shown the levels of myristic acid, palmitoleic acid, and oleic acid to be higher in women with PCOS, with conflicting results (33–35). In another study, *de novo* fatty acid synthesis of myristic acid, palmitoleic acid, and oleic acid in subcutaneous adipose stem cells of normal-weight PCOS patients was increased compared to that in controls (36). According to a serum metabolomics study of 20 women with PCOS, myristic acid and palmitoleic acid levels were significantly higher in IR PCOS patients than in non-IR PCOS patients (33). In contrast, another research group reported that palmitoleic acid and oleic acid, but not myristic acid, were strongly associated with IR in girls with PCOS (37). It is unclear why studies on women with PCOS have yielded conflicting results, but this may be due, in part, to the small number of PCOS cases in the studies. In addition, differences in patient characteristics and lipid extraction and analysis methods were observed. To our knowledge, few studies have explored the role of cis-vaccenic acid and homo-gamma-linolenic acid in PCOS (38). Our data, for the first time, showed that both cis-vaccenic acid and homo-gamma-linolenic acid were associated with IR in a relatively large cohort of PCOS patients, emphasizing the need for further studies to clearly define the role of these two fatty acids in PCOS and determine the functional mechanism underlying the actions of insulin.

Leptin and adiponectin, which are adipokines secreted by adipocytes, have a profound influence on insulin sensitivity (39). Women with PCOS present with adipokine alterations, such as increased leptin levels and decreased adiponectin levels. Fatty acid concentration is an important factor that can influence adipokines (40). PCOS patients with a higher n-3 PUFA intake have may have increased serum adiponectin and reduced leptin concentrations; however, the results have been mixed (41). In this study, 16 fatty acids were positively associated with serum leptin, the most significant of which were palmitoleic acid and homo-gamma-linolenic acid. We speculate that these two fatty acids play an important role in IR through leptin-related mechanisms. Previously, homo-gamma-linolenic acid was found to be positively associated with plasma leptin throughout pregnancy in a prospective study of 201 pregnant women (42). The mechanism by which these two fatty acids might affect the level of leptin is unclear, and thus, further study is needed to understand how they contribute to the biology of PCOS.

5 Conclusion

In summary, we report that two distinct reproductive and metabolic subtypes of women with PCOS have unique fatty acid profiles. Our data demonstrated thata distinct fatty acid signature comprising high levels of myristic acid (C14:0),palmitoleic acid (C16:1),oleic acid (C18:1n-9C),cis-vaccenic acid (C18:1n-7), and homo-gamma-linolenic acid (C20:3n-6) is particularly associated with insulin-related metabolic risk in women with PCOS, independent of BMI. Additionally, DHA was positively associated with SHBG levels. Although the underlying mechanisms are not fully understood, our findings provide new evidence supporting the important role of these fatty acids in PCOS. Further studies are needed to verify these findings in larger cohorts of PCOS patients.

Data availability statement

The original contributions presented in the study are included in the article/Supplementary Material. Further inquiries can be directed to the corresponding authors.

Ethics statement

The studies involving human participants were reviewed and approved by Institutional Review Board of Tianjin Medical University General Hospital. The patients/participants provided their written informed consent to participate in this study.

Author contributions

YT and XS designed and provided support during the study. ML, HZ, YW, and XS collected all the clinical data and blood samples. ML and JS performed the experiments. YT, JZ, and HC analyzed the data. YT drafted the manuscript. XB and XS revised the article. All authors contributed to the article and approved the submitted version.

Funding

This research was supported by the National Natural Science Foundation of China (82171625, 81701410); the Natural Science Foundation of Tianjin (20JCQNJC00470); and Beijing-Tianjin-Hebei Basic Research Cooperation Program (19JCZDJC65000(Z), 19JCZDJC65000). This research was funded by the Tianjin Key Medical Discipline (Specialty) Construction Project (TJYXZDXK-031A).

Acknowledgments

We especially thank all the participants in this study. We would like to thank Editage (www.editage.com) for English language editing.

Conflict of interest

The authors declare that the research was conducted in the absence of any commercial or financial relationships that could be construed as a potential conflict of interest.

Publisher's note

Supplementary material

The Supplementary Material for this article can be found online at: https://www.frontiersin.org/articles/10.3389/fendo.2023.1077590/full#supplementary-material

References

1. Azziz R, Carmina E, Chen Z, Dunaif A, Laven JS, Legro RS, et al. Polycystic ovary syndrome. *Nat Rev Dis Primers* (2016) 2:16057. doi: 10.1038/nrdp.2016.57

2. McCartney CR, Marshall JC. CLINICAL PRACTICE. polycystic ovary syndrome. *N Engl J Med* (2016) 375:54–64. doi: 10.1056/NEJMcp1514916

3. Legro RS, Kunselman AR, Dunaif A. Prevalence and predictors of dyslipidemia in women with polycystic ovary syndrome. *Am J Med* (2001) 111:607–13. doi: 10.1016/S0002-9343(01)00948-2

4. Li R, Zhang Q, Yang D, Li S, Lu S, Wu X, et al. Prevalence of polycystic ovary syndrome in women in China: A large community-based study. *Hum Reprod* (2013) 28:2562–9. doi: 10.1093/humrep/det262

5. Luo X, Cai WY, Wu XK. Prevalence, pattern and predictors for dyslipidemia of Chinese women with polycystic ovary syndrome. *Front Cardiovasc Med* (2021) 8:790454. doi: 10.3389/fcvm.2021.790454

6. Wild RA, Rizzo M, Clifton S, Carmina E. Lipid levels in polycystic ovary syndrome: Systematic review and meta-analysis. *Fertil Steril* (2011) 95:1073–9.e1-11. doi: 10.1016/j.fertnstert.2010.12.027

7. Shawish MI, Bagheri B, Musini VM, Adams SP, Wright JM. Effect of atorvastatin on testosterone levels. *Cochrane Database Syst Rev* (2021) 1:CD013211. doi: 10.1002/14651858.CD013211.pub2

8. Liu T, Liu D, Song X, Qu J, Zheng X, Li J, et al. Lipid metabolism was associated with oocyte in vitro maturation in women with polycystic ovarian syndrome undergoing unstimulated natural cycle. *Front Cell Dev Biol* (2021) 9:719173. doi: 10.3389/fcell.2021.719173

9. Imamura F, Micha R, Wu JH, de Oliveira Otto MC, Otite FO, Abioye AI, et al. Effects of saturated fat, polyunsaturated fat, monounsaturated fat, and carbohydrate on glucose-insulin homeostasis: Asystematic review and meta-analysis of randomised controlled feeding trials. *PloS Med* (2016) 13:e1002087. doi: 10.1371/journal.pmed.1002087

10. Pickens CA, Sordillo LM, Zhang C, Fenton JI. Obesity is positively associated with arachidonic acid-derived 5- and 11-hydroxyeicosatetraenoic acid (HETE). *Metabolism* (2017) 70:177–91. doi: 10.1016/j.metabol.2017.01.034

11. Yu Y, Tan P, Zhuang Z, Wang Z, Zhu L, Qiu R, et al. Untargeted metabolomic approach to study the serum metabolites in women with polycystic ovary syndrome. *BMC Med Genomics* (2021) 14:206. doi: 10.1186/s12920-021-01058-y

12. Spałkowska M, Mrozińska S, Gałuszka-Bednarczyk A, Gosztyła K, Przywara A, Guzik J, et al. The PCOS patients differ in lipid profile according to their phenotypes. *Exp Clin Endocrinol Diabetes* (2018) 126:437–44. doi: 10.1055/s-0043-121264

13. Dapas M, Lin FTJ, Nadkarni GN, Sisk R, Legro RS, Urbanek M, et al. Distinct subtypes of polycystic ovary syndrome with novel genetic associations: an unsupervised, phenotypic clustering analysis. *PloS Med* (2020) 17:e1003132. doi: 10.1371/journal.pmed.1003132

14. Rotterdam ESHRE/ASRM-Sponsored PCOS consensus working group. Revised 2003 consensus on diagnostic criteria and long-term health risks related to polycystic ovary syndrome (PCOS). *Hum Reprod* (2004) 19:41–7. doi: 10.1093/humrep/deh098

15. Haoula Z, Ravipati S, Stekel DJ, Ortori CA, Hodgman C, Daykin C, et al. Lipidomic analysis of plasma samples from women with polycystic ovary syndrome. *Metabolomics* (2015) 11:657–66. doi: 10.1007/s11306-014-0726-y

16. Moran LJ, Mundra PA, Teede HJ, Meikle PJ. The association of the lipidomic profile with features of polycystic ovary syndrome. *J Mol Endocrinol* (2017) 59:93–104. doi: 10.1530/JME-17-0023

17. Mousa A, Huynh K, Ellery SJ, Strauss BJ, Joham AE, de Courten B, et al. Novel lipidomic signature associated with metabolic risk in women with and without polycystic ovary syndrome. *J Clin Endocrinol Metab* (2022) 107:e1987–99. doi: 10.1210/clinem/dgab931

18. Li S, Chu Q, Ma J, Sun Y, Tao T, Huang R, et al. Discovery of novel lipid profiles in PCOS: do insulin and androgen oppositely regulate bioactive lipid production? *J Clin Endocrinol Metab* (2017) 102:810–21. doi: 10.1210/jc.2016-2692

19. Lu L, Li X, Lv L, Xu Y, Wu B, Huang C. Dietary and serum n-3 PUFA and polycystic ovary syndrome: a matched case-control study. *Br J Nutr* (2022) 128:114–23. doi: 10.1017/S0007114521003007

20. Sachdeva G, Gainder S, Suri V, Sachdeva N, Chopra S. Comparison of the different PCOS phenotypes based on clinical metabolic, and hormonal profile, and their response to clomiphene. *Indian J Endocrinol Metab* (2019) 23:326–31. doi: 10.4103/ijem.IJEM_30_19

21. Zhu JL, Chen Z, Feng WJ, Long SL, Mo ZC. Sex hormone-binding globulin and polycystic ovary syndrome. *Clin Chim Acta* (2019) 499:142–8. doi: 10.1016/j.cca.2019.09.010

22. Kasim-Karakas SE, Almario RU, Gregory L, Wong R, Todd H, Lasley BL. Metabolic and endocrine effects of a polyunsaturated fatty acid-rich diet in polycystic ovary syndrome. *J Clin Endocrinol Metab* (2004) 89:615–20. doi: 10.1210/jc.2003-030666

23. Yuan J, Wen X, Jia M. Efficacy of omega-3 polyunsaturated fatty acids on hormones, oxidative stress, and inflammatory parameters among polycystic ovary syndrome: A systematic review and meta-analysis. *Ann Palliat Med* (2021) 10:8991–9001. doi: 10.21037/apm-21-2018

24. Selva DM, Hammond GL. Peroxisome-proliferator receptor gamma represses hepatic sex hormone-binding globulin expression. *Endocrinology* (2009) 150:2183–9. doi: 10.1210/en.2008-1289

25. Sepilian V, Nagamani M. Effects of rosiglitazone in obese women with polycystic ovary syndrome and severe insulin resistance. *J Clin Endocrinol Metab* (2005) 90:60–5. doi: 10.1210/jc.2004-1376

26. Delarue J, Magnan C. Free fatty acids and insulin resistance. *Curr Opin Clin Nutr Metab Care* (2007) 10:142–8. doi: 10.1097/MCO.0b013e328042ba90

27. Samuel VT, Shulman GI. The pathogenesis of insulin resistance: Integrating signaling pathways and substrate flux. *J Clin Invest* (2016) 126:12–22. doi: 10.1172/JCI77812

28. Ghosh A, Gao L, Thakur A, Siu PM, Lai CWK. Role of free fatty acids in endothelial dysfunction. *J BioMed Sci* (2017) 24:50. doi: 10.1186/s12929-017-0357-5

29. Wen H, Gris D, Lei Y, Jha S, Zhang L, Huang MT, et al. Fatty acid-induced NLRP3-ASC inflammasome activation interferes with insulin signaling. *Nat Immunol* (2011) 12:408–15. doi: 10.1038/ni.2022

30. Mansouri A, Gattolliat CH, Asselah T. Mitochondrial dysfunction and signaling in chronic liver diseases. *Gastroenterology* (2018) 155:629–47. doi: 10.1053/j.gastro.2018.06.083

31. Holte J, Bergh T, Berne C, Lithell H. Serum lipoprotein lipid profile in women with the polycystic ovary syndrome: Relation to anthropometric, endocrine and metabolic variables. *Clin Endocrinol (Oxf)* (1994) 41:463–71. doi: 10.1111/j.1365-2265.1994.tb02577.x

32. Niu Z, Lin N, Gu R, Sun Y, Feng Y. Associations between insulin resistance, free fatty acids, and oocyte quality in polycystic ovary syndrome during in vitro fertilization. *J Clin Endocrinol Metab* (2014) 99:E2269–76. doi: 10.1210/jc.2013-3942

33. Dong F, Deng D, Chen H, Cheng W, Li Q, Luo R, et al. Serum metabolomics study of polycystic ovary syndrome based on UPLC-QTOF-MS coupled with a pattern recognition approach. *Anal Bioanal Chem* (2015) 407:4683–95. doi: 10.1007/s00216-015-8670-x

34. Szczuko M, Zapałowska-Chwyć M, Drozd A, Maciejewska D, Starczewski A, Stachowska E. Metabolic pathways of oleic and palmitic acid are intensified in PCOS patients with normal androgen levels. *Prostaglandins Leukot Essent Fatty Acids* (2017) 126:105–11. doi: 10.1016/j.plefa.2017.09.001

35. Escobar-Morreale HF, Samino S, Insenser M, Vinaixa M, Luque-Ramírez M, Lasunción MA, et al. Metabolic heterogeneity in polycystic ovary syndrome is determined by obesity: Plasma metabolomic approach using GC-MS. *Clin Chem* (2012) 58:999–1009. doi: 10.1373/clinchem.2011.176396

36. Leung KL, Sanchita S, Pham CT, Davis BA, Okhovat M, Ding X, et al. Dynamic changes in chromatin accessibility, altered adipogenic gene expression, and total versus de novo fatty acid synthesis in subcutaneous adipose stem cells of normal-weight polycystic ovary syndrome (PCOS) women during adipogenesis: Evidence of cellular programming. *Clin Epigenet* (2020) 12:181. doi: 10.1186/s13148-020-00970-x

37. Cree-Green M, Carreau AM, Rahat H, Garcia-Reyes Y, Bergman BC, Pyle L, et al. Amino acid and fatty acid metabolomic profile during fasting and hyperinsulinemia in girls with polycystic ovarian syndrome. *Am J Physiol Endocrinol Metab* (2019) 316:E707–18. doi: 10.1152/ajpendo.00532.2018

38. Zhang XJ, Huang LL, Su H, Chen YX, Huang J, He C, et al. Characterizing plasma phospholipid fatty acid profiles of polycystic ovary syndrome patients with and without insulin resistance using GC-MS and chemometrics approach. *J Pharm BioMed Anal* (2014) 95:85–92. doi: 10.1016/j.jpba.2014.02.014

39. Francisco V, Sanz MJ, Real JT, Marques P, Capuozzo M, Ait Eldjoudi D, et al. Adipokines in non-alcoholic fatty liver disease: are we on the road toward new biomarkers and therapeutic targets? *Biol (Basel)* (2022) 11:1237. doi: 10.3390/biology11081237

40. Prostek A, Gajewska M, Kamola D, Bałasińska B. The influence of EPA and DHA on markers of inflammation in 3T3-L1 cells at different stages of cellular maturation. *Lipids Health Dis* (2014) 13:3. doi: 10.1186/1476-511X-13-3

41. Salek M, Clark CCT, Taghizadeh M, Jafarnejad S. N-3 fatty acids as preventive and therapeutic agents in attenuating PCOS complications. *EXCLI J* (2019) 18:558–75. doi: 10.17179/excli2019-1534

42. Lepsch J, Farias DR, Dos Santos Vaz J, de Jesus Pereira Pinto T, da Silva Lima N, Freitas Vilela AA, et al. Serum saturated fatty acid decreases plasma adiponectin and increases leptin throughout pregnancy independently of BMI. *Nutrition* (2016) 32:740–7. doi: 10.1016/j.nut.2016.01.016

frontiers | Frontiers in Endocrinology

TYPE Original Research
PUBLISHED 19 May 2023
DOI 10.3389/fendo.2023.1164371

OPEN ACCESS

EDITED BY
Changyin Zhou,
Guangdong Second Provincial General Hospital, China

REVIEWED BY
Ludovica Vincenzi,
Sapienza University of Rome, Italy
Yu-Chiao Yi,
Taichung Veterans General Hospital, Taiwan
Nenghui Liu,
Central South University, China

*CORRESPONDENCE
Jiali Cai
jialicai@xmu.edu.cn
Jianzhi Ren
rjz174@126.com

RECEIVED 12 February 2023
ACCEPTED 02 May 2023
PUBLISHED 19 May 2023

CITATION
Liu L, Jiang X, Liu Z, Chen J, Yang C, Chen K, Yang X, Cai J and Ren J (2023) Oocyte degeneration in a cohort adversely affects clinical outcomes in conventional IVF cycles: a propensity score matching study. *Front. Endocrinol.* 14:1164371. doi: 10.3389/fendo.2023.1164371

Oocyte degeneration in a cohort adversely affects clinical outcomes in conventional IVF cycles: a propensity score matching study

Lanlan Liu[1,2], Xiaoming Jiang[1], Zhenfang Liu[1], Jinghua Chen[1], Chao Yang[1], Kaijie Chen[1], Xiaolian Yang[1], Jiali Cai[1,2]* and Jianzhi Ren[1]*

[1]Reproductive Medicine Center, The Affiliated Chenggong Hospital of Xiamen University, Xiamen, China, [2]Medical College, Xiamen University, Xiamen, China

Background: Oocyte degeneration was mostly described in intracytoplasmic sperm injection (ICSI) cycles; there is no report showing the relationship between oocyte degeneration and clinical outcomes in conventional *in vitro* fertilization (IVF) cycles. This retrospective study using the propensity score (PS) matching method aimed to explore whether the presence of oocyte degeneration in conventional IVF cycles would affect the sibling embryo development potential and clinical outcomes.

Methods: Patients with at least one oocyte degenerated after short-term insemination and stripping were defined as the degeneration (DEG) group, while patients with no oocyte degenerated were defined as the non-degeneration (NONDEG) group. The PS matching method was used to control for potential confounding factors, and a multivariate logistic regression analysis was made to evaluate whether the presence of oocyte degeneration would affect the cumulative live birth rate (CLBR).

Results: After PS matching, basic characteristics were similar between the two groups, oocyte yield was significantly higher in the DEG group than the NON-DEG group ($P < 0.05$), mature oocyte number, 2 pronuclear (2PN) embryo number, 2PN embryo clearage rate, "slow" embryo number, "accelerated" embryo number, rate of cycles with total day 3 embryo extended culture, number of frozen embryo transfer (FET) cycles, transferred embryo stage, transferred embryo number, and live birth rate in fresh embryo transfer cycles were all similar between the two groups ($P > 0.05$), but the 2PN fertilization rate, available embryo number, high-quality embryo number, "normal" embryo number, frozen embryo number, blastocyst formation rate, and no available embryo cycle rate were all significantly lower in the DEG group than the NON-DEG group ($P < 0.05$). The cumulative live birth rate was also significantly lower in the DEG group than in the NON-DEG group (70.2% vs. 74.0%, $P = 0.0019$). Multivariate logistic regression analysis further demonstrated that the presence of oocyte degeneration in conventional IVF cycles adversely affects the CLBR

both before (OR = 0.83, 95% CI: 0.75–0.92) and after (OR = 0.82, 95% CI: 0.72–0.93) PS matching.

Conclusion: Our findings together revealed that the presence of oocyte degeneration in a cohort of oocytes may adversely affect subsequent embryo development potential and clinical outcomes in conventional IVF cycles.

KEYWORDS

oocyte degeneration, conventional IVF, embryo development potential, clinical outcome, cumulative live birth

Introduction

Oocyte degeneration is a common phenomenon in both conventional *in vitro* fertilization (IVF) and intracytoplasmic sperm injection (ICSI) cycles, but it is mostly described in ICSI cycles (1, 2). The presence of degenerated oocytes may be an indicator of either laboratory performance or oocyte quality (2). It is proposed that the presence of degenerated oocyte or empty zona pellucida at ovum pick-up (OPU) before ICSI correlates with the quality of the entire oocyte cohort (3–5). However, several authors argued that oocyte degeneration in ICSI cycles is neither technician nor physician dependent but reflects the inherent oocyte quality, as the changes in the ICSI technician or the stripping technician were not associated with the oocyte degeneration rate (1). Nevertheless, ICSI remained a strong confounder in the reported studies and the performance of ICSI may vary among embryologists and clinics. The random fluctuation of ICSI performance may also mask the association between oocyte quality and oocyte degeneration.

The invasive procedure of ICSI is absent in conventional IVF cycles, which provided an opportunity to evaluate the association between oocyte quality and oocyte degeneration without confounding ICSI performance. Oocyte degeneration could be confirmed during oocyte denudation or at the time of fertilization assessment with retracted and/or darkened ooplasm or without zona pellucida the next day after OPU during conventional IVF cycles (1, 6). However, data regarding oocyte degeneration in conventional IVF cycles remained very limited. Only one study reported a negative association between oocyte degeneration and the IVF outcome (7). However, both conventional IVF cycles and ICSI cycles were all included in that study. Meanwhile, oocyte degeneration was assessed at the time of OUP, as we know, oocytes were surrounded by layers of granulosa cells after retrieval. Oocyte degeneration like retracted ooplasm within the zona pellucid is difficult to confirm at the time of OPU, and cumulative live birth was also not studied in that study.

Most of the previous studies regarding oocyte degeneration associated the degeneration rate with the implantation rate following fresh embryo transfer (7, 8). These study designs may lead to selection bias as they could not include certain patients such as patients with exceeded responses or planning a freeze-all procedure. If oocyte degeneration correlates with the quality of the entire oocyte cohort, the cumulative outcomes of the oocyte cohort should be a better measure than the outcome of a single transfer.

In this study, we aimed to investigate whether the presence of oocyte degeneration in conventional IVF cycles on the OPU day would affect the sibling embryo quality and clinical outcomes in a retrospective cohort including 16,823 conventional IVF cycles, of which 2,776 cycles presented at least one oocyte degenerated. A propensity score (PS) matching method was used to account for comparability between the two groups by balancing the biases and confounders, and multivariate logistic regression was carried out to confirm the findings.

Materials and methods

Institutional review board approval for this study was obtained from the Ethical Committee of Medical College Xiamen University. Informed consent was not necessary because this retrospective research was based on non-identifiable records.

Study subjects

This retrospective study was performed at the reproductive medicine center of The Affiliated Chenggong Hospital of Xiamen University. Patients who underwent conventional IVF treatment from 2013 to 2019 were enrolled and retrospectively analyzed. The exclusion criteria were as follows: (a) patients proposed to take IVF treatment but eventually underwent early rescue ICSI treatment because less than 50% of mature oocytes excluded their second poly body. (b) Patients got no live birth but still had frozen embryos 2 years later after oocyte collection in one OPU cycle. A total of 14,665 patients who took 16,823 conventional IVF cycles were included, of which 2,776 cycles presented at least one oocyte degenerated after short-term insemination and denuding on the OPU day, and 12,921 cycles took fresh embryo transfer. Cycles with at least one oocyte degenerated were defined as the degeneration

group (DEG Group), and cycles with no oocytes degenerated were defined as the non-degeneration group (NON DEG Group).

Laboratory procedures and embryo assessment

Most patients in our center used a Gonadotropin-releasing hormone (GnRH) agonist or an antagonist protocol as we previously described (9, 10); some patients with advanced age or poor ovarian reserve used "other protocols" like the mild stimulation protocol, natural cycle, or luteal-phase stimulation protocol. Ovarian response was monitored using transvaginal ultrasound measurements of follicular growth and the serum E_2 level every 1–3 days. Oocyte retrieval was performed using transvaginal ultrasound, and a 17 G needle (Cook Medical) was used for oocyte pick-up.

Insemination was carried out using conventional IVF, cumulus–oocyte complexes were incubated with approximately 1.5–3 × 10^5 progressively motile spermatozoa in fertilization culture medium (K-SIFM, Cook) for approximately 5 h, and then oocytes were denuded for the observation of the second poly body. Patients with more than 50% mature oocytes excluding the second poly body underwent conventional IVF treatment, while early rescue ICSI was performed on patients with less than 50% mature oocytes excluding the second poly body 6 h after insemination. Early rescue ICSI patients were excluded in this study. Considering oocyte degeneration definition in ICSI cycles (1, 2), degeneration oocytes in this study were defined as those broken to pieces during stripping or being noted by retracted and/or darkened ooplasm or with empty zona pellucid after denudation for the observation of the second poly body after stripping.

Embryos were cultured in single droplets after fertilization, and oocytes and embryos were cultured in COOK series medium (KSIFM, KSICM, or KSIBM, Cook Medical, Bloomington, IN) in traditional incubators (C200, Labotech, Gottingen, Germany) at 37°C, 6% CO_2, and 5% O_2. Fertilization was checked approximately 17–18 h post-insemination under an inverted microscope. Day 3 embryo assessment and grading system were based on the number of embryo blastomeres, fragmentation, and symmetry; 2PN embryos on day 3 were assessed and divided into four different grades according to the ASEBIR embryo assessment criteria (6). Grade 1 and grade 2 embryos were considered as high-quality embryos; grade 1, grade 2, and grade 3 embryos were considered as available embryos, while grade 4 embryos, arrested embryos, and embryos with all blastomere degenerated or lysed were usually deserted. Meanwhile, as for embryo development kinetics, according to the Istanbul consensus (6), "normal" embryos have 7–9 cells on day 3, "slow" embryos have 6 or fewer cells on day 3, and "accelerated" embryos have >9 cells on day 3. For blastocyst assessment, we used the Gardner grading system (11), and we previously described it in detail (9). Blastocysts with poor morphology scores (≤CC) or low expansion grades (grade 1–2) were not cryopreserved or transferred.

A vitrification protocol was used for embryo cryopreservation, which employed 15% dimethyl sulfoxide, 15% ethylene glycol, and 0.6 M sucrose as cryoprotectants. For embryo thawing, embryos were directly immersed into a thawing solution (TS) containing 1 M sucrose at 37°C for 1 min. Then, they were sequentially incubated in each of the following solutions for 3 min: 0.5 M sucrose, 0.25 M sucrose, and sucrose-free TS, and embryos were placed in blastocyst culture medium (K-SIBM, COOK, IN, USA) and cultured normally.

Embryo transfer was performed using a COOK catheter (K-JETS-7019-SIVE, COOK, IN, USA) under trans-abdominal ultrasound guidance.

Cumulative live birth calculation

The cumulative live birth rate (CLBR) was calculated in this study, and we used a short-term calculation method as previously described (12). The CLBR was presented as live birth episodes per woman per egg collection over a 2-year period to account for the first live birth.

Statistical analysis

Oocyte degeneration in conventional IVF cycles occurs occasionally, and there were differences in basic characteristics between the DEG Group and the NON DEG Group; thus, we used the PS matching method to tackle potential confounders and selection biases in this study. PSs were calculated using logistic regression based on potential variables related to the outcomes. The variables included female age, male age, freeze-all strategy, ovarian stimulation protocol, infertility type, OPU order, the duration of infertility, whether complicated with polycystic ovary syndrome, whether complicated with endometriosis, whether complicated with tubal factor, female BMI, baseline hormone levels, antral follicle count (AFC), gonadotropin total dose, the length of stimulation, gonadotropin starting dose, E_2 level on the hCG day, and survival oocyte number (retrieved oocyte number minus degenerated oocyte number). Considering degenerated oocytes decreased the survival oocyte number and may affect cumulative live birth, we take the survival oocyte number as a variable in the PS matching method. A one-to-one nearest neighbor matching method without replacement was performed to match data between the DEG group and the NON DEG group with a caliper width equal to 0.2. PS matching was performed by using the MatchIt package in R software (13). The cobalt package (14) was used to test the balance. Standard differences (D) were calculated to evaluate the balance of the distribution of the baseline characteristics between the two groups before and after PS matching. $D < 0.1$ was used as the threshold to indicate a negligible difference in the mean or prevalence of a covariate between exposure groups (15).

Data were presented as mean (SD) and median (first quartile and third quartile) for continuous variables and n (percentage) for categorical variables. Continuous variables were analyzed using the Wilcoxon test, and categorical variables were analyzed using the chi-square test or Fisher's exact test; $P < 0.05$ was considered to be significant. All analyses were performed by using R statistic software 4.12 (16).

Multivariate logistic regression analysis was also performed to evaluate the association between oocyte degeneration presence and the probability of cumulative live birth, with adjustments made for important covariates and potential confounding factors.

We used generalized additive models (GAMs) to verify whether there is a dose-dependent association between degeneration and CLBR (17). In GAMs, the degree of degeneration and other continuous covariates were fitted as smooth terms. Because the smooth estimator only demonstrated the contribution of the covariate fitted to a given smooth function to the response variable, we plotted the degeneration against the prediction to demonstrate a dose response on a cumulative live birth.

Results

In this study, 16,823 IVF cycles were enrolled and analyzed, 3,748 oocytes in 2,776 cycles were found degenerated after fertilization, the oocyte degeneration rate is 2.48% (3,748/151,047), and the degeneration cycle rate is 16.50% (2,776/16,823).

After PS matching, 2,776 cycles in the NON DEG group were matched by their counterparts in the DEG group. Basic characteristics before and after PS matching are shown in Table 1. Before matching (left panel), significant differences were observed between the DEG group and the NON DEG group, including female age, male age, embryo freeze-all cycle rate, the rate of the GnRH agonist protocol, basal FSH level, AFC, the length of stimulation, E_2 level on the hCG day, and survival oocyte number (D > 0.1). After matching (right panel), all the baseline characteristics became very comparable between the two groups (D < 0.1). Distributions of the PSs before and after PS matching are shown in Supplementary Figure S1.

Table 2 shows the outcomes of the DEG group and the NON DEG group before and after PS matching. After PS matching, oocyte yield was significantly higher in the DEG group than the NON DEG group ($P < 0.05$), mature oocyte number, fertilization oocyte number, 2PN embryo number, 2PN embryo clearage rate, "slow" embryo number, "accelerated" embryo number, the rate of cycles with total day 3 extended embryo culture, the number of FET cycles, transferred embryo stage, transferred embryo number, and live birth rate in fresh cycles were all similar between the two groups ($P > 0.05$), but the 2PN fertilization rate, both on the basis of oocyte yield (2PN number/oocyte yield *100%) as shown in Table 2 and on the basis of the survival oocyte number (2PN number/survival oocyte number *100%, 65.2 ± 21.5 vs. 62.3 ± 22.6, P < 0.001, in matched cohort) were all significantly lower in the DEG group than the NON DEG group ($P < 0.05$). The available embryo number, high-quality embryo number, "normal" embryo number with seven to nine cells on day 3, frozen embryo number, blastocyst formation rate, and no available embryo cycle rate were all significantly lower in the DEG group than the NON DEG group ($P < 0.05$). These findings revealed that the presence of oocyte degeneration in a cohort of oocytes may affect subsequent embryo development potential. The cumulative live birth rate was also significantly lower in the DEG group than the NON DEG group (70.2% vs. 74.0%, $P = 0.0019$) after PS matching.

We also conducted a multivariate logistic regression analysis, with adjustments made for important covariates and potential confounding factors; logistic regression analysis results in Table 3 further demonstrated that the presence of oocyte degeneration in

TABLE 1 Baseline characteristics of the degeneration (DEG) group and non-degeneration (NON DEG) group before and after propensity score (PS) matching.

Variables	Before matching			After matching		
	NON DEG (N = 14,047)	DEG (N = 2,776)	*D	NON DEG (N = 2,776)	DEG (N = 2,776)	*D
Female's age, year			-0.1717			0.0469
Mean (SD)	31.9 (4.62)	31.2 (4.25)		31.0 (4.21)	31.2 (4.25)	
Median [Min, Max]	31.0 [20.0, 48.0]	31.0 [20.0, 45.0]		30.0 [20.0, 46.0]	31.0 [20.0, 45.0]	
Male's age, year			-0.1193			0.0128
Mean (SD)	33.6 (5.17)	33.0 (4.93)		33.0 (4.90)	33.0 (4.93)	
Median [Min, Max]	33.0 [22.0, 60.0]	32.0 [22.0, 59.0]		32.0 [22.0, 56.0]	32.0 [22.0, 59.0]	
Freeze-all cycle (%)	2,300 (16.4%)	818 (29.5%)	**0.1309**	801 (28.9%)	818 (29.5%)	0.0061
Stimulation protocols						
GnRH agonist (%)	9,178 (65.3%)	2,139 (77.1%)	**0.1172**	2,165 (78.0%)	2,139 (77.1%)	-0.0094
GnRH antagonist (%)	2,856 (20.3%)	375 (13.5%)	-0.0682	367 (13.2%)	375 (13.5%)	0.0029
Other protocols (%)	2,013 (14.3%)	262 (9.4%)	-0.0489	244 (8.8%)	262 (9.4%)	0.0065
Primary infertility (%)	5,569 (39.6%)	1,201 (43.3%)	-0.0362	1,200 (43.2%)	1,201 (43.3%)	-0.0004
OPU order						

(Continued)

TABLE 1 Continued

Variables	Before matching			After matching		
	NON DEG (N = 14,047)	DEG (N = 2,776)	*D	NON DEG (N = 2,776)	DEG (N = 2,776)	*D
1	11,358 (80.9%)	2,358 (84.9%)	0.0409	2,366 (85.2%)	2,358 (84.9%)	-0.0029
2	2,027 (14.4%)	344 (12.4%)	-0.0204	348 (12.5%)	344 (12.4%)	-0.0014
≧3	662 (4.7%)	74 (2.7%)	-0.0205	62 (2.2%)	74 (2.7%)	0.0043
Duration of infertility, year			-0.0015			0.0151
Mean (SD)	4.21 (3.13)	4.21 (3.05)		4.16 (3.00)	4.21 (3.05)	
Median [Min, Max]	3.50 [0.04, 31.0]	3.50 [0.10, 23.0]		3.50 [0.10, 25.0]	3.50 [0.10, 23.0]	
PCOs (%)	915 (6.5%)	203 (7.3%)	0.008	201 (7.2%)	203 (7.3%)	0.0007
Endometriosis (%)	1,744 (12.4%)	347 (12.5%)	0.0008	341 (12.3%)	347 (12.5%)	0.0022
Tubal factor (%)	10,452 (74.4%)	2,048 (73.8%)	-0.0063	2,058 (74.1%)	2,048 (73.8%)	-0.0036
Female BMI, kg/cm^2			-0.0836			-0.0279
Mean (SD)	21.2 (2.26)	21.0 (2.26)		21.1 (2.29)	21.0 (2.26)	
Median [Min, Max]	21.2 [13.5, 46.8]	21.0 [15.5, 46.2]		21.0 [14.3, 46.2]	21.0 [15.5, 46.2]	
Basal FSH, IU/l			**-0.1161**			0.0245
Mean (SD)	8.20 (2.99)	7.88 (2.79)		7.81 (2.72)	7.88 (2.79)	
Median [Min, Max]	7.50 [0.05, 41.3]	7.25 [0.10, 41.5]		7.16 [0.05, 41.3]	7.25 [0.10, 41.5]	
Basal LH, IU/l			0.0679			-0.0146
Mean (SD)	4.84 (2.93)	5.05 (3.07)		5.09 (3.11)	5.05 (3.07)	
Median [Min, Max]	4.24 [0.01, 51.6]	4.37 [0.05, 38.6]		4.45 [0.01, 30.9]	4.37 [0.05, 38.6]	
Basal PRL, ng/ml			0.0423			-0.0122
Mean (SD)	15.6 (8.47)	16.1 (10.4)		16.2 (9.14)	16.1 (10.4)	
Median [Min, Max]	14.1 [0.19, 162]	14.1 [0.17, 298]		14.3 [0.22, 162]	14.1 [0.17, 298]	
Basal E_2, pg/ml			-0.0356			0.019
Mean (SD)	45.9 (31.1)	44.9 (25.7)		44.5 (23.5)	44.9 (25.7)	
Median [Min, Max]	41.0 [0.03, 747]	41.0 [0.10, 499]		41.0 [2.0, 321]	41.0 [0.10, 499]	
Antral follicle count			**0.1892**			-0.0156
Mean (SD)	10.1 (5.43)	11.1 (5.41)		11.2 (5.40)	11.1 (5.41)	
Median [Min, Max]	9.00 [1.00, 32.0]	10.0 [1.0, 30.0]		10.0 [1.0, 30.0]	10.0 [1.0, 30.0]	
Total dose of GN, IU			0.0462			-0.0088
Mean (SD)	2,280 (700)	2,310 (643)		2,310 (648)	2,310 (643)	
Median [Min, Max]	2,250 [0, 8,480]	2,250 [0, 8,100]		2,250 [0, 8,210]	2,250 [0, 8,100]	
Length of stimulation, day			**0.1523**			-0.0139
Mean (SD)	11.1 (3.07)	11.5 (2.55)		11.5 (2.74)	11.5 (2.55)	
Median [Min, Max]	11.0 [0, 19.0]	11.0 [0, 18.0]		11.0 [0, 17.0]	11.0 [0, 17.0]	
GN starting dose, IU			-0.0568			-0.0042
Mean (SD)	199 (43.1)	196 (39.7)		197 (38.7)	196 (39.7)	
Median [Min, Max]	225 [0, 300]	225 [0, 300]		225 [0, 300]	225 [0, 300]	
E_2 level of hCG day			**0.3415**			0.0187

(Continued)

10.3389/fendo.2023.1164371

TABLE 1 Continued

Variables	Before matching			After matching		
	NON DEG (N = 14,047)	DEG (N = 2,776)	*D	NON DEG (N = 2,776)	DEG (N = 2,776)	*D
Mean (SD)	2,980 (2,450)	3,910 (2730)		3,860 (2,720)	3,910 (2,730)	
Median [Min, Max]	2,430 [0, 105,000]	3,520 [0, 45,500]		3,490 [0, 43,800]	3,520 [0, 45,500]	
Survival oocyte number			**0.4405**			0.0041
Mean (SD)	8.29 (5.59)	11.1 (6.47)		11.1 (6.50)	11.1 (6.47)	
Median [Min, Max]	7.00 [1.00, 52.0]	10.0 [1.00, 45.0]		10.0 [1.00, 52.0]	10.0 [1.00, 45.0]	

Data were presented as mean ± SD and median [first quartile, third quartile] for continuous variables and n (percentage) for categorical variables. *D: Standardized difference. The absolute value of D ≥ 0.1 is printed in bold. The absolute value of D is less than 0.1, cohorts can be considered to be balanced with respect to the demographics being assessed. PCOS, polycystic ovarian syndrome; BMI, body mass index; FSH, follicle-stimulating hormone; LH, luteinizing hormone; PRL, prolactin; E_2, estradiol; GN, gonadotropin.

conventional IVF cycles adversely affect the cumulative live birth rate both before (OR = 0.83, 95% CI: 0.75–0.92) and after PS matching (OR = 0.82, 95% CI: 0.72–0.93). Meanwhile, with the GMA method, we found that the oocyte degeneration rate is negatively correlated with the cumulative live birth rate in an OPU cycle in a dose–response manner, results were shown in Figure 1.

Discussion

To our best knowledge, this is the first study to investigate oocyte degeneration in conventional IVF cycles on the OPU day. Despite the surviving number of oocytes and the patient's characteristics being comparable following PS matching, our results showed that the cumulative live birth rate of the completed cycles was significantly decreased in the DEG group than that in the non-DEG group, suggesting an overall decrease in the oocyte quality. It was also supported by the findings that the numbers of available embryos, high-quality embryos, and "normal" embryos with seven to nine cells on day 3 were all significantly lower in the DEG group than in the NON-DEG group. For patients who had all their embryos extended culture, the blastocyst formation rate was also decreased with the presence of oocyte degeneration. Taken together, these results revealed that the presence of oocyte degeneration in a cohort of oocytes in conventional IVF cycles may be an unfavorable predictor for subsequent embryo development potential and clinical outcomes.

In this study, we found that the percentage of conventional IVF cycles with oocyte degeneration on the OPU day is 16.50%, which is similar to previously reported at the time of OPU in both conventional IVF cycles and ICSI cycles (7). On the other hand, however, the oocyte degeneration rate among all oocytes retrieved was 2.48% in the present study, which is much lower than those reported in ICSI cycles (8). The difference might suggest the role of the invasive procedure of ICSI on the occurrence of oocyte degeneration.

In ICSI cycles with oocyte degeneration, several studies reported that oocyte degeneration was not an indicator of the live birth rate (8, 18), and Rosen et al. (1) concluded that "the remaining cohort of retrieved oocytes appears to be unaffected by an uncompromised implantation rate." Our matched results also showed a similar live birth rate between the DEG group and the NONDEG group following fresh ET. However, the comparison is limited by several biases. First, the analyses on fresh ET cycles excluded certain types of patients, such as patients with an extremely high ovarian response or patients who failed to have day 5 blastocysts. As shown in our study, the latter may take a higher proportion in the DEG group. Second, including only fresh ET cycles omitted the contribution of surplus embryos of the cohort. As shown in previous studies (8, 18), the presence of oocyte degeneration in ICSI cycles is also associated with a decreased number of good-quality embryos. If the initial fresh ET attempt fails, the number and quality of the remaining embryos are key determinants for subsequent success.

Our study conflicted with the work of Hu et al., which suggested that the cumulative live birth rate in young women was not affected by the presence of oocyte degeneration (18).The controversial results may be caused by the different approaches of insemination (IVF vs. ICSI) or the heterogeneity of patients. The severity of male infertility might also contribute to embryo development competence (19) and therefore affect the cumulative outcome. The ICSI cohorts are expected to have more severe male infertility factors than IVF cohorts. The difference in the cumulative live birth rate between the two studies may also support the heterogeneity of the population.

In addition to the insemination protocol and male infertility, the degree of ovarian response might also affect the evaluation of the association between oocyte degeneration and cycle outcomes. Pride et al. (4) reported cycles with a higher number of oocytes correlated with the increased presence of DEG oocytes. Cinar et al. (20) reported that the oocyte degeneration rate (DEG/total oocyte) increased when more oocytes were collected per cycle, and the fertilization rate and cleavage rate in DEG cycles were significantly lower. These data suggested that DEG cases are more likely to aggregate in high responders, who are expected to have higher cumulative outcomes (21, 22). On the other hand, the presence of degenerated oocytes in the DEG patients may lead to fewer available oocytes in comparison with the NON DEG patients with similar oocyte yield. Both situations may either over- or underestimate the association between oocyte degeneration and oocyte quality. To

TABLE 2 Clinical outcomes of DEG group and NON DEG group before and after PS matching.

Variables	Before matching			After matching		
	NON DEG (N = 14,047)	DEG (N = 2,776)	*P*	NON DEG (N = 2,776)	DEG (N = 2,776)	P
Oocyte yield			<0.001			<0.001
Mean (SD)	8.29 (5.59)	12.5 (6.56)		11.1 (6.50)	12.5 (6.56)	
Median [Min, Max]	7.00 [1.00, 52.0]	12.0 [2.0, 46.0]		10.0 [1.00, 52.0]	12.0 [2.00, 46.0]	
Mature oocyte number			<0.001			0.874
Mean (SD)	7.54 (5.19)	10.0 (6.04)		10.1 (6.06)	10.0 (6.04)	
Median [Min, Max]	6.00 [1.00, 46.0]	9.00 [1.0, 44.0]		9.00 [1.00, 45.0]	9.00 [1.00, 44.0]	
Fertilization oocyte number			<0.001			0.218
Mean (SD)	6.94 (4.92)	9.10 (5.72)		9.28 (5.77)	9.10 (5.72)	
Median [Min, Max]	6.00 [0, 41.0]	8.00 [0, 39.0]		8.00 [0, 39.0]	8.00 [0, 39.0]	
2PN embryo number			<0.001			0.0723
Mean (SD)	5.32 (3.94)	6.93 (4.67)		7.12 (4.59)	6.93 (4.67)	
Median [Min, Max]	4.00 [0, 27.0]	6.00 [0, 36.0]		6.00 [0, 27.0]	6.00 [0, 36.0]	
Normal fertilization rate (%)			<0.001			<0.001
Mean (SD)	65.1 (24.8)	53.6 (19.5)		65.2 (21.5)	53.6 (19.5)	
Median [Min, Max]	66.7 [0, 100]	56.1 [0, 94.4]		66.7 [0, 100]	56.1 [0, 94.4]	
Cleavage rate of 2PN embryo (%)			0.017			0.0679
Mean (SD)	94.2 (20.7)	94.8 (18.5)		96.5 (14.1)	94.8 (18.5)	
Median [Min, Max]	100 [0, 100]	100 [0, 100]		100 [0, 100]	100 [0, 100]	
Available embryo number			<0.001			0.0452
Mean (SD)	4.78 (3.84)	6.25 (4.49)		6.46 (4.40)	6.25 (4.49)	
Median [Min, Max]	4.00 [0, 27.0]	6.00 [0, 34.0]		6.00 [0, 27.0]	6.00 [0, 34.0]	
High-quality embryo number			<0.001			0.0064
Mean (SD)	3.23 (2.95)	4.11 (3.51)		4.32 (3.45)	4.11 (3.51)	
Median [Min, Max]	3.00 [0, 20.0]	3.00 [0, 28.0]		4.00 [0, 20.0]	3.00 [0, 28.0]	
"Slow" embryo number			<0.001			0.219
Mean (SD)	2.32 (2.39)	3.08 (2.95)		3.16 (2.94)	3.08 (2.95)	
Median [Min, Max]	2.00 [0, 23.0]	2.00 [0, 22.0]		2.00 [0, 23.0]	2.00 [0, 22.0]	
"Normal" embryo number			<0.001			0.0132
Mean (SD)	3.43 (2.99)	4.29 (3.45)		4.47 (3.38)	4.29 (3.45)	
Median [Min, Max]	3.00 [0, 29.0]	4.00 [0, 24.0]		4.00 [0, 21.0]	4.00 [0, 24.0]	
"Accelerated" embryo number			<0.001			0.514
Mean (SD)	0.560 (1.10)	0.709 (1.30)		0.724 (1.28)	0.709 (1.30)	
Median [Min, Max]	0 [0, 13.0]	0 [0, 14.0]		0 [0, 10.0]	0 [0, 14.0]	
Percentage of cycles with total day 3 embryo extended culture (%)	10,327 (73.5%)	1,737 (62.6%)	<0.001	1,762 (63.5%)	1,737 (62.6%)	0.505
Blastocyst formation rate (%)			0.271			<0.001
Mean (SD)	52.5 (31.5)	54.7 (27.9)		59.6 (25.2)	54.7 (27.9)	
Median [Min, Max]	58.3 [0, 100]	58.8 [0, 100]		62.5 [0, 100]	58.8 [0, 100]	

(Continued)

TABLE 2 Continued

Variables	Before matching			After matching		
	NON DEG (N = 14,047)	DEG (N = 2,776)	*P*	NON DEG (N = 2,776)	DEG (N = 2,776)	P
Frozen embryo number			<0.001			0.0181
Mean (SD)	2.40 (2.73)	3.32 (3.25)		3.52 (3.32)	3.32 (3.25)	
Median [Min, Max]	2.00 [0, 20.0]	3.00 [0, 26.0]		3.00 [0, 20.0]	3.00 [0, 26.0]	
No available embryo cycle rate (%)	668 (4.8%)	116 (4.2%)	0.205	59 (2.1%)	116 (4.2%)	<0.001
Number of FET cycle			<0.001			0.282
Mean (SD)	0.568 (0.820)	0.718 (0.920)		0.754 (0.954)	0.718 (0.920)	
Median [Min, Max]	0 [0, 6.00]	0 [0, 6.00]		0 [0, 5.00]	0 [0, 6.00]	
Transferred embryo stage in fresh cycle			<0.001			0.166
day 2	1,047 (9.5%)	142 (7.7%)		121 (6.3%)	142 (7.7%)	
day 3	8,765 (79.1%)	1,442 (78.3%)		1,503 (78.4%)	1,442 (78.3%)	
day 5	1,267 (11.4%)	258 (14.0%)		292 (15.2%)	258 (14.0%)	
Transferred embryo number in fresh cycle			0.553			0.362
1	4,071 (36.7%)	654 (35.5%)		690 (36.0%)	654 (35.5%)	
2	6,818 (61.5%)	1,158 (62.9%)		1,205 (62.9%)	1,158 (62.9%)	
3	190 (1.7%)	30 (1.6%)		21 (1.1%)	30 (1.6%)	
Fresh cycle LB rate (%)	5,504 (49.7%)	1,001 (54.3%)	<0.001	1,046 (54.6%)	1,001 (54.3%)	0.904
Cumulative LB rate (%)	9,028 (64.3%)	1,949 (70.2%)	<0.001	2,054 (74.0%)	1,949 (70.2%)	0.0019

Data were presented as mean ± SD and median [first quartile, third quartile] for continuous variables and n (percentage) for categorical variables. PN, pronuclei; FET, frozen embryo transfer; LB, live birth; "slow" embryo, embryos with 6 or fewer cell numbers on day 3; "normal" embryo, embryos with 7–9 cell numbers on day 3; "accelerated" embryo, embryos with >9 cell number on day 3.

make a better estimation of the effect of oocyte degeneration, we considered the survival oocyte number (the retrieved oocyte number minus the degenerated oocyte number) as a baseline characteristic in the PS matching method.

Atzmon et al. (7) reported that the frequency of DEG oocytes per cycle was negatively correlated with the pregnancy rate in both IVF cycles and ICSI cycles at OPU, and this study is in agreement with our results. With the GMA method, we found that the oocyte degeneration rate is negatively correlated with the cumulative live birth rate in an OPU cycle in a dose–response manner. While the occurrence of low-prevalence events might be affected by the random fluctuation of data, the dose–response association may support a causal relationship (23).

As we know, oocyte quality predominantly determines embryo quality (24–26), and oocyte morphology may affect subsequent embryo cleavage patterns and development potential (27, 28). Oocyte quality is affected by various factors like the body mass index (29), blood lipid level, and blood estrogen level (30), but the cause of oocyte degeneration was less clear. Several studies reported controversial associations between oocyte degeneration and ovarian stimulation or ovarian response (7, 20). In one study, patients with the GnRH agonist protocol had a higher risk of DEG oocytes (7), while Cinar et al. (20) reported that the GnRH antagonist protocol was correlated with more damaged oocytes. On the other hand, the E_2 level was demonstrated to be very important during oocyte development and maturation (31); Rosen et al. (1) reported that a high level of E_2 on the hCG day may be negatively associated with the degeneration rate in GnRH agonist protocols, while Palermo et al. (32) reported that the oocyte degeneration rate increased in patients who took more gonadotropin administration and had a lower E_2 level on the hCG day. Factors like the ovarian stimulation protocol and high levels of E_2 are known to affect the physiological status of women and thus affect IVF outcomes (33–36). However, with adjustment for these factors, our study suggested that the effect of oocyte degeneration in a cohort is not mediated or confounded by the physiological or cycle-based parameters. Our study may support the hypothesis that oocyte degeneration is likely a function of the inherent oocyte quality and reflects the cohort of embryo development potential.

While ICSI is absent in the conventional IVF cycles, oocyte degeneration may also be affected by technical factors, such as OPU needles and oocyte denudation pipettes. Pride et al. (4) deduced that the mechanical forces during oocyte pick-up may cause oocyte damage and affect cycle outcomes. Atzmon et al. reported that different types of needles used for OPU were associated with oocyte degeneration at OPU (7). In our center, we routinely used the 17G needle for oocyte pick-up; thus, this factor was also not discussed in this study. As for the oocyte denudation pipette, if the diameter of the stripping pipette is too small, then oocytes may be strongly compressed during striping and may result in the damage of zona pellucida and subsequent oocyte

10.3389/fendo.2023.1164371

TABLE 3 Multivariate logistic regression analysis for the cumulative live birth rate.

Variable	Category	Before matching			After matching		
		OR	95% CI	*P*	OR	95% CI	*P*
Oocyte degeneration	Degeneration group vs. control group	0.83	0.75, 0.92	0.001	0.82	0.72, 0.93	<0.001
Female age	Per year increased	0.92	0.91, 0.93	<0.001	0.94	0.91, 0.96	<0.001
Male age	Per year increased	1	0.99, 1.01	0.8	1	0.98, 1.02	0.8
Stimulation protocol							
1	Antagonist vs. agonist protocol	0.62	0.54, 0.72	<0.001	0.53	0.40, 0.71	<0.001
2	Other protocols vs. agonist protocol	0.62	0.55, 0.69	<0.001	0.66	0.53, 0.83	0.003
Infertility type	Secondary infertility vs. primary infertility	1.12	1.03, 1.22	0.019	1.17	1.01, 1.36	0.028
OPU time							
Order 2 vs. 1	2 vs. 1	0.97	0.88, 1.08	>0.9	0.92	0.76, 1.11	0.532
Order 3 or more vs. 1	≥3 vs. 1	0.73	0.61, 0.87	0.008	0.61	0.41, 0.91	0.016
Duration of infertility	Per year increased	0.97	0.96, 0.98	<0.001	0.97	0.95, 0.99	0.041
PCOS	Yes vs. no	0.75	0.62, 0.91	0.007	0.79	0.56, 1.13	0.8
Endometriosis	Yes vs. no	1.11	0.99, 1.24	0.058	0.96	0.79, 1.18	0.8
Tubal factor	Yes vs. no	1.16	1.06, 1.26	0.003	1.15	0.98, 1.34	0.025
BMI	Per unit increased	1.01	0.99, 1.03	0.092	1.02	0.98, 1.05	0.025
Basal FSH	Per unit increased	0.97	0.96, 0.98	<0.001	0.96	0.93, 0.98	0.021
Basal LH	Per unit increased	1.01	0.99, 1.02	0.4	1.02	0.99, 1.05	0.3
Basal PRL	Per unit increased	1	1.00, 1.00	0.8	1	1.00, 1.01	0.3
Basal E_2	Per unit increased	1	1.00, 1.00	0.2	1	1.00, 1.00	0.4
AFC	Per AFC increased	1.02	1.01, 1.03	<0.001	1.02	1.00, 1.03	0.047
The total dose of GN	Per 75 units increased	0.97	0.95, 0.98	<0.001	0.95	0.92, 0.98	0.001
Length of simulation	Per day increased	1.13	1.08, 1.18	<0.001	1.14	1.05, 1.25	0.011
GN starting dose	Per unit increased	1.22	1.07, 1.39	0.052	1.13	0.87, 1.49	0.2
E_2 level on hCG day	Per 100 units increased	1.01	1.01, 1.02	<0.001	1.01	1.01, 1.01	<0.001
Survival oocyte number	Per oocyte increased	1.09	1.08, 1.10	<0.001	1.09	1.07, 1.10	<0.001
Freeze all or not	Freeze all cycle vs. fresh embryo transfer cycle	0.77	0.69, 0.86	<0.001	0.72	0.60, 0.86	<0.001

OPU, oocyte pick-up; PCOS, polycystic ovarian syndrome; BMI, body mass index; AFC, antral follicle count; FSH, follicle-stimulating hormone; LH, luteinizing hormone; PRL, prolactin; E_2, estradiol; GN, gonadotropin; OR, odds ratio; CI, confidence interval.

degeneration. In our center, we made a series of pipettes with different diameters before denudation, and we select the proper pipette for oocyte stripping; thus, oocyte degeneration would be widely avoided during stripping.

This study was limited by its retrospectively observational design, and the results could be screwed by unrecorded or unmeasured confounders. Although PS matching was used to minimize the confounding bias, the sample size decreased after PS matching, and the loss of unmatched samples may include biased ones; thus, we also analyzed the pre-matched data by using multivariable logistic regression analysis and got the same reassuring conclusion.

In most clinics during conventional IVF procedures, cumulus–oocyte complexes are usually incubated with spermatozoa overnight and the real oocyte structure is unknown on the oocyte pick-up day (37, 38). The oocyte morphology on the OPU day may reflect the real oocyte characteristics, without confounding the delayed effect of previous stress during denudation or OPU. Short-term insemination and early denudation provide a chance to observe oocyte degeneration of conventional IVF patients on the OPU day. Short-term insemination combined with early rescue ICSI could efficiently prevent the occurrence of total fertilization failure and got similar clinical outcomes compared with traditional IVF with overnight co-incubation of gametes (39, 40). This study was based on a cohort of patients receiving short-term insemination; caution should be taken when generalizing the conclusion to clinics using traditional IVF with overnight coincubation of gametes.

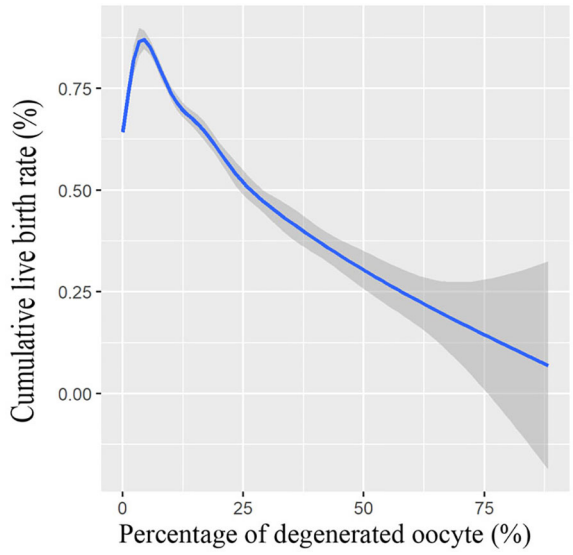

FIGURE 1
Association between cumulative live birth rate and percentage of degenerated oocytes. Shade indicates confident intervals. Model was fitted with GAM, adjusted for female age, male age, freeze-all cycle rate, ovarian stimulation protocol, primary infertility rate, OPU order, duration of infertility, polycystic ovary syndrome patient rate, endometriosis patient rate, tubal factor patient rate, female BMI, baseline hormone levels, antral follicle count (AFC), the total dose of gonadotropin, length of stimulation, gonadotropin starting dose, E2 level on hCG day, and survival oocyte number (retrieved oocyte number minus degenerated oocyte number).

Conclusions

In conclusion, we first reported oocyte degeneration in conventional IVF cycles on the OPU day in this study. Our results showed that the oocyte degeneration rate and degeneration cycle rate on the OPU day in conventional IVF cycles were all much lower than in ICSI cycles (2, 8). The presence of oocyte degeneration in a cohort of oocytes in conventional IVF cycles may adversely affect subsequent embryo development potential, and the cumulative live birth rate was also significantly lower in the DEG group than in the NON DEG group. These results together conferred that oocyte degeneration in conventional IVF cycles may adversely affect oocyte development potential and clinical outcomes.

Data availability statement

The original contributions presented in the study are included in the article/Supplementary Material. Further inquiries can be directed to the corresponding authors.

Ethics statement

The studies involving human participants were reviewed and approved by Ethical Committee of Medical College Xiamen University. Written informed consent for participation was not required for this study in accordance with the national legislation and the institutional requirements.

Author contributions

LL, JLC, and JR contribute to conception and design. JHC, CY, KC, and XY contribute to the acquisition of data. LL, XJ, and ZL contributed to the analysis and interpretation of data. All authors contributed to drafting the article or revising it critically for important intellectual content. All authors contributed to the article and approved the submitted version.

Funding

This work was supported by the National Natural Science Foundation of China (grant number 22176159) and the Xiamen medical advantage subspecialty construction project (grant number 2018296).

Acknowledgments

The authors thank all the staff in our center, especially the embryologists in our lab for their support in generating this manuscript. We would like to thank Xinli Wang for her assistance in the data processing.

Conflict of interest

The authors declare that the research was conducted in the absence of any commercial or financial relationships that could be construed as a potential conflict of interest.

Publisher's note

Supplementary material

The Supplementary Material for this article can be found online at: https://www.frontiersin.org/articles/10.3389/fendo.2023.1164371/full#supplementary-material

SUPPLEMENTARY TABLE S1
Original data was shown in Table S1.

SUPPLEMENTARY FIGURE S1
Distributions of the distances (propensity scores) before and after PS matching were plotted in Figure S1.

References

1. Rosen MP, Shen S, Dobson AT, Fujimoto VY, McCulloch CE, Cedars MI. Oocyte degeneration after intracytoplasmic sperm injection: a multivariate analysis to assess its importance as a laboratory or clinical marker. *Fertil Steril* (2006) 85(6):1736–43. doi: 10.1016/j.fertnstert.2005.12.017

2. E. S. I. Grp, E. S. I. Grp and M. Alpha Scientists Reprod. The Vienna consensus: report of an expert meeting on the development of art laboratory performance indicators. *Hum Reprod Open* (2017) 2017(2):494–510. doi: 10.1093/European/hox011

3. Lazzaroni-Tealdi E, Barad DH, Albertini DF, Yu Y, Kushnir VA, Russell H, et al. Oocyte scoring enhances embryo-scoring in predicting pregnancy chances with IVF where it counts most. *PloS One* (2015) 10(12):e0143632. doi: 10.1371/journal.pone.0143632

4. Oride A, Kawasaki H, Hara T, Ohta H, Kyo S. Characterization of oocyte retrieval cycles with empty zona pellucida. *Reprod Med And Biol* (2018) 17(1):71–6. doi: 10.1002/rmb2.12071

5. Rienzi L, Balaban B, Ebner T, Mandelbaum J. The oocyte. *Hum Reprod* (2012) 27:2–21. doi: 10.1093/humrep/des200

6. M. Alpha Scientists in Reproductive and E. S. Interest and E. Group of. The Istanbul consensus workshop on embryo assessment: proceedings of an expert meeting. *Hum Reprod (Oxford England)* (2011) 26(6):1270–83. doi: 10.1093/humrep/der037

7. Michaeli M, Atzmon Y, Poltov D, Rotfarb N, Lebovitz O, Aslih N, et al. Degenerated oocyte in the cohort adversely affects IVF outcome. *J Ovarian Res* (2020) 13(1):109–16. doi: 10.1186/s13048-020-00708-6

8. Liu L, Cai J, Li P, Jiang X, Ren J. Clinical outcome of cycles with oocyte degeneration after intracytoplasmic sperm injection. *Syst Biol In Reprod Med* (2017) 63(2):113–9. doi: 10.1080/19396368.2016.1272648

9. Liu L, Cai J, Chen J, Liu Z, Jiang X, Chen H, et al. : day-3-embryo fragmentation is associated with singleton birth weight following fresh single blastocyst transfer: a retrospective study. *Front Endocrinol* (2022) 2022:919283(13). doi: 10.3389/fendo.2022.919283

10. Cai J, Liu L, Zheng J, Zhang L, Jiang X, Li P, et al. Differential response of AMH to GnRH agonist among individuals: the effect on ovarian stimulation outcomes. *J Assisted Reprod Genet* (2018) 35(3):467–73. doi: 10.1007/s10815-017-1095-z

11. Lane M, Gardner DK, Stevens J, Schlenker T, Schoolcraft WB. Blastocyst score affects implantation and pregnancy outcome: towards a single blastocyst transfer. *Fertil Steril* (2000) 73(6):1155–8. doi: 10.1016/s0015-0282(00)00518-5

12. McLernon D, Maheshwari A, Bhattacharya S. Cumulative live birth rate: time for a consensus? *Hum Reprod* (2015) 30(12):2703–7. doi: 10.1093/humrep/dev263

13. Imai K, Ho DE, King G, Stuart EA. MatchIt: nonparametric preprocessing for parametric causal inference. *J Stat Software* (2011) 42(8):1–28. doi: 10.1186/s40246-018-0156-4

14. Greifer N. Cobalt: covariate balance tables and plots. In: *R package version 4.3.2* (2022). Available at: https://www.R-project.org/, 2023-2-10

15. Austin PC. An introduction to propensity score methods for reducing the effects of confounding in observational studies. *Multivar Behav Res* (2011) 46(3):399–424. doi: 10.1080/00273171.2011.568786

16. R. C. Team. R: a language and environment for statistical computing. In: *R foundation for statistical computing*. Vienna, Austria (2022). Available at: https://CRAN.R-project.org/package=cobalt. 2023-2-10

17. Wood SN. Fast stable restricted maximum likelihood and marginal likelihood estimation of semiparametric generalized linear models. *J R Stat Soc (B)* (2011) 73(1):3–36. doi: 10.1111/j.1467-9868.2010.00749.x

18. Liu Y, Hu X, Zhang X, Lee P, Wen Y, Ding C, et al. Oocyte degeneration after ICSI is not an indicator of live birth in young women. *Front Endocrinol* (2021) 12:705733. doi: 10.3389/fendo.2021.705733

19. Atzmon Y, Peer A, Aslih N, Bilgory A, Estrada D, Raya YSA, et al. Male Genome influences embryonic development as early as pronuclear stage. *Andrology* (2022) 10 (3):525–33. doi: 10.1111/andr.13133

20. Demir B, Cinar O, Dilbaz S, Saltek S, Aydin S, Goktolga U. Does empty zona pellucida indicate poor ovarian response on intra cytoplasmic sperm injection cycles? *Gynecol Endocrinol* (2012) 28(5):341–4. doi: 10.3109/09513590.2011.631632

21. Shi H, Zhao Z, Li J, Zhang Y, Chen C, Guo Y. Cumulative live birth rates according to the number of oocytes retrieved following the "freeze-all" strategy. *Reprod Biol Endocrinol* (2020) 18(1):14. doi: 10.1186/s12958-020-00574-3

22. Drakopoulos P, Polyzos NP, Parra J, Pellicer A, Santos-Ribeiro S, Tournaye H, et al. Cumulative live birth rates according to the number of oocytes retrieved after the first ovarian stimulation for *in vitro* fertilization/intracytoplasmic sperm injection: a multicenter multinational analysis including ~15,000 women. *Fertil Steril* (2018) 110 (4):661–70. doi: 10.1016/j.fertnstert.2018.04.039

23. Hill AB. The environment and disease: association or causation? *Proc R Soc Med* (1965) 58(5):295–300. doi: 10.1177/0141076814562718

24. Keefe D, Kumar M, Kalmbach K. Oocyte competency is the key to embryo potential. *Fertil Steril* (2015) 103(2):317–22. doi: 10.1016/j.fertnstert.2014.12.115

25. Bassil R, Casper RF, Mariano J, Smith R, Haas J, Mehta C, et al. Can oocyte diameter predict embryo quality? *Reprod Sci* (2021) 28(3):904–8. doi: 10.1007/s43032-020-00306-3

26. Yuan P, Guo Q, Guo H, Lian Y, Zhai F, Yan Z, et al. The methylome of a human polar body reflects that of its sibling oocyte and its aberrance may indicate poor embryo development. *Hum Reprod* (2021) 36(2):318–30. doi: 10.1093/humrep/deaa292

27. Bartolacci A, Intra G, Coticchio G, dell'Aquila M, Patria G, Borini A. Does morphological assessment predict oocyte developmental competence? a systematic review and proposed score. *J Of Assisted Reprod And Genet* (2022) 39(1):3–17. doi: 10.1007/s10815-021-02370-3

28. Faramarzi A, Khalili MA, Ashourzadeh S. Oocyte morphology and embryo morphokinetics in an intra-cytoplasmic sperm injection programme. is there a relationship? *Zygote* (2017) 25(2):190–6. doi: 10.1017/s0967199417000041

29. Bartolacci A, Buratini J, Moutier C, Guglielmo MC, Novara PV, Brambillasca F, et al. Maternal body mass index affects embryo morphokinetics: a time-lapse study. *J Assist Reprod Genet* (2019) 36(6):1109–16. doi: 10.1007/s10815-019-01456-3

30. Wang S, Wang J, Jiang Y, Jiang W. Association between blood lipid level and embryo quality during *in vitro* fertilization. *Medicine* (2020) 99(13):e19665. doi: 10.1097/md.0000000000019665

31. Cadoret V, Dalbies-Tran R, Desmarchais A, Elis Sébastien, Maillard V, Monget P, et al. A comparative analysis of oocyte development in mammals. *Cells* (2020) 9 (4):1002. doi: 10.3390/cells9041002

32. Palermo GD, Alikani M, Bertoli M, Colombero LT, Moy F, Cohen J, et al. Oolemma characteristics in relation to survival and fertilization patterns of oocytes treated by intracytoplasmic sperm injection. *Hum Reprod* (1996) 11(1):172–6. doi: 10.1093/oxfordjournals.humrep.a019012

33. Zhang C, Zhang Yu, Shu J, Guo J, Chang H-M, Leung PCK, et al. Adjuvant treatment strategies in ovarian stimulation for poor responders undergoing IVF: a systematic review and network meta-analysis. *Hum Reprod Update* (2020) 26(2):247–63. doi: 10.1093/humid/dmz046

34. Racca A, Martinez F, Rodríguez I, Polyzos NP. Ovarian stimulation for oocyte donation: a systematic review and meta-analysis. *Hum Reprod Update* (2021) 27 (4):673–96. doi: 10.1093/humid/dmab008

35. Liu B, Yang Y, Wu G, Yang J. Exploration of the value of progesterone and progesterone/estradiol ratio on the hCG trigger day in predicting pregnancy outcomes of PCOS patients undergoing IVF/ICSI: a retrospective cohort study. *Reprod Biol Endocrinol* (2021) 19(1):184. doi: 10.1186/s12958-021-00862-6

36. Li J, Liu Yu, Zhang W, Guo Y. Association between serum oestradiol level on the hCG administration day and neonatal birthweight after IVF-ET among 3659 singleton live births. *Sci Rep* (2021) 11(1):6084. doi: 10.1038/s41598-021-85692-7

37. Huang Z, Li J, Wang L, Yan J, Shi Y, Li S. Brief co-incubation of sperm and oocytes for *in vitro* fertilization techniques. *Cochrane Database Of Systematic Rev* (2013) 30(4):CD009391. doi: 10.1002/14651858.CD009391.pub2

38. Le Bras A, Hesters L, Gallot V, Tallet C, Tachdjian G, Frydman N. Shortening gametes co-incubation time improves live birth rate for couples with a history of fragmented embryos. *Syst Biol Reprod Med* (2017) 63(5):331–7. doi: 10.1080/19396368.2017.1336581

39. Liu H, He Y, Zheng H, Li Li, Fu X, Liu J. Effect of early cumulus cells removal and early rescue ICSI on pregnancy outcomes in high-risk patients of fertilization failure. *Gynecol Endocrinol* (2018) 34(8):689–93. doi: 10.1080/09513590.2018.1433159

40. Yin M, Kong P, Tang C, Zhu X, Bukulmez O, Chen M, et al. Effects of early cumulus cell removal on treatment outcomes in patients undergoing *In vitro* fertilization: a retrospective cohort study. *Endocrinol (Lausanne)* (2021) 12:669507 (1). doi: 10.3389/fendo.2021.669507

frontiers | Frontiers in Endocrinology

TYPE Original Research
PUBLISHED 22 June 2023
DOI 10.3389/fendo.2023.1119599

OPEN ACCESS

EDITED BY
Shunfeng Cheng,
Qingdao Agricultural University, China

REVIEWED BY
Guantai Ni,
First Affiliated Hospital of Wannan Medical College, China
Ferdinando Antonio Gulino,
Azienda di Rilievo Nazionale e di Alta Specializzazione (ARNAS) Garibaldi, Italy

*CORRESPONDENCE
Yonghong Lin
linyhcd2011@163.com
Zhenglin Yang
zliny@yahoo.com

†These authors have contributed equally to this work and share first authorship

RECEIVED 09 December 2022
ACCEPTED 09 June 2023
PUBLISHED 22 June 2023

CITATION
Yu X, He L, Lin W, Zheng X, Zhang L, Yu B, Wang Y, Yang Z and Lin Y (2023) Long-term menopause exacerbates vaginal wall support injury in ovariectomized rats by regulating amino acid synthesis and glycerophospholipid metabolism. *Front. Endocrinol.* 14:1119599. doi: 10.3389/fendo.2023.1119599

Long-term menopause exacerbates vaginal wall support injury in ovariectomized rats by regulating amino acid synthesis and glycerophospholipid metabolism

Xia Yu[1†], Li He[2†], Wenyi Lin[3†], Xuemei Zheng[2], Ling Zhang[2], Bo Yu[3], Yanjun Wang[2], Zhenglin Yang[4*] and Yonghong Lin[2*]

[1]Department of Clinical Laboratory, Chengdu Women's and Children's Central Hospital, Sichuan Provincial People's Hospital, School of Medicine, University of Electronic Science and Technology of China, Chengdu, Sichuan, China, [2]Department of Obstetrics and Gynecology, Chengdu Women's and Children's Central Hospital, School of Medicine, University of Electronic Science and Technology of China, Chengdu, Sichuan, China, [3]Department of Medical Pathology, Chengdu Women's and Children's Central Hospital, School of Medicine, University of Electronic Science and Technology of China, Chengdu, Sichuan, China, [4]Sichuan Provincial Key Laboratory for Human Disease Gene Study and Institute of Laboratory Medicine, Sichuan Provincial People's Hospital, University of Electronic Science and Technology of China, Chengdu, China

Purpose: Menopause is a risk factor for pelvic organ prolapse (POP) and is frequently associated with diminished vaginal wall support. To uncover relevant molecular mechanisms and provide potential therapeutic targets, we evaluated changes in the transcriptome and metabolome of the vaginal wall in ovariectomized rats to identify important molecular changes.

Methods: Sixteen adult female Sprague–Dawley rats were randomly assigned to either the control or menopause group. Seven months after the operation, hematoxylin and eosin (H&E) staining and Masson trichrome staining were used to observe changes in the rat vaginal wall structure. Differentially expressed genes (DEGs) and metabolites (DEMs) in the vaginal wall were detected by RNA-sequencing and LC–MS, respectively. Gene Ontology (GO) and Kyoto Encyclopedia of Genes and Genomes (KEGG) analyses of DEGs and DEMs were performed.

Results: We verified that long-term menopause causes vaginal wall injury by H&E and Masson trichrome staining. From the multiomics analyses, 20,669 genes and 2193 metabolites were identified. Compared with the control group, 3255 DEGs were found in the vaginal wall of long-term menopausal rats. Bioinformatics analysis showed that the DEGs were mainly enriched in mechanistic pathways, including cell–cell junction, extracellular matrix, muscle tissue developments, the PI3K-Akt signaling pathway, the MAPK signaling pathway, tight junctions and the Wnt signaling pathway. Additionally, 313 DEMs were found, and they consisted mostly of amino acids and their metabolites. DEMs were also enriched in mechanistic pathways, such as glycine, serine and threonine metabolism, glycerophospholipid metabolism, gap junctions and ferroptosis.

Coexpression analysis of DEGs and DEMs revealed that biosynthesis of amino acids (isocitric acid and *PKM*) and glycerophospholipid metabolism (1-(9Z-hexadecenoyl)-sn-glycero-3-phosphocholine and *PGS1*) are critical metabolic pathways, suggesting that POP induced by menopause may be associated with the regulation of these processes.

Conclusion: The findings showed that long-term menopause greatly exacerbated vaginal wall support injury by decreasing the biosynthesis of amino acids and interfering with glycerophospholipid metabolism, which may result in POP. This study not only clarified that long-term menopause exacerbates damage to the vaginal wall but also provided insight into the potential molecular mechanisms by which long-term menopause induces POP.

KEYWORDS

pelvic organ prolapse, menopause, vaginal wall, mechanical properties, transcriptomic, metabolomic

Introduction

Pelvic organ prolapse (POP) is a common pelvic floor dysfunction (PFD) that lowers the quality of life for almost half of all women globally. Increased life expectancy and efforts to improve quality of life have led to an increase in both the prevalence of POP and the number of women seeking medical attention for their symptoms, resulting in increased financial and medical costs (1). Between 2010 and 2050, the number of women in the United States who have POP is anticipated to rise by 46%, from 3.3 million to 4.9 million (2). In the United States, 10% - 20% of women have pelvic floor reconstruction surgery to cure prolapse (3); however, complications such mesh exposure and recurrence can still occur (4). Therefore, exploring the mechanism of action of POP is crucial for the development of new therapeutic strategies.

Postmenopausal, low-estrogen environments are a risk factor for the development of POP (5). As age increased from 20-29 years old to over 50 years old, the likelihood of experiencing symptomatic POP also increased. The odds ratio for symptomatic POP-Q stage II or higher rose from 1.34 (95% CI, 1.32-1.45) to 7.34 (95% CI, 4.34-12.41) (6). And the prevalence of symptomatic POP is 30% - 40% in postmenopausal women (5). According to these findings, the researchers further conducted estrogen supplementation therapy for postmenopausal patients with POP, but the clinical therapeutic effect remains controversial (7, 8). Therefore, it is urgent to elucidate the molecular mechanism of POP induced by low estrogen environment in order to find therapeutic targets.

Multiomics analysis methods can be applied to clarify the pathophysiology of disease and the underlying mechanisms (9). Moreover, gene expression profiles for the entire genome can be provided through transcriptomics. Metabolomics offers large-scale informative data about metabolic changes that reflect genetic, epigenetic, and environmental influences on cellular physiology. Transcriptomics and metabolomics have recently been employed to investigate the postmenopausal, low estrogen environment. Lu et al. found that the metabolic pathways of patients with premature ovarian insufficiency were abnormal, and some metabolites, such as fumarate, arachidonic acid and acetoacetic acid, were altered in the patient's serum. The DEGs that were found in patients with premature ovarian insufficiency were mainly associated with extracellular matrix (ECM)/structural organization, different types of junctions, and various catabolic/metabolic/biosynthetic processes. In addition, cytokine–cytokine receptor interactions, the PI3K-Akt signaling pathway, and the MAPK signaling pathway was also enriched, which have close regulatory effects on cellular mechanical properties (10, 11). Zhu et al. demonstrated that abnormal ECM synthesis and metabolism affected the pelvic support system, which led to the occurrence and progression of POP (12). Moreover, in our recent studies, we constructed focal adhesion signaling pathway-related ceRNA networks in POP by transcriptome analysis, which were found to be associated with mechanical properties (13). We also revealed that abnormal metabolic regulatory pathways and gene transcription expression were closely related to the occurrence of POP on the uterosacral ligaments (14). However, the genetic transcription and metabolic effects of prolonged menopause on the vaginal wall tissue, an important part of the pelvic floor support structure, have not been elucidated.

In this study, to address these issues, we constructed an animal model of POP by removing both ovaries in rats and used a postoperative care period of up to seven months to create a long-term menopausal environment, followed by a multiomic analysis of the rat vaginal wall tissue including transcriptomics and metabolomics. To our knowledge, this is the first study to use a multiomics analysis to investigate the specific mechanism by which prolonged menopause exacerbates support damage to the vaginal wall in rats and to provide targets that may interfere with the occurrence of POP.

Materials and methods

Animals and ovariectomy surgery

Female Sprague–Dawley rats weighing between 190 and 220 g and two months old were purchased from the Chengdu Dashuo Laboratory Animal Co., Ltd. Individually housed rats were kept in a specific pathogen-free environment with free access to food and water in a 12:12 light:dark cycle and a temperature range of 22–26°C and humidity range of 45–55%. The ethics committee of the Chengdu Women's and Children's Central Hospital approved the use of lab animals for our research objectives in accordance with the guidelines from the Animal Experimental Center.

The rats were randomly assigned to either the control group (Con, n=8) or the menopausal group (Meno, n=8) after a week of acclimation. An intraperitoneal injection of 1% pentobarbital sodium (0.4 mL/100 g) was used to anesthetize the rats. A 2-cm ventral midline incision was performed in the upper abdomen while the area was sterile. Bilateral ovaries were removed from the Meno group. The ovaries in the control group were exposed but not removed. After seven months of postoperative care, as shown in Figure 1, the rats were sacrificed.

Sample collection

The rats were sacrificed, and whole blood retrieved by direct cardiac puncture was used to measure serum estrogen. Approximately 4 mm of vaginal wall tissue close to the cervix was incised, fixed in 10% neutral buffered formalin and embedded in paraffin for histological tests. Transcriptomics and metabolomics investigations were conducted on the remaining tissue. Prior to analysis, each sample was kept at -80°C.

Serum estrogen measurements

Following the ovariectomy, the serum E2 levels were measured seven months later through enzyme-amplified chemiluminescence using the collected blood samples (Atellica IM1600, Siemens). Estradiol and progesterone assay analytical sensitivity limits were 15 pg/mL (references range of 20-2000 pg/mL).

H&E and Masson trichrome staining

For the morphological analysis, a 3-μm thick cross-section of a paraffin-embedded vaginal wall tissue from each group was stained with Masson trichrome and H&E. The samples were scanned using the K-Viewer (1.7.0.23) X64 digital pathology scanning system at magnifications of ×4 and ×10.

Transcriptome sequencing and data analysis

Total RNA was extracted from the samples using TRIzol reagent (Invitrogen, USA). An Agilent 5400 system (Agilent Technologies, USA) was used to measure RNA concentrations and integrity. The RNA sample preparations used a total of 1 g of RNA per sample as input material. Metware Biotechnology Co., Ltd. (Wuhan, China) prepared the cDNA libraries for sequencing on the Illumina Novaseq 6000 using the NEBNext®Ultra RNA Library Prep Kit. To filter the original data, fastp v 0.23.2 was used. Reads with adapters, sequences with more than 10% unknown nucleotides (N), and a quality rating of less than 50% (Q-value ≤20) were removed.

Clean reads served as the foundation for all further analyses. HISATv2.1.0 software was used to build the index, download the reference genome Rnor6.0.103 (http://ftp.ensembl.org/pub/release-103/fasta/rattusnorvegicus/) and associated annotation files, and compare clean reads to the reference genome. The length of each gene and the number of reads mapped to it were used to compute the FPKM of each gene. Using DESeq2 software (v1.22.1), the differential expression between the two groups was examined. DEGs were defined as genes with |log2FC| > 1 and q-value < 0.05. We used KEGG pathway analysis and GO functions to estimate the potential biological roles of the DEGs, the clusterProfiler R package (v3.14.3) was employed.

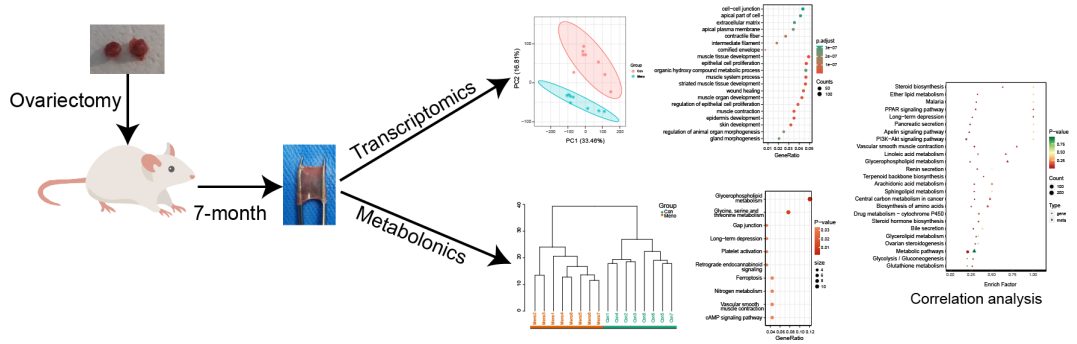

FIGURE 1
The research strategy adopted in the present study.

Metabolite profiling analysis

MetWare (Wuhan, China) carried out the extract analysis, metabolite identification, and quantification in accordance with their established practices and earlier research [14]. After the raw data had been processed, the unique metabolites for the two-group analysis were identified using the absolute VIP (VIP ≥ 1), *P*-value ($p < 0.05$, Student's t test), and absolute Log2FC (|Log2FC| ≥ 1.0) values.

Coexpression network analysis of the metabolome and transcriptome

According to the fold changes of each DEG and each DEM, the Pearson correlation coefficients were calculated using the EXCEL application. Correlations with coefficients of $R^2 > 0.8$ were chosen.

Results

Estrogen concentrations decrease during prolonged menopause

To verify the effect of ovariectomies on estrogen levels, we analyzed serum estrogen concentrations in rats seven months after ovariectomies by chemiluminescence. The blood levels of estrogen in the control group fluctuated within a normal range (38.13 pg/ml - 75.74 pg/ml), but seven months after ovariectomy, they plummeted to a low level (18.86 pg/ml - 33.74 pg/ml), and there was a significant difference between the two groups ($p < 0.001$) (Figure 2). Therefore, vaginal wall tissues from the menopause group and the control group seven months after surgery were selected as material samples for transcriptomic and metabolomic analysis.

Histological staining revealed abnormal vaginal wall tissue structure

As shown in Figure 3, H&E and Masson's trichrome staining were used to evaluate the histology of the vaginal wall and to examine the histopathological changes in the tissue after long-term menopause. In the control group, the vaginal epithelial layer was abundant, collagen deposition was dense in the lamina propria, the normal orderly arrangement of smooth muscle layers was maintained, the muscle cells were clearly outlined, and there was a thick adventitia layer. However, in the Meno group, histological analysis showed a significant reduction in the thickness of the vaginal epithelial layer, a sparse state of collagen deposition in the lamina propria, a disordered arrangement of smooth muscle with a significantly reduced content, and the adventitia layer became thinner. Therefore, long-term menopause weakens the tissue structure of the vaginal wall, resulting in a decline from the epithelial layer to the adventitia layer, which exacerbates the decline in the support capacity of the vaginal wall.

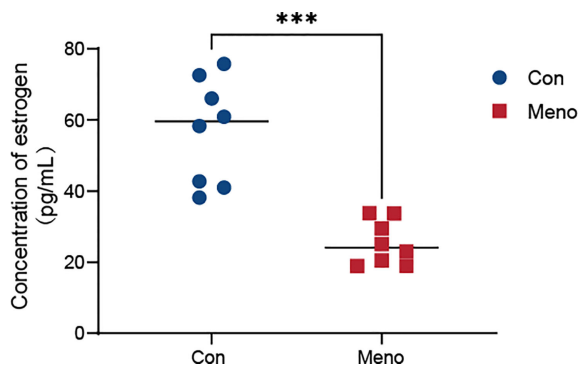

FIGURE 2
Serum estrogen levels in the Con group and the Meno group (n=8, ***$P < 0.001$).

Transcriptome analysis reveals altered molecular expression of vaginal wall tissue in rats after long-term menopause

To explore the molecular events occurring in the vaginal wall of long-term postmenopausal rats, transcriptome analysis was performed on vaginal wall tissue in rats seven months after ovary removal (Meno) and without ovary removal (Con). After removing the low-quality reads, a total of 721,846,394 clean reads were obtained. The percentages of Q30 and GC were 90.94–92.02% and 47.86–50.59%, respectively, indicating that the transcriptome sequencing data was high quality. The PCA results showed that the transcriptome of the Meno group was very different from that of the control group (Figure 4A). A total of 20,669 genes were functionally annotated in the databases (Additional file 1). Moreover, 3255 (1677 up- and 1578 down-regulated) DEGs (| fold change| > 2 and q-value < 0.05) were identified in the comparison of Con vs. Meno (Figures 4B, C) (Additional file 2). Overall, the results suggested that long-term menopause can induce transcriptional changes in the vaginal parietal tissue. The raw data can be found at https://www.ncbi.nlm.nih.gov/geo/query/acc.cgi?acc=GSE220515.

Functional analysis of DEGs in pathways related to mechanical properties

To further evaluate the biological functions of the DEGs in the vaginal wall tissue of long-term menopausal rats, we performed Gene Ontology (GO) and Kyoto Encyclopedia of Genes and Genomes (KEGG) enrichment analyses (Additional File 3). The results showed that the GO terms significantly enriched by the DEGs in the Meno group vs. the Con group were closely related to mechanical properties, including cell–cell junction, apical part of cell, extracellular matrix, muscle tissue developments, and epithelial cell proliferation (Figure 4D). The KEGG pathway analysis of the DEGs in the Meno group vs. the Con group also exhibited signaling pathways related to mechanical properties, including the PI3K-Akt signaling pathway, the MAPK signaling pathway, cytokine–cytokine receptor interaction, calcium signaling pathways, tight junctions and the Wnt signaling pathway (Figures 4E). Therefore, the results showed that long-term menopause can regulate complex biological pathways related to the mechanical support of vaginal wall tissue.

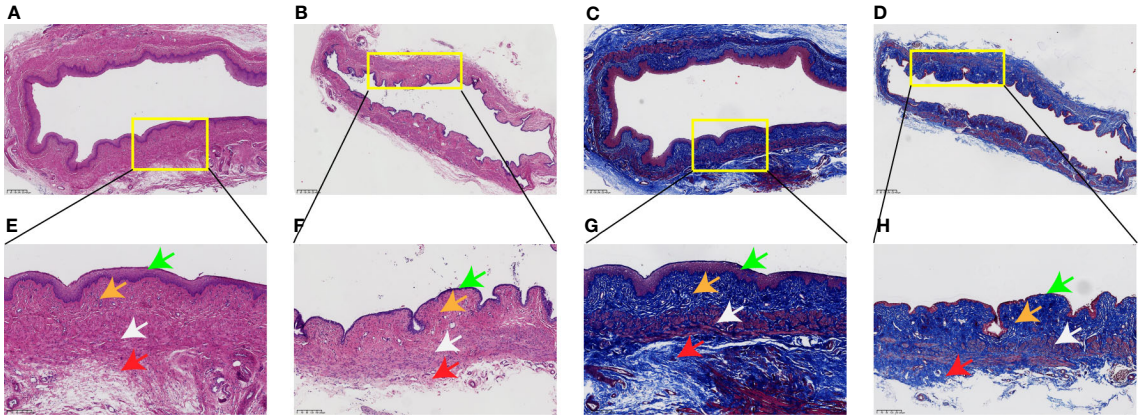

FIGURE 3
Rat vaginal wall tissue stained with H&E and Masson's trichrome. H&E staining of the Con group **(A)** ×4, **(E)** ×10, and Meno group **(B)** ×4, **(F)** ×10. Masson's trichrome staining of the Con group **(C)** ×4, **(G)** ×10, and Meno group **(D)** ×4, **(H)** ×10. Epithelial layer (green arrows), lamina propria (orange arrows), muscle layers (white arrows) and adventitia layer (red arrows).

Metabolomic analysis reveals disturbances in amino acid synthesis and metabolites associated with mechanical pathways

For further analysis of metabolites of long-term menopausal rat vaginal wall tissue, untargeted (global) metabolomics using liquid chromatography high-resolution mass spectrometry (LC–MS) was carried out to obtain a comprehensive comparative analysis of metabolites. A total of 2193 metabolites were obtained in all samples (Additional File 4) and clearly divided into two groups based on PCA (Figure 5A). The orthogonal partial least squares discriminant analysis (OPLS-DA) model was then used to further investigate the DEMs between the groups. The OPLS-DA results show that the Meno and Con groups are scattered in two different

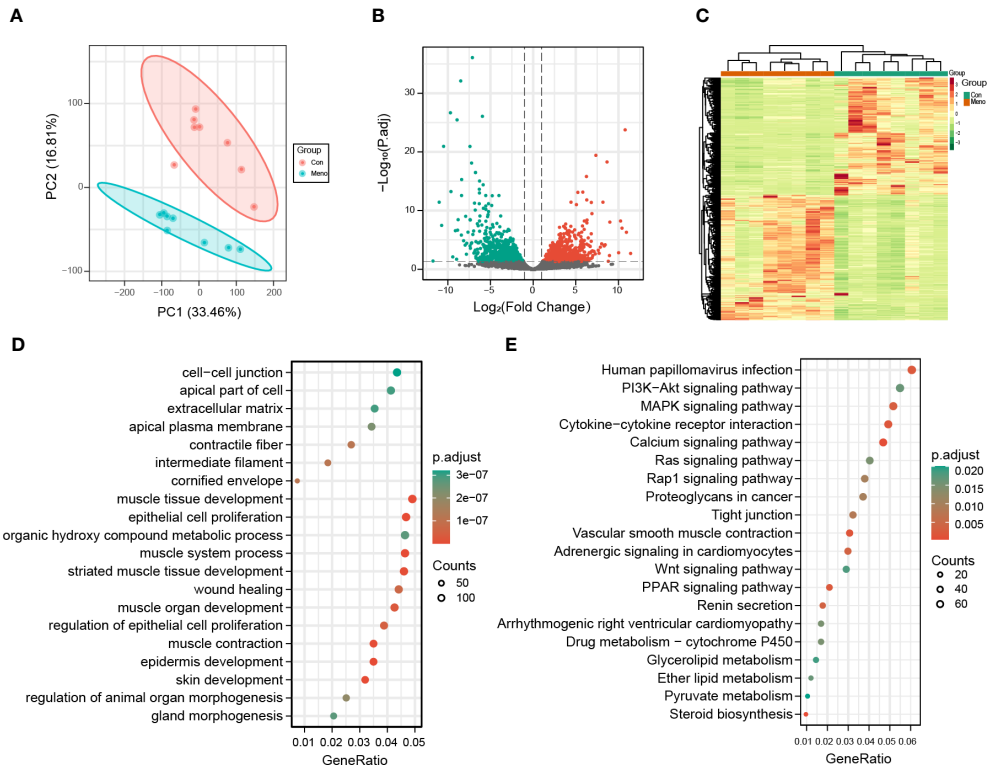

FIGURE 4
Transcriptomic analysis of the Con and Meno groups. **(A)** PCA plots of the two groups. **(B)** Volcanic distribution maps of the Con group and Meno groups. **(C)** Heatmaps of significant differentially expressed genes. **(D-E)** Bubble plots showing GO and KEGG enrichment analysis pathways of differentially expressed genes.

geographic regions (Figure 5B). The OPLS-DA model has a satisfactory fit, strong predictive power, goodness-of-fit and predictive power values (R^2X = 0.453, R^2Y = 0.996, Q^2 = 0.84, p < 0.005) (Figure 5C). We also carried out cluster analysis on 16 samples. The samples that clustered together showed higher similarity among the samples, as shown in Figure 5D. Based on the VIP > 1 and *P value* < 0.05, the number of upregulated and downregulated metabolites in the Meno group vs. the Con group was 119 and 194, respectively (Figure 5E) (Additional File 5). The was nearly perfect separation between the Meno group and the Con group. Then, these DEMs were summarized into 20 groups, mainly divided into amino acids and their metabolites (46), benzene and substituted derivatives (38), heterocyclic compounds (37), organic acids and their derivatives (33), FA (30), alcohols and amines (28) and others (Figure 5F). After qualitative and quantitative analysis of the detected amino acids and their metabolites, we combined the groups and showed the differential fold changes between amino acids and their metabolites in the two groups, as shown in Figure 5G. The histogram showed that the expression of more than 30 amino acids and their metabolites in the Meno group were reduced compared to those in the Con group. This suggests that prolonged menopause leads to a significant decrease in amino acid synthesis. Similarly, the top 10 KEGG enrichment analyses showed that the DEMs were associated with glycine, serine and threonine metabolism (Figure 5H) (Additional File 6). In addition, the most obvious pathway of DEM enrichment was glycerophospholipid metabolism, which is closely related to cellular mechanical properties. Moreover, the DEMs were also enriched in other pathways associated with mechanical properties, including gap junctions and ferroptosis. The results showed that long-term menopause can induce changes in metabolites involved in cellular mechanical properties.

Coexpression analysis of DEGs and DEMs revealed that the decreased mechanical support of the vaginal wall was closely related to biosynthesis of amino acids and glycerophospholipid metabolism

To investigate the relationship between the DEGs and DEMs in the vaginal wall tissues of rats experiencing long-term menopause, a coexpression analysis was carried out and displayed by a nine-quadrant plot (Figure 6A) (Pearson correlation coefficient > 0.8, p < 0.05; Additional File 7). The lower left quadrant results showed that the proportion of positively correlated substances with decreased gene expression and decreased metabolite expression accounted for most of the DEGs and DEMs. The KEGG pathway coenriched by the two omics was used to draw the bubble map, and the results showed that the DEGs and DEMs were significantly enriched in biosynthesis of amino acids and glycerophospholipid metabolism (Figure 6B). Then, the results of a canonical correlation analysis (CCA), a multivariate statistical analysis technique that uses the correlation between pairs of comprehensive variables to reflect the overall correlation between two groups, revealed DEGs and DEMs play a role in the biosynthesis of amino acids and glycerophospholipid metabolism (Figures 6C, F). In addition, the role of DEGs and DEMs in the biosynthesis of amino acids and glycerophospholipid metabolism was further investigated and significantly correlations were found between isocitric acid and *PKM*, 1-(9Z-hexadecenoyl)-sn-glycero-3-phosphocholine and *PGS1*, respectively. Therefore, we further investigated the expression of isocitric acid, *PKM*, 1-(9Z-hexadecenoyl)-sn-glycero-3-phosphocholine and *PGS*, and their expression was reduced in the long-term menopausal state (Figures 6D, E, G, H). The integrated analysis of transcriptomics

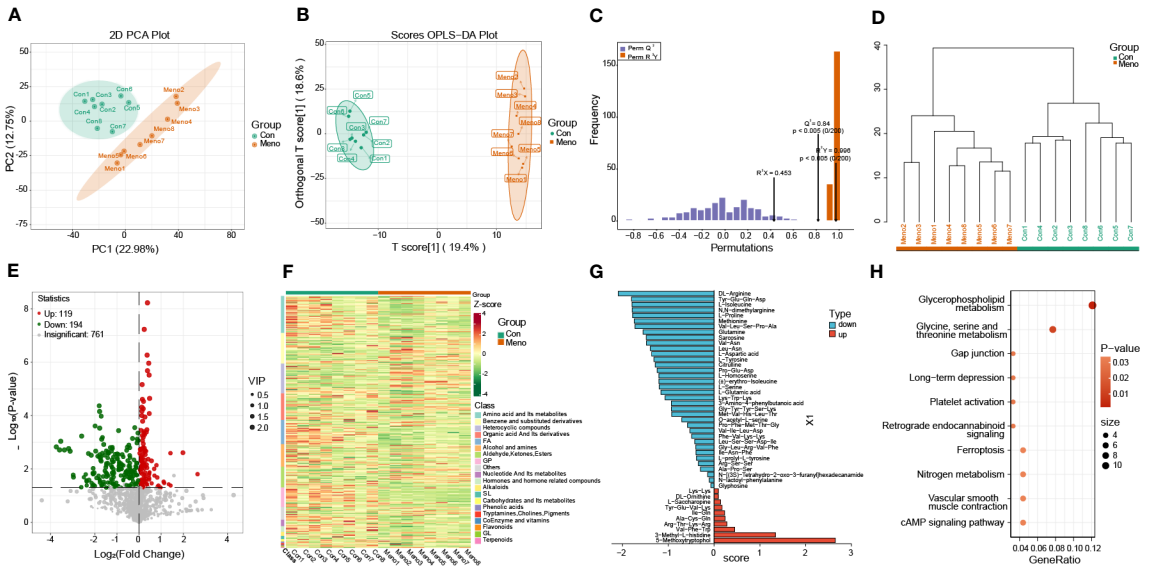

FIGURE 5
Metabolomics analysis of the Con and Meno groups. **(A)** PCA plot of the two groups. **(B)** The OPLS-DA score plot and **(C)** OPLS-DA model test chart demonstrated favorable discrimination between the Con and Meno groups, R^2X=0.453, R^2Y=0.996, Q^2 = 0.84, p < 0.05. **(D)** Cluster analysis plot of differentially expressed metabolites (DEMs) in the Con and Meno groups. **(E, F)** Volcano map and heatmap of the DEMs in the Con vs. Meno groups. **(G)** OPLS-DA model shows fold changes in the expression of amino acids and their metabolism between the two groups. **(H)** Bubble plot showing pathway enrichment analysis related to DEGs in the Con and Meno groups.

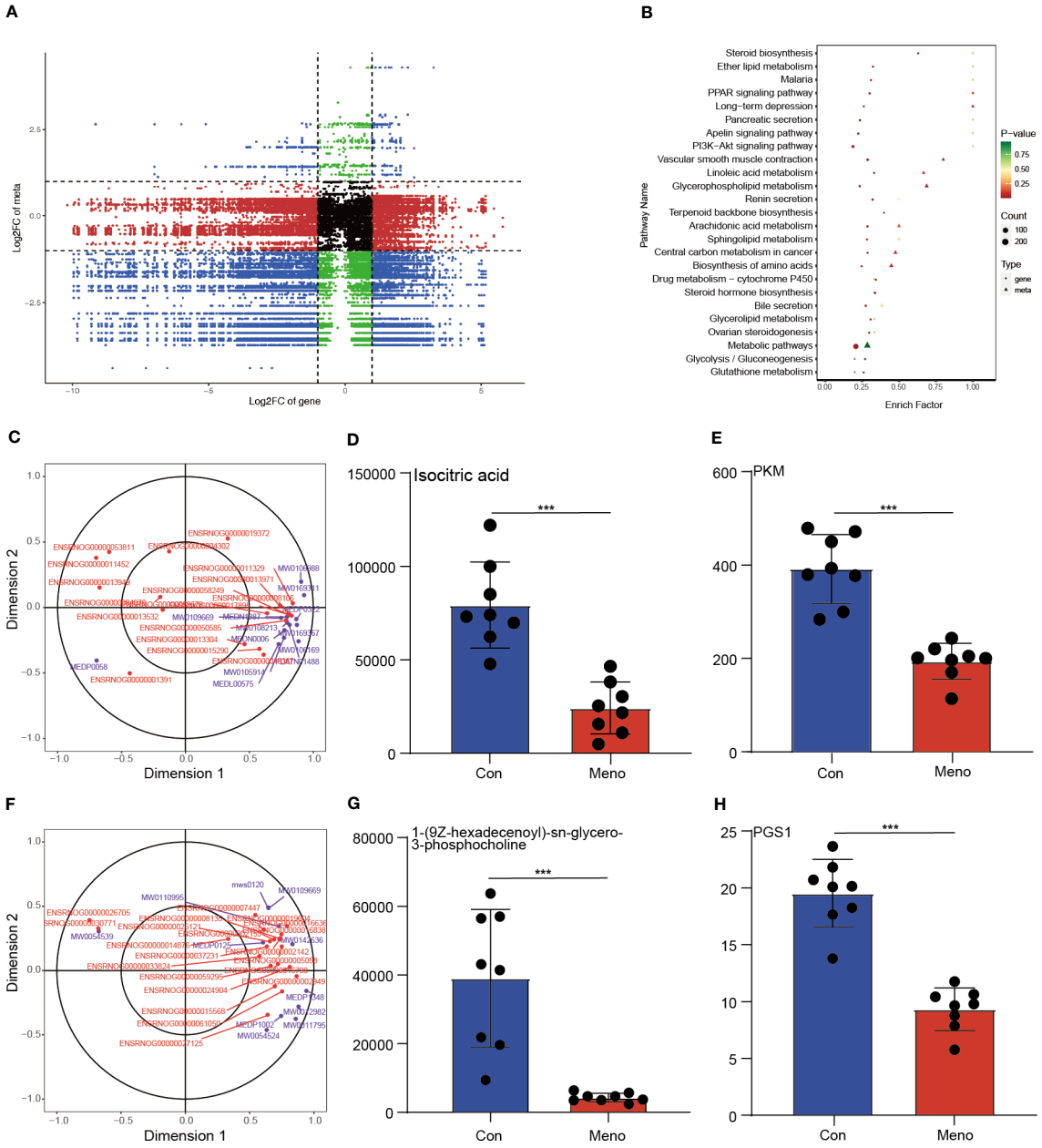

FIGURE 6
Integration of the transcriptome and metabolomic data analysis. **(A)** The nine-quadrant plot shows the coexpression analysis of DEGs and DEMs. **(B)** The bubble chart shows the common enriched pathways of DEGs and DEMs. Canonical correlation analysis (CCA) results reveal the role of DEGs and DEMs in amino acid biosynthesis **(C)** and glycerophospholipid metabolism **(F)**. The histogram shows the expression levels of isocitric acid **(D)**, *PKM* **(E)**, 1-(9Z-hexadecenoyl)-sn-glycero-3-phosphocholine **(G)** and *PGS1* **(H)** in the Con and Meno groups (n=8, ***$P < 0.001$).

and metabolomics further revealed that the decreased mechanical support of vaginal wall tissue in rats during long-term menopause was closely related to the biosynthesis of amino acids and glycerophospholipid metabolism.

Discussion

In this study, to explore the impact of long-term menopause on POP and to provide possible therapeutic targets, we used a comprehensive analysis of transcriptomics and metabolomics to investigate the changes in the vaginal wall in a rat model with bilateral ovary removal after a postoperative care period of seven months. The results showed that long-term menopause can exacerbate the decreased vaginal wall support, mainly through interference with the biosynthesis of amino acids and glycerophospholipid metabolism, which are involved in the occurrence of POP.

To determine the successful establishment of a POP animal model by bilateral ovariectomy in rats, serum estrogen levels were measured and the pathological structure of the rat vaginal wall tissue was detected. Consistent with previous reports, the serum

estrogen level in rats seven months after bilateral oophorectomy was significantly lower than that of the control group (15), and the structure of the vaginal wall was also abnormal. The pathological results showed that long-term menopause resulted in thinning of the vaginal wall (16). Moreover, a sparse state of collagen deposition and a disordered arrangement of smooth muscle with a significantly reduced content were found. According to a report on the biaxial mechanical response, these changes in the vaginal wall reduced maximum muscle tone (17).

To investigate the potential mechanism by which prolonged menopause affects the mechanical properties of the vaginal wall, we compared the transcription profiles of the Con group and Meno group vaginal wall tissues to identify DEGs. GO and KEGG pathway enrichment analyses indicated that these DEGs had notable correlations with cellular mechanical pathways, including extracellular matrix, cell–cell junctions, muscle tissue developments, the PI3K-Akt signaling pathway, the MAPK signaling pathway, tight junctions and the Wnt signaling pathway. The ECM is a highly dynamic structure that is present in all tissues and continuously undergoes controlled remodeling. In addition to serving as a structural support for tissue elasticity and integrity, the ECM also functions to communicate mechanical signals to cells that control adhesion, migration, proliferation, and apoptosis within the matrix. These signals are transmitted by ECM constituents acting as ligands for cell receptors such as integrins (18). Several studies have reported the use of ECM remodeling to construct animal models of POP (19–21) and the selection of ECM remodeling as a therapeutic target (22). Moreover, the site of cell-ECM adhesion is limited by the application of fibronectin micropatterns. According to Théry et al., the ECM has an impact on the strength of intra- and intercellular forces as well as the stability of cell–cell junction placement (23). The tight junction and cell–cell junction molecular landscapes are diverse, containing transmembrane proteins that form intercellular bonds and a variety of cytoplasmic proteins that remodel the junctional connection to the cytoskeleton and transform mechanical cues into cellular responses (24), which involve the PI3K-Akt signaling pathway (25), MAPK signaling pathway (26) and Wnt signaling pathway (27). In addition, using single-cell RNA-seq analysis, Zhu et al. also showed dysregulation of the ECM and cell-cell communication patterns in the prolapse of the anterior vaginal wall (28). In POP samples, the interactions of smooth muscle cells with fibroblasts and macrophages were increased, which may affect tissue regeneration, such as muscle tissue development and matrix organization. In addition, in the process mechanical transduction pathway signaling, the metabolism of substances is an important biological process for the production of biosynthetic macromolecules (29). Additionally, Alarab et al. discovered that menopause affects the genes involved in the metabolism of the vaginal extracellular matrix (30). The unnatural accumulation of numerous significant metabolites that profoundly affected cellular function was caused by disorganized metabolic processes.

Herein, untargeted metabolomics was used to further investigate the decreased mechanical support of the vaginal wall in rats with prolonged menopause. From our data, the expression of more than 30 amino acids and their metabolites in the Meno group was reduced compared to that in the Con group, and DEMs were also mainly enriched in cellular mechanic-related pathways, such as glycine, serine and threonine metabolism, glycerophospholipid metabolism, gap junctions and ferroptosis. Collagen, the most abundant protein in the body, is necessary to preserve the ECM's structure and strength, and glycine, proline, and hydroxyproline (Hyp) make up 57% of t collagen's overall amino acid content (AAs) (31). Long-term menopause decreases the expression of amino acids and their metabolites, especially those involved in glycine, serine and threonine metabolism, which are closely related to ECM remodeling and leads to gap junction disturbances. Glycerophospholipid metabolism is closely related to the formation of cell membranes, in which many biological processes take place through mechanical signaling (32). Ferroptosis is closely associated with amino acid, lipid, and iron metabolism. The formation of cell–cell contacts in epithelial cell monolayers is thought to improve resistance to ferroptosis induction (33). Our findings show significant thinning of the vaginal epithelial layer after long-term menopause; however, more studies are needed to confirm whether this change promotes ferroptosis and leads to POP. At present, this is the first study to suggest that ferroptosis may be related to the occurrence of POP.

Furthermore, this study integrated transcriptome and metabolome data from our biological model, and revealed a significant correlation between the DEGs and DEMs that is associated with amino acid biosynthesis and glycerophospholipid metabolism. Additionally, isocitric acid and *PKM*, 1-(9Z-hexadecenoyl)-sn-glycero-3-phosphocholine and *PGS1* were found to have the highest correlation in these pathways. Yan et al. reported that modulation of *PKM* splicing inhibited hepatocyte metabolic reprogramming and could be a target for the treatment of hepatocellular carcinoma (34). However, the *PKM* as a target for the treatment of POP needs to be further explored. In our previous studies of the uterosacral ligaments in patients with POP, we also reported that *PGS1* was involved in glycerophospholipid metabolism alterations (14). The uterosacral ligaments and the vaginal wall are both important tissues that make up the pelvic floor support, and abnormal expression of *PGS1* was found in both of these tissues, so *PGS1* may be an important target for the treatment of POP.

Although this study found the DEGs, DEMs and related enrichment pathways that were involved in the decreased vaginal wall support in rats during long-term menopause, this study has limitations. First, the animal model of POP created by bilateral ovariectomy of rats does not accurately represent the characteristics of clinical POP patients. Follow-up studies require the collection of tissue from a large sample of POP patients to determine more representative results. Second, there was a lack of estrogen supplementation in this experiment, and there was a lack of strong evidence to determine whether the screened DEGs and DEMs could be used as therapeutic targets. Therefore, studies need to further investigate the DEGs and DEMs to clarify their

potential as therapeutic targets for POP. In addition, this research demonstrated the enrichment of molecular pathways of the DEGs and DEMs, such as the Wnt signaling pathway. However, more cell experiments are needed to confirm whether these pathways play a crucial role in the occurrence of POP caused by long-term menopause.

In summary, we used transcriptome and untargeted metabolome analyses to comprehensively analyze the gene expression profiles and metabolic profiles involved in the development of POP due to prolonged menopause, which leads to decreased vaginal wall support. According to our findings, long-term menopause alters the expression of genes associated with mechanical properties in the vaginal wall and the levels of multiple metabolites involved in various metabolic pathways. In addition, correlation analysis showed that multiple DEGs were substantially associated with DEMs. Together, these studies may provide a new understanding of the underlying mechanisms driving menopausal-induced POP, particularly in exacerbating vaginal wall support injury, and the findings can also be used to target molecular interventions for POP using drug-available gene databases. More research is needed to clarify the mechanism of interaction between differential gene expression in vaginal walls and its associated key metabolites, as well as to evaluate its potential as a therapeutic target for POP.

Data availability statement

The original contributions presented in the study are publicly available. This data can be found here: https://www.ncbi.nlm.nih.gov/geo/query/acc.cgi?acc=GSE220515.

Ethics statement

The animal study was reviewed and approved by the ethics committee of the Chengdu Women's and Children's Central Hospital.

Author contributions

ZY and YL: conceptualization, supervision. XY: methodology, writing-original draft preparation, data curation, visualization. LH and WL: methodology, data curation, writing - reviewing and editing. LZ: formal analysis. XZ, BY and YW: methodology, data curation. All authors have read and approved the content of the manuscript.

Funding

This project was supported by Natural Science Foundation of Sichuan Province [grant number 2022NSFSC0815], Sichuan Medical Health and Health Promotion Association [grant number KY2022SJ0015], Youth Innovation Foundation of Sichuan Provincial Medical [grant number Q21060], the Yingcai Scheme, Chengdu Women's and Children's Central Hospital [grant number YC2021004 and YC2022001].

Acknowledgments

We thank AJE Academic Services (https://www.aje.cn) for English-language editing and review services.

Conflict of interest

The authors declare that the research was conducted in the absence of any commercial or financial relationships that could be construed as a potential conflict of interest.

Publisher's note

Supplementary material

The Supplementary Material for this article can be found online at: https://www.frontiersin.org/articles/10.3389/fendo.2023.1119599/full#supplementary-material

References

1. Wang B, Chen Y, Zhu X, Wang T, Li M, Huang Y, et al. Global burden and trends of pelvic organ prolapse associated with aging women: an observational trend study from 1990 to 2019. *Front Public Health* (2022) 10:975829. doi: 10.3389/fpubh.2022.975829

2. Wu JM, Hundley AF, Fulton RG, Myers ER. Forecasting the prevalence of pelvic floor disorders in U.S. women: 2010 to 2050. *Obstet Gynecol* (2009) 114:1278–83. doi: 10.1097/AOG.0b013e3181c2ce96

3. Wilkins MF, Wu JM. Lifetime risk of surgery for stress urinary incontinence or pelvic organ prolapse. *Minerva Ginecol* (2017) 69:171–7. doi: 10.23736/S0026-4784.16.04011-9

4. Lallemant M, Clermont-Hama Y, Giraudet G, Rubod C, Delplanque S, Kerbage Y, et al. Long-term outcomes after pelvic organ prolapse repair in young women. *J Clin Med* (2022) 11:6112. doi: 10.3390/jcm11206112

5. Tinelli A, Malvasi A, Rahimi S, Negro R, Vergara D, Martignago R, et al. Age-related pelvic floor modifications and prolapse risk factors in postmenopausal women. *Menopause* (2010) 17:204–12. doi: 10.1097/gme.0b013e3181b0c2ae

6. Pang H, Zhang L, Han S, Li Z, Gong J, Liu Q, et al. A nationwide population-based survey on the prevalence and risk factors of symptomatic pelvic organ prolapse in adult women in China - a pelvic organ prolapse quantification system-based study. *BJOG* (2021) 128:1313–23. doi: 10.1111/1471-0528.16675

7. Vodegel EV, Zwolsman SE, Vollebregt A, Duijnhoven RG, Bosmans JE, Speksnijder L, et al. Cost-effectiveness of perioperative vaginally administered estrogen in postmenopausal women undergoing prolapse surgery (EVA trial): study protocol for a multicenter double-blind randomized placebo-controlled trial. *BMC Womens Health* (2021) 21:439. doi: 10.1186/s12905-021-01587-9

8. Marschalek M-L, Bodner K, Kimberger O, Morgenbesser R, Dietrich W, Obruca C, et al. Sexual function in postmenopausal women with symptomatic pelvic organ prolapse treated either with locally applied estrogen or placebo: results of a double-masked, placebo-controlled, multicenter trial. *J Sexual Med* (2022) 19:1124–30. doi: 10.1016/j.jsxm.2022.04.007

9. Yang L, Yang Y, Huang L, Cui X, Liu Y. From single- to multi-omics: future research trends in medicinal plants. *Brief Bioinform* (2023) 24:bbac485. doi: 10.1093/bib/bbac485

10. Metsiou DN, Deligianni D, Giannopoulou E, Kalofonos H, Koutras A, Athanassiou G. Adhesion strength and anti-tumor agents regulate vinculin of breast cancer cells. *Front Oncol* (2022) 12:811508. doi: 10.3389/fonc.2022.811508

11. Li Z, Peng F, Liu Z, Li S, Li L, Qian X. Mechanobiological responses of astrocytes in optic nerve head due to biaxial stretch. *BMC Ophthalmol* (2022) 22:368. doi: 10.1186/s12886-022-02592-8

12. Li L, Ma Y, Yang H, Sun Z, Chen J, Zhu L. The polymorphisms of extracellular matrix-remodeling genes are associated with pelvic organ prolapse. *Int Urogynecol J* (2022) 33:267–74. doi: 10.1007/s00192-021-04917-5

13. Yu X, He L, Chen Y, Lin W, Liu H, Yang X, et al. Construction of a focal adhesion signaling pathway-related ceRNA network in pelvic organ prolapse by transcriptome analysis. *Front Genet* (2022) 13:996310. doi: 10.3389/fgene.2022.996310

14. Yu X, Chen Y, He L, Liu H, Yang Z, Lin Y. Transcriptome and metabolome analyses reveal the interweaving of immune response and metabolic regulation in pelvic organ prolapse. *Int Urogynecol J* (2022) [Online ahead of print]. doi: 10.1007/s00192-022-05357-5

15. Zhang W, Wu H, Xu Q, Chen S, Sun L, Jiao C, et al. Estrogen modulation of pain perception with a novel 17beta-estradiol pretreatment regime in ovariectomized rats. *Biol Sex Differ* (2020) 11:2. doi: 10.1186/s13293-019-0271-5

16. You S, Liu S, Dong X, Li H, Zhu Y, Hu L. Intravaginal administration of human type III collagen-derived biomaterial with high cell-adhesion activity to treat vaginal atrophy in rats. *ACS Biomater Sci Eng* (2020) 6:1977–88. doi: 10.1021/acsbiomaterials.9b01649

17. Clark GL, Pokutta-Paskaleva AP, Lawrence DJ, Lindsey SH, Desrosiers L, Knoepp LR, et al. Smooth muscle regional contribution to vaginal wall function. *Interface Focus* (2019) 9:20190025. doi: 10.1098/rsfs.2019.0025

18. Bonnans C, Chou J, Werb Z. Remodelling the extracellular matrix in development and disease. *Nat Rev Mol Cell Biol* (2014) 15:786–801. doi: 10.1038/nrm3904

19. Liu X, Zhao Y, Gao J, Pawlyk B, Starcher B, Spencer JA, et al. Elastic fiber homeostasis requires lysyl oxidase-like 1 protein. *Nat Genet* (2004) 36:178–82. doi: 10.1038/ng1297

20. Rahn DD, Acevedo JF, Roshanravan S, Keller PW, Davis EC, Marmorstein LY, et al. Failure of pelvic organ support in mice deficient in fibulin-3. *Am J Pathol* (2009) 174:206–15. doi: 10.2353/ajpath.2009.080212

21. Budatha M, Roshanravan S, Zheng Q, Weislander C, Chapman SL, Davis EC, et al. Extracellular matrix proteases contribute to progression of pelvic organ prolapse in mice and humans. *J Clin Invest* (2011) 121:2048–59. doi: 10.1172/JCI45636

22. Gudde AN, van Velthoven MJJ, Roovers JWR, Kouwer PHJ, Guler Z. Polyisocyanides as a substrate to trigger vaginal fibroblast functioning in an *in vitro* model for prolapse repair. *Biomater Adv* (2022) 141:213104. doi: 10.1016/j.bioadv.2022.213104

23. Tseng Q, Duchemin-Pelletier E, Deshiere A, Balland M, Guillou H, Filhol O, et al. Spatial organization of the extracellular matrix regulates cell-cell junction positioning. *Proc Natl Acad Sci U S A* (2012) 109:1506–11. doi: 10.1073/pnas.1106377109

24. Angulo-Urarte A, van der Wal T, Huveneers S. Cell-cell junctions as sensors and transducers of mechanical forces. *Biochim Biophys Acta Biomembr* (2020) 1862:183316. doi: 10.1016/j.bbamem.2020.183316

25. He J, Zhang N, Zhu Y, Jin R, Wu F. MSC spheroids-loaded collagen hydrogels simultaneously promote neuronal differentiation and suppress inflammatory reaction through PI3K-akt signaling pathway. *Biomaterials* (2021) 265:120448. doi: 10.1016/j.biomaterials.2020.120448

26. Orsini EM, Perelas A, Southern BD, Grove LM, Olman MA, Scheraga RG. Stretching the function of innate immune cells. *Front Immunol* (2021) 12:767319. doi: 10.3389/fimmu.2021.767319

27. Choi RB, Robling AG. The wnt pathway: an important control mechanism in bone's response to mechanical loading. *Bone* (2021) 153:116087. doi: 10.1016/j.bone.2021.116087

28. Li Y, Zhang QY, Sun BF, Ma Y, Zhang Y, Wang M, et al. Single-cell transcriptome profiling of the vaginal wall in women with severe anterior vaginal prolapse. *Nat Commun* (2021) 12:87. doi: 10.1038/s41467-020-20358-y

29. Romani P, Valcarcel-Jimenez L, Frezza C, Dupont S. Crosstalk between mechanotransduction and metabolism. *Nat Rev Mol Cell Biol* (2021) 22:22–38. doi: 10.1038/s41580-020-00306-w

30. Shynlova O, Bortolini MA, Alarab M. Genes responsible for vaginal extracellular matrix metabolism are modulated by women's reproductive cycle and menopause. *Int Braz J Urol* (2013) 39:257–67. doi: 10.1590/S1677-5538.IBJU.2013.02.15

31. Li P, Wu G. Roles of dietary glycine, proline, and hydroxyproline in collagen synthesis and animal growth. *Amino Acids* (2018) 50:29–38. doi: 10.1007/s00726-017-2490-6

32. Zhang Y, Daday C, Gu RX, Cox CD, Martinac B, de Groot BL, et al. Visualization of the mechanosensitive ion channel MscS under membrane tension. *Nature* (2021) 590:509–14. doi: 10.1038/s41586-021-03196-w

33. Wu J, Minikes AM, Gao M, Bian H, Li Y, Stockwell BR, et al. Intercellular interaction dictates cancer cell ferroptosis via NF2-YAP signalling. *Nature* (2019) 572:402–6. doi: 10.1038/s41586-019-1426-6

34. Chen D, Wang Y, Lu R, Jiang X, Chen X, Meng N, et al. E3 ligase ZFP91 inhibits hepatocellular carcinoma metabolism reprogramming by regulating PKM splicing. *Theranostics* (2020) 10:8558–72. doi: 10.7150/thno.44873

frontiers | Frontiers in Endocrinology

TYPE Original Research
PUBLISHED 22 June 2023
DOI 10.3389/fendo.2023.1122004

OPEN ACCESS

EDITED BY
Changyin Zhou,
Guangdong Second Provincial General Hospital, China

REVIEWED BY
Santasree Banerjee,
Beijing Genomics Institute (BGI), China
Xue Feng Xie,
Guangdong Second Provincial General Hospital, China

*CORRESPONDENCE
Hua-Lin Huang
huanghualin@csu.edu.cn
Wanjuan Song
2594118999@qq.com

†These authors have contributed equally to this work

RECEIVED 12 December 2022
ACCEPTED 01 June 2023
PUBLISHED 22 June 2023

CITATION
Huang F, Zeng J, Liu D, Zhang J, Liang B, Gao J, Yan R, Shi X, Chen J, Song W and Huang H-L (2023) A novel frameshift mutation in *DNAH6* associated with male infertility and asthenoteratozoospermia. *Front. Endocrinol.* 14:1122004. doi: 10.3389/fendo.2023.1122004

A novel frameshift mutation in *DNAH6* associated with male infertility and asthenoteratozoospermia

Fei Huang†, Jun Zeng†, Dan Liu†, Jing Zhang, Boluo Liang, Jingping Gao, Rong Yan, Xiaobo Shi, Jianlin Chen, Wanjuan Song* and Hua-Lin Huang*

Reproductive Medicine Center, Department of Obstetrics and Gynecology, The Second Xiangya Hospital, Central South University, Changsha, China

Introduction: Asthenoteratozoospermia is one of the most common causes of male infertility. Several genes have been identified as genetic causative factors, but there is a considerable genetic heterogeneity underlying asthenoteratozoospermia. In this study, we performed a genetic analysis of two brothers from a consanguineous Uighur family in China to identify gene mutations causative for asthenoteratozoospermia-related male infertility.

Methods: Two related patients with asthenoteratozoospermia from a large consanguineous family were sequenced by whole-exome sequencing and Sanger sequencing to identify disease-causing genes. Scanning and transmission electron microscopy analysis revealed ultrastructural abnormalities of spermatozoa. Quantitative real-time PCR (qRT-PCR) analysis and immunofluorescence (IF) analysis were used to assess the expression of the mutant messenger RNA (mRNA) and protein.

Results: A novel homozygous frameshift mutation (c.2823dupT, p.Val942Cysfs*21) in *DNAH6* was identified in both affected individuals and was predicted to be pathogenic. Papanicolaou staining and electron microscopy revealed multiple morphological and ultrastructural abnormalities of affected spermatozoa. qRT-PCR and IF analysis showed abnormal expression of DNAH6 in affected sperm, probably due to premature termination code and decay of abnormal 3′ untranslated region (UTR) region of mRNA. Furthermore, intracytoplasmic sperm injection could achieve successful fertilization in infertile men with *DNAH6* mutations.

Discussion: The novel frameshift mutation identified in DNAH6 may contribute to asthenoteratozoospermia. These findings expand the spectrum of genetic mutations and phenotypes associated with asthenoteratozoospermia and may be useful for genetic and reproductive counseling in male infertility.

KEYWORDS

infertility, asthenoteratozoospermia, sperm flagella, *DNAH6*, mutation, premature termination codon

Introduction

Infertility is a challenging health and social problem that affects 10%–15% of couples worldwide (1). A male factor is implicated in approximately half of infertility cases (2). Asthenoteratozoospermia, which describes sperm with reduced motility and obvious morphological abnormalities, is one of the most common factors in male infertility (3). Genetic causes of asthenoteratozoospermia include primary ciliary dyskinesia (PCD) and multiple morphological abnormalities of the sperm flagella (MMAF). PCD (mendelian inheritance in man (MIM): 244400) is characterized by dysfunction of motile cilia and flagella, leading to chronic rhinosinusitis, bronchiectasis, and heterotaxis (4), whereas MMAF is characterized by various morphological abnormalities of flagella (absent, short, bent, coiled, and irregular) (5). To date, 22 genes related to spermatogenesis or ciliogenesis have been identified as causative for MMAF, resulting in primary infertility without PCD (6–10). There is, therefore, a considerable genetic heterogeneity underlying asthenoteratozoospermia, not all of which has been accounted for.

Dynein axonemal heavy chain 6 (*DNAH6*; MIM: 603336), a member of the dynein protein family, is located at 2p11.2 in humans. *DNAH6* contains 77 exons and encodes a 4,158–amino acid protein (11, 12), and it plays an important role in multiple microtubule-associated motor protein complexes involved in ciliary and flagellar morphology and motility (13). Flagella and cilia are hair-like, microtubule-based structures with the same axoneme, formed by an ordered 9 + 2 arrangement of nine doublets of microtubules (A and B) and a central pair of microtubules (14). Dynein is arranged in complex arrays of single-headed, heterodimeric, and heterotrimeric outer dynein arm (ODA) and inner dynein arm (IDA) complexes (15). DNAH6 is a putative IDA and is required for motile cilia function (16). Several *DNAH6* mutations are known to cause severe sperm motility disorders and dysplasia of the fibrous sheath–MMAF (16, 17). *DNAH6* mutations may be related to MMAF in the absence of other PCD symptoms (18) but have recently been identified in patients with respiratory cilia disease leading to the evolution of PCD (16). *DNAH6* variants have also been implicated in lung function changes in patients with cystic fibrosis (19). In humans, loss-of-function mutations in *DNAH6* have been implicated in male infertility, such as globozoospermia, acephalic spermatozoa syndrome and azoospermia, and even premature ovarian insufficiency (20–22). However, the full spectrum of causative mutations in *DNAH6* is unknown, and there are a few reports of pathogenic *DNAH6* variations in Chinese populations.

Here, we identified a novel homozygous mutation in *DNAH6* in two infertile men with MMAF. We applied whole-exome sequencing (WES) and Sanger sequencing to a proband with idiopathic infertility and asthenoteratozoospermia from a consanguineous Uyghur family and subsequently identified the same homozygous mutation in his infertile brother. The brothers harboring the homozygous *DNAH6* mutation showed reduced progressive sperm motility, multiple morphological sperm malformations, and successful fertilization with intracytoplasmic sperm injection (ICSI) treatment. Our study adds to the *DNAH6* mutations reported in different patients with different diseases (Table S1), and the identification of this *DNAH6* mutation paves the way for a biomarker of asthenoteratozoospermia.

Materials and methods

Study participants

The proband (family member IV-1, 28 years old) and his family members in a consanguineous Chinese Uyghur family (Xinjiang, China) were recruited from the Reproductive Medicine Center in the Obstetrics and Gynecology Department of The Second Xiangya Hospital of Central South University for genetic counseling for primary infertility treatment. He was diagnosed with infertility 9 years before our study, and the initial physical and andrological examinations showed a normal body mass index and excluded associated diseases, such as hypogonadotropic hypogonadism, cryptorchidism, varicocele, seminal ductal obstruction, testicular trauma, and andrological tumor. The proband's parents (III-1 and III-2) were first-degree cousins. The patient's brother (IV-3) was also infertile for 4 years, and both wives had no fertility-related disorders (Table S2). Written informed consent was obtained from the study participants, and the study was approved by the Ethics Committee of The Second Xiangya Hospital of Central South University (Changsha, China).

Semen and sperm morphology analysis

Semen samples were collected from the affected patients through masturbation after 3–5 days of sexual abstinence. Three repeated semen analyses were performed according to the World Health Organization (WHO, 2021) guidelines (23). Papanicolaou staining was used to assess sperm morphology, and morphological abnormalities of the flagella were classified as absent, short, coiled, bent, or irregular. For each subject, the percentages of morphologically normal and abnormal spermatozoa were documented according to the WHO guidelines.

Transmission electron microscopy

Spermatozoa from the affected individual were fixed in 2.5% glutaraldehyde (Sigma-Aldrich) overnight at 4°C. Samples were immersed in 1% osmium tetroxide (OsO_4, Taab), dehydrated in graded ethanol, and embedded in Taab812, dodecenylsuccinic anhydride, methylnadic anhydride, and dimethylaminomethyl phenol (Taab). Ultrathin 70- to 90-nm sections were contrast-stained with uranyl acetate and lead citrate, and we examined them by using a Tecnai G2 Spirit TWIN transmission electron microscope (FEI, USA) with a Gatan Orius CCD camera system.

WES and Sanger sequencing

Peripheral blood samples were collected from family members (III-2, IV-1, IV-3, IV-5, and IV-9). Genomic DNA samples were

extracted from peripheral blood using the QIAamp DNA Blood Mini Kit (QIAGEN). The patients (IV-1 and IV-3) underwent WES using the BGI Genomics platform (BGI-Shenzhen, China). The Agilent SureSelect Human All Exon v6 Kit (Agilent) was used to capture known exons and exon–intron boundary sequences (24, 25). Functional annotation and further filtering was performed using the 1000 Genomes Project, gnomAD, the database of single-nucleotide polymorphisms, and Exome Aggregation Consortium based on ANNOVAR. Potential pathogenicity was predicted *in silico* using SIFT, MutationTaster, PROVEAN, Polyphen-2, and CADD. Candidate variants were identified as previously described (26): (i) allele frequency <1% in the 1000 Genomes Project and gnomAD database as above; (ii) nonsynonymous or splicing variants, or coding INDELs; and (iii) *in silico* predicted to be pathogenic. The detailed variant interpretation and analysis pipeline were schematically presented previously (27, 28). Sanger sequencing was used to test family members and control subjects for the candidate pathogenic gene variants identified in the proband. Sanger sequencing was performed as a confirmatory test using the ABI 3730XL automated sequencer (Applied Biosystems, USA) according to the manufacturer's instructions. The PCR primers are listed in Table S3 and were synthesized by Tsingke Biotechnology Co., Ltd. (Beijing, China).

Expression analysis

Total RNA was extracted from blood tissue of fertile adult donors who provided written informed consent for study participation and infertile patients using TRIzol reagent (Invitrogen). RNA (1 μg) was reverse-transcribed into cDNA using the HiScript III 1st Strand cDNA Synthesis Kit (+gDNA wiper) (Vazyme) according to the manufacturer's instructions. We performed qPCR by using the ChamQ SYBR qPCR Master Mix (Vazyme) on a LightCycler96 real-time PCR product detection system (Roche, Switzerland) with specific primers of *DNAH6* mRNA (Table S3) to assess relative expression. Statistical analysis was performed using Student's *t*-test in the Graphpad Prism 9.0 program (***$p < 0.001$). We also performed splicing analysis by using 2× Taq Plus Master Mix II (Vazyme) with specific primers listed in Table S3. The products were sequenced on an ABI 3730XL automated sequencer, and the sequencing results were analyzed using Chromas software (v2.6.5, Technelysium Pty Ltd., South Brisbane, Australia).

Immunofluorescence analysis

Sperm samples were incubated with mouse monoclonal antibody targeting α-tubulin (T5168, Sigma-Aldrich; 1:1,000), rabbit polyclonal antibody targeting DNAH6 (ab122333, Abcam; 1:100), secondary antibodies [Alexa Fluor 488 anti-mouse immunoglobulin G (IgG) (A21121, Life Technologies; 1:1,000) and Alexa Fluor 555 anti-rabbit IgG (A31572, Life Technologies; 1:1,000)], and 4′,6-diamidino-2-phenylindole (DAPI). Fluorescence signals were captured using a BX-51 fluorescence microscope (Olympus, Japan). Images were analyzed using VideoTesT-FISH software (v.2.0, VideoTesT, St. Petersburg, Russia).

In vitro fertilization and ICSI

In vitro fertilization (IVF) and ICSI procedures were performed as previously described (29). In brief, the female underwent a stimulation procedure and oocyte retrieval 35–36 h later after injection of human chorionic gonadotropin. Sperm samples collected from the patient were processed by conventional discontinuous density gradient centrifugation and swim-up procedures according to the WHO guidelines. For IVF, each oocyte was co-incubated with sperm to occur naturally. For ICSI, normal morphology spermatozoa were selected, immobilized, and injected into the oocyte cytoplasm. Then, the oocytes were cultured sequentially in cleavage embryo and blastocyst culture medium at 37°C under 5% CO_2. Fertilization rates were evaluated on the morning of days 1–5 after oocyte retrieval.

Results

Clinical characteristics of the infertile patients

In the present study, we recruited a consanguineous Uyghur family consisting of two patients (IV-1 and IV-3) that were suffering from primary infertility (Figure 1A). The two patients were diagnosed with primary infertility, and both wives excluded fertility-related disorders. No apparent organic anomalies were found in the male reproductive system and the respiratory system by physical and andrological examination. Physical examination of the men revealed normal testicular size, external genital development, and bilateral spermatic veins. There was no history of respiratory disorders, situs inversus, exposure to hazardous environments, or drug/alcohol abuse in either man. Semen analysis showed adequate sperm concentration but abnormal motility, diagnosed as asthenoteratozoospermia, and sperm motility was significantly lower in IV-3 than in IV-1 (e.g., progressive motility, 2.4% vs. 21.3%) (Table 1). In the two patients (IV-1 and IV-3), the serum follicle-stimulating hormone, luteinizing hormone, and testosterone were within normal ranges, their karyotype were 46,XY, and no azoospermia factor microdeletion was found. The male cousin (IV-7) was the only IV generation male with a biologic offspring. The female member (IV-9), aged 20 years, was currently clinically normal (Table S2), with a normal menstrual cycle, normal development of the female reproductive system, and no history of respiratory disease. The pattern of inheritance of male infertility in the consanguineous families is consistent with an autosomal recessive homozygous mutation in the affected brothers.

Sperm morphology by light and electron microscopy

To investigate sperm morphology and flagellar ultrastructural abnormalities in the two men harboring the *DNAH6* variant, we performed Papanicolaou staining, microscopic examination, and

10.3389/fendo.2023.1122004

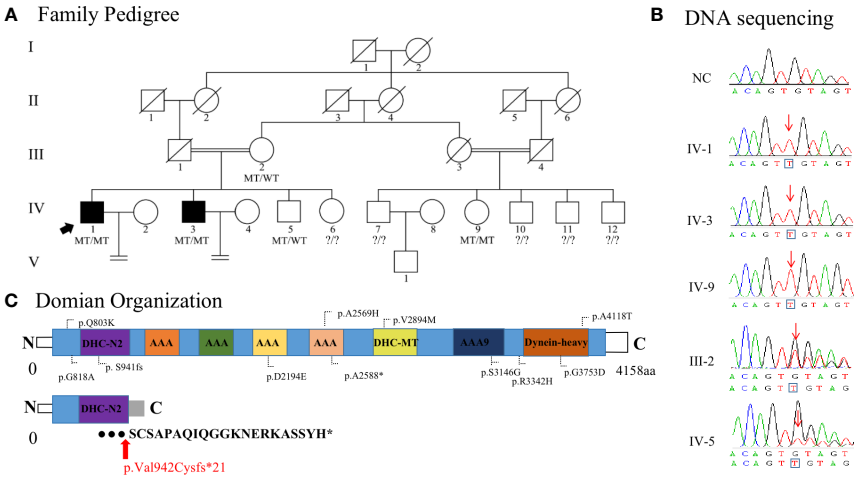

FIGURE 1
Identification of homozygous *DNAH6* variants in men with asthenoteratozoospermia. **(A)** Pedigrees of the Uyghur consanguineous families affected by homozygous *DNAH6* variants. Circles denote female family members, squares male family members, and solid symbols affected members. The double lines denote a consanguineous marriage, slashes denote deceased family members, and equal signs denote infertility. WT indicates wild type in the normal allele, MT indicates mutant type (c.2823dupT, p.Val942Cysfs*21) in *DNAH6*, and arrow indicates the index patient (family member IV-1). **(B)** Sanger sequencing results are shown on the right side. The variant positions are indicated by red arrows. **(C)** Structure of DNAH6 protein; predicted functional domains are shown together with the position of novel and old mutations identified in patients with asthenoteratozoospermia. The novel variant positions are indicated by red arrows. Expression analysis of DNAH6 mRNA and protein in the spermatozoa from a normal male control and men harboring homozygous *DNAH6* variants.

TABLE 1 Semen characteristics and sperm morphology in men harboring homozygous deleterious *DNAH6* variants.

Individual	Semen (ml)	Concentration (10^6/ml)	Number of motility sperm	Progressive motility (%)	Motility (%)
IV-1	2.5	48.3	525	21.3	42.9
IV-3	2	21.8	40	2.4	7.9
Reference limits	1.5 [a]	15.0 [a]	3.0 [a]	32.0 [a]	40.0 [a]

Individual	Absent flagella (%)	Short flagella (%)	Coiled flagella (%)	Angulation (%)	Irregular caliber (%)	Abnormal head and neck (%)
IV-1	6	39	18	7	2.2	2
IV-3	8	45	27	8	3	3
Reference limits	–	–	–	–	–	–

[a]Reference limits according to the WHO standards.

scanning and transmission electron microscopy (SEM and TEM, respectively) analyses of the sperm from these individuals (IV-1 and IV-3). Papanicolaou staining and SEM showed that most spermatozoa had abnormal tails, including short, coiled, bent, occasionally absent flagella, and irregular flagella compared to unaffected controls (Figures 2A, B). TEM revealed ultrastructural disruption of affected spermatids, with disordered peripheral dense fibers, serious distortions in axonemes, including sporadic to partial or complete absence of the central complex (9 + 1 or 9 + 0), and frequent absence of outer doublet microtubules (DMT; 8 + 0, 8 + 2). Dynein arms (inner or both) were frequently absent from the axoneme peripheral doublets, and the axoneme was sometimes completely disrupted. Spermatozoa from healthy controls showed the typical "9 + 2" axoneme microtubule structure (Figure 2C).

Identification of the *DNAH6* variant

We performed WES to identify a potential genetic basis for asthenoteratozoospermia in the proband and his brother. WES produced 126.34 million clean reads and 116.27 million total effective reads, with 99.91% of the reads mapping to the human reference genome. The mean sequencing depth on target regions was 120.93, and 98.98% of target regions were covered 10× or more. A total of 98,802 single-nucleotide polymorphisms and 14,863 indels were detected in the proband. As the patients were from a consanguineous family, homozygous variants implicated in infertility phenotypes were prioritized. After screening, only one novel homozygous frameshift variant (NM_001370.2: exon 17: c.2823dupT, p.Val942Cysfs*21) in *DNAH6*, known to cause

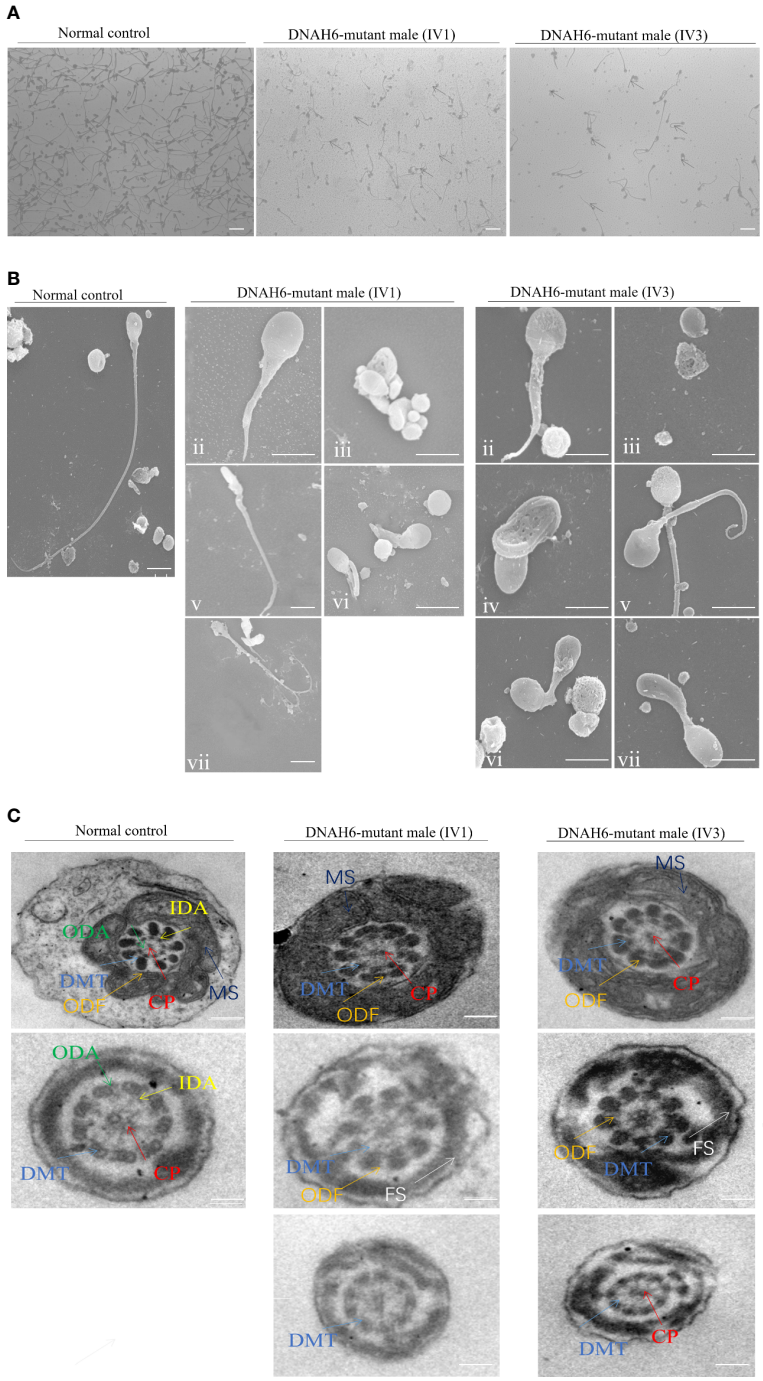

FIGURE 2
The phenotype of spermatozoa from the patient and a healthy control. **(A)** Staining for the spermatozoa obtained from a fertile control individual (NC) and men harboring *DNAH6* variants. Compared to the spermatozoa of NC, which presented long, smooth tails, most spermatozoa obtained from men harboring *DNAH6* variants displayed typical MMAF phenotypes, such as short, absent, coiled, and irregular flagella. Scale bars, 5 mm. **(B)** SEM analysis of the spermatozoa obtained from a fertile control individual (NC) and men harboring homozygous *DNAH6* variants. **(i)** Normal morphology of the spermatozoon from a healthy control male. (ii–vii) Most spermatozoa obtained from men harboring homozygous *DNAH6* variants displayed typical MMAF phenotypes, including short (ii), absent (iii), bent (iv), coiled (v), and irregular flagella (vi and vii). Scale bars, 5 µm. **(C)** Cross-sections of the midpiece and principal piece of the sperm flagella in the sperm obtained from NC displayed typical "9 + 2" microtubule structure and peri-axoneme structure. The axoneme microtubule structure, including nine pairs of peripheral doublet microtubules (DMT; indicated with white arrows) and the central pair of microtubules (CP; indicated with blue arrows), is visible. The ODAs (indicated with yellow arrows) and IDAs (indicated with red arrows) are also visible. The peri-axoneme structure includes a helical mitochondrial sheath (MS; indicated with green arrows), nine outer dense fibers (ODFs; indicated with orange arrows), and the fiber sheath (FS; indicated with pink arrows). Cross-sections of the midpiece, principal piece, and endpiece of the spermatozoa obtained from men harboring *DNAH6* variants revealed that typical axonemal anomalies were disorder, including partial or complete absence of peripheral doublet microtubules and the central pair of microtubules and dynein arms, whereas other axoneme microtubule structures seemed to be unaffected. Scale bars, 200 nm.

10.3389/fendo.2023.1122004

asthenozoospermia, fulfilled these criteria. The record of this variant in public databases (ClinVar, gnomAD, and 1000 Genomes) showed in Table 2. *In silico* functional prediction classified the c.2823dupT variant as deleterious with SIFT, MutationTaster (a score near or equal to 1), PROVEAN (score of −9.06), PolyPhen-2 (score of 1.000, specificity of 1.00, and sensitivity of 0.00), and CADD (score of 19.6) (Table 2). The *DNAH6* homozygous variants in the affected individuals (IV-1 and IV-3) and female member (IV-9) and the *DNAH6* heterozygous variants in the proband's brother (IV-5) and mother (III-2) were further confirmed by Sanger sequencing (Figure 1B), consistent with autosomal recessive inheritance. The frameshift variant was not detected in a sample of 300 Chinese male controls.

Effect and expression of the *DNAH6* variant

Evolutionary conservation analysis showed that valine 942 in human DNAH6 is highly conserved between species, suggesting that this site is functionally important. The frameshift variant was located in key functional domains of the coding protein and was predicted to result in a premature termination codon (PTC) at site 961 (Figure 1C).

To explore the impact of the *DNAH6* p.Val942Cysfs*21 variant, we performed immunostaining (IF) and qPCR assays to detect the DNAH6 protein and mRNA levels in the two patients. IF showed that DNAH6 protein was located along the neck and along the entire length of the sperm flagella in a control individual, but only in the neck of mutant sperm (Figure 3B). In addition, qRT-PCR analysis of nonsense-mediated mRNA decay demonstrated that DNAH6 happened to terminate at the PTC position and to decay of abnormal 3′ UTR region of the mRNA (Figure 3A), whereas splicing analysis showed no alternative splicing (Figure S1).

In vitro fertilization, intracytoplasmic sperm injection, and pregnancy outcome

The proband couple underwent two cycles at our clinic in 2020. In the first IVF cycle, 15 oocytes were received and only one good-quality embryo was available. Unfortunately, this resulted in an early unexplained miscarriage after transfer. In the second half-ICSI cycle, 13 oocytes were obtained, of which six were fertilized with IVF and seven with ICSI. Only one oocyte was fertilized by IVF, and no good-quality embryo was obtained. Meanwhile, six in the seven oocytes were successfully fertilized by ICSI, whereas one was fertilized abnormally. Finally, three good-quality embryos were formed, suggesting that spermatozoa harboring *DNAH6* mutations can produce viable embryos with ICSI treatment. However, the proband's wife did not become pregnant after transfer (Table 3).

Discussion

Asthenoteratozoospermia describes the absence or reduction of motile sperm in the ejaculate, and it is a known cause of male infertility (~19% of infertile men) (1, 30). However, the causes of asthenoteratozoospermia remain unclear. Here, we discovered and validated a novel homozygous frameshift mutation p.Val942Cysfs*21 in *DNAH6* by both WES and Sanger sequencing. This *DNAH6* variant is absent in population analyses and was predicted to be damaging by several *in silico* analyses. The homozygous *DNAH6* p.Val942Cysfs*21 mutation results in a typical asthenoteratozoospermia phenotype, with no obvious phenotypic differences between our patients and other previously reported cases of asthenoteratozoospermia, regardless of the mutations involved (31).

Note that the homozygous mutation in *DNAH6* was identified in this family. The male family members (IV-10, IV-11, and IV-12) are suggested to examine the *DNAH6* p.Val942Cysfs*21 mutation, which is helpful for their choice of childbearing methods. The single female family member IV-9 is homozygous for the mutation and is unmarried, whose reproductive outcome needs to be followed. There were a lot of severe abnormal morphologies and ultrastructural disruptions in the affected sperm. Pathogenicity analyses showed that DNAH6 was abnormally expressed in spermatozoa from the men harboring the variant. In contrast to the DNAH6 protein in the neck and the entire length of normal control sperm and the absence of DNAH6 staining in the spermatozoa of other previously reported patients (32), the mutant DNAH6 was only present in the neck of our patient's sperm. We propose that the difference could be explained by the instability of the structure of the truncated protein. The observation of residual mRNA expression and decay of the mRNA 3′ UTR tail of the mutant *DNAH6* gene supports our hypothesis.

Dynein is a component of microtubule-associated motor protein complexes and plays an important role in cilial and flagellar motility or in the cytoplasm, where it mediates intercellular movement and

TABLE 2 Homozygous deleterious *DNAH6* variants identified in men with asthenoteratozoospermia.

variant [a]	Amino acid change	Zygosity	1000 Genomes Project	East Asians in gnomAD	All individuals in gnomAD	SIFT	Mutation Taster	PROVEAN[b]	PolyPhen-2	CADD[c]
c.2823dupT	p.Val942Cysfs*21	Homozygous	0	0	0.00003428	D	D	−9.06 (D)	1.000 (D)	19.6 (D)

D damage.
[a]The NCBI reference sequence number of DNAH6 is NM 001370.2.
[b]Variants with scores lower than −2.5 (cutoff) are predicted to be deleterious.
[c]Variants with CADD values greater than 4 are considered to be deleterious.

10.3389/fendo.2023.1122004

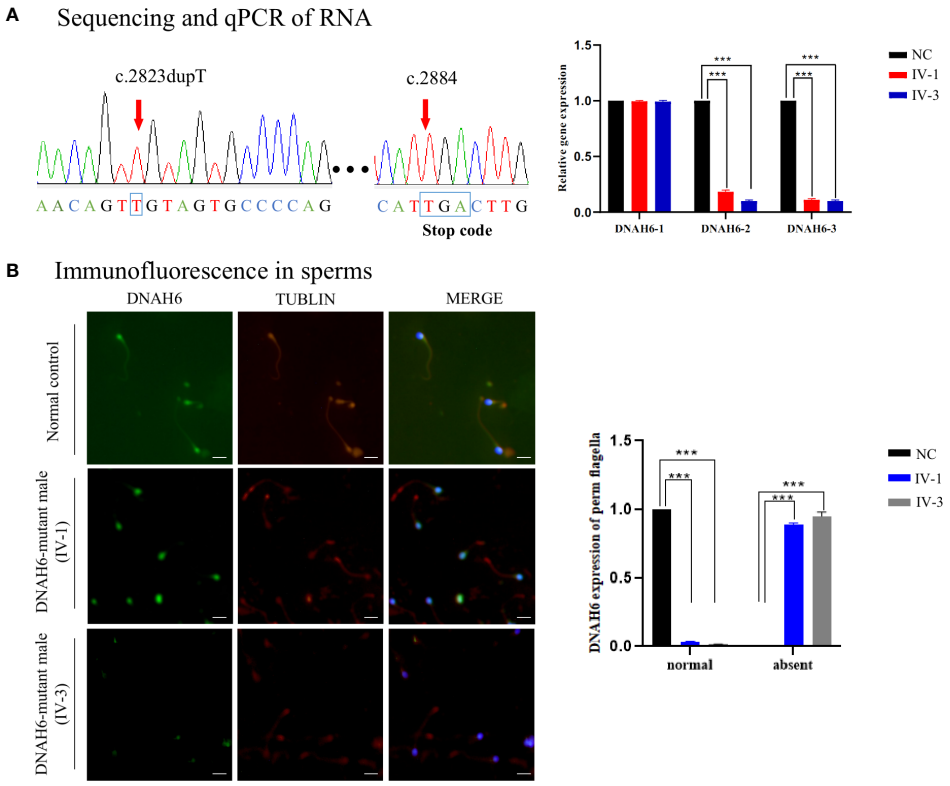

FIGURE 3
DNAH6 expression in men with asthenoteratozoospermia. **(A)** Real-time quantitative PCR analysis indicated that the abundance of homozygous DNAH6 mRNA was significantly reduced in the sperm from men harboring *DNAH6* variants and sequence analysis that it happened to terminate at the PTC position, when compared to that of a normal control man. Data represent the means + standard error of measurement of three independent experiments. Two-tailed Student's paired or unpaired t-tests were used as appropriate (***$p < 0.001$). **(B)** Representative images of spermatozoa obtained from a fertile control individual (NC) and men harboring *DNAH6* variants (IV-1 and IV-3) stained with the anti-DNAH6 antibody, anti−a-tubulin antibody, and DAPI. Staining results revealed that DNAH6 was localized in the neck and almost reduced in the sperm flagella obtained from men harboring *DNAH6* variants but localized in the neck and tail of the sperm obtained from the NC. Representative data are provided to illustrate the typical staining observed in *DNAH6*-associated cases. Scale bars, 5 mm.

cytoskeletal remodeling (13). DNAH6 is mainly expressed in the human testis and is needed for motile cilia function (16, 21). Mutations in *DNAH6* have been associated with PCD and heterotaxy caused by the central pair complex motile cilia dysfunction (16). Mutations in two IDA heavy-chain protein-encoding genes, *DNAH1* (MIM: 603332) and *DNAH2* (MIM: 603333), and two ODA heavy chain components, *DNAH8* (MIM: 603337) and *DNAH17* (MIM: 610063), have been described in individuals with isolated male infertility due to asthenoteratozoospermia. *DNAH1* is required for the formation of IDAs in spermatozoa and is important for the assembly and biogenesis of the flagellar axoneme, and mutations in *DNAH1* cause MMAF and other PCD-associated symptoms (33). *DNAH6* can act both recessively and possibly through trans-heterozygous interactions with other PCD genes such as *DNAH1* or *DNAH5*. Dynein is involved in spermatogenesis, and other patients with a rare

TABLE 3 Clinical outcomes of IVF/ICSI treatment cycles using the for spermatozoa from men harboring homozygous DNAH6 variants.

Patient	Female age (years)	Male age (years)	Duration of infertility (years)	Cycles	Insemination method	Total no. of oocytes	Total fertilization rate (%)	Normal fertilization rate (%)	Good-quality embryo rate (%)	No. of live births (n)
IV-1	25	27	9	1	IVF	15	4/15 (26.7)	2/15 (13.3)	1/15 (6.7)	0
				2	IVF	6	1/6	0	0	0
					ICSI	7	7/7 (100)	6/7 (85.7)	3/7 (42.9)	0
IV-3	23	24	5	NA	–	–	–	–	–	0

homozygous missense mutation in *DNAH6* exhibited azoospermia and oligozoospermia and male infertility (21, 34). *DNAH6* deficiency is also associated with asthenoteratozoospermia in the absence of other PCD symptoms (18). Our phenotypic analysis revealed that the men carrying the *DNAH6* variant displayed typical MMAF phenotypes, including reduced sperm motility and MMAF, without other PCD symptoms. TEM analysis further revealed partial defects or loss of the dynein arms and severe disorganization or aberration of axonemal or other peri-axonemal microtubule structures in spermatozoa. Therefore, DNAH6 is beneficial for flagellar axoneme assembly during spermatogenesis, and the asthenoteratozoospermia-associated phenotypes in these cases are likely to be caused by homozygous variants in *DNAH6*.

From the clinical perspective, ICSI is an assisted reproductive technology that is an effective method to achieve successful conception in infertile men with MMAF (35–39). Previous studies have reported success with ICSI in a series of individuals with MMAF-related gene mutations. For example, MMAF-affected individuals with biallelic variants in *DNAH1*, *DNAH8*, or *TTC29* have good clinical outcomes following ICSI (40–42), whereas failed pregnancies have been reported in MMAF-affected men with *CEP135* (MIM: 611423), *DNAH17*, or *CFAP65* variants (21, 43, 44). It has also been reported that patients with MMAF with *DNAH6* mutations do not achieve pregnancy (18). In our study, fertilization was also achieved with ICSI (7 of 7, 100%), whereas 23.8% (5 of 21) with IVF. However, whether successful ICSI outcomes can be achieved in patients with MMAF with *DNAH6* mutations requires further investigation.

Conclusion

In conclusion, our experimental observations in human subjects show that a novel frameshift mutation in *DNAH6* can induce MMAF-associated asthenoteratozoospermia. This finding expands the spectrum of genetic mutations associated with MMAF and asthenoteratozoospermia. Additional functional analysis of specific *DNAH6* mutations would provide further important information about the underlying genetic causes of male infertility, allowing genetic counselors and clinicians to develop personalized treatment plans.

Data availability statement

The primary data for this study are available from the corresponding author upon reasonable request.

Ethics statement

The studies involving human participants were reviewed and approved by the Institutional Review Board from the Ethics Committee of the Second Xiangya Hospital, Central South University. The patients/participants provided their written informed consent to participate in this study.

Author contributions

H-LH and WS: Data collection or management, data analysis, and manuscript revision process. FH and JuZ: Project development, data analysis, and manuscript editing. DL and JiZ: Data analysis and manuscript editing. BL, JG, and RY: Manuscript editing and revision. XS and JC: Data collection or management, data analysis, and manuscript writing. All authors contributed to the article and approved the submitted version.

Funding

This study was funded by the National Natural Science Foundation of China (No. 81501248), the Science and Technology Innovation Program of Hunan Province (2021RC3031), the Scientific Research Program of Hunan Provincial Health Commission (20220503347), and the Open Research Program of Key Laboratory of Regenerative Biology of Chinese Academy of Sciences (KLRB202010).

Acknowledgments

The authors thank all the doctors, nurses, and embryologists in the Reproductive Medicine Center of The Second Xiangya Hospital for their clinical work.

Conflict of interest

The authors declare that the research was conducted in the absence of any commercial or financial relationships that could be construed as a potential conflict of interest.

Publisher's note

Supplementary material

The Supplementary Material for this article can be found online at: https://www.frontiersin.org/articles/10.3389/fendo.2023.1122004/full#supplementary-material

SUPPLEMENTARY FIGURE 1
Sanger sequencing results of splicing analysis in men harboring *DNAH6* variants. The variant positions are indicated by red arrows.

References

1. Krausz C, Riera-Escamilla A. Genetics of male infertility. *Nat Rev Urol* (2018) 15:369–84. doi: 10.1038/s41585-018-0003-3

2. Choy JT, Eisenberg ML. Male Infertility as a window to health. *Ferti Steri* (2018) 110:810–4. doi: 10.1016/j.fertnstert.2018.08.015

3. Shahrokhi SZ, Salehi P, Alyasin A, Taghiyar S, Deemeh MR. Asthenozoospermia: cellular and molecular contributing factors and treatment strategies. *Andrologia* (2020) 52:e13463. doi: 10.1111/and.13463

4. Storm van's Gravesande K, Omran H. Primary ciliary dyskinesia: clinical presentation, diagnosis and genetics. *Ann Med* (2005) 37:439–49. doi: 10.1080/07853890510011985

5. Ben Khelifa M, Coutton C, Zouari R, Karaouzène T, Rendu J, Bidart M, et al. Mutations in DNAH1, which encodes an inner arm heavy chain dynein, lead to Male infertility from multiple morphological abnormalities of the sperm flagella. *Am J Hum Genet* (2014) 94:95–104. doi: 10.1016/j.ajhg.2013.11.017

6. Tang SY, Wang X, Li WY, Yang XY, Li Z, Liu WJ, et al. Biallelic mutations in CFAP43 and CFAP44 cause Male infertility with multiple morphological abnormalities of the sperm flagella. *Am J Hum Genet* (2017) 100:854–64. doi: 10.1016/j.ajhg.2017.04.012

7. Shen Y, Zhang F, Li F, Jiang X, Yang Y, Li X, et al. Loss-of-function mutations in QRICH2 cause male infertility with multiple morphological abnormalities of the sperm flagella. *Nat Commun* (2019) 10(1):433. doi: 10.1038/s41467-018-08182-x

8. He X, Liu C, Yang X, Lv M, Ni X, Li Q, et al. Bi-allelic loss-of-function variants in CFAP58 cause flagellar axoneme and mitochondrial sheath defects and asthenoteratozoospermia in humans and mice. *Am J Hum Genet* (2020) 107:514–26. doi: 10.1016/j.ajhg.2020.07.010

9. Sironen A, Shoemark A, Patel M, Loebinger MR, Mitchison HM. Sperm defects in primary ciliary dyskinesia and related causes of male infertility. *Cell Mol Life Sci* (2020) 77:2029–48. doi: 10.1007/s00018-019-03389-7

10. Tu C, Cong J, Zhang Q, He X, Zheng R, Yang X, et al. Bi-allelic mutations of DNAH10 cause primary male infertility with asthenoteratozoospermia in humans and mice. *Am J Hum Genet* (2021) 108:1466–77. doi: 10.1016/j.ajhg.2021.06.010

11. Hom EFY, Witman GB, Harris EH, Dutcher SK, Kamiya R, Mitchell DR, et al. A unified taxonomy for ciliary dyneins. *Cytoskeleton* (2011) 68:555–65. doi: 10.1002/cm.20533

12. Vaughan KT, Mikami A, Paschal BM, Holzbaur EL, Hughes SM, Echeverri CJ, et al. Multiple mouse chromosomal loci for dynein-based motility. *Genomics* (1996) 36:29–38. doi: 10.1006/geno.1996.0422

13. Roberts AJ, Kon T, Knight PJ, Sutoh K, Burgess SA. Functions and mechanics of dynein motor proteins. *Nat Rev Mol Cell Biol* (2013) 14:713–26. doi: 10.1038/nrm3667

14. Ishikawa T. Axoneme structure from motile cilia. *Cold Spring Harb Perspect Biol* (2017) 9(1):a028076. doi: 10.1101/cshperspect.a028076

15. Kollmar M. Fine-tuning motile cilia and flagella: evolution of the dynein motor proteins from plants to humans at high resolution. *Mol Biol Evol* (2016) 33:3249–67. doi: 10.1093/molbev/msw213

16. Li Y, Yagi H, Onuoha EO, Damerla RR, Francis R, Furutani , et al. DNAH6 and its interactions with PCD genes in heterotaxy and primary ciliary dyskinesia. *PloS Genet* (2016) 12:e1005821. doi: 10.1371/journal.pgen.1005821

17. Oud MS, Houston BJ, Volozonoka L, Mastrorosa FK, Holt GS, Alobaidi BKS, et al. Exome sequencing reveals variants in known and novel candidate genes for severe sperm motility disorders. *Hum Reprod* (2021) 36:2597–611. doi: 10.1093/humrep/deab099

18. Tu C, Nie H, Meng L, Yuan S, He W, Luo A, et al. Identification of DNAH6 mutations in infertile men with multiple morphological abnormalities of the sperm flagella. *Sci Rep* (2019) 9:15864. doi: 10.1038/s41598-019-52436-7

19. Blue E, Louie TL, Chong JX, Hebbring SJ, Barnes KC, Rafaels NM, et al. Variation in cilia protein genes and progression of lung disease in cystic fibrosis. *Ann Am Thorac Society* (2018) 15:440–8. doi: 10.1513/AnnalsATS.201706-451OC

20. Li L, Sha YW, Xu X, Mei LB, Qiu PP, Ji ZY, et al. DNAH6 is a novel candidate gene associated with sperm head anomaly. *Andrologia* (2018). doi: 10.1111/and.12953

21. Gershoni M, Hauser R, Yogev L, Lehavi O, Azem F, Yavetz H, et al. A familial study of azoospermic men identifies three novel causative mutations in three new human azoospermia genes. *Genet Med* (2017) 19:998–1006. doi: 10.1038/gim.2016.225

22. Liu H, Wei X, Sha Y, Liu W, Gao H, Lin J, et al. Whole-exome sequencing in patients with premature ovarian insufficiency: early detection and early intervention. *J Ovarian Res* (2020) 13:114. doi: 10.1186/s13048-020-00716-6

23. World Health Organization. *WHO laboratory manual for the examination and processing of human semen. 6th ed.* Geneva, Switzerland: WHO Press (2021). p. 276.

24. Han P, Wei G, Cai K, Xiang X, Deng WP, Li YB, et al. Identification and functional characterization of mutations in LPL gene causing severe hypertriglyceridaemia and acute pancreatitis. *J Cell Mol Med* (2020) 24:1286–99. doi: 10.1111/jcmm.14768

25. Dai Y, Liang S, Dong X, Zhao Y, Ren H, Guan Y, et al. Whole exome sequencing identified a novel DAG1 mutation in a patient with rare, mild and late age of onset muscular dystrophy-dystroglycanopathy. *J Cell Mol Med* (2019) 23:811–8. doi: 10.1111/jcmm.13979

26. Zeng J, Sun Y, Zhang J, Wu X, Wang Y, Quan R, et al. Identification of zona pellucida defects revealed a novel loss-of-function mutation in ZP2 in humans and rats. *Front Endocrinol* (2023) 14. doi: 10.3389/fendo.2023.1169378

27. Zhang R, Chen S, Han P, Chen F, Kuang S, Meng Z, et al. Whole exome sequencing identified a homozygous novel variant in CEP290 gene causes meckel syndrome. *J Cell Mol Med* (2020) 24:1906–16. doi: 10.1111/jcmm.14887

28. Zheng Y, Xu J, Liang S, Lin D, Banerjee S. Whole exome sequencing identified a novel heterozygous mutation in HMBS gene in a Chinese patient with acute intermittent porphyria with rare type of mild anemia. *Front Genet* (2018) 9:129. doi: 10.3389/fgene.2018.00129

29. Zeng J, Yao Z, Zhang Y, Tian F, Liao T, Wu L, et al. Fertilization and neonatal outcomes after early rescue intracytoplasmic sperm injection: a retrospective analysis of 16,769 patients. *Arch Gynecol Obstet* (2022) 306:249–58. doi: 10.1007/s00404-022-06445-z

30. Agarwal A, Mulgund A, Hamada A, Chyatte MR. A unique view on male infertility around the globe. *Reprod Biol Endocrinol* (2015) 13:37. doi: 10.1186/s12958-015-0032-1

31. Inaba K. Sperm flagella: comparative and phylogenetic perspectives of protein components. *Mol Hum Reprod* (2011) 17:524–38. doi: 10.1093/molehr/gar034

32. Mazaheri Moghaddam M, Mazaheri Moghaddam M, Hamzeiy H, Baghbanzadeh A, Pashazadeh F, Sakhinia E, et al. Genetic basis of acephalic spermatozoa syndrome, and intracytoplasmic sperm injection outcomes in infertile men: a systematic scoping review. *J Assist Reprod Genet* (2021) 38:573–86. doi: 10.1007/s10815-020-02008-w

33. Imtiaz F, Allam R, Ramzan K, Al-Sayed M. Variation in DNAH1 may contribute to primary ciliary dyskinesia. *BMC Med Genet* (2015) 16:14. doi: 10.1186/s12881-015-0162-5

34. Chemes HE, Alvarez Sedo C. Tales of the tail and sperm head aches: changing concepts on the prognostic significance of sperm pathologies affecting the head, neck and tail. *Asian J Androl* (2012) 14:14–23. doi: 10.1038/aja.2011.168

35. Yang S, Gao L, Wang W, Ding J, Xu Y, Li H, et al. Successful intracytoplasmic sperm injection with testicular spermatozoa from a man with multiple morphological abnormalities of the sperm flagella: a case report. *J Assist Reprod Genet* (2018) 35:247–50. doi: 10.1007/s10815-017-1057-5

36. Chemes HE, Rawe VY. Sperm pathology: a step beyond descriptive morphology. origin, characterization and fertility potential of abnormal sperm phenotypes in infertile men. *Hum Reprod Update* (2003) 9:405–28. doi: 10.1093/humupd/dmg034

37. Yang SM, Yang XY, Ding Y, Li H, Wang W, Liu JY, et al. Intracytoplasmic sperm injection outcomes in Chinese men with multiple morphological abnormalities of sperm flagella. *Asian J Androl* (2016) 18:809–11. doi: 10.4103/1008-682X.167722

38. Liu C, He X, Liu W, Yang S, Wang L, Li W, et al. Bi-allelic mutations in TTC29 cause Male subfertility with asthenoteratospermia in humans and mice. *Am J Hum Genet* (2019) 105:1168–81. doi: 10.1016/j.ajhg.2019.10.010

39. Payne D, Flaherty SP, Jeffrey R, Warnes GM, Matthews CD. Andrology: successful treatment of severe male factor infertility in 100 consecutive cycles using intracytoplasmic sperm injection. *Hum Reprod* (1994) 9:2051–7. doi: 10.1093/oxfordjournals.humrep.a138392

40. Yang Y, Jiang C, Zhang X, Liu X, Li J, Qiao X, et al. Loss-of-function mutation in DNAH8 induces asthenoteratospermia associated with multiple morphological abnormalities of the sperm flagella. *Clin Genet* (2020) 98:396–401. doi: 10.1111/cge.13815

41. Wambergue C, Zouari R, Fourati Ben Mustapha S, Martinez G, Devillard F, Hennebicq S, et al. Patients with multiple morphological abnormalities of the sperm flagella due to DNAH1 mutations have a good prognosis following intracytoplasmic sperm injection. *Hum Reprod* (2016) 31:1164–72. doi: 10.1093/humrep/dew083

42. Whitfield M, Thomas L, Bequignon E, Schmitt A, Stouvenel L, Montantin G, et al. Mutations in DNAH17, encoding a sperm-specific axonemal outer dynein arm heavy chain, cause isolated Male infertility due to asthenozoospermia. *Am J Hum Genet* (2019) 105:198–212. doi: 10.1016/j.ajhg.2019.04.015

43. Sha YW, Xu X, Mei LB, Li P, Su ZY, He XQ, et al. A homozygous CEP135 mutation is associated with multiple morphological abnormalities of the sperm flagella (MMAF). *Gene* (2017) 633:48–53. doi: 10.1016/j.gene.2017.08.033

44. Wang WL, Tu CF, Nie HC, Meng LL, Li Y, Yuan SM, et al. Biallelic mutations in CFAP65 lead to severe asthenoteratospermia due to acrosome hypoplasia and flagellum malformations. *J Med Genet* (2019) 56:750–7. doi: 10.1136/jmedgenet-2019-106031

frontiers | Frontiers in Endocrinology

TYPE Systematic Review
PUBLISHED 29 June 2023
DOI 10.3389/fendo.2023.1147306

OPEN ACCESS

EDITED BY
Shunfeng Cheng,
Qingdao Agricultural University, China

REVIEWED BY
Rafeah Pakri Mohamed,
UCSI University, Malaysia
Jing-Cai Liu,
Nanjing Agricultural University, China

*CORRESPONDENCE
Jaya Kumar
jayakumar@ukm.edu.my
Abdul Kadir Abdul Karim
abdulkadir73@ppukm.ukm.edu.my

RECEIVED 18 January 2023
ACCEPTED 07 June 2023
PUBLISHED 29 June 2023

CITATION
Karunyam BV, Abdul Karim AK, Naina Mohamed I, Ugusman A, Mohamed WMY, Faizal AM, Abu MA and Kumar J (2023) Infertility and cortisol: a systematic review. *Front. Endocrinol.* 14:1147306. doi: 10.3389/fendo.2023.1147306

Infertility and cortisol: a systematic review

Bheena Vyshali Karunyam[1], Abdul Kadir Abdul Karim[1*], Isa Naina Mohamed[2], Azizah Ugusman[3], Wael M. Y. Mohamed[4,5], Ahmad Mohd Faizal[1], Muhammad Azrai Abu[1] and Jaya Kumar[3*]

[1]Department of Obstetrics and Gynaecology, Faculty of Medicine, Universiti Kebangsaan Malaysia, Kuala Lumpur, Malaysia, [2]Department of Pharmacology, Faculty of Medicine, Universiti Kebangsaan Malaysia, Kuala Lumpur, Malaysia, [3]Department of Physiology, Faculty of Medicine, Universiti Kebangsaan Malaysia, Kuala Lumpur, Malaysia, [4]Basic Medical Science Department, Kulliyyah of Medicine, International Islamic University Malaysia, Kuantan, Malaysia, [5]Department of Clinical Pharmacology, Faculty of Medicine, Menoufia University, Shebin El-Kom, Egypt

Introduction: Stress and infertility form a complex relationship. In line with this, various stress-related biological markers have been investigated in infertility.

Methods: This systematic review was performed using PRISMA guidelines (i) to report whether cortisol is highly present in infertile patients compared to fertile control; (ii) to report whether there is any significant difference in the cortisol level in infertile subjects that conceive and those that didn't at the end of assisted reproduction treatments. Original articles involving human (male and female) as subjects were extracted from four electronic databases, including the list of references from the published papers. Sixteen original full-length articles involving male (4), female (11), and both genders (1) were included.

Results: Findings from studies that compared the cortisol level between infertile and fertile subjects indicate that (i) Male: three studies reported elevated cortisol level in infertile patients and one found no significant difference; (ii) Female: four studies reported increased cortisol level in infertile subjects and three studies found no significant difference. Findings from studies that measured the cortisol level from infertile patients that conceived and those that didn't indicate that (i) Male: one study reported no significant difference; (ii) Female: one study reported elevated cortisol in infertile patients that conceived, whereas two studies reported increased cortisol in infertile patients that was unable to conceive. Five studies found no significant difference between the groups.

Discussion: In the present review we only included the cortisol value that was measured prior to stimulation or IVF treatment or during natural or spontaneous cycles, despite this, there are still variations in the sampling period, assessment techniques and patients' characteristics. Hence, at present, we are still unable to conclude that cortisol is significantly elevated in infertile patients. We warrant future studies to standardize the time of biological sample collection and other limitations that were addressed in the review to negate the unwanted influencing factors.

KEYWORDS

cortisol, infertility, subfertility, HPA, fertility, pregnancy, stress, sterility

10.3389/fendo.2023.1147306

1 Introduction

Infertility is defined as a disease characterized by failure to conceive after one year or more of regular, unprotected sexual intercourse due to an impaired male or female reproductive system (1). Infertility can be categorized into primary and secondary. Primary infertility is applicable for a woman that has never been diagnosed with a clinical pregnancy and fulfills the criteria for being classified as infertile, whereas a male who was not able to initiate a pregnancy with his female partner and meets the criteria for having infertility is diagnosed to have primary infertility. A woman that unable to conceive once again after previously being diagnosed with a clinical pregnancy and successfully giving birth is known to have secondary infertility. A similar classification is also applicable to males not being able to initiate pregnancy with their female partners but having done so previously (1, 2).

Based on data-driven from 195 countries in the span of 17 years (1990 to 2017), the global burden of infertility has been on the rise, with the age-standardized prevalence rate of infertility increased by 0.37% per annum for females, and 0.29% per annum for males (3). The same study also reported that the age group 35-39 had the highest prevalence rate (3). A wide range of factors has been associated with male and female infertilities including physical problems, lifestyle issues, genetic makeup, psychological problems, and hormonal disorders due to idiopathic reasons (4, 5). The impact of stress-induced psychoendocrinological changes on human reproductive function has been heavily studied over the decades (6, 7), resulting in the discovery of the role of various endogenous hormones including cortisol, catecholamines, vasopressin, gonadotrophins, thyroids, growth hormone, prolactin, and insulin in stress mechanisms (8, 9). Changes in some of these hormones were reported in infertility (10–14). This has led to research questions about whether (i) stress hormones are significantly elevated in infertility (i) causal relationship between elevated stress hormones and infertility, (ii) stress hormones as potential markers of infertility-related risk factors, and (iii) stress hormones as markers of ART outcome prediction.

Cortisol, the primary stress hormone released through the activation of the hypothalamus-pituitary-adrenal (HPA) axis was reported to affect human reproductive function through immunosuppression (15). The effect of cortisol on *in vitro* fertilization (IVF) treatment outcomes was systematically reviewed in the past, and the results were conflicting, with three studies reporting favorable IVF treatment outcomes in the presence of high cortisol levels and five studies reporting low cortisol to positively influence successful outcomes (16). Different treatment cycles during IVF treatment may directly influence the level of cortisol, for instance, hormonal stimulation and invasive procedures-induced stress as well. In the present review, our main aim is to determine the changes in cortisol levels in both male and female infertility in the absence of interference from assisted reproductive technology (ART) treatment procedures. Therefore, for studies that compared the cortisol level between female infertile subjects that conceived and those that didn't at the end of ART, we only included the cortisol level that was assessed prior to stimulation or induction.

2 Methods

2.1 Search strategy

The studies were obtained from four online databases including SCOPUS, Web of Science, PubMed, and Ovid MEDLINE from 1946 until September 2022. The last search was formed on 22nd September 2022. The search strategy involved the combination ("AND") of the following keywords: 1) corti* (cortisol, corticosteroid) OR hydrocorti* (hydrocortisone) OR glucocorti* (glucocorticoid); 2) infertil* (infertility, infertile) OR subfertil* (subfertility, subfertile). In addition, the references of all retrieved articles were reviewed for relevant citations.

2.2 Inclusion criteria

All full-length original research articles published in the English language and using humans (male or female or both) as subjects that investigated cortisol and infertility were included. For studies involving female subjects, only studies that recruited infertile subjects, and their biological specimens taken prior to a stimulated cycle or during unstimulated or spontaneous cycles were included. Among these, only studies that compared the differences in cortisol levels between fertile and infertile groups, and the pregnancy outcomes of the infertile subjects were included.

2.3 Exclusion criteria

Case series, case studies, books, reviews, letters to the editors, animal studies, cell culture studies, and conference abstracts were excluded. Human studies that specifically looked into infertile subjects with neurological or psychiatric comorbidities were excluded.

2.4 Article selection

The articles retrieved from the four databases were independently reviewed by 2 authors (BVK and JK). Any disagreement in the selection process was resolved through discussion to reach a consensus. In general, the articles were screened through three stages. First, articles that did not meet the inclusion criteria were rejected based on their titles. Second, articles that were irrelevant to infertility and cortisol were eliminated based on the abstracts. Third, the remaining articles' methods, and results were carefully reviewed, and the articles that did not meet the inclusion criteria were eliminated. Reasons for exclusion included (i) if it was not clearly mentioned whether the biological samples to measure cortisol level was taken prior to or after the hormonal stimulation during the infertility treatment, (ii) if the participants were not diagnosed with infertility, (iii) for pre- and post-treatment studies, cortisol level was not assessed prior to treatment, (iv) if the infertile subjects were diagnosed with mood disorders, (v) if the biological samples were taken after induced ovulation, (vi) if the subjects have undergone surgical procedures (varicocelectomy), (vii) infertility patients who

were at a stage prior to, during, or after their intrauterine insemination or IVF treatment, (viii) if the biological samples were collected after the embryo transfer, (ix) not reporting absolute cortisol levels.

3 Results

Initially, we identified 10,886 articles from four online databases including Ovid MEDLINE (6,843), SCOPUS (2,021), Web of Science (954), and PubMed (1,068). From this, we identified 280 articles through title screening (Ovid MEDLINE: 63, SCOPUS: 75, Web of Science: 70, and PubMeD: 72). Following the removal of duplicates, we found 143 articles. These articles' abstracts, methods, and results were reviewed based on the inclusion criteria, and this was followed by the rejection of 127 articles. In the end, we included 16 full-length original articles involving males (4), females (11), and both genders (1) as subjects in this systematic review (Figure 1).

3.1 Study designs and sample characteristics

The study designs that were employed for studies involving male subjects only are case-control prospective studies (17–20), with a total of 400 subjects involving age-matched, healthy fertile controls and infertile subjects. Only one study stated the average age of the participants, infertile (32.4 ± 6.7 years) and fertile (32.7 ± 4.8 to 33.1 ± 5.4 years) (17). Three studies provided the age range of the participants, which was, in general, ranging from 25 to 38 years (18–20) (Table 1). One study recruited 150 subjects from both genders, with their age ranging from 30.9 ± 4.9 to 35.3 ± 3.5 years. The study design employed was prospective (21) (Table 2).

Studies involving female subjects employed designs such as cross-sectional (22, 23), prospective cohort (10), case-control study (24–26), case-control prospective study (7, 27), and prospective study (28–30). The total number of participants recruited was 1102. In general, ten studies reported the average age of the separate groups of patients recruited, such as fertile control (23.5 ± 0.4 to 34 ± 5 years) and infertile group (24.4 ± 0.3 to 33.4 ± 2.3 years) and infertile/pregnant (32.75 ± 5.78 to 36.3 ± 4.76 years) and infertile/non-pregnant (32.94 ± 4.04 to 36.35 ± 3.97 years) (7, 10, 22–29). One study provided the age range of the participants recruited (23-47 years) (30) (Table 3).

The diagnosis or types of infertility specified were diminished ovarian reserve (21), ovulatory disturbance (21), tubal factor (7, 21), unexplained (23, 27), idiopathic hyperprolactinemia (22), oligomenorrhea (25), and endometriosis (21). Some of the studies reported the types of infertility as female factor, male factor, and mixed (24), male factor, female factor, and unexplained (28), primary and secondary (29), normozoospermic infertility (18, 19), oligozoospermia (17, 18), cryptozoospermia (17), azoospermia infertility (17), asthenozoospermia infertility (18), and unknown origin (19). Whereas some studies did not report the diagnosis or types of infertility involved (10, 20, 30) (Table 4).

In general, the infertile females' mean duration of infertility was ranging from 18.37 months to 8.47 ± 5.83 years. Some studies did not report the duration of infertility (10, 17–20, 22, 25, 29, 30). One of the studies reported the subjects' duration of the marriage, which was ranging from 8.03 ± 4.68 to 8.47 ± 5.83 years (23). Another study reported the duration of infertility treatment, 3.1 ± 1.6 years, and the period of waiting before the treatment, 4.3 ± 1.5 years (7) (Table 5).

Some studies recruited newly diagnosed infertile patients (10, 17, 20, 21, 23–25). In some studies, infertile patients have already been exposed to infertility treatment in the past (7, 30). Whereas some studies did not report whether the recruited infertile patients were novices or have prior infertility treatment experience (18, 19, 22, 25–27, 29) (Table 6).

3.2 Cortisol measurement

Various types of biological samples were collected to assess the cortisol level in the study subjects including serum (7, 10, 18–20, 22, 23, 25–29), saliva (21), and hair (24). Two studies used blood samples but did not specify whether plasma or serum was used for cortisol assessment (17, 30) (Table 7).

Some studies collected the biological specimens in the morning only (7, 10, 17–22, 25, 28, 29), around 0730-0900, upon waking up,

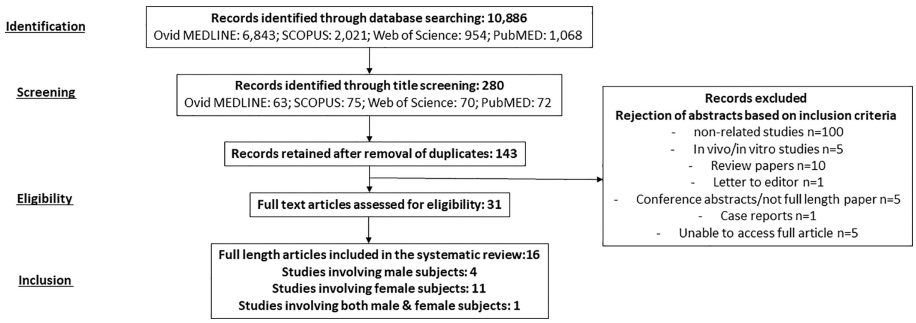

FIGURE 1
A summary of literature search, screening, and selection of studies based on Preferred Reporting Items for Systematic Reviews and Meta-Analyses (PRISMA) guideline.

TABLE 1 Characteristics of the included studies: Male.

References	Title	Study Design	Sample size & Age	Duration of infertility	Inclusion criteria	Cause(s) of infertility	Methods of cortisol measurement	Day, time and types of biological sample collected	Methods & Results	Conclusion
(20)	Impact of emotional disorders on semen quality in men treated for infertility	Case-control prospective study	112 men (60 fertile control vs 52 low fertility) [27 -33 years]	–	Men aged between 27-33, BMI 18.5-24.9, non-smokers, no problem drinking, no history of medications, unable to conceive after 12 months of regular unprotected sexual intercourse with fertile female partner.	None specified	Cortisol level was measured in a standard laboratory.	Serum cortisol collected in the morning	Mean cortisol level was significantly higher in the low fertility group (165.35 µg/dL), compared to the control (130.78 µg/dL) ($p < 0.001$). Higher Beck Depression Inventory (BDI) was significantly associated with higher cortisol level ($r=0.657$, $p<0.001$). Higher State-Trait Anxiety Inventory (STAI-1 and STAI-2) scores were significantly associated with higher cortisol [STAI-1 ($r=0.697$, $p<0.001$) STAI-2 ($r=0.665$, $p<0.001$)]	Anxiety and depression in subfertile males are associated with increased secretion of prolactin and cortisol.
(17)	Male Fertility: Endocrine Stress Parameters and Coping	Case control prospective study	48 men (14 impaired fertility vs 34 fertile) (average age: Group A: 33.1 ± 5.4, Group B: 32.7 ± 4.8, Group C: 32.4 ± 6.7 to years	–	Male patients aged 18 to 45: Group A: normozoospermia, elevated prolactin (>360 IU/L). Group B: normozoospermia, normal prolactin (<360 IU/L) Group C: impaired fertility, azoospermia or oligozoospermia, or cryptozoospermia	oligozoospermia, cryptozoospermia or azoospermia	Cortisol was assessed using with chemiluminescence immunoassay.	Blood; morning	The cortisol level in group A (612.9 nmol/L) was significantly higher than Group B (478.1 nmol/L) ($p<0.05$). There was no significant difference between group A+B (557.4 ± 143.4 nmol/L) and group C (580.7± 134.1 nmol/L) in cortisol level. There was no significant difference in depression scores between the groups, based on SVF120 the total of coping strategy was significantly higher in infertile group.	No significant change in cortisol was seen in impaired fertility group, however no comparison was made between Group B and C alone.
(18)	Mucuna pruriens Reduces Stress and Improves the Quality of Semen in Infertile Men	Case-control prospective study	120 men (aged 30-38 years old)	–	Men (30–38 years); healthy control: had previously initiated at least 1 pregnancy and with normal semen profile; infertile group: attending infertility clinic, of same socioeconomic and ethnic status (Indo Aryan) and BMI (19 to 24 kgm2), not on nutritional supplement or vitamins	normozoospermic infertility, Oligozoospermic infertility, asthenozoospermic infertility	Serum cortisol levels were assessed by radioimmunoassay	Venous blood samples; morning (0800h) and evening (1600h)	The morning and evening serum cortisol levels were significantly higher in the infertile groups [morning cortisol ug/dL: normozoospermic (14.1 ± 3.0; $P<0.01$), oligozoospermic(21.5 ± 0.7; $P<0.01$) and asthenozoospermic(28.0 ± 1.0; $P<0.01$)] and [evening cortisol: normozoospermic(10.1 ± 1.6; $P < 0.01$), oligozoospermic 13.3 ± 4.6 (; $P< 0.01$) and asthenozoospermic (16.8 ± 1.3; $P< 0.01$) compared to the healthy	The cortisol level was significantly higher in infertile subjects compared to healthy fertile subjects.

(Continued)

10.3389/fendo.2023.1147306

TABLE 1 Continued

References	Title	Study Design	Sample size & Age	Duration of infertility	Inclusion criteria	Cause(s) of infertility	Methods of cortisol measurement	Day, time and types of biological sample collected	Methods & Results	Conclusion
									control [morning: 10.2 ± 0.2, evening: 5.0 ± 0.6]	
(19)	Withania somnifera Improves Semen Quality in Stress-Related Male Fertility	120 total- 60 healthy men, normozoospermic infertile men (20), normozoospermic infertile men under psychological stress (20), normozoospermic infertile men who were cigarette smokers (20) [25-38 years]	Case-control Prospective study	–	Men (aged 25-38 years old) - Control: healthy fertile men who had initiated at least 1 pregnancy and has normal sperm count; Men attending infertility treatment divided into (i) normozoospermic infertile men, (ii) normozoospermic infertile men under psychological stress and (iii) normozoospermic infertile men who were cigarette smokers.	Normozoospermic infertility; infertility of unknown etiology	Serum cortisol was assessed based on method of Foster and Dunn [Foster & Dunn, 1974] (radioimmunoassay)	Blood; collected in the morning (0800h) and evening (1600h)	The mean serum level in the infertile group was higher than the control group in both morning and evening. The cortisol level in healthy fertile group was 10.84 ± 1.63 μg/dL in the morning and 5.8 ± 1.33 μg/dL in the evening.	The cortisol level was significantly higher in infertile subjects compared to healthy fertile subjects.

10.3389/fendo.2023.1147306

10.3389/fendo.2023.1147306

TABLE 2 Characteristics of the included studies: Male and Female.

References	Title	Study Design	Sample size & Age	Duration of infertility	Inclusion criteria	Cause(s) of infertility	Methods of cortisol measurement	Day, time and types of biological sample collected	Methods & Results	Conclusion
(21)	Stress in couples undergoing assisted reproductive technology	Prospective study	150 patients/75 couples (Mean age, female pregnant: 30.9 ± 4.9, male pregnant: 32.2 ± 4.1, female not pregnant: 33.9 ± 3.9, male not pregnant: 35.3 ± 3.5 years)	From 5.5 ± 3.5 to 5.5 ± 2.4 years	Couples with primary infertility in their first ART treatment cycle, with a BMI of 20.0–29.9 kg/m2.	Primary infertility, female factor: endometriosis, ovulatory disorders, and poor ovarian reserve, and tubal factor Male factor based on WHO criteria (2010)	Cortisol level was measure using enzyme-linked immunosorbent assay.	Saliva; collected at 15, 30, and 60 min upon waking up prior to the start of gonadotropins in GnRH antagonist cycle (first day of their ART cycle)	There was no significant difference in cortisol levels between different interval upon waking up (15, 30, and 60 mins) in male and female samples. The median value of cortisol level was significantly higher in women who became pregnant than those who did not [24.7 ng/ml (19.9–63.1) vs. 20.7 (10.4–30.4), respectively]. No significant difference was seen in the cortisol level of male between the two groups.	Based on the interval after waking up, the study discovered no statistically significant variation in cortisol levels. However, pregnant women's cortisol levels were higher than those of non-pregnant women, while no such difference was seen in males.

and some studies collected samples on multiple time points, such as 15, 30, and 60 minutes after waking up (21). Two studies collected the biological specimens in both morning and evening (18, 19). Whereas some studies did not report the time of biological specimen collection (24, 26, 27) (Table 8).

The results of cortisol levels were reported in numerous units due to differences in the measuring techniques. Some have reported their results in μg/dL (10, 18–20, 26, 27), nmol/L (7, 17, 28), ng/mL (21), g/dL (30), μg/mL (23), μg/L (29), μmol/L (25), pg/mg (24), and nm/L (22) (Table 9).

Techniques employed in the studies to measure the cortisol level were chemiluminescence immunoassay (10, 17), radioimmunoassay (18, 19, 25, 28, 30), enzyme-linked immunosorbent assay (ELISA) (21, 22, 24, 27), liquid chromatography-mass chromatography (23, 29), and dissociation-enhanced lanthanide fluoroimmunoassay (DELFIA) (7). Two studies did not specify the techniques (20, 26) (Table 10).

Some studies specified the time of female biological specimen collection as early follicular phase or luteal phase or ovulation phase or prior to the stimulation day (7, 10, 22, 26–30). Some reported the specimens were taken during the time of recruitment or while on the waiting list for treatment or prior to the beginning of treatment (21, 23–25) (Table 11).

3.3 Cortisol levels in infertility: male and both genders

A study that assessed the cortisol levels in both male and female patients found no significant difference in the levels of cortisol among males with conceived and non-conceived female partners following the IVF treatment (21) (Table 12). Four studies evaluated the cortisol levels in infertile male patients only. Among these, three studies reported elevated cortisol levels among infertile males compared to healthy controls (18–20). One study found no significant difference between infertile and healthy controls (17) (Table 13).

3.4 Cortisol levels in infertility: female

Among the studies that recruited female subjects, seven studies compared the cortisol levels between the infertile and fertile female subjects. Out of these, four studies reported elevated cortisol levels in infertile female subjects compared to the fertile group (10, 22, 23, 26). Three studies found no significant difference in the cortisol levels between the fertile and infertile subjects (7, 25, 27) (Table 14). Nine studies measured the cortisol levels prior to treatment or stimulation in infertile subjects that conceived at the end of IVF treatment and those that did not. Two studies reported elevated cortisol levels in infertile female subjects that could not conceive following IVF compared to those who could (10, 26). However, five studies found no significant difference in the cortisol levels between the conceived, infertile female subjects and those did not (7, 24, 28–30). In contrast, one study reported that the median value of cortisol was higher among females that conceived compared to those who did not (21) (Table 15).

TABLE 3 Characteristics of the included studies: Female.

References	Title	Study Design	Sample size & Age	Duration of infertility	Inclusion criteria	Cause(s) of infertility	Methods of cortisol measurement	Day, time and types of biological sample collected	Findings	Conclusion/ comments
(22)	Endocrine Markers of Fertility Potential in Reproductive Age Women with Idiopathic Hyperprolactinemia (HP)	Cross sectional study	82: 27 healthy women 23.6 ± 0.3 years old, 33 patients with endocrine sub fertility with idiopathic HP (24.4 ± 0.3 years old), and 22 fertile women with idiopathic HP with mean age of 23.5 ± 0.4 years old.	Not stated	Group 0: healthy women who had pregnancy in 2 years back without any gynaecological pathology, without any lactation history Group 1: Infertility for at least two years of unprotected, timed intercourse, and a stable increase of serum prolactin level. Group 2: women with pregnancy 2 years back year but serum prolactin level was increased. The diagnosis of HP occurred before pregnancy and a year after child-birth.	IdiopathicHyperprolactinemia	Serum cortisol was assessed using ("Elisas") immunoassay analyzer "Ultra Microplate Reader - Elx808"(USA).	Serum; from 8 to 9 am, within the early follicular phase (5-7 days of the menstrual cycle).	Group 0: 475,27 ± 140,59 Group 1 503,84 ± 238,21and Group 2 700,18 ± 352,59nm/l. The cortisol level was higher in the subfertile patients in relation to fertile women in condition of hyperprolactinemia by 37%.	Infertility due to idiopathic hyperprolactinemia elevates serum cortisol level. However, we need to take into account the altered prolactin level in this case, which may disrupt the function of HPA axis, hence the level of cortisol. This may not be the case for the other types of infertility.
(27)	Intensive hormone monitoring in women with unexplained infertility: evidence for subtle abnormalities suggestive of diminished ovarian reserve	Case-control prospective study	24 (12 infertile and 12 healthy control) average age of infertile women 33.2 ± 1.3 years; healthy: 32.8 ± 1.2	4.4 ± 0.8 years	25-40 years old; normal tubal and peritoneal anatomy; 121 ovulatory menstrual cycles from 26 to 32 days; BMI between 18 and 28 (kg/m2>. The male partner had no evidence of male factor infertility.	Unexplained infertility	Serum cortisol level was measured with ELISA using streptavidin technology as the detection system.	blood was taken every other day until the onset of menstruation.	No significant differences in the cortisol level between the groups (P = 0.141), nor was the interaction between group and phase (P = 0.72).	Unexplained infertility had no significant effect on serum cortisol level.
(10)	Interactions of Cortisol and Prolactin with Other Selected Menstrual Cycle	prospective cohort study.	305 (205 infertile [26.7 ± 1.9 years] and 100 fertile	Not stated	primary infertility; first entered for infertility therapy, no prior hormone treatment, patent	Nothing specified	On the third day of the cycle cortisol level was assessed using electrochemiluminescence	Serum; obtained in the morning (3rd day of the cycle and 7 days after ovulation)	Infertile women recorded higher cortisol compared to the control during each phase of the	Increased cortisol in infertile women decreased the pre-ovulatory LH peak and estradiol,

(Continued)

10.3389/fendo.2023.1147306

TABLE 3 Continued

References	Title	Study Design	Sample size & Age	Duration of infertility	Inclusion criteria	Cause(s) of infertility	Methods of cortisol measurement	Day, time and types of biological sample collected	Findings	Conclusion/ comments
	Hormones Affecting the Chances of Conception in Infertile Women		women [26.8 ± 1.8 years]		fallopian tubes; no male factors.		method using the Cobas c6000 analyzer.		menstrual cycle ($p < 0.001$) 3rd day, control: 138.54, infertile: 157.50 ug/dL 7th day after ovulation, control: 143.91, infertile: 216.51 ug/dL. Cortisol level after ovulation in infertile group was negatively correlated with LH during ovulation, progesterone after ovulation, estradiol during and post-ovulation, follicle size, and endometrial thickness during and post-ovulation ($r<0$, $p<0.05$). 17 out of 205 infertile women achieved pregnancy (8.3%). Women with + HCG test had significantly lower level of cortisol compared to those with -HCG test result ($p < 0.001$; 3rd day of the cycle 113.12 versus 161.62 µg/dL; during ovulation 162.24 versus 216.95 µg/dL; after ovulation 163.18 versus 221.46 µg/dL, respectively).	postovulatory estradiol, affecting the endometrial growth, and conception chances.
(25)	Low 11-deoxycortisol to cortisol conversion reflects extra-adrenal factors in	Case-control study	49 (clomiphene citrate-resistant infertile=26,	Not stated	normoestrogenic, normo-gonadotroph, oligomenorrhoeic, witha history of	oligomenhorrea	Cortisol level was assessed using solid-phase 3H radioimmunoassay	Serum; Collected between 0800 and 0900, after 12 h of fasting.	Comparisons of morning cortisol levels indicated similar morning cortisol	The authors concluded that extra adrenal factors were involved in

(Continued)

10.3389/fendo.2023.1147306

TABLE 3 Continued

References	Title	Study Design	Sample size & Age	Duration of infertility	Inclusion criteria	Cause(s) of infertility	Methods of cortisol measurement	Day, time and types of biological sample collected	Findings	Conclusion/ comments
	the majority of women with normo-gonadotrophic normo-estrogenic infertility		obese ovulatory control=11, lean ovulatory control=12). Mean age of infertile subjects 33 ± 5 (25 ± 44) obese (34 ± 5), lean 33 ± 4		oligomenorrhoea, otherwise healthy and had no endocrine disorders			Blood collected more than 3 months prior to inclusion in the study.	concentrations (0.47 ± 0.15, 0.45 ± 0.16 and 0.47 ± 0.18 nmol/l) between 3 groups.	infertility syndromes studied.
(23)	SIRTI and cortisol in unexplained infertile females; a cross sectional study, in Karachi Pakistan	cross sectional study	135 infertile cases (31.13 ± 5.7) and 207 fertile control (31.22 ± 6.02)	Duration of marriage, 8.03 ± 4.68 for fertile, and 8.47 ± 5.83 years for infertile groups	Infertile: duration of infertility more than two years, subjects aged between 16 and 45 years, from all ethnic backgrounds. Control: healthy females, aged between 16 and 50 years, with a child less than 5 years of age, from all ethnic groups.	Unexplained infertility	Serum cortisol was assessed using enzyme linked immunosorbent assay (ELISA) kits.	Venous blood; collected from 8 till 9 am	The cortisol level in fertile females was 9.98 ± 1.88 (ug/ml), and infertile group was 15.66 ± 7.73(ug/ml), which is significantly higher in the infertile group (<0.01).	In unexplained infertility cortisol level is significantly elevated.
(24)	Hair Cortisol Concentrations as a Biomarker to Predict a Clinical Pregnancy Outcome after an IVF Cycle: A Pilot Feasibility Study	Case-control study	43 subjects with a mean age of 36.3 ± 4.36 years [pregnant: 36.3 ± 4.76, non pregnant: 36.35 ± 3.97]	18.37 (± 8.68) in months	BMI of 19–30 kg/m2, no prior fertility treatments, undergoing *in vitro* fertilization with intracytoplasmic sperm injection (IVF/ICSI) or *in vitro* fertilization with preimplantation genetic diagnosis (IVF/PGD), with delayed embryo transfer under the	Female factor (46.5%), male factor (37.2%), mixed factor (16.2%)	Hair cortisol concentration was measured with a salivary ELISA cortisol kit and expressed in pg/mg	Hair sample was collected on T1: 2nd consultation with reproductive endocrinologist prior to first IVF cycle; T2: 12 weeks following post-transfer visit with the study coordinators (T2), days before human	For pregnant women HCC at T1 was 364.63 (571.44) [mean (SD)] and non-pregnant women was 181.06 (169.74) Women with a negative pregnancy test had higher HCC at T2 (181.06 pg/mg vs. 741.06 pg/mg, $p < 0.001$) but HCC at T2 was not statistically different between pregnant women when compared to	HCC might be a promising biomarker to calculate the probability of pregnancy in women using assisted reproductive technologies.

(Continued)

10.3389/fendo.2023.1147306

TABLE 3 Continued

References	Title	Study Design	Sample size & Age	Duration of infertility	Inclusion criteria	Cause(s) of infertility	Methods of cortisol measurement	Day, time and types of biological sample collected	Findings	Conclusion/ comments
					(GnRH) antagonist protocol			chorionic gonadotropin pregnancy test.	non-pregnant women. There were no statistical differences between HCC at T1 and HCC at T2. When BMI, time of infertility, number of follicles and age were included in model as covariates, an interaction effect was noticed between HCC at T1 and T2 F (1, 31) = 0.71, p = 0.01, and η2 = 0.16	
(28)	Pituitary-adrenal and sympathetic nervous system responses to psychiatric disorders in women undergoing *in vitro* fertilization treatment	Prospective study.	264 (The infertile patient that remained non-pregnant, mean age was 33.4 (3.9). vs Infertile that conceived 33.1 (4.1)	7.0 (3.5) years.	Women that came for their first cycle of IVF or ICSI treatment, regular menstrual cycles and no hormonal contraceptive use.	Male factor, female factors, and explained	Cortisol level was measured by radioimmunoassay	Blood samples were taken in the luteal phase before treatment (T1) and on the day of oocyte retrieval (T2) between 8:00 and 9:00 AM.	There is no significant difference in cortisol levels at T1 between the pregnant and nonpregnant women, but at T2, serum cortisol was lower in the conception cycles (P<.001). Serum cortisol in nonpregnant women on T1 was 238.7 (78.2) (nmol/L). Follicular cortisol in the nonpregnant group was significantly higher than the pregnant group (P<.001). Serum cortisol on T2 was significantly correlated with the respective follicular values in all patients (P<.001).	Cortisol concentration imposes negative influence on pregnancy outcome in infertility treatment.
(29)	Prospective study of pregnancy outcome	Prospective study	128 (pregnant vs	Not stated	Women aged 40 and below,	Primary and secondary	Serum cortisol level was measured through	Blood samples were collected	No significant difference was found	The authors found significantly higher

(Continued)

10.3389/fendo.2023.1147306

TABLE 3 Continued

References	Title	Study Design	Sample size & Age	Duration of infertility	Inclusion criteria	Cause(s) of infertility	Methods of cortisol measurement	Day, time and types of biological sample collected	Findings	Conclusion/ comments
	between perceived stress and stress-related hormones		non-pregnant: Mean age ranging from pregnant: 32.75 ± 5.28, non-pregnant: 32.94 ± 4.04)		undergoing the first IVF cycle, capable of completing anxiety and stress test		enzyme-linked immunosorbent assay.	at 8:00–8:30 on the morning of menstrual cycle day 3	in cortisol, between the pregnant (18.4 ug/L) and nonpregnant (21.4 ug/L) groups. The cortisol level was significantly related to SDS score.	level of salivary amylase and angiotensin II compared to cortisol in non-pregnant infertile women than the pregnant ones.
(7)	The influence of stress and state anxiety on the outcome of IVF-treatment: Psychological and endocrinological assessment of Swedish women entering IVF-treatment	Case-control prospective study	44 (22 infertile vs 22 fertile controls) infertile (33.4 ± 2.3 years) and fertile (33.1 ± 2.5 years old)	infertility treatment for 3.1 ± 1.6 years and waiting list before treatment was 4.3 ± 1.5 years	Infertile: Primary/ secondary infertility, regular menstruation, male partners with normal spermiogram on at least 2 occasions; control: fertile, regular menstruation	Tubal infertility	Serum cortisol level was assessed using DELFIA fluoroimmunoassay kits	Blood samples; collected during a normal natural cycle in the morning between 07.30 h and 08.30 h, on days 3, 10–15 and 19–26.	There was a significant difference in the serum cortisol ($p>0.01$) during the entire menstrual cycle. There was no significant difference in the plasma cortisol measured between 8–12 o'clock on cycle day 3 between the pregnant and non-pregnant infertile women, and between fertile and infertile women. No significant correlation was reported between the hormonal measure and Karolinska Scales of Personality variables and total STAI scores.	On day 3 of the cycle no significant difference was seen in the cortisol level between the study groups.
(26)	Reproductive problems and intensity of anxiety and depression in women treated for infertility	Case-control study	200 (fertile control 100 and infertile 100) Mean age: infertile: 26.7 ± 1.9 Years, fertile: 26.8 ± 1.8	Not stated	Infertile: Women aged 23–30 with infertility Control: Fertile women with at least two children, and used the mechanical means	None specified	Cortisol level was assessed at Diagnostyka Group authorized laboratory	Blood was collected on day of ovulation (without hormonal stimulation)	The serum cortisol concentration was higher in infertile women (212 µg/dl and 217 µg/dl on average) than fertile women (141 µg/dl and 144 µg/dl on average). Cortisol also	Emotional state of women undergoing IVF treatment is worse than fertile women.

(Continued)

10.3389/fendo.2023.1147306

TABLE 3 Continued

References	Title	Study Design	Sample size & Age	Duration of infertility	Inclusion criteria	Cause(s) of infertility	Methods of cortisol measurement	Day, time and types of biological sample collected	Findings	Conclusion/ comments
					of contraception during the study.				was higher in non-pregnant women (217 µg/dl and 221 µg/dl on average) than pregnant women (162 µg/dl and 163 µg/dl on average). In infertile women, the cortisol level during and post-ovulation is positively correlated with the severity of trait and state anxiety, symptoms of anxiety and depression.	
(30)	Psychological and Hormonal Changes in the Course of in Vitro Fertilization	Prospective study	113	Not stated	Women (age 23-47), completed elementary education, had been previously treated for infertility for at least 2 years, no history of psychological or psychiatric disorders.	Not stated	Cortisol concentration was assessed using the Coat-A-Count and the Double Antibody kits	Baseline measures were taken during early follicular phase (days 3-5 of the cycle), in the morning	The conceived and non-conceived groups recorded normal range of cortisol level at about 15-17 ~µg/dl and remained in this range until the ovum pickup day. On embryo transfer day, a decline in cortisol level was seen in both groups. In luteal phase on expectation of pregnancy results, the cortisol level was increased to 21-22 µg/dl in both groups. Significance correlation was found between cortisol and prolactin level in phase I, III, and IV of IVF treatment in non-conceiving group.	Hormonal and endorphin mediation may play an important role in successful IVF outcome.

10.3389/fendo.2023.1147306

10.3389/fendo.2023.1147306

TABLE 4 Types of infertility.

Types of infertility														
Diminished ovarian reserve	Ovulatory Disturbance	Tubal factor	Unexplained	Idiopathic Hyperprolactinemia	Oligomenorrea	Endometriosis	Not Stated	Normozoospermia infertility	Oligozoo Spermia inferility	Cryptozoospermia	Azoospermia	Asthenozoospermia	Unkown origin	female factor, male factor, mixed	male factor, female factor, explained	primary/secondary
(21)	(21)	(7, 21)	(23, 27)	(22)	(25)	(21)	(10, 20, 30)	(18, 19)	(17, 18)	(17)	(17)	(18)	(19)	(24)	(28)	(29)

4 Discussion

4.1 Male: infertile vs fertile

Four studies reported changes in blood cortisol levels in healthy fertile and infertile males, with one reporting no significant difference (17), and three found significantly higher cortisol in infertile male patients (18–20). Out of these four studies, only three studies specified the causes of infertility which included normozoospermic, oligozoospermic, cryptozoospermic, azoospermic, asthenozoospermic, and unknown infertility (17, 18). None of the studies reported a significant direct correlation between cortisol levels and infertility characteristics investigated. One study reported higher Beck Depression Inventory (BDI), and State-Trait Anxiety Inventory (STAI-1 and STAI-2) scores to be significantly associated with higher cortisol levels in infertile patients, and BDI score also significantly negatively correlated with sperm count and ejaculate volume. Lower STAI-1 and STAI-2 scores were associated with a higher percentage of sperm with progressive motility (20). A recent systematic review reported mental disorders such as depression, sleep disorders, addiction, eating disorders, and stress negatively impact fertility in males and females (6). It is not within the scope of the present review to relate stress with infertility, nevertheless perceived stress, anxiety, and depression was reported in the past to elevate cortisol level (32, 33).

Harth and Linse (17) found no significant difference in the blood cortisol levels between infertile subjects (normozoospermic, cryptozoospermic, or azoospermic) and a combined cortisol level from Group A (normozoospermic, high prolactin, and stress levels) and Group B (normozoospermic, normal stress and prolactin levels), 580.7 nmol/L (infertile) against 557.4 nmol/L (Group A +B). Nevertheless, earlier reports on prolactin showed that prolactin may directly induce adrenal steroidogenesis, thus increasing the level of cortisol (34, 35). This should be taken into consideration when interpreting the results. In the same study, the cortisol level in Group B subjects was much lower, 478.1 nmol/L, however, no description was given of the individual comparison between group B and C. Harth and Linse (17) recruited participants between the age range of 18-45 years old, a much wider range, whereas the other three studies recruited between the age of 27-33 (20), 30-38 (18), and 25-38 (19) years old participants, with the lowest age being 25 and oldest 38. The average age of the participants recruited by (17) was 32.7 ± 4.8 to 33.1 ± 5.4 years old, whereas the other three studies did not report the participants' average age. Cortisol is synthesized from cortisone by the enzyme 11β-hydroxysteroid dehydrogenase type 1 (11βBHSD1) and converted to inactive cortisone by 11β-hydroxysteroid dehydrogenase type 2 (11βBHSD2). Age alters the activity of 11βBHSD2 (36). Furthermore, an increase of 17 nmol/L in serum cortisol per year of age was reported. This accounts for approximately 32% of the difference in serum cortisol levels between patients (R2 = 0.315; 36).

Two studies (18, 19) reported the morning cortisol level (10.2 to 10.84 μg/dL) to be higher than the evening cortisol level (5.0 to 5.8 μg/dL) in healthy fertile subjects, which is in line with circadian cortisol rhythmicity reported in the past (37–39). Normozoospermia (18, 19), asthenozoospermia (18), and

TABLE 5 Duration of infertility.

Duration of infertility	
Stated	Not stated
(7) [infertility treatment: 3.1 ± 1.6 years, and waiting list before treatment: 4.3 ± 1.5 years] (21) [5.5 ± 3.5 to 5.5 ± 2.4 years] (23) [duration of marriage: 8.47 ± 5.83 years] (24) [18.37 ± 8.68 months] (27) [4.4 ± 0.8 years] (28) [7.0 (3.5) years]	(10, 17–20, 22, 25, 26, 29, 30)

unknown origin (19) were reported as infertility-related factors in infertile males with higher cortisol. To date, very little literature is available to physiologically link asthenozoospermia to altered cortisol levels. At the preclinical level, asthenozoospermia induced via the inactivation of AMP-activated protein kinase-α1 (AMPKα1) in mice caused no significant changes in plasma cortisol level (40).

4.2 Female: infertile vs fertile and infertile/pregnant vs infertile/non-pregnant

Four studies found that the cortisol level in infertile females was significantly higher compared to fertile females (10, 22, 23, 26). Out of this, only one study reported a significant negative correlation between high cortisol (after ovulation) and LH level during ovulation, progesterone level after ovulation, estradiol level during and post-ovulation, follicle size and endometrial thickness during and post-ovulation (10). One study recruited infertile patients with idiopathic hyperprolactinemia hence elevated cortisol levels due to the direct effect of enhanced prolactin on adrenal steroidogenesis should be considered in the interpretation of results (34, 35). Three studies reported no significant difference in the cortisol level (7, 25, 27). All seven studies measured cortisol using serum samples taken in the morning, except for two studies that did not state the time of biological specimen collection (26, 27). In general, studies that reported elevated cortisol levels in infertile females recruited a larger pool of participants (929 subjects in four studies) compared to the studies that reported no significant difference in the cortisol level (117 subjects in three studies). The average age of participants recruited by studies reporting significant differences in the cortisol level (control: 23.6 ± 0.3 to 31.22 ± 6.02; infertile: 24.4 ± 0.3 to 31.13 ± 5.7 years old) is also lower compared to the studies that found no significant difference in the cortisol (control: 32.8 ± 1.2 to 34 ± 5; infertile: 33 ± 4 to 33.4 ± 2.3 years old). Higher age of the control group (in studies that found no significant difference in cortisol level) may have reduced the deficit in the cortisol value between study groups due to the aging-related effects on cortisol value (36, 41).

Two studies reported higher cortisol in infertile/non-pregnant patients (10, 26), however, none of the studies reported a significant association with pregnancy outcomes. Five studies found no significant change in the cortisol level (7, 24, 28–30). Both sets of studies recruited an almost similar pool of participants (525 versus 595 subjects). In general, the average age of participants in studies with elevated cortisol is in their 20s. Infertility factor such as idiopathic hyperprolactinemia (22) was reported in infertile females with elevated cortisol. Hyperandrogenism was reported in PCOS due to dysregulation of 11β-hydroxysteroid dehydrogenase (42, 43).

The menstrual cycle is known to affect the activity of the HPA axis which can result in variation in cortisol synthesis, such as higher cortisol levels during the luteal phase compared to the follicular phase (31). 14 out of 17 selected studies collected the biological specimen for cortisol analysis in the morning, and four studies did not specify the time of collection (10, 17, 20, 30). Physiological cortisol level is usually higher in the morning, especially 30-45 minutes after awakening and gradually reduces for the rest of the day under normal conditions (44).

Eight out of 17 selected studies did not report whether the recruited infertile patients have any prior exposure to IVF treatment procedures. Anticipatory stress was associated with higher stress reactivity for cortisol (45) and higher stress task-induced increase in cortisol (46). Contrary to this, some researchers found no significant association between cortisol awakening response and stress anticipation (47). Furthermore, reports on the effects of stress during and prior to IVF treatment on pregnancy outcomes have been conflicting (48, 49). It will be interesting to see in future studies whether there is a significant difference in stress and stress-related hormones among infertile patients that undergoing ART treatment for the first time and those with prior exposure.

Based on the data we have listed, while high cortisol may have been reported in most of the infertile subjects, this is not always the case (Tables 13–15). It is challenging to ascribe infertility to cortisol levels due to the presence of various other confounding factors. The complex interactions of multiple hormones, each of which plays a specialized role in regulating fertility, make the human reproductive

TABLE 6 Prior exposure to IVF treatment.

Prior exposure to IVF treatment		
First time IVF	Prior IVF exposure	Not stated
(10, 17, 20, 21, 23, 24, 28)	(7, 30)	(18, 19, 22, 25–27, 29)

TABLE 7 Types of biological specimen collected.

Types of biological sample collected			
Blood	Serum	Hair	Saliva
(17, 30)	(7, 10, 18–20, 22, 23, 25, 27–29)	(24)	(21)

TABLE 8 Time of biological specimen collection.

Biological specimen collection (time)		
Not stated	Morning	Evening
(24, 26, 27)	(7) [0730-0830] (10) (17) (18) [0800] (19) [0800] (20) (21) [15, 30, 60 mins after waking up] (22) [0800-0900] (23) [0800-0900] (25) [0800-0900] (28) [0800-0900] (29) [0800-0830] (30)	(18) [1600] (19) [1600]

system even more complex. The stress hormone cortisol interacts with this complex hormonal network and has the potential to cause disruptions (50), which is still poorly understood. Finding the precise mechanisms through which cortisol affects infertility is challenging due to the complexity of the hormonal pathways and feedback mechanisms involved in fertility regulation. Nevertheless, a majority of results have linked chronically elevated cortisol levels with disrupted reproductive endocrinology based on observational and correlational data. For instance, excessive amounts of cortisol might interfere with GnRH's pulsatile release, which controls the menstrual cycle and ovulation. This can result in irregular or absent ovulation and, ultimately, infertility (51, 52). High cortisol levels could inhibit LH and FSH release as well, which affects ovarian function and lowers the likelihood of pregnancy. The menstrual cycle is hampered by increased secretion of cortisol and prolactin in infertile women by lowering pre-ovulatory LH peak and E2 and post-ovulatory E2 levels that alter endometrial development and thus lower the likelihood of conception (10). However, it's crucial to remember that some people might be more resilient to the effects of cortisol on reproductive function. In line with this, it was reported that psychopathology, stress, and hair cortisol concentration scores were higher for pregnant women with poorer resilience than for those with better resilience (53). The likelihood that someone would experience infertility due to cortisol can depend on a variety of variables, including genetic differences, general health state, and stress resilience. It is difficult to establish a universal link between cortisol and infertility owing to this individual diversity.

In the present review, we noticed a large span in the age difference of the recruited study participants. The relationship between age and infertility is complex, with aging older having a significant role in both men's and women's declining fertility (54–56). In women, the quality and quantity of eggs decrease during aging, resulting in a decreased ovarian reserve (57), which leads to a longer time to conceive, decreased fertility, and a higher risk of pregnancy-related complications (58, 59). An increase in paternal age also has an impact on reproductive outcomes in males, affecting sperm volume, motility, and morphological changes that may result in decreased fertility (55). Individuals' stress response systems may change as they get older (60), which could have an impact on how cortisol is regulated. Age-related changes in cortisol patterns, such as a diurnal cortisol fluctuation (61, 62), or changes in overall cortisol output (63). These alterations may be caused by aging-related effects on the hypothalamic-pituitary-adrenal (HPA) axis, the system that regulates cortisol. The relationship between cortisol and age might be bidirectional. Aging-related elements including long-term underlying illness (64), endocrinological changes (65), or psychological stressors (66) could affect cortisol levels. On the contrary, cortisol dysregulation by itself may hasten aging (67, 68), resulting in a complicated interplay between

TABLE 9 Unit of cortisol concentration.

Cortisol concentration (unit)								
µg/dL	nmol/L	ng/ml	g/dL	µg/ml	µg/L	µmol/L	pg/mg	nm/L
(10, 17, 18, 20, 26, 27)	(7, 17, 28)	(21)	(30)	(23)	(29)	(25)	(24)	(22)

TABLE 10 Cortisol measurement technique.

Cortisol measurement (technique)					
Not stated	Chemiluminescence Immunoassay	Radioimmunoassay	ELISA	LC-MS	DELFIA fluoroimmunoassay
(20, 26)	(10, 17)	(18, 19, 25, 28, 30)	(21–24, 27)	(29)	(7)

TABLE 11 Day of biological specimen collection.

Day of biological specimen collection [female subjects]	
Early/mid follicular phase/luteal/ovulatory phase	Prior to the study
(7) [on day 3 of normal natural cycle] (22) [within the early follicular phase, 5-7 days of menstrual cycle] (26) [On the day of ovulation] (27) [every other day until onset of menstruation] Wdowiak et al., 2020 [3rd day of cycle and 7th day after ovulation] (28) [luteal phase before treatment] (29) [Day 3 of menses] (30) [Day 4-5]	(21) [1st day of ART cycle prior to hormonal stimulation] (23) [Blood withdrawn at the time of recruitment] (24) (25) [3 months prior to the study]

cortisol levels and age. While cortisol and age can both have an independent impact on fertility, they may also affect fertility synergistically. The delicate hormonal balance required for fertility can also be upset by altered cortisol levels linked to long-term stress or by age-related changes in cortisol regulation (10, 52). Hormonal imbalances brought on by cortisol may make the age-related decline in fertility worse and aid infertility.

Stress has long been thought to affect fertility as well as other areas of general well-being (69). While stress is associated with elevated cortisol (70), proving a direct cause-and-effect relationship between cortisol and fertility is challenging, and thus it necessitates more research. The delicate hormonal balance involved in reproductive processes is thought to be affected by prolonged exposure to elevated cortisol levels, which may affect fertility. Based on existing literature, in both genders, prolonged stress has been associated with diminished reproductive functions (71, 72). Even though cortisol is part of the stress-fertility relationship, it's vital to understand that fertility is a complex process that governed by a myriad of factors. Stress affects fertility indirectly through psychological and physiological impacts such as change in lifestyle factors (73, 74), sleep quality (75, 76), and sexual behavior (77). Understanding the connection between cortisol and fertility presents a substantial problem in separating the precise effects of cortisol from the general stress response. Individual variation in stress reactions and coping mechanisms further complicates the interpretation of research findings. While some people can handle stress better than others, some may be more susceptible to its negative consequences (78). Furthermore, patients who are diagnosed as infertile suffer from a great deal of emotional instability as a result of their condition, increasing the risk of anxiety, depression, and other mood disorders substantially. Infertility drugs like leuprolide, gonadotropins, and clomiphene can affect the patient's psychological well-being causing side effects such as irritability, anxiety, and depression. Hence, it is often challenging to distinguish between the psychological impacts of infertility and the adverse effects of the medications when evaluating symptoms in women receiving infertility-related pharmacotherapy (70). Therefore, it is important to note that stress can cause infertility, and vice versa, and given the complexity, pinpointing cortisol's exact function in the relationship between stress and fertility is challenging at present.

TABLE 12 Cortisol level in male infertile patients (Infertile/pregnant vs infertile/non-pregnant).

Infertile/pregnant vs Infertile/non-pregnant (Male cortisol level)		
Infertile/pregnant > infertile/non-pregnant	Infertile/ pregnant < infertile/ non-pregnant	No significant difference
		(21)

5 Strength and limitations

To our knowledge, this is the first systematic review that investigated the changes in cortisol levels in infertile male and female patients. Prior to this review, Massey et al. (2014) conducted a systematic review of cortisol levels and IVF treatment outcomes and reported three studies to associate higher cortisol with favorable IVF outcomes and five studies to relate lower cortisol to IVF success. The present review aimed to report whether cortisol is highly present in infertile patients compared to fertile healthy subjects, infertile patients who conceived, and those who didn't at the end of the ART. We only included studies that reported the cortisol level in the unstimulated/ natural cycle or prior to hormonal stimulation to rule out changes in cortisol levels due to hormonal stimulation.

One of the limitations we faced in the analysis was variation in the sampling period for studies involving female subjects as the biological specimens were collected on different days of natural cycles such as early follicular phase, day of ovulation, and days after ovulation. Future studies should standardize the time of biological specimen collection.

6 Conclusion and future direction

A complex relationship exists between psychological well-being and infertility, where infertility can cause stress to patients through

TABLE 13 Cortisol level in male infertile patients (Infertile vs fertile).

Infertile vs fertile (Male cortisol level)		
Infertile > fertile	Fertile > infertile	No significant difference
(18) (19) (20)		(17)

TABLE 14 Cortisol level in female infertile patients (Infertile vs fertile).

Infertile vs fertile (Female cortisol level)		
Infertile > fertile	Fertile > infertile	No significant difference
(10) (22) (23) (26)		(7) (25) (27)

TABLE 15 Cortisol level in female infertile patients (Infertile/pregnant vs infertile/non-pregnant).

Infertile/pregnant vs Infertile/non-pregnant (Female cortisol level)		
Infertile/pregnant > infertile/non-pregnant	Infertile/pregnant < infertile/non-pregnant	No significant difference
(21)	(10) (26)	(7) (24) (28) (29) (30)

emotional and financial burdens, and mental health disorders such as depression and anxiety could lead to infertility. Biological markers of stress have been extensively investigated and correlated to various health-related problems, including infertility. Seven out of eleven studies that compared the cortisol level between fertile and infertile subjects found significantly higher cortisol in the infertile group. Out of this, only one study correlated cortisol levels with infertility markers. On a separate note, out of 8 studies, only 3 reported significantly higher cortisol levels in infertile subjects that could not conceive at the end of ART. Based on the evidence we gathered through this review, at present, due to variations in study designs, sampling periods, and patients' characteristics, it is still unclear if high cortisol level causes infertility in males and females. In the present review, we only included the cortisol value that was measured prior to stimulation or IVF treatment, despite this, there are still variations in the sampling period as the collection of biological specimens was carried out during different time phases of the menstrual cycle such as follicular and luteal phases. Hence, we warrant future studies to standardize the time of biological sample collection to negate the unwanted influencing factors.

Data availability statement

The original contributions presented in the study are included in the article/supplementary material. Further inquiries can be directed to the corresponding authors.

Author contributions

BK, AK, and JK contributed to conception and design; BK, AK, and JK contributed to data acquisition; BK, AK, and JK were involved in the analysis, interpretation, and drafting of the manuscript; IM, AU, WM, AF and AA revise the manuscript critically for important intellectual content. The version to be published has received final approval from all authors.

Funding

This research was funded by Faculty of Medicine, Universiti Kebangsaan Malaysia, and Ministry of Higher Education (FRGS/1/2020/SKK0/UKM/03/1).

Acknowledgments

The authors would like to thank the Faculty of Medicine, Universiti Kebangsaan Malaysia.

Conflict of interest

The authors declare that the research was conducted in the absence of any commercial or financial relationships that could be construed as a potential conflict of interest.

Publisher's note

References

1. Vander Borght M, Wyns C. Fertility and infertility: definition and epidemiology. *Clin Biochem* (2018) 62:2–10. doi: 10.1016/j.clinbiochem.2018.03.012

2. Zegers-Hochschild F, David Adamson G, Dyer S, Racowsky C, De Mouzon J, Sokol R, et al. The international glossary on infertility and fertility care, 2017. *Hum Reprod* (2017) 32(9):1786–801. doi: 10.1093/humrep/dex234

3. Sun H, Gong T-T, Jiang Y-T, Zhang S, Zhao Y-H, Wu Q-J. Global, regional, and national prevalence and disability-adjusted life-years for infertility in 195 countries and territories, 1990–2017: results from a global burden of disease study, 2017. *Aging (Albany NY)* (2019) 11(23):10952. doi: 10.18632/aging.102497

4. Babakhanzadeh E, Nazari M, Ghasemifar S, Khodadadian A. Some of the factors involved in male infertility: a prospective review. *Int J Gen Med* (2020) 13:29. doi: 10.2147/IJGM.S241099

5. Bala R, Singh V, Rajender S, Singh K. Environment, lifestyle, and female infertility. *Reprod Sci* (2021) 28(3):617–38. doi: 10.1007/s43032-020-00279-3

6. Szkodziak F, Krzyżanowski J, Szkodziak P. Psychological aspects of infertility. a systematic review. *J Int Med Res* (2020) 48(6):0300060520932403. doi: 10.1177/0300060520932403

7. Csemiczky G, Landgren B-M, Collins A. The influence of stress and state anxiety on the outcome of IVF-treatment: psychological and endocrinological assessment of Swedish women entering IVF-treatment. *Acta Obstet Gynecol Scandinavica: ORIGINAL ARTICLE* (2000) 79(2):113–8. doi: 10.1034/j.1600-0412.2000.079002113.x

8. Russell G, Lightman S. The human stress response. *Nat Rev Endocrinol* (2019) 15 (9):525–34. doi: 10.1038/s41574-019-0228-0

9. Ranabir S, Reetu K. Stress and hormones. *Indian J Endocrinol Metab* (2011) 15 (1):18. doi: 10.4103/2230-8210.77573

10. Wdowiak A, Raczkiewicz D, Janczyk P, Bojar I, Makara-Studzińska M , Wdowiak-Filip A. Interactions of cortisol and prolactin with other selected menstrual cycle hormones affecting the chances of conception in infertile women. *Int J Environ Res Public Health* (2020) 17(20):7537. doi: 10.3390/ijerph17207537

11. Zehravi M, Maqbool M, Ara I. Polycystic ovary syndrome and infertility: an update. *Int J Adolesc Med Health* (2022) 34(2):1–9. doi: 10.1515/ijamh-2021-0073

12. Kwon W-S, Park Y-J, Kim Y-H, Kim I-C, Pang M-G. Vasopressin has detrimental effect on male fertility. *Biol Rep* (2012) 87:354–4. doi: 10.1093/biolreprod/87.s1.354

13. Korevaar TIM, Mínguez-Alarcón L, Messerlian C, de Poortere RA, Williams PL, Broeren MA, et al. Association of thyroid function and autoimmunity with ovarian reserve in women seeking infertility care. *Thyroid* (2018) 28:1349–58. doi: 10.1089/thy.2017.0582

14. Albu D, Albu A. Is growth hormone administration essential for *in vitro* fertilization treatment of female patients with growth hormone deficiency? *Syst Biol Reprod Med* (2019) 65(1):71–4. doi: 10.1080/19396368.2018.1492044

15. Vedhara K, Miles JNV, Sanderman R, Ranchor AV. Psychosocial factors associated with indices of cortisol production in women with breast cancer and controls. *Psychoneuroendocrinology* (2006) 31(3):299–311. doi: 10.1016/j.psyneuen.2005.08.006

16. Massey AJ, Campbell B, Raine-Fenning N, Aujla N, Vedhara K. The association of physiological cortisol and IVF treatment outcomes: a systematic review. *Reprod Med Biol* (2014) 13(4):161–76. doi: 10.1007/s12522-014-0179-z

17. Harth W, Linse R. Male Fertility: endocrine stress parameters and coping. *Dermatol Psychosomatics/Dermatol und Psychosomatik* (2004) 5(1):22–9. doi: 10.1159/000078051

18. Shukla KK, Mahdi AA, Ahmad MK, Jaiswar SP, Shankwar SN, Tiwari SC. Mucuna pruriens reduces stress and improves the quality of semen in infertile men. *Evidence-Based Complement Altern Med* (2010) 7(1):137–44. doi: 10.1093/ecam/nem171

19. Mahdi AA, Shukla KK, Ahmad MK, Rajender S, Shankhwar SN, Singh V, et al. Withania somnifera improves semen quality in stress-related male fertility. *Evidence-Based Complement Altern Med* (2011) 2011. doi: 10.1093/ecam/nep138

20. Wdowiak A, Bien A, Iwanowicz-Palus G, Makara-Studzińska M, Bojar I. Impact of emotional disorders on semen quality in men treated for infertility. *Neuro-endocrinol Lett* (2017) 38(1).

21. Tuncay G, Yıldız S, Karaer A, Reyhani I, Özgöcer T, Ucar C, et al. Stress in couples undergoing assisted reproductive technology. *Arch Gynecol Obstet* (2020) 301 (6):1561–7. doi: 10.1007/s00404-020-05549-8

22. Atalyan AV, Shelokhov LF, Kolesnikova LI. Endocrine markers of fertility potential in reproductive age women with idiopathic hyperprolactinemia. *J Pharm Res Int* (2020) 32(23):71–7. doi: 10.9734/jpri/2020/v32i2330790

23. Alam F, Khan TA, Ali R, Tariq F, Rehman R. SIRTI and cortisol in unexplained infertile females; a cross sectional study, in Karachi Pakistan. *Taiwanese J Obstet Gynecol* (2020) 59(2):189–94. doi: 10.1016/j.tjog.2020.01.004

24. C. Santa-Cruz D, Caparros-Gonzalez RA, Romero-Gonzalez B, Peralta-Ramirez MI, Gonzalez-Perez R, García-Velasco JA. Hair cortisol concentrations as a biomarker to predict a clinical pregnancy outcome after an IVF cycle: a pilot feasibility study. *Int J Environ Res Public Health* (2020) 17(9):3020. doi: 10.3390/ijerph17093020

25. Dolfing JG, Tucker KE, Lem CM, Uittenbogaart J, Verzijl JC, Schweitzer DH. Low 11-deoxycortisol to cortisol conversion reflects extra-adrenal factors in the majority of women with normo-gonadotrophic normo-estrogenic infertility. *Hum Reprod* (2003) 18(2):333–7. doi: 10.1093/humrep/deg082

26. Wdowiak A, Makara-Studzińska M, Raczkiewicz D, Cyranka K. Reproductive problems and intensity of anxiety and depression in women treated for infertility. *Psychiatr Pol* (2022) 56(1):153–70. doi: 10.12740/PP/125885

27. Leach RE, Moghissi KS, Randolph JF, Reame NE, Blacker CM, Ginsburg KA, et al. Intensive hormone monitoring in women with unexplained infertility: evidence for subtle abnormalities suggestive of diminished ovarian reserve. *Fertil Steril.* (1997) 68 (3):413–20. doi: 10.1016/s0015-0282(97)00222-7

28. An Y, Wang Z, Ji H, Zhang Y, Wu K. Pituitary-adrenal and sympathetic nervous system responses to psychiatric disorders in women undergoing *in vitro* fertilization treatment. *Fertil Steril.* (2011) 96(2):404–8. doi: 10.1016/j.fertnstert.2011.05.092

29. Cui Y, Yu H, Meng F, Liu J, Yang F. Prospective study of pregnancy outcome between perceived stress and stress-related hormones. *J Obstet Gynaecol Res* (2020) 46 (8):1355–63. doi: 10.1111/jog.14278

30. Merari D, Feldberg D, Elizur A, Goldman J, Modan B. Psychological and hormonal changes in the course of *in vitro* fertilization. *J Assist Reprod Genet* (1992) 9 (2):161–9. doi: 10.1007/BF01203757

31. Rohleder N, Schomner NC, Hellhammer R, Engle R, Kirschbaum C. Sex differences in glucocorticoid sensitivity of proinflamatorycytokine production after psychosocial stress. *Psychosom Med* (2001) 63:966–72. doi: 10.1097/00006842-200111000-00016

32. Barbaresco GQ, Reis AVP, Da Rocha Lopes G, Pereira Boaventura L, Freitas Castro A, Ferreira Vilanova TC, et al. Effects of environmental noise pollution on perceived stress and cortisol levels in street vendors. *J Toxicol Environ Health* (2019) 82 (5):331–7. doi: 10.1080/15287394.2019.1595239

33. Jia Y, Liu L, Sheng C, Cheng Z, Cui L, Li M, et al. Increased serum levels of cortisol and inflammatory cytokines in people with depression. *J nervous Ment Dis* (2019) 207(4):271–6. doi: 10.1097/NMD.0000000000000957

34. Glasow A, Breidert M, Haidan A, Anderegg U, Kelly PA, Bornstein SR. Functional aspects of the effect of prolactin (PRL) on adrenal steroidogenesis and distribution of the PRL receptor in the human adrenal gland. *J Clin Endocrinol Metab* (1996) 81(8):3103–11. doi: 10.1210/jcem.81.8.8768882

35. Levine S, Muneyyirci-Delale O. Stress-induced hyperprolactinemia: pathophysiology and clinical approach. *Obstet Gynecol Int* (2018) 2018:9253083. doi: 10.1155/2018/9253083

36. Campino C, Martinez-Aguayo A, Baudrand R, Carvajal CA, Aglony M, Garcia H, et al. Age-related changes in 11βhydroxysteroid dehydrogenase type 2 activity in normotensive subjects. *Am J Hypertens* (2013) 26(4):481–7. doi: 10.1093/ajh/hps080

37. Clow A, Hucklebridge F, Stalder T, Evans P, Thorn L. The cortisol awakening response:more than a measure of HPA axis function. *Neurosci Biobehav Rev* (2010) 35:97–103. doi: 10.1016/j.neubiorev.2009.12.011

38. Wilhelm I, Born J, Kudielka BM, Schlotz W, Wüst S. Is the cortisol awakening rise a response to awakening? *Psychoneuroendocrinology* (2007) 43(4):358–66. doi: 10.1016/j.psyneuen.2007.01.008

39. Petrowski K, Schmalbach B, Stalder T. Morning and evening type: the cortisol awakening response in a sleep laboratory. *Psychoneuroendocrinology* (2020) 112:104519. doi: 10.1016/j.psyneuen.2019.104519

40. Tartarin P, Guibert E, Toure A, Ouiste C, Leclerc J, Sanz N, et al. Inactivation of AMPKα1 induces asthenozoospermia and alters spermatozoa morphology. *Endocrinology* (2012) 153(7):3468–81. doi: 10.1210/en.2011-1911

41. Titman A, Price V, Hawcutt D, Chesters C, Ali M, Cacace G, et al. Salivary cortisol, cortisone and serum cortisol concentrations are related to age and body mass index in healthy children and young people. *Clin Endocrinol* (2020) 93(5):572–8. doi: 10.1111/cen.14294

42. Rodin A, Thakkar H, Taylor N, Richard C. Hyperandrogenism in polycystic ovary syndrome–evidence of dysregulation of 11β-hydroxysteroid dehydrogenase. *New Engl J Med* (1994) 330(7):460–5. doi: 10.1056/NEJM199402173300703

43. Tsilchorozidou T, Honour JW, Conway GS. Altered cortisol metabolism in polycystic ovary syndrome: insulin enhances 5α-reduction but not the elevated adrenal steroid production rates. *J Clin Endocrinol Metab* (2003) 88(12):5907–13. doi: 10.1210/jc.2003-030240

44. Wüst S, Federenko I, Hellhammer DH, Kirschbaum Genetic factors C. Perceived chronic stress, and the free cortisol response to awakening. *Psychoneuroendocrinology* (2000) 25:707–20. doi: 10.1016/S0306-4530(00)00021-4

45. Juster R-P, Perna A, Marin M-F, Sindi S, Lupien SJ. Timing is everything: anticipatory stress dynamics among cortisol and blood pressure reactivity and recovery in healthy adults. *Stress* (2012) 15(6):569–77. doi: 10.3109/10253890.2012.661494

46. Pulopulos MM, Vanderhasselt M-A, De Raedt R. Association between changes in heart rate variability during the anticipation of a stressful situation and the stress-induced cortisol response. *Psychoneuroendocrinology* (2018) 94:63–71. doi: 10.1016/j.psyneuen.2018.05.004

47. Powell DJ, Schlotz W. Daily life stress and the cortisol awakening response: testing the anticipation hypothesis. *PloS One* (2012) 7(12):e52067. doi: 10.1371/journal.pone.0052067

48. Xu H, Ouyang N, Li R, Tuo P, Mai M, Wang W. The effects of anxiety and depression on *in vitro* fertilization outcomes of Chinese women. *Psychol Health Med* (2017) 22:37–43. doi: 10.1080/13548506.2016.1218031

49. Boivin J, Griffiths E, Venetis CA. Emotional distress in infertile women and failure of assisted reproductive technologies: meta-analysis of prospective psychosocial studies. *BMJ* (2011) 342:d223. doi: 10.1136/bmj.d223

50. Galst JP. The elusive connection between stress and infertility: a research review with clinical implications. *J Psychother Integration* (2018) 28(1):1. doi: 10.1037/int0000081

51. Breen KM, Karsch FJ. Does cortisol inhibit pulsatile luteinizing hormone secretion at the hypothalamic or pituitary level? *Endocrinology* (2004) 145(2):692–8. doi: 10.1210/en.2003-1114

52. Morrison AE, Fleming S, Levy MJ. A review of the pathophysiology of functional hypothalamic amenorrhoea in women subject to psychological stress, disordered eating, excessive exercise or a combination of these factors. *Clin Endocrinol* (2021) 95(2):229–38. doi: 10.1111/cen.14399

53. García-León MÁ, Caparrós-González RA, Romero-González B, González-Perez R, Peralta-Ramírez I. Resilience as a protective factor in pregnancy and puerperium: its relationship with the psychological state, and with hair cortisol concentrations. *Midwifery* (2019) 75:138–45. doi: 10.1016/j.midw.2019.05.006

54. du Fossé NA, Marie-Louise P, van der Hoorn JMM, van Lith SleC , Lashley EELO. Advanced paternal age is associated with an increased risk of spontaneous miscarriage: a systematic review and meta-analysis. *Hum Reprod Update* (2020) 26 (5):650–69. doi: 10.1093/humupd/dmaa010

55. Johnson SL, Dunleavy J, Gemmell NJ, Nakagawa S. Consistent age-dependent declines in human semen quality: a systematic review and meta-analysis. *" Ageing Res Rev* (2015) 19:22–33. doi: 10.1016/j.arr.2014.10.007

56. Pinheiro R, Lomelino ALA, Pinto AM, Donato H. Advanced maternal age: adverse outcomes of pregnancy, a meta-analysis. *Acta Med portuguesa* (2019) 32 (3):219–26. doi: 10.20344/amp.11057

57. Amanvermez R, Tosun M. An update on ovarian aging and ovarian reserve tests. *Int J fertil steril* (2016) 9:411. doi: 10.22074/ijfs.2015.4591

58. Llarena N, Hine C. Reproductive longevity and aging: geroscience approaches to maintain long-term ovarian fitness. *Journals Gerontol: Ser A* (2021) 76(9):1551–60. doi: 10.1093/gerona/glaa204

59. Cavazos-Rehg PA, Krauss MJ, Spitznagel EL, Bommarito K, Madden T, Olsen MA, et al. Maternal age and risk of labor and delivery complications. *Maternal Child Health J* (2015) 19:1202–11. doi: 10.1007/s10995-014-1624-7

60. Chen K, Shen W, Zhang Z, Xiong F, Ouyang Q, Luo C. Age-dependent decline in stress response capacity revealed by proteins dynamics analysis. *Sci Rep* (2020) 10 (1):15211. doi: 10.1038/s41598-020-72167-4

61. Agbedia OO, Varma VR, Seplaki CL, Seeman TE, Fried LP, Li L, et al. Blunted diurnal decline of cortisol among older adults with low socioeconomic status. *Ann N Y Acad Sci* (2011) 1231:56–64. doi: 10.1111/j.1749-6632.2011.06151.x

62. Johar H, Emeny RT, Bidlingmaier M, Reincke M, Thorand B, Peters A, et al. Blunted diurnal cortisol pattern is associated with frailty: a cross-sectional study of 745 participants aged 65 to 90 years. *J Clin Endocrinol Metab* (2014) 99(3):E464–8. doi: 10.1210/jc.2013-3079

63. Gonzalez Rodriguez E, Marques-Vidal P, Aubry-Rozier B, Papadakis G, Preisig M, Kuehner C, et al. Diurnal salivary cortisol in sarcopenic postmenopausal women: the OsteoLaus cohort. *Calcified Tissue Int* (2021) 109(5):499–509. doi: 10.1007/s00223-021-00863-y

64. Schoorlemmer RM, Peeters GM, van Schoor NM, Lips P. Relationships between cortisol level, mortality and chronic diseases in older persons. *Clin Endocrinol (Oxf).* (2009) 71(6):779–86. doi: 10.1111/j.1365-2265.2009.03552.x

65. Yiallouris A, Tsioutis C, Agapidaki E, Zafeiri M, Agouridis AP, Ntourakis D, et al. Adrenal aging and its implications on stress responsiveness in humans. *Front Endocrinol (Lausanne).* (2019) 10:54. doi: 10.3389/fendo.2019.00054

66. Zapater-Fajarí M, Crespo-Sanmiguel I, Pulopulos MM, Hidalgo V, Salvador A. Resilience and psychobiological response to stress in older people: the mediating role of coping strategies. *Front Aging Neurosci* (2021) 13:632141. doi: 10.3389/fnagi.2021.632141

67. McAuley MT, Kenny RA, Kirkwood TBL, Wilkinson DJ, Jones JJL, Miller VM. A mathematical model of aging-related and cortisol induced hippocampal dysfunction. *BMC Neurosci* (2009) 10(1):1–14. doi: 10.1186/1471-2202-10-26

68. Valbuena Perez JV, Linnenberger R, Dembek A, Bruscoli S, Riccardi C, Schulz MH, et al. Altered glucocorticoid metabolism represents a feature of macroph-aging. *Aging Cell* (2020) 19(6):e13156. doi: 10.1111/acel.13156

69. Rooney KL, Domar AD. The relationship between stress and infertility. *Dialogues Clin Neurosci* (2018) 20(1):41–7. doi: 10.31887/DCNS.2018.20.1/klrooney

70. Stalder T, Steudte-Schmiedgen S, Alexander N, Klucken T, Vater A, Wichmann S, et al. Stress-related and basic determinants of hair cortisol in humans: a meta-analysis. *Psychoneuroendocrinology* (2017) 77:261–74. doi: 10.1016/j.psyneuen.2016.12.017

71. Joseph DN, Whirledge S. Stress and the HPA axis: balancing homeostasis and fertility. *Int J Mol Sci* (2017) 18(10):2224. doi: 10.3390/ijms18102224

72. Nargund VH. Effects of psychological stress on male fertility. *Nat Rev Urol* (2015) 12(7):373–82. doi: 10.1038/nrurol.2015.112

73. Wright C, Milne S, Leeson H. Sperm DNA damage caused by oxidative stress: modifiable clinical, lifestyle and nutritional factors in male infertility. *Reprod biomed Online* (2014) 28(6):684–703. doi: 10.1016/j.rbmo.2014.02.004

74. Ilacqua A, Izzo G, Emerenziani GP, Baldari C, Aversa A. Lifestyle and fertility: the influence of stress and quality of life on male fertility. *Reprod Biol Endocrinol* (2018) 16:1–11. doi: 10.1186/s12958-018-0436-9

75. Kloss JD, Perlis ML, Zamzow JA, Culnan EJ, Gracia CR. Sleep, sleep disturbance, and fertility in women. *Sleep Med Rev* (2015) 22:78–87. doi: 10.1016/j.smrv.2014.10.005

76. Palnitkar G, Phillips CL, Hoyos CM, Marren AJ, Bowman MC, Yee BJ. Linking sleep disturbance to idiopathic male infertility. *Sleep Med Rev* (2018) 42:149–59. doi: 10.1016/j.smrv.2018.07.006

77. Bodenmann G, Atkins DC, Schär M, Poffet V. The association between daily stress and sexual activity. *J Family Psychol* (2010) 24(3):271–9. doi: 10.1037/a0019365

78. Nasca C, Bigio B, Zelli D, Nicoletti F, McEwen BS. Mind the gap: glucocorticoids modulate hippocampal glutamate tone underlying individual differences in stress susceptibility. *Mol Psychiatry* (2015) 20(6):755–63. doi: 10.1038/mp.2014.961

frontiers | Frontiers in Endocrinology

TYPE Original Research
PUBLISHED 05 July 2023
DOI 10.3389/fendo.2023.1222635

OPEN ACCESS

EDITED BY
Changyin Zhou,
Guangdong Second Provincial General Hospital, China

REVIEWED BY
Long Zhang,
Xi'an Jiaotong University, China
Yang Guo,
Peking University, China

*CORRESPONDENCE
Zhongyi Sun
sunzhy199481@hotmail.com
Lan Li
lli@qau.edu.cn

†These authors share first authorship

RECEIVED 15 May 2023
ACCEPTED 19 June 2023
PUBLISHED 05 July 2023

CITATION
Han B, Guo J, Zhou B, Li C, Qiao T, Hua L, Jiang Y, Mai Z, Yu S, Tian Y, Zhang X, Lu D, Wang B, Sun Z and Li L (2023) Chestnut polysaccharide rescues the damaged spermatogenesis process of asthenozoospermia-model mice by upregulating the level of palmitic acid. *Front. Endocrinol.* 14:1222635. doi: 10.3389/fendo.2023.1222635

Chestnut polysaccharide rescues the damaged spermatogenesis process of asthenozoospermia-model mice by upregulating the level of palmitic acid

Baoquan Han[1,2†], Jiachen Guo[1†], Bo Zhou[3†], Chunxiao Li[1], Tian Qiao[1], Lei Hua[2], Yinuo Jiang[2], Zihang Mai[2], Shuai Yu[1], Yu Tian[1], Xiaoyuan Zhang[1], Dongliang Lu[2], Bin Wang[2], Zhongyi Sun[2*] and Lan Li[1*]

[1]College of Life Sciences, Qingdao Agricultural University, Qingdao, China, [2]Department of Urology, Shenzhen University General Hospital, Shenzhen, China, [3]Department of Urology, Daping Hospital, Army Medical University, Chongqing, China

Introduction: In recent years, the quality of male semen has been decreasing, and the number of male infertilities caused by asthenozoospermia is increasing year by year, and the diagnosis and treatment of patients with asthenozoospermia are gradually receiving the attention of the whole society. Due to the unknown etiology and complex pathogenesis, there is no specific treatment for asthenozoospermia. Our previous study found that the administration of chestnut polysaccharide could alter the intestinal microbiota and thus improve the testicular microenvironment, and rescue the impaired spermatogenesis process by enhancing the expression of reproduction-related genes, but its exact metabolome-related repairment mechanism of chestnut polysaccharide is still unclear.

Methods and results: In this study, we studied the blood metabolomic changes of busulfan-induced asthenozoospermia-model mice before and after oral administration of chestnut polysaccharide with the help of metabolome, and screened two key differential metabolites (hydrogen carbonate and palmitic acid) from the set of metabolomic changes; we then analyzed the correlation between several metabolites and between different metabolites and intestinal flora by correlation analysis, and found that palmitic acid in the blood serum of mice after oral administration of chestnut polysaccharide had different degrees of correlation with various metabolites, and palmitic acid level had a significant positive correlation with the abundance of *Verrucomicrobia*; finally, we verified the role of palmitic acid in rescuing the damaged spermatogenesis process by using asthenozoospermia-model mice, and screened the key target gene for palmitic acid to play the rescuing effect by integrating the analysis of multiple databases.

Discussion: In conclusion, this study found that chestnut polysaccharide rescued the damaged spermatogenesis in asthenozoospermia-model mice by upregulating palmitic acid level, which will provide theoretical basis and technical support for the use of chestnut polysaccharide in the treatment of asthenozoospermia.

KEYWORDS

chestnut polysaccharide, palmitic acid, asthenozoospermia, spermatogenesis, hydrogen carbonate

Highlights

1. Hydrogen carbonate may be significantly involved with the chestnut polysaccharide rescue process.

2. Upregulated palmitic acid is important for rescuing the damaged spermatogenesis process by using chestnut polysaccharide.

3. Palmitic acid may rescue the damaged spermatogenesis process of asthenozoospermia-model mice via enhancing *PPARA* expression.

Introduction

Currently, infertility affects approximately 60 to 80 million couples worldwide at a rate of 15% (1), and the World Health Organization (WHO) ranks infertility as the third most common disease after oncology and cardiovascular disease, with male factors accounting for approximately 50% of infertility (2). In recent years, the quality of male semen is decreasing, the number of male infertilities is increasing year by year, and the issue of male reproductive health is of concern to the whole society. From the perspective of semen quality, male infertility is usually a condition caused by reduced semen quality, with the most common clinical manifestations being low sperm count (oligospermia), poor sperm motility (weak spermatozoa) and abnormal sperm shape (abnormal spermatozoa). According to the latest WHO clinical guidelines, patients with a sperm progressive motility (PR) <32% in semen are diagnosed with weak spermatozoa, which is characterized by reduced sperm motility and decreased sperm motility (3). In 2003, Curi et al. reported that 80% of male infertility was associated with impaired sperm motility and 20% of male infertility was directly related to low sperm motility (4), this study fully demonstrates that weak spermatozoa are an important cause of the occurrence of male infertility, and considering that normal sperm motility is necessary for the completion of fertilization, and that male infertility patients with weak spermatozoa have significantly reduced sperm motility as a clinical manifestation, sperm motility is essential for maintaining normal male fertility.

Due to the unknown etiology and complex pathogenesis, there is no specific treatment for weak spermatozoa, and researchers have been investigating the use of antioxidant therapy or lifestyle changes to improve sperm quality. Studies have shown that lifestyle changes can significantly improve semen quality and sperm motility, such as reducing smoking and alcohol consumption can improve sperm motility (5). In addition, studies have found that obese patients can improve testicular function and enhance sperm motility through weight loss and regular exercise. Also, increasing the number of intercourse and ejaculation can improve sperm motility (6). Whereas antioxidant therapy is widely used by clinicians to improve sperm quality (7), it is now commonly used clinically through supplementation with carnitine (8), vitamin E (9), selenium (10), or acetylcysteine (11) to improve semen quality. However, the therapeutic potential of antioxidants remains controversial because of insufficient clinical sample sizes (12). In addition, some therapeutic approaches, including L-carnitine, are inefficient, costly, or have potential side effects when used, and there is still an urgent need for efficient, low-cost, and non-toxic alternative therapies for the effective treatment of weak spermatozoa.

Chestnut (*Castanea mollissima Blume*) is a plant of the family Crustaceae, which is widely grown in most parts of China and is an ingredient of traditional Chinese medicine. Chestnut is rich in nutrients such as starch, soluble sugar, crude fiber, protein, amino acids, and minerals (13). In recent years, polysaccharides have received increasing attention due to their multiple biological activities such as antioxidant, anti-inflammatory, immunostimulatory, anti-proliferative and anti-cancer (14, 15). Chestnut polysaccharides are the main components in chestnuts and consist of monosaccharides in the α or β conformation, linked by glycosidic bonds (16). Chestnut polysaccharides (CPs) include many monosaccharides such as glucose, rhamnose, arabinose, galactose, xylose, mannose, and fructose. CPs have been shown to have anticancer activity (17) and anti-fatigue effect. In addition, chestnut extract was found to improve the tolerance and survival of lactic acid bacteria in the gastrointestinal tract (18), and a recent study (19) showed that the addition of chestnut starch to the diet of mice altered the ratio of cecum-associated microorganisms and associated carbohydrate metabolites (e.g., acetic acid). In addition, chestnut starch induced changes in the expression of several genes in cecum epithelial cells, including those involved in energy production, cell cycle and cell junctions (20). This also confirmed that the components of chestnut starch can alter the gut microbiota and affect the expression of microbial metabolites and host genes, providing an important theoretical basis for the development of this project. Our team discovered that chestnut polysaccharide could enhance the expression of reproduction-related genes (STRA8, DAZL, SYCP1, SYCP3 and TNP1) to rescue the impaired spermatogenesis process (21). Moreover, another study confirmed that CPs can restore the impaired spermatogenesis process by adjusting the gut microbiota and intestinal structure (19), which also laid an important foundation for the subsequent research work of this project.

Palmitic acid (PA) is a major saturated fatty acid commonly found in sperm (22). In 2008, a study showed that PA levels were higher in semen samples from patients with asthenozoospermia than in the normal population (23). in addition, Kiernan et al. found that the addition of PA to an extender improved sperm quality in bulls (24). A recent clinical study found a positive correlation between high PA intake and the incidence of asthenozoospermia (25), while Andersen et al. also found a positive correlation between PA in sperm and total sperm count, further confirming the importance of PA for sperm production (22). Recent studies reported that PA has an important effect on maintaining linear motility and viability of porcine spermatozoa (26), which provides an important theoretical basis for conducting this study.

Metabolomics is an emerging histology that emerged after genomics, transcriptomics, and proteomics with the goal of quantitatively describing metabolite changes in organisms. This histological approach can reflect events downstream of gene expression and is closer to the actual phenotype than proteomics and genomics (27). Our previous study found that the administration of chestnut polysaccharide could alter the intestinal microbiota and

thus improve the testicular microenvironment, and rescue the impaired spermatogenesis process by enhancing the expression of reproduction-related genes, but its exact metabolome-related repairmen mechanism of chestnut polysaccharide is still unclear. In this study, we studied the blood metabolomic changes of busulfan-induced asthenozoospermia-model mice before and after oral administration of chestnut polysaccharide with the help of metabolome, which will provide a more in-depth dissection of the molecular mechanism of chestnut polysaccharide rescuing the impaired spermatogenesis process and provide a new direction for the clinical prevention and treatment of asthenozoospermia.

Materials and methods

The design of this study

Based on the existing research reports and experimental validation (Figure 1A), we conducted the following design for this study as displayed in Figure 1C: we set up a total of four experimental groups, including control group (Ctrl), oral administration of chestnut polysaccharide group (CPs), asthenozoospermia-model group (Bus) and chestnut polysaccharide rescue group (Bus+CPs). The treatment was started from 3 weeks of age, and subsequently, after one spermatogenic cycle (5 weeks), blood serum samples from different treatment groups were collected for metabolome assay analysis, and the metabolite composition and differential metabolite functions among different groups were analyzed in detail by various methods, so as to determine the effects of CPs on the serum metabolome of asthenozoospermia-model mice and the key metabolites that play important roles in rescuing damaged spermatogenesis process.

Breeding environment of mice

Male ICR mice were purchased from Vital River Laboratory Animal Technology Co., Ltd (Beijing, China). The mice were kept in a house with a 12-hour cycle of light and12-hour cycle of dark and a constant temperature (22–23°C) and had free access to food and water during the experimental phase. The Animal Care and Ethics Committee of Qingdao Agricultural University approved the study, which was conducted in accordance with the National Institutes of Health guidelines for the care and use of laboratory animals (NIH Publications no. 8023).

Information of CPs and busulfan

The CPs used in this study were brought from Wo Te Lai Si bio-technology co., Ltd (Lan Zhou, China) and busulfan (B2635, Germany) was brought from Sigma-Aldrich company.

Treatment of mice

Busulfan was used to establish the asthenozoospermia model of male sterility. Different treatment groups (10 mice per group) are as described in "The design of this study". The asthenozoospermia-model mice were treated with busulfan at the concentration of 40 mg per kg body weight. Fresh CPs solutions were prepared daily and 0.1ml of CPs solution were given orally per day at the rate of 0.1mg per kg body weight every mouse.

Collection of samples

After five-week treatment, mice were slaughtered in accordance with animal welfare requirements, and the tissues were collected for further analysis. Mouse blood samples are collected as follows: grasp the skin of the animal's neck with the left hand, take the lateral position to press it lightly on the experimental table, the left thumb and forefinger press the animal's eye skin to the back of the neck as much as possible, so that the animal's eye is filled with blood and protrudes, and the eyeball is removed with curved forceps, and the mouse is inverted with the head downward to make the blood flow out. After that, the blood serum was extracted and stored at -80°C until use.

Tissue immunofluorescence

Collected testes were fixed in 4% paraformaldehyde and kept in a refrigerator at 4°C overnight, then subsequently stored in different concentrations of dehydrating solutions. The dehydrated testicular samples were then embedded in paraffin and the resulting paraffin blocks were sectioned at 5 μm thickness following standard histological procedures. Sections were deparaffinized and hydrated in xylene and ethanol. Antigen retrieval was performed using citrate solution. Sections were then blocked with blocking buffer [3% bovine serum albumin (BSA, Solarbio, A8020, China), 10% normal goat serum in TBS buffer] at room temperature for 30 min. Each section was incubated with primary antibodies-DAZL (Abcam, ab215718, USA) and secondary antibodies (Beyotime, A0516, China) then sections were imaged under an Olympus fluorescence microscope (Olympus, BX51, Tokyo, Japan).

Metabolites extraction and UHPLC-MS/MS analysis

Blood serum samples from treated mice were collected, placed in Eppendorf tubes per 100 μL, and resuspended with prechilled 80% methanol in a well vortex. Dilute part of the supernatant with LC-MS grade water to a final concentration containing 53% methanol. Samples are then transferred to a new Eppendorf tube and centrifuged at 15,000 g, 4°C for 20 min. Finally, the supernatant

10.3389/fendo.2023.1222635

is injected into the LC-MS/MS system for analysis. UHPLC-MS/MS analysis was performed using the Vanquish UHPLC System (Thermo Fisher Scientific Technologies) and the Orbitrap Q ExactiveTM high-frequency mass spectrometer (Thermo Fisher Scientific Inc.) at Novogene Co., Ltd. (Beijing, China). The Q ExactiveTM HF mass spectrometer operates in positive/negative polarity mode with a spray voltage of 3.5 kV, a capillary temperature of 320°C, a sheath flow rate of 35 arb, an auxiliary gas flow rate of 10 arb, an S-lens RF level of 60, and an auxiliary gas heater temperature of 350°C.

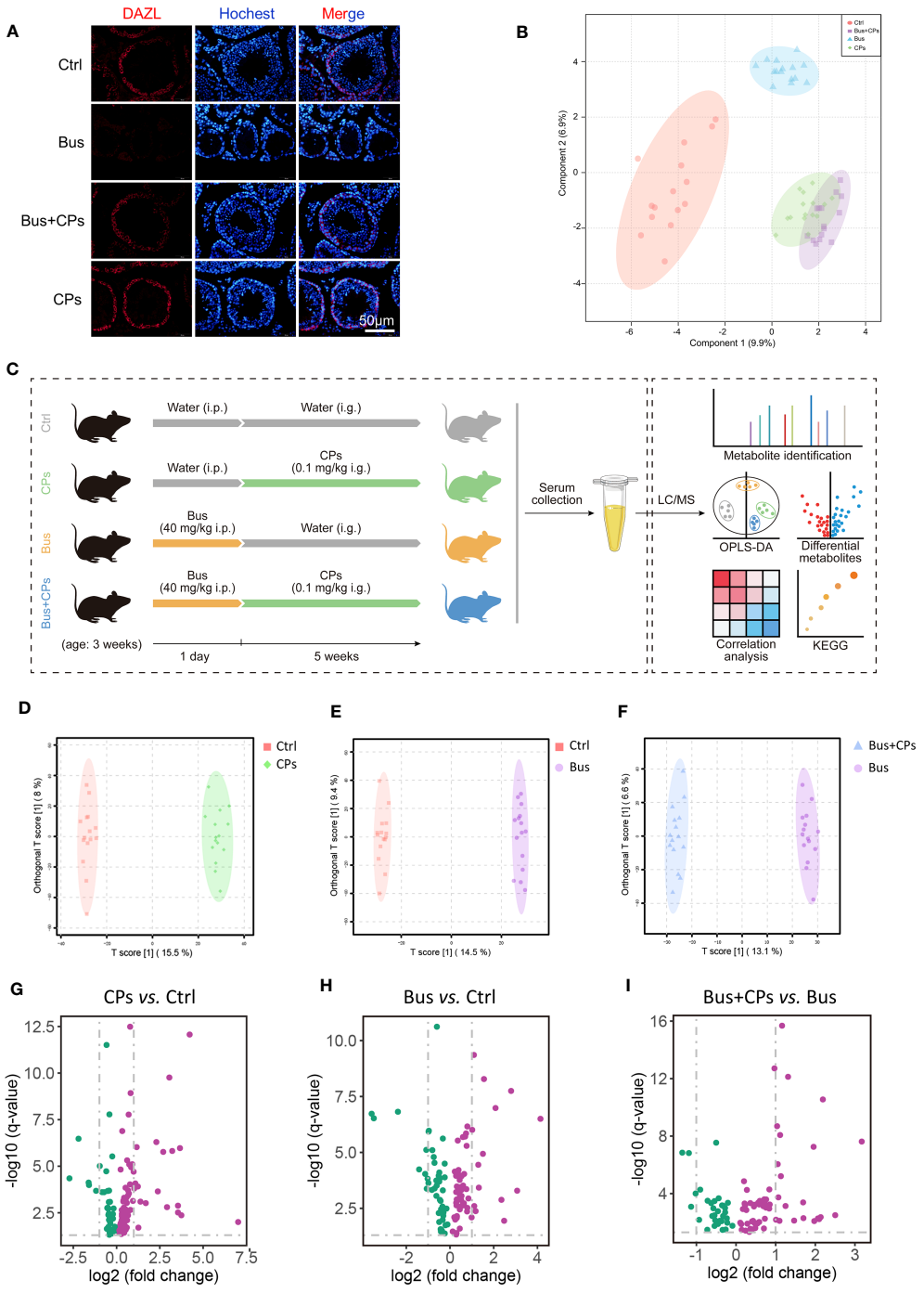

FIGURE 1
Study design and CPs-produced changes in metabolic features. **(A)** Histopathology photos of DAZL staining of mice testes; **(B)** the beta diversity analysis between the different groups by Principal Coordinates Analysis (PCoA); **(C)** the whole design of the study; **(D-F)**. the Orthogonal Partial least squares discriminant analysis (OPLS-DA) of diverse groups; **(G-I)**. the volcano map of differential expressed metabolites from different comparison groups.

Metabolite profiling from different samples

Raw data files generated by UHPLC-MS/MS were processed using the Compound Discoverer 3.1 (Thermo Fisher Scientific, USA) to perform peak alignment, peak picking, and quantitation for each metabolite. Subsequently, peak intensities were normalized to the total spectral intensity. The normalized data was used to predict the molecular formula based on additive ions, molecular ion peaks, and fragment ions. Peaks were then matched with the mzCloud, mzVault, and MassList databases to obtain accurate qualitative and relative quantitative results. Statistical analyses were performed using the statistical software R (v.3.4.3), Python (v.2.7.6) and CentOS (v.6.6), When data were not normally distributed, normal transformations were attempted using the area normalization method. These metabolites were annotated using the KEGG database, HMDB database and LIPIDMaps database. Orthogonal Partial least squares discriminant analysis (OPLS-DA) were performed using metaX (flexible and comprehensive software for processing metabolomics data). We used univariate analysis (t-test) to calculate the statistical significance (p-value). Metabolites with VIP >1, *p*value <0.05, and log2 (fold change) ≥0 or log2 (fold change) ≤0 were considered to be differential metabolites. Volcano plots were used to filter metabolites of interest which were based on log2 (fold change) and -log10 (*p* value) of metabolites with ggplot2 in R language. For clustering heat maps, the data were normalized using z-scores of the intensity areas of differential metabolites and were plotted using the pheatmap package in R language. Correlation between differential metabolites were analyzed by cor () in R language (Pearson method). Statistically significant correlations between differential metabolites were calculated by cor.mtest () in R language. *p* value <0.05 was considered to be statistically significant and correlation plots were plotted using the corrplot package in R language. Functions of these metabolites and metabolic pathways were studied using the SMPDB database. Metabolic pathways enrichment of differential metabolites was performed; when the ratio was satisfied by x/n > y/N, the metabolic pathway was considered to be enriched, when the P-value of the metabolic pathway <0.05, the pathway was considered as significantly enriched.

Prediction of target genes of candidate metabolite and expression profiling of target genes in different databases

Upon confirming the candidate metabolite, we predicted target genes of candidate metabolite using the Swiss Target-Prediction webtool (http://swisstargetprediction.ch/) and STITCH Database (http://stitch.embl.de/cgi/), then candidate genes were further screened by sorting according to the probability value and intersecting from two gene sets. After that, we conducted expression profiling of target gene from The Human Protein Atlas (https://www.proteinatlas.org/) to further explore its role.

Detection of the promoting effects of the candidate metabolite in rescuing damaged spermatogenesis process *in vivo*

In this part of the experiment, asthenozoospermia-model mice were prepared with the aid of busulfan, with reference to existing literature (28, 29). Three-week-old male mice were used as experimental subjects, and a control group (Ctrl), a busulfan and metabolite co-injection group (Bus+PA), and a busulfan injection group (Bus) were set up, with six mice in each group. The candidate metabolite intraperitoneal injection concentration was calculated based on the concentrations screened in the preliminary experiment. After one spermatogenic cycle, testicular tissues of different treatment groups were collected and testicular coefficients were analyzed; sperm quality of mice in different treatment groups were also statistically analyzed through CASA to verify the effect of metabolite on sperm motility.

Correlation analysis of 16S rDNA and metabolite profiling from blood serum

Based on our previous report (19), after completing metabolomics analyses of the blood serum, the Phylum that were significantly different after 16S rDNA profiling were correlated with the metabolites that were significantly different from the metabolite profiling based on Pearson's correlation coefficient. Heat maps were drawn to measure the degree of association between species diversity and metabolites in environmental samples.

Code availability

Analysis scripts employing these packages (and associated usage notes) are available from the authors upon request.

Data availability

The microbiota raw sequencing data generated in this study have been uploaded to the Genome Sequence Archive (GSA) with the accession number CRA004367 that are publicly accessible at https://ngdc.cncb.ac.cn/gsa. Metabolomics data employed in this study are available from the authors upon request.

Statistical analysis

All experiments were repeated at least 3 times and results were expressed as the mean ± SEM. SPSS software one-way analysis of variance (ANOVA) following by LSD multiple comparison test was used for data analysis and we defined $p < 0.05$ as a significant difference.

Results

Chestnut polysaccharide produced significant changes on the metabolome of asthenozoospermia-model mice

Consistent with our previous study (19), busulfan could significantly reduce the germ cells in seminiferous tubes, and CPs treatment effectively restored busulfan-impaired spermatogenesis, as evidenced by the increased number of germ cells in the Bus+Cps group mice (Figure 1A). After completing the UHPLC-MS/MS analysis, we firstly conducted the PCoA analysis of different samples and the results displayed that the spatial distribution of the Bus +CPs group and the CPs group was more similar which means similar components, while the Bus+CPs group was closer to the Ctrl group than the Bus group, indicating that CPs had a certain rescue effect on busulfan-induced spermatogenesis disorders (Figure 1B). Subsequently, the OPLS-DA analysis results (Figure 1D-F) further validated the influence of CPs or busulfan on metabolome components, especially for the asthenozoospermia-model mice (Figure 1F). In addition, the volcano plots (Figure 1G-I) were used to further show the metabolites differences between different groups. Based on these results, there were 38 significantly downregulated metabolites and 76 significantly upregulated metabolites in CPs vs Ctrl comparison; 46 downregulated metabolites and 61 upregulated metabolites in Bus vs Ctrl comparison; 32 downregulated metabolites and 64 upregulated metabolites in Bus+CPs vs Bus comparison. Above results demonstrated that CPs produced significant changes on the metabolome of asthenozoospermia-model mice, which further verified the important role of CPs-induced metabolome change in rescuing damaged spermatogenesis process.

Besides, the overall display of metabolites from three comparison showed large differences (Figure 2A), especially in Bus+CPs vs Bus comparison. It was found that after CPs gavage, more metabolites in asthenozoospermia-model group mice increased significantly than other two comparisons. Nevertheless, the Bus group had more significantly decreased metabolites than other two comparisons, which indicated that busulfan may severely damaged the spermatogenesis process by downregulating some important metabolites in mice. Also, it was detected that there was a significant different metabolome between the CPs and Ctrl groups, which suggests that CPs may have other potential effects in other biological process.

Hydrogen carbonate may be significantly involved with the chestnut polysaccharide-mediated rescue process

After confirming the effect of CPs on the metabolic composition of asthenozoospermia-model mice, we subsequently conducted a more in-depth study of the differential metabolites in different groups. Through cross-comparison analysis of the differential metabolites in the three comparison groups, we screened and obtained 21 differential metabolites that coexisted in the three comparison groups (Figure 2B), and with the help of functional enrichment analysis of the 21 differential metabolites, we found that among these core 21 differential metabolites, hydrogen carbonate and palmitic acid play an important role. We then correlated the top 50 differential metabolites in the three comparison groups and found that hydrogen carbonate and palmitic acid were also among the top 50 differential metabolites in the chestnut polysaccharide group, whereas hydrogen carbonate was not found among the top 50 differential metabolites in the model mice, which also demonstrated that oral administration of chestnut polysaccharide affected the hydrogen carbonate content in mice (Figure 2C). Subsequently, we performed heat map analysis (Figure 3A) and Stamp analysis (Figure 3C) on the metabolite composition of mice in the salvage and asthenozoospermia-model mice, and found that the hydrogen carbonate content of mice in the asthenozoospermia-model mice was significantly down-regulated after feeding chestnut polysaccharide, which suggest hydrogen carbonate may be significantly involved with the chestnut polysaccharide-mediated rescue process and also provides an important reference for the subsequent related studies.

Upregulated palmitic acid is important for rescuing the damaged spermatogenesis process by using chestnut polysaccharide

In addition to the preliminary confirmation of the important role of hydrogen carbonate in the salvage of damaged spermatogenesis by chestnut polysaccharide, we found that palmitic acid also produced significant changes in the metabolome of chestnut polysaccharide-salvaged mice (Figure 2B), and the functional enrichment analysis revealed that palmitic acid plays an important role in biological processes such as “Glycerolipid metabolism”, “Fatty Acid metabolism”, “Fatty Acid Biosynthesis” and “Steroid Biosynthesis” (Figure 2C). Similarly, the correlation analysis of the top 50 differential metabolites in the three comparative groups showed that palmitic acid was included in the top 50 differential metabolites in all three comparisons, which is a preliminary evidence that the administration of chestnut polysaccharides can affect the spermatogenesis process by affecting palmitic acid content (Figure 2D). Subsequent heat map analysis (Figures 3A, B) and Stamp analysis (Figure 3D) revealed that the palmitic acid content was significantly up-regulated in the asthenozoospermia-model mice after feeding chestnut polysaccharide, which further demonstrated that upregulated palmitic acid is important for rescuing the damaged spermatogenesis process by using chestnut polysaccharide and provided an important basis for the follow-up work of this study.

Palmitic acid could rescue the damaged spermatogenesis process of asthenozoospermia -model mice via enhancing PPARA expression

After initially determining the important role of palmitic acid upregulation in the rescue of impaired spermatogenesis by chestnut polysaccharide, we further verified the effect of palmitic acid by using asthenozoospermia-model mice, and the results showed that chestnut polysaccharide had the effect of improving semen quality (Figures 4A, B), especially on semen density, in addition, the sperm motility of asthenozoospermia-model mice receiving chestnut polysaccharide was also increased to some extent; subsequently, according to the cross comparison analysis between the Swiss Target-Prediction webtool and STITCH database, the key target gene of palmitic acid, *Ppara*, was screened (Figure 3E). The protein expression of PPARA in different tissues was also analyzed based on The Human Protein Atlas database, and the results showed that the protein was highly expressed in testis, which also indicated that this protein may play an important role in the physiological function of testis (Figure 3E) and this result provided an important theoretical basis for the subsequent use of chestnut polysaccharide in the treatment of asthenozoospermia.

Interestingly, in our association analysis based on previous gut microbiome results (19), we found that only one phylum *Cyanobacteria* was significantly negatively associated with

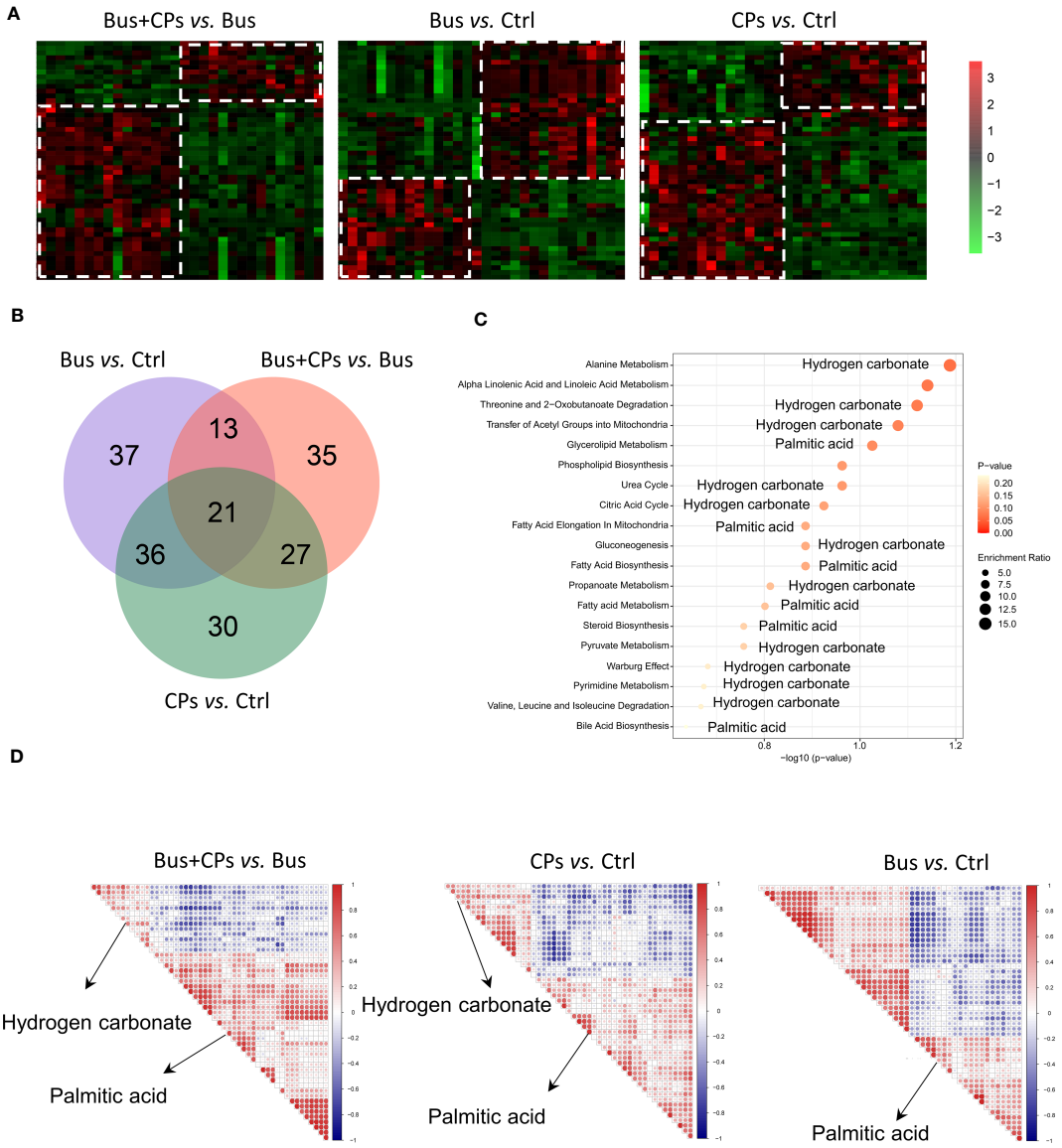

FIGURE 2
The candidate metabolites screening. **(A)** the expression heatmap of differential expressed metabolites from diverse comparison groups; **(B)** the cross-comparison analysis of the differential metabolites in the three comparison groups; **(C)** the enrichment analysis of the core 21 differential metabolites of the four comparison groups using the SMPDB database; **(D)** the correlation analysis of the top 50 differential metabolites in the three comparative groups.

10.3389/fendo.2023.1222635

bicarbonate, and most of the remaining bacteria were negatively associated, but not significantly (Figure 4C), while only one phylum *Verrucomicrobia* was significantly positively associated with palmitic acid, and most of the remaining bacteria were positively associated, but not significantly, suggesting that *Cyanobacteria* and *Verrucomicrobia* have important roles in maintaining normal spermatogenesis.

Discussion

In this study, we studied the blood metabolomic changes of busulfan-induced asthenozoospermia-model mice before and after oral administration of chestnut polysaccharide with the help of metabolome, and screened two key differential metabolites (hydrogen carbonate and palmitic acid) from the set of

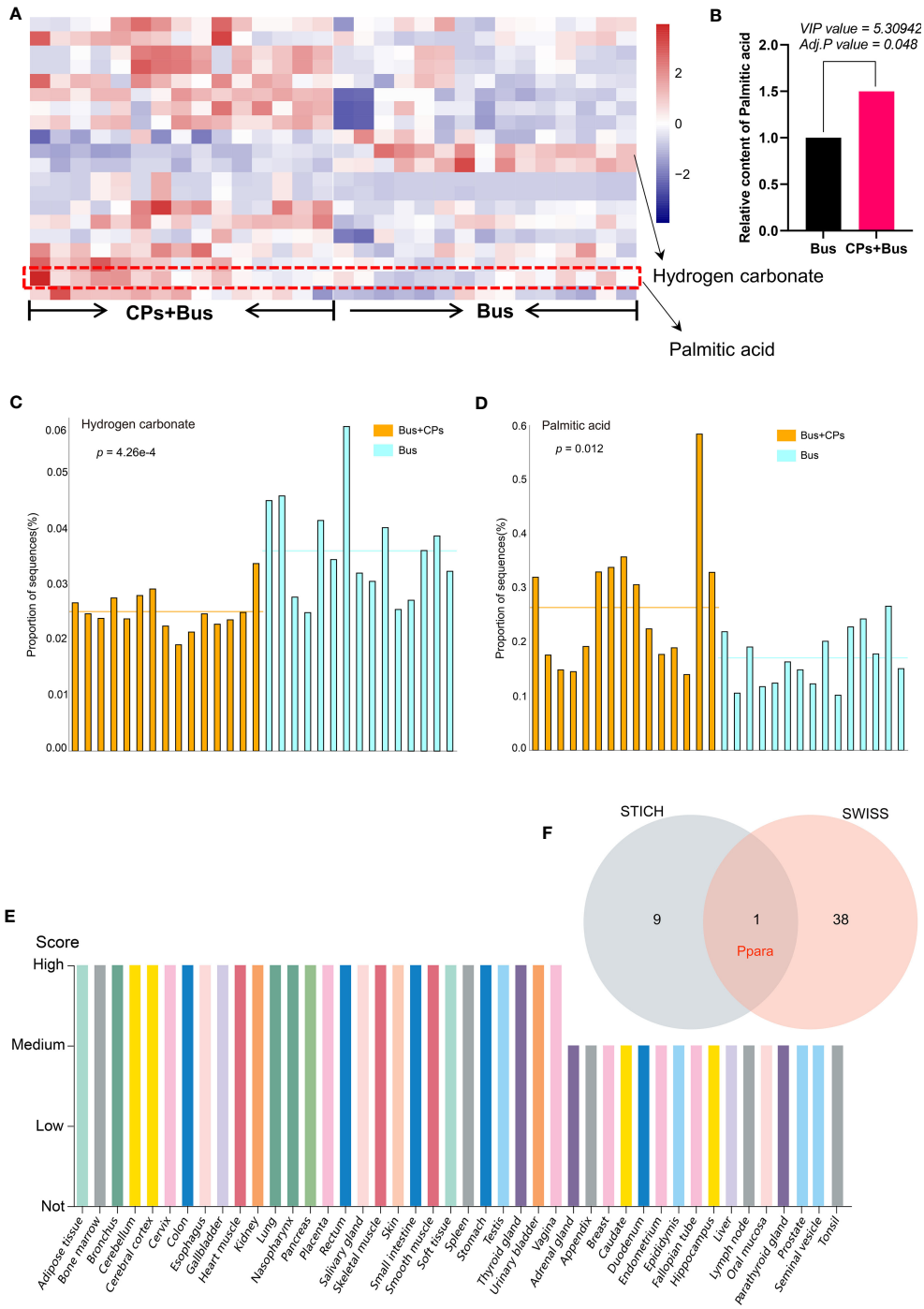

FIGURE 3
The expression display of key differential metabolites and screening of candidate target gene. **(A)** the heat map presentation of partial differential metabolites of the different groups in each sample; **(B)** the quantitative analysis of the palmitic acid from different groups; **(C, D)**. the STAMP analysis of Hydrogen carbonate and palmitic acid difference between groups; **(E)** the expression profiling of PPARA gene from The Human Protein Atlas; **(F)** the prediction and screening of target gene using different tools.

10.3389/fendo.2023.1222635

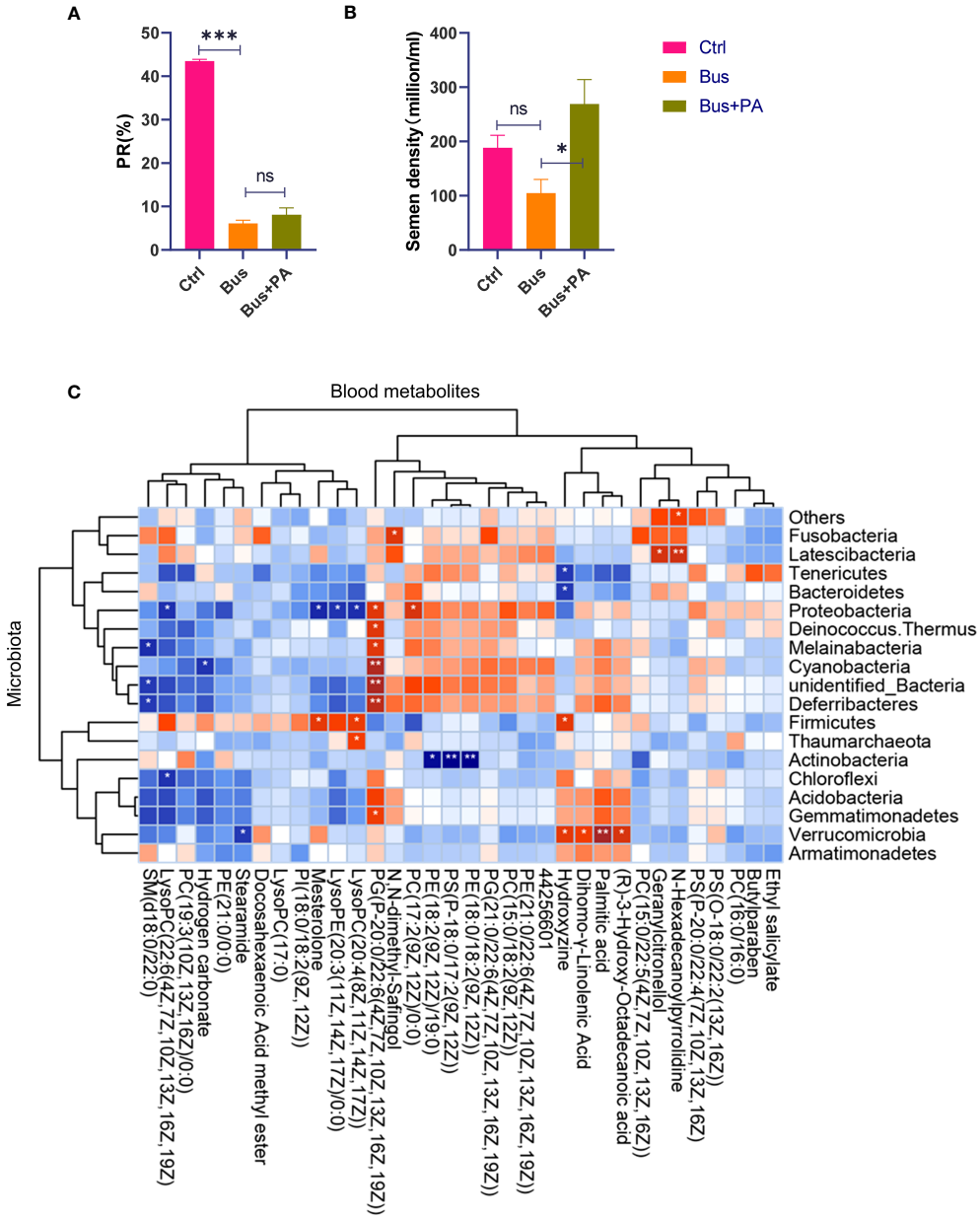

FIGURE 4
The function verification of palmitic acid on semen quality in vitro and correlation analysis of 16S rDNA and metabolite profiling. **(A)** the statistical analysis of sperm motility from different groups. The asterisk (*) represents a significant difference and the asterisk (***) represents a very significant difference. The abbreviation ns represents a non-significant difference; **(B)** the statistical analysis of semen density from different groups; **(C)** CPs-associated changes in metabolic features and their microbial associations. The asterisk (* or **) represents a significant association. The blue block represents a negative correlation and the red block represents a positive correlation.

metabolomic changes; we then analyzed the correlation between several metabolites and between different metabolites and intestinal flora by correlation analysis, and found that palmitic acid in the blood serum of mice after oral administration of chestnut polysaccharide had different degrees of correlation with various metabolites, and palmitic acid level had a significant positive correlation with the abundance of *Verrucomicrobia*; finally, we verified the role of palmitic acid in rescuing the damaged spermatogenesis process by using asthenozoospermia-model mice, and confirmed the key target gene for palmitic acid to play the rescuing effect by integrating the analysis of multiple databases. In conclusion, this study found that chestnut polysaccharide rescued the damaged spermatogenesis in asthenozoospermia-model mice by upregulating palmitic acid level, which will provide theoretical basis and technical support for the use of chestnut polysaccharide in the treatment of asthenozoospermia.

It is known that hydrogen carbonate has a crucial role in spermatogenesis (30–33), and the present study further revealed that hydrogen carbonate may be significantly involved in the rescue process mediated by chestnut polysaccharide with the help of metabolomic analysis technique, while further confirming the important role of hydrogen carbonate in spermatogenesis.

However, the specific mechanism of action of how chestnut polysaccharide affects hydrogen carbonate is unclear, which will provide us with references and new ideas for our subsequent studies.

The most important point found in this study is that chestnut polysaccharide can significantly increase the expression level of palmitic acid and further improve the impaired spermatogenesis process by increasing the protein expression of PPARA. Previous studies have shown that palmitic acid has an important effect on maintaining semen quality and improving sperm motility (22, 24, 26), and the present study also demonstrated that palmitic acid has a certain effect on salvaging spermatogenic damage with the help of asthenozoospermia-model mice, which also an important theoretical basis for the subsequent in-depth exploration of how palmitic acid enhances the mechanism of action of spermatogenesis through up-regulation of *Ppara* gene expression. In addition, the mechanism of how chestnut polysaccharide increases palmitic acid level and the is still unclear, which will be the direction of our subsequent research.

In conclusion, the present study demonstrated that chestnut polysaccharide significantly altered metabolome of asthenozoospermia-model mice, especially upregulating palmitic acid level, further proving that chestnut polysaccharide has an ameliorative and salvage effect on mice with weak spermatozoa, which will provide theoretical basis and technical support for the use of chestnut polysaccharide in the treatment of asthenozoospermia.

Data availability statement

The datasets presented in this study can be found in online repositories. The names of the repository/repositories and accession number(s) can be found below: https://ngdc.cncb.ac.cn/gsa, CRA004367. Other data employed in this study are available from the authors upon request.

Ethics statement

The animal study was reviewed and approved by The Animal Care and Ethics Committee of Qingdao Agricultural University.

Author contributions

LL and ZS designed the research. BH, JG, and BZ performed the research. CL, TQ, ZM, YJ, and SY generated the data. LH, XZ, and YT analyzed the data. DL and BW provided project oversight. BH, JG, and BZ wrote the paper. All authors contributed to the article and approved the submitted version.

Funding

Funding to support this work was provided by the National Natural Science Foundation of China (82271637 and 31572225), Natural Science Foundation of Shenzhen (JCYJ20220531103004008), Chongqing Natural Science Foundation of China (Cstc2019jcyj-msxmX0277), and Taishan Scholar Foundation of Shandong Province (ts20190946).

Acknowledgments

We are grateful for the technical support provided by Novogene Co., Ltd. (Beijing, China).

Conflict of interest

The authors declare that the research was conducted in the absence of any commercial or financial relationships that could be construed as a potential conflict of interest.

Publisher's note

References

1. Fakhro KA, Elbardisi H, Arafa M, Robay A, Rodriguez-Flores JL, Al-Shakaki A, et al. Point-of-care whole-exome sequencing of idiopathic male infertility. *Genet Med* (2018) 20:1365–73. doi: 10.1038/gim.2018.10

2. Agarwal A, Mulgund A, Hamada A, Chyatte MR. A unique view on male infertility around the globe. *Reprod Biol Endocrinol* (2015) 13:37. doi: 10.1186/s12958-015-0032-1

3. Shahrokhi SZ, Salehi P, Alyasin A, Taghiyar S, Deemeh MR. Asthenozoospermia: cellular and molecular contributing factors and treatment strategies. *Andrologia* (2020) 52:e13463. doi: 10.1111/and.13463

4. Curi SM, Ariagno JI, Chenlo PH, Mendeluk GR, Pugliese MN, Sardi Segovia LM, et al. Asthenozoospermia: analysis of a large population. *Arch Androl* (2003) 49:343–9. doi: 10.1080/01485010390219656

5. Boeri L, Capogrosso P, Ventimiglia E, Pederzoli F, Cazzaniga W, Chierigo F, et al. Heavy cigarette smoking and alcohol consumption are associated with impaired sperm parameters in primary infertile men. *Asian J Androl* (2019) 21:478–85. doi: 10.4103/aja.aja_110_18

6. Welliver C, Benson AD, Frederick L, Leader B, Tirado E, Feustel P, et al. Analysis of semen parameters during 2 weeks of daily ejaculation: a first in humans study. *Transl Androl Urol* (2016) 5:749–55. doi: 10.21037/tau.2016.08.20

7. Kefer JC, Agarwal A, Sabanegh E. Role of antioxidants in the treatment of male infertility. *Int J Urol* (2009) 16:449–57. doi: 10.1111/j.1442-2042.2009.02280.x

8. Garolla A, Maiorino M, Roverato A, Roveri A, Ursini F, Foresta C. Oral carnitine supplementation increases sperm motility in asthenozoospermic men with normal sperm phospholipid hydroperoxide glutathione peroxidase levels. *Fertility Sterility* (2005) 83:355–61. doi: 10.1016/j.fertnstert.2004.10.010

9. Ener K, Aldemir M, Işık E, Okulu E, Özcan MF, Uğurlu M, et al. The impact of vitamin e supplementation on semen parameters and pregnancy rates after

varicocelectomy: a randomised controlled study. *Andrologia* (2016) 48:829–34. doi: 10.1111/and.12521

10. Scott R, MacPherson A, Yates RW, Hussain B, Dixon J. The effect of oral selenium supplementation on human sperm motility. *Br J Urol* (1998) 82:76–80. doi: 10.1046/j.1464-410x.1998.00683.x

11. Jannatifar R, Parivar K, Roodbari NH, Nasr-Esfahani MH. Effects of n-acetyl-cysteine supplementation on sperm quality, chromatin integrity and level of oxidative stress in infertile men. *Reprod Biol Endocrinol* (2019) 17:24. doi: 10.1186/s12958-019-0468-9

12. Steiner AZ, Hansen KR, Barnhart KT, Cedars MI, Legro RS, Diamond MP, et al. The effect of antioxidants on male factor infertility: the males, antioxidants, and infertility (MOXI) randomized clinical trial. *Fertility Sterility* (2020) 113:552–60.e3. doi: 10.1016/j.fertnstert.2019.11.008

13. Borges O, Gonçalves B, de Carvalho JLS, Correia P, Silva AP. Nutritional quality of chestnut (Castanea sativa mill.) cultivars from Portugal. *Food Chem* (2008) 106:976–84. doi: 10.1016/j.foodchem.2007.07.011

14. Han J, Guo D, Sun X-Y, Wang J-M, Ouyang J-M, Gui B-S. Repair effects of astragalus polysaccharides with different molecular weights on oxidatively damaged HK-2 cells. *Sci Rep* (2019) 9:9871. doi: 10.1038/s41598-019-46264-y

15. Gao J, Zhang T, Jin Z-Y, Xu X-M, Wang J-H, Zha X-Q, et al. Structural characterisation, physicochemical properties and antioxidant activity of polysaccharide from lilium lancifolium thunb. *Food Chem* (2015) 169:430–8. doi: 10.1016/j.foodchem.2014.08.016

16. Jeddou KB, Chaari F, Maktouf S, Nouri-Ellouz O, Helbert CB, Ghorbel RE. Structural, functional, and antioxidant properties of water-soluble polysaccharides from potatoes peels. *Food Chem* (2016) 205:97–105. doi: 10.1016/j.foodchem.2016.02.108

17. Tang M, Hou F, Wu Y, Liu Y, Ouyang J. Purification, characterization and tyrosinase inhibition activity of polysaccharides from chestnut (Castanea mollissima bl.) kernel. *Int J Biol Macromolec* (2019) 131:309–14. doi: 10.1016/j.ijbiomac.2019.03.065

18. Blaiotta G, La Gatta B, Di Capua M, Di Luccia A, Coppola R, Aponte M. Effect of chestnut extract and chestnut fiber on viability of potential probiotic lactobacillus strains under gastrointestinal tract conditions. *Food Microbiol* (2013) 36:161–9. doi: 10.1016/j.fm.2013.05.002

19. Sun ZY, Yu S, Tian Y, Han BQ, Zhao Y, Li YQ, et al. Chestnut polysaccharides restore impaired spermatogenesis by adjusting gut microbiota and the intestinal structure. *Food Funct* (2022) 13:425–36. doi: 10.1039/D1FO03145G

20. Lee E-S, Song E-J, Nam Y-D, Nam TG, Kim H-J, Lee B-H, et al. Effects of enzymatically modified chestnut starch on the gut microbiome, microbial metabolome, and transcriptome of diet-induced obese mice. *Int J Biol Macromolec* (2020) 145:235–43. doi: 10.1016/j.ijbiomac.2019.12.169

21. Yu S, Zhao Y, Zhang FL, Li YQ, Shen W, Sun ZY. Chestnut polysaccharides benefit spermatogenesis through improvement in the expression of important genes. *Aging* (2020) 12:11431–45. doi: 10.18632/aging.103205

22. Andersen JM, Rønning PO, Herning H, Bekken SD, Haugen TB, Witczak O. Fatty acid composition of spermatozoa is associated with BMI and with semen quality. *Andrology* (2016) 4:857–65. doi: 10.1111/andr.12227

23. Tavilani H, Goodarzi MT, Doosti M, Vaisi-Raygani A, Hassanzadeh T, Salimi S, et al. Relationship between seminal antioxidant enzymes and the phospholipid and fatty acid composition of spermatozoa. *Reprod BioMed Online* (2008) 16:649–56. doi: 10.1016/S1472-6483(10)60478-6

24. Kiernan M, Fahey AG, Fair S. The effect of the *in vitro* supplementation of exogenous long-chain fatty acids on bovine sperm cell function. *Reproduction Fertility Dev* (2013) 25:947–54. doi: 10.1071/RD12204

25. Eslamian G, Amirjannati N, Rashidkhani B, Sadeghi M-R, Baghestani A-R, Hekmatdoost A. Dietary fatty acid intakes and asthenozoospermia: a case-control study. *Fertility Sterility* (2015) 103:190–8. doi: 10.1016/j.fertnstert.2014.10.010

26. Zhu Z, Li R, Feng C, Liu R, Zheng Y, Hoque SAM, et al. Exogenous oleic acid and palmitic acid improve boar sperm motility via enhancing mitochondrial β-oxidation for ATP generation. *Anim (Basel)* (2020) 10:591. doi: 10.3390/ani10040591

27. Rinschen MM, Ivanisevic J, Giera M, Siuzdak G. Identification of bioactive metabolites using activity metabolomics. nature reviews. *Mol Cell Biol* (2019) 20:353–67. doi: 10.1038/s41580-019-0108-4

28. Zhang P, Feng Y, Li L, Ge W, Yu S, Hao Y, et al. Improvement in sperm quality and spermatogenesis following faecal microbiota transplantation from alginate oligosaccharide dosed mice. *Gut* (2021) 70:222–5. doi: 10.1136/gutjnl-2020-320992

29. Zhao Y, Zhang P, Ge W, Feng Y, Li L, Sun Z, et al. Alginate oligosaccharides improve germ cell development and testicular microenvironment to rescue busulfan disrupted spermatogenesis. *Theranostics* (2020) 10:3308–24. doi: 10.7150/thno.43189

30. Bernardino RL, Carrageta DF, Sousa M, Alves MG, Oliveira PF. pH and male fertility: making sense on pH homeodynamics throughout the male reproductive tract. *Cell Mol Life Sci* (2019) 76:3783–800. doi: 10.1007/s00018-019-03170-w

31. Delgado-Bermúdez A, Yeste M, Bonet S, Pinart E. A review on the role of bicarbonate and proton transporters during sperm capacitation in mammals. *Int J Mol Sci* (2022) 23:99. doi: 10.3390/ijms23116333

32. Gadella BM, Van Gestel RA. Bicarbonate and its role in mammalian sperm function. *Anim Reprod Sci* (2004) 82-83:307–19. doi: 10.1016/j.anireprosci.2004.04.030

33. Liu Y, Wang D-K, Chen L-M. The physiology of bicarbonate transporters in mammalian reproduction. *Biol Reprod* (2012) 86:99. doi: 10.1095/biolreprod.111.096826

frontiers | Frontiers in Endocrinology

TYPE Review
PUBLISHED 27 July 2023
DOI 10.3389/fendo.2023.1194089

OPEN ACCESS

EDITED BY
Changyin Zhou,
Guangdong Second Provincial General Hospital, China

REVIEWED BY
Xianyi Cai,
Hefeng Central Hospital, China
Komal Thapa,
Chitkara University, India

*CORRESPONDENCE
Yulan Li
east_tale@aliyun.com

†These authors have contributed equally to this work and share first authorship

RECEIVED 26 March 2023
ACCEPTED 30 June 2023
PUBLISHED 27 July 2023

CITATION
Yao Y, Wang B, Jiang Y, Guo H and Li Y (2023) The mechanisms crosstalk and therapeutic opportunities between ferroptosis and ovary diseases. *Front. Endocrinol.* 14:1194089. doi: 10.3389/fendo.2023.1194089

The mechanisms crosstalk and therapeutic opportunities between ferroptosis and ovary diseases

Ying Yao[1†], Bin Wang[1†], Yanbiao Jiang[1], Hong Guo[1] and Yulan Li[2*]

[1]The First School of Clinical Medicine, Lanzhou University, Lanzhou, China, [2]Department of Anesthesiology, The First Hospital of Lanzhou University, Lanzhou, China

Ferroptosis, a form of regulated cell death, was first defined in 2012. Ferroptosis mainly involves iron-driven lipid peroxidation damage of cells. This process is regulated by iron homeostasis, redox balance, lipid metabolism, glutathione metabolism, and various disease signaling pathways. Iron is one of the key mineral elements that regulate the physiological function of women and the development of ovarian tumors. Occurrence of Ferroptosis has some hidden dangers and advantages in ovary diseases. Some scholars have shown that ferroptosis of ovarian granulosa cells (GC) promotes the development of ovarian dysfunction and polycystic ovary syndrome (PCOS). Interestingly, drug-resistant ovarian cancer cells are very sensitive to ferroptosis, suggesting that pharmacological positive and negative regulation of ferroptosis has great potential in the treatment of benign ovarian diseases and ovarian cancer. This article aimed to assess how ferroptosis occurs and the factors controlling ferroptosis. Moreover, we summarize how ferroptosis can be used to predict, diagnose and target treatment ovary disease. Meanwhile, we also evaluated the different phenomena of Ferroptosis in ovarian diseases. It aims to provide new directions for the research and prevention of female reproductive diseases.

KEYWORDS

ovarian diseases, ferroptosis, iron metabolism, lipid peroxidation, therapeutics

1 Introduction

Ferroptosis was originally defined as iron-mediated lipid peroxidation damage, which is closely related to the physiological and pathological mechanisms of the ovary. Although iron is a micromineral component, it is essential in various biological processes, including oxygen transport, energy metabolism, cell growth, and differentiation. Women have some unique physiological characteristics, such as excessive menstrual volume, increased maternal blood volume during pregnancy, fetal development, and postpartum blood loss. Therefore, adult women usually need more iron than men (1). However, iron is a ‘ double-edged sword ‘ and thus should be carefully used while taking measures to prevent iron deficiency. Iron overload

can increase unstable iron content in the body. Excessive free active iron can cause lipid peroxidation of polyunsaturated fatty acids in the cell membrane in a non-enzymatic manner. Furthermore, excessive free active iron can cause a Fenton reaction with free radicals, leading to oxidative damage to the cell membrane (2). Ferroptosis is mainly determined by the balance of the antioxidant mechanism. Glutathione peroxidase 4 (GPX4), as an antioxidant enzyme, can reduce ferroptosis by converting toxic lipid peroxides into corresponding non-toxic alcohols. Notably, GPX4 activity is affected by glutathione (GSH) and the trace element selenium (3). In addition, transcription factors, such as activating transcription factor 4 (ATF4), nuclear factor erythroid 2-related factor 2 (Nrf2), and p53, can exert antioxidant effects by regulating the GSH/GPX4 pathway (4, 5).

The ovary is a female gonad that mainly produces eggs, ovulates, and secrete sex hormones, collectively known as the reproductive and endocrine functions of the ovary. Follicle is the basic functional unit of human reproduction. Follicle is mainly composed of oocytes and GC, which are interconnected through gap junctions and paracrine pathways. GC provide oocytes with ATP and small molecular energy metabolites required for growth and development through the above pathways (6). Therefore, the number and function of germ cells are closely related to the normal function of the ovary. Both genetic and environmental factors impact the fate of germ cells. Some studies have shown that oxidative stress is the main cause of many female reproductive disorders, which can decrease oocyte quality (7). The oxidative modification of lipids in the membrane bimolecular layer (especially lipid peroxidation) significantly regulates oxidative stress in cells (8). Oxidative stress and an inflammatory state associated with ferroptosis exist in the ovarian GC of patients with PCOS and endometriosis (EMs) (9, 10). Meanwhile, oxidative damage and chronic inflammation are the classic etiologies of ovarian aging (7, 11). As a result, many scholars have studied whether ferroptosis plays a role in this process and how ovarian function can be improved. In addition, the emergence of ferroptosis has made many researchers see the hope of inhibiting the growth of tumor cells due to the infinite growth characteristics of tumor cells. As a result, several mechanism studies have been conducted to improve clinical diagnosis, prediction, and treatment.

In summary, several key and common environmental factors affecting the fate of germ cells, such as metabolism, inflammation, and oxidative stress, are associated with the existing ferroptosis effect. As a result, research on the role of ferroptosis in the female reproductive system has gradually attracted much attention. Therefore, a phased summary and critical analysis of this research progress are necessary to clarify the main findings, problems, and challenges around this topic for future research. This study aimed to analyze the classical regulatory mechanism of ferroptosis and its role in the development and treatment of ovarian diseases.

2 The discovery of ferroptosis

The concept of ferroptosis was formally proposed by Dixon in 2012 (8). Yang and Stockwell (12) investigated the mechanism of action of small molecule compounds (Erastin and RSL3) with a selective lethal effect on RAS mutant cell lines, and discovered that the two compounds could kill cancer cells by increasing intracellular iron content and accumulating oxidizing substances. Moreover, this particular form of cell death can be inhibited by iron-chelating agents or antioxidants (which capture lipophilic free radicals). Dixon et al. (8) studied the unique morphological, biochemical, and genetic characteristics involved in erastin-induced cell death and found that: morphologically, mitochondrial shrinkage, ridge reduction, disappearance, and membrane density increase; biochemical aspects showed intracellular iron deposition and lipid peroxidation; hereditary evidence demonstrated that erastin-induced cell death is regulated by a specific genetic network (genes related to iron metabolism). Finally, the process was named "ferroptosis" due to the unique characterization of this cell death pattern and its demand for iron. Erastin can selectively destroy tumor cells or protect non-tumor cells exposed to specific oxidative conditions by manipulating ferroptosis.

3 Ferroptosis regulation mechanism

Ferroptosis is a controlled iron-dependent lipid peroxidation cell death controlled by many metabolic pathways, such as redox reactions, iron homeostasis, glutathione metabolism and lipids (Figure 1).

3.1 Iron metabolism and ferroptosis

Dietary iron from various sources, such as meat, fish, and poultry is the main source of iron in the body under physiological conditions (13). Iron is mainly absorbed in the upper part of the small intestine. The human body has developed precise mechanisms for keeping iron levels in balance (iron homeostasis). Briefly, most Fe^{3+} in food is first reduced to Fe^{2+} by reductases, such as duodenal cytochrome B, then transported into cells through the divalent metal transporter 1 (DMT1) on the apical membrane of intestinal epithelial cells. Some iron entering the cell goes to the blood through the basolateral membrane, and the rest is temporarily stored in the cell as ferritin. Ferroportin 1 (FPN1), made by the SLC40A1 gene, is the only ferrous export protein found in mammals. Fe^{2+} leaves the intestinal epithelial cells through the pathway mediated by FPN1 when the intracellular iron is too high (14). Subsequently, Fe^{2+} is oxidized to Fe^{3+} and tightly bound to transferrin (TF) at a ratio of 2:1. TF is mainly present in the plasma, which binds to the cell surface transferrin receptor 1 (TfR1) to supply the iron needed by most tissues of the body (15). Besides the dietary iron absorbed by intestinal cells, the body also releases iron through iron storage tissues, such as the liver and spleen (16).

The body's system of checks and balances keeps iron levels in a dynamic balance under normal conditions. Hepcidin (HEPC), which comes from the liver, can "sense" how much iron is in the body, stop intestinal absorption of iron and prevent iron release. Serum iron levels are reduced by negatively regulating the expression of duodenal iron transporters (DMT1 and FPN1) and TfR1 (17). Iron metabolism is also associated with intracellular

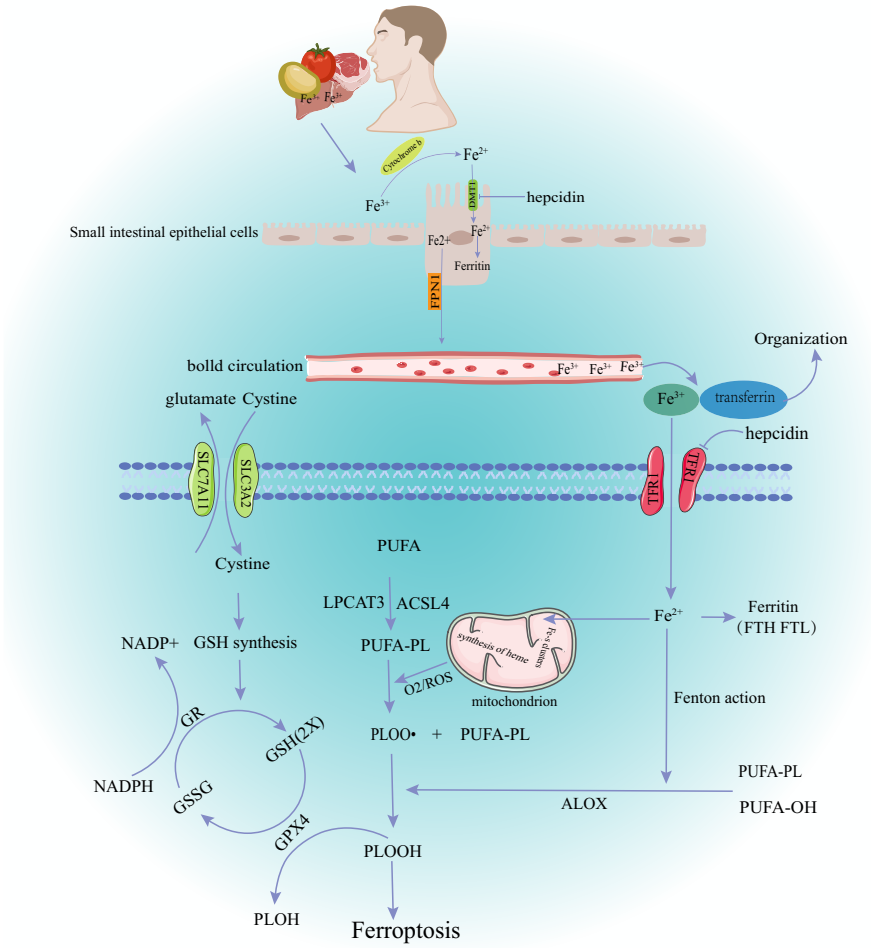

FIGURE 1
The main mechanism of ferroptosis. DMT1, divalent metal transporter 1; FPN1, ferroportin1; TFR1, Transferrin Receptor 1; GSH, glutathione; GR, Glutathion Reductase; GSSH, oxidized glutathione; GPX4, glutathione peroxidase 4; NADPH, Nicotinamide Adenine Dinucleotide Phosphate; ROS, reactive oxygen species; PUPA, polyunsaturated fatty acid; LPCAT3, Recombinant Lysophosphatidylcholine Acyltransferase 3; ACSL4,acyl-CoA synthetase long-chain family member 4; PLOOH, phospholipid hydroperoxide glutathione peroxidase.

post-transcriptional regulation. This mechanism is mediated by the central regulator of cellular iron metabolism, iron regulatory proteins (IRP1 and IRP2). IRP can bind to the iron response element (IRES) in mRNA encoding key iron regulatory proteins, including DMT1, ferritin heavy chain (FTH), TfR1, and ferritin, thereby stabilizing iron absorption, utilization, storage, and output (18). Furthermore, increased expression of hypoxia-inducible factor-2 (HIF-2), autophagy-related gene (ATG)-activated nuclear receptor coactivator 4 (NCOA4), and heme oxygenase 1 (HO-1) can regulate iron level changes in the body via the IRP pathway, ferritin autophagy, and senescent erythrocyte heme degradation (19–21). Iron in cells exists in two different forms during this regulation (Fe^{2+} and Fe^{3+}). The redox reactions and other pathophysiological processes that these two valence iron ions take part in depend on the transfer of electrons between them. Fe^{3+} is relatively stable and binds to TF mainly for iron storage and transport. Fe^{2+}, free iron ions, forms an unstable iron pool (LIP) in cells, which is transferred to mitochondria and participates in the formation of iron-dependent protein complexes, iron-sulfur clusters, heme, and other metabolic processes. Excessive Fe^{2+} can react with lipid radicals and H_2O_2 to produce a large amount of reactive oxygen species (ROS), which can damage membrane lipids, proteins, DNA, and other biological macromolecules, causing ferroptosis (22).

3.2 Glutathione metabolism and ferroptosis

GPX4 is an antioxidant enzyme found in mammalian cells. GPX4 prevents ferroptosis by changing toxic phospholipid hydrogen peroxide (PLOOH) into non-toxic alcohols (3). GSH is an essential cofactor of GPX4. GPX4 can turn lipid peroxides into hydroxyl compounds and oxidize glutathione. The cell membrane cystine/glutamate transporter (System Xc-, composed of two subunits of SLC7A11 and SLC3A2L) can take extracellular cystine into the cell and transport glutamate out of the cell when GSH is

consumed in large quantities. Cystine is used by the cell to make GSH, which is crucial for keeping the redox balance inside and outside the cell (23). GPX4 activity depends on how well the XC-GSH-GPX4 axis works and other factors that control it. Selenium (Se) is an essential trace element for the formation of the selenoprotein glutathione peroxidase. Selenium directly affects GPX4 activity and cell sensitivity to ferroptosis (24). Selenium participates in GPX4 maturation through mevalonate pathway. However, statins can block this pathway (25). Some transcription factors can also regulate the relationship between glutathione metabolism and ferroptosis. ATF4 and Nrf2 mediate the expression of solute carrier family member 11 (SLC7A11) under stress conditions, protecting cells from ferroptosis induced by cystine starvation and excessive accumulation of ROS (4). SLC7A11 is a target of the tumor suppressor gene p53. Overexpression of some tumor genes can promote ubiquitination and degradation of p53, up-regulate SLC7A11, GPX4, antioxidant enzymes superoxide dismutase 1 (SOD-1), and SOD-2, and accelerate tumor progression by inhibiting ferroptosis in tumor cells. This also provides a target mechanism for tumor therapy (5). Recent studies have shown that the GTP cyclohydrolase-1-Tetrahydrobiopterin (GCH1-BH4) and FSP1-CoQ10-NAD (P) H pathways can inhibit ferroptosis in a way that is both parallel and synergistic with the traditional GSH/GPX4 antioxidant pathway (26, 27).

3.3 Lipid peroxidation and ferroptosis

Peroxidation of polyunsaturated fatty acid phospholipids (PUFA-PLs) in the plasma membrane is a major cause of ferroptosis (28). PUFA-PLs form carbon-centered phospholipid free radicals (PL•) after losing diallyl hydrogen atoms. PL•reacts with molecular oxygen to form phospholipid peroxide radicals (PLOO•), which can remove and bind hydrogen from adjacent PUFA-PLs to form lipid peroxides (PL-OOH). A large amount of PL-OOH and lipid radicals [PLOO• and alkoxyphospholipid radicals (PLO•)] can react with PUFA-PLs again if it is not converted to the corresponding alcohol by GPX4, leading to PLOOH accumulation (29). Several toxic oxides produced by this chain reaction can destroy the fluidity and structural stability of cell membranes, leading to cell rupture and death. Lipid peroxidation can also be achieved through enzymatic methods. Some lipoxygenases (LOX) (dioxygenases targeting polyunsaturated fatty acid phospholipids) can directly oxidize polyunsaturated fatty acids in biofilms, thus inducing ferroptosis (30). The non-enzymatic lipid peroxidation is mainly induced by excessive ferrous ions (Fe^{2+}) or spontaneous occurrence of lipid radicals or hydroxyl radicals (•OH). Phospholipid peroxy radicals are relatively unstable and can react with Fe^{2+}, resulting in a chain expansion of phospholipid peroxidation, thus triggering ferroptosis signals (2). In summary, the level of lipid peroxidation in cells depends on the polyunsaturated fatty acids in the lipids. Acyl-CoA synthetase long-chain family member 4 (ACSL4) and lysophosphatidylcholine acyltransferase 3 (LPCAT3) can increase phospholipid PUFA content. Therefore, increased expression or activity of ACSL4 and LPCAT3 may promote ferroptosis in various pathophysiological contexts. Many studies have explored the treatment of different diseases based on the above mechanisms. For example, studies have explored how ACSL4 inhibitors can improve organ ischemia-reperfusion injury and how LPCAT3 inhibitors can reshape the polyunsaturated phospholipid content of human cells to prevent ferroptosis (31, 32).

3.4 Transcription factors and ferroptosis

P53 and Nrf2, as widely reported transcription factors, participate in the metabolism of iron and reactive oxygen species by regulating SLC7A11, arachidonate 12-lipoxygenase (ALOX12) gene, NOQ1, HO-1, heme type I fluorosynthase and the frontotemporal hairline (FTHL) gene (33). However, recent studies have reported other transcription factors, including forkhead box O3a (FoxO3a), which participates in cell metabolism, mitochondrial dysfunction, and oxidative stress. Glucose deprivation activates AMPK/FoxO3a by binding to FoxO3a and inhibiting SLC7A11 expression, thus preventing erastin-induced ferroptosis. The absence of FoxO3a promotes ferroptosis through mitochondrial membrane potential hyperpolarization, oxygen consumption, and lipid peroxidation accumulation (34). Furthermore, activation transcription factor 3 (Atf3) reduces Acsl4m6 A modification level by up-regulating FTO expression, thus inhibiting ferroptosis (35). Repressor element 1-silencing transcription factor (REST) can regulate gene expression under hypoxia. REST knockdown can decrease ferroptosis marker GPX4 and significantly up-regulate ACSL4 in hypoxia-injured renal tubular epithelial cells (RTECs) rather than apoptosis-related proteins (Bcl-2 and Bax) (36). Furthermore, GPX4 is the downstream target of Kruppel-like factor11 (KLF11). In addition, the transcription factor KLF11 inhibits the proliferation of lung adenocarcinoma (LUAD) cells and promotes their chemosensitivity by participating in the GPX4-related ferroptosis pathway (37). The environment in which these transcription factors operate, such as energy metabolism and oxidative stress, is a common cause of most diseases, including ovarian tumors, POI, and PCOS. Besides, mitochondrial dysfunction, hypoxia, and methylation of genes are closely related to ovarian dysfunction (38–40). Therefore, further studies should confirm whether these transcription factors participate in ferroptosis regulation in ovarian diseases.

4 The relationship between ferroptosis and ovarian diseases

4.1 Ovarian aging

Ovarian aging is the process of gradual decline of ovarian function. There are two main types of ovarian aging: physiological and pathological. Physiological ovarian aging (NOA) is the gradual loss of ovarian reserve function in older

women until they reach menopause while pathological ovarian aging is the premature ovarian failure caused by various pathogenic factors, including decreased ovarian reserve (DOR), ovarian insufficiency (POI) and poor ovarian response (POR) (41). Ferroptosis occurs during ovarian aging. Zheng et al. (42) showed that ACSL4 expression and ferroptosis increased in the ovaries of aged rats. The 4-hydroxy-2-nonenal (HNE) is the most sensitive marker. Besides, Zheng et al. tested five different monoclonal antibodies against HNE-modified proteins and found that HNEJ-1 is the most promising way to track ferroptosis in isolated tissues and proteins. This result indicates that ferroptosis is involved in physiological aging. However, only a few studies have explored the physiological significance of ferroptosis due to the lack of easy-to-implement and reliable methods and tools for directly monitoring ferroptosis in physiological environments. A study (43) confirmed that Tf, ferritin (Ft)) and TfR1 are abnormally up-regulated in the NOA rats based on proteomics analysis, *in vivo*, and *in vitro* research. This results in increased levels of active iron and total iron, nitrite/nitrate, 3-nitrotyrosine and HNE in aging ovaries. The ferroptosis-induced aging of the ovaries is also related to hormone secretion, which is an important function of germ cells. Ferritin inhibits the biosynthesis of estradiol in ovarian granulosa cells *in vitro* by up-regulating NF-κB and inducible nitric oxide synthase (iNOS). An adenovirus carrying ferritin light chain/heavy chain and transferrin can up-regulate NF-κB/INOS and down-regulate Nrf2/GPX4 in the ovaries of 3-month-old rats, confirming that oxidative stress-inflammatory response is mediated by iron homeostasis disorder in ovarian aging. Furthermore, Basonuclin 1 (BNC1) participates in follicular development, lipid metabolism, and redox homeostasis of oocytes (44). Therefore, BNC1 gene defects can lead to premature follicular activation and excessive atresia. Further studies have found that BNC1 deficiency triggers ferroptosis of oocytes through the Nrf2-YAP pathway, thus decreasing ovarian reserve. Also, inhibition of the YAP signal or ferroptosis can significantly rescue POI caused by BNC1 mutation. In addition, animal experiments have found that ferroptosis, cell oxidation, and vascular endothelial growth factor (VEGF) in primordial follicles are significantly increased in the ovaries of obese mice, suggesting that ferroptosis can activate immature ovarian follicles. Primordial follicle depletion is characterized by the death and activation of primordial follicles (45). Obesity has become a modern disease due to the changes in modern work and eating habits and thus may aggravate reproductive endocrine problems. Therefore, future studies should assess the relationship among ferroptosis, energy metabolism, and abnormal body fat rate.

4.2 Polycystic ovarian syndrome (PCOS)

PCOS is a heterogeneous gynecological disease associated with sex hormone disorders and insulin resistance. PCOS is also affected by genetic, environmental, and metabolic factors (46). PCOS is mainly characterized by ovarian granulosa cell dysfunction (47). The overexpression of MIR-93-5p in GC of PCOS patients can inhibit the expression of GPX4, SLC7A11, and Nrf2, and promote the accumulation of lipid reactive oxygen species and MDA, leading to apoptosis and ferroptosis. However, miR-93-5p silencing can prevent GC dysfunction (10). High homocysteine (Hcy) levels are associated with insulin resistance and sex hormone levels. Shi et al. found that the expression of ASCL4 and DMT1, which regulate lipid metabolism and iron metabolism, is significantly higher in Hcy-treated KGN cells than in the control group (48). These studies have shown that GC ferroptosis promotes PCOS development. In addition, PCOS patients are characterized by mitochondrial dysfunction. Mitochondrial dysfunction increases oxidative stress levels, causing or aggravating hyperandrogenism, insulin resistance, and obesity, interfering with follicular development, and thus affecting the menstrual and reproductive functions of PCOS women. As a result, some researchers (49) have shown that the activation of ferroptosis may be associated with an abnormal pregnancy (abortion) in PCOS patients. Animal tests have also shown that ferroptosis can occur in the uterus of pregnant women with PCOS, making the endometrium less receptive. Transmission electron microscopy has also shown that pregnant women with PCOS have reduced mitochondrial volume, concentrated mitochondrial membrane density, no mitochondrial ridge, and ruptured mitochondrial outer membrane (key characteristics of mitochondrial morphological changes during ferroptosis). Meanwhile, changes in mitochondrial function may also be due to ROS caused by iron elevation during ferroptosis related to mitophagy. Increased TFRC expression increases iron content, which brings NOX1 to PTEN induced putative kinase 1 (PINK1), thus promoting mitochondrial aggregation and mitophagy. As a result, cytochrome C is released into the cytoplasm to activate ACSL4 and cause lipid peroxidation, thus stopping follicular development. Therefore, the TFRC/NOX1/PINK1/ACSL4 pathway may be a potential target for PCOS (50). However, Zhang et al. recently found that n-3 polyunsaturated fatty acids (n-3 PUFAs) can activate the Hippo signaling pathway, inhibit yes-associated protein 1 (YAP1) from entering the nucleus, weaken the interaction between YAP1 and Nrf2, and increase the sensitivity of ovarian GC to ferroptosis. As a result, GC can alleviate follicular development arrest caused by abnormal proliferation of GC (51). In summary, oxidative stress, mitochondrial dysfunction, and abnormal secretion of nutritional factors associated with ferroptosis in GC affect the growth and development of ovaries. However, GC can alleviate follicular development arrest caused by excessive proliferation through ferroptosis. Therefore, further studies should confirm whether such a contradictory critical point is related to the degree of insulin resistance, body fat rate, or number of follicles in PCOS patients.

4.3 Ovarian cancer

Ovarian cancer (OC) is one of the most common tumors in women. OC is common in middle-aged and elderly women and seriously threatens the lives and health of women (52). Besides, the incidence rate of OC is increasing yearly. Furthermore, OC has hidden symptoms, with no clear clinical manifestations in the early stages. As a result, over 75% of OC patients are diagnosed at an advanced stage, which is related with poor therapeutic effect and

high mortality (53). Therefore, the mechanism and therapeutic targets of OC occurrence and development should be determined to formulate effective treatment strategies and improve the overall survival rate of patients.

Cell death is a natural and irreversible process. Cancer cells invasively damage the body due to their infinite proliferation, loss of polarity, and decreased adhesion. However, mitochondrial dysfunction usually occurs during tumor growth since they have to make a lot of energy to maintain tumor growth ("high metabolism"). The high metabolism produces a large amount of ROS and transmits proliferation signals to promote tumor development (54). Therefore, ferroptosis is crucial in the biological process that stops rapid growth of tumor cells (55). Several tumors, including OC, grow faster when they take in and hold on to too much iron (56). High-grade serous ovarian cancer tissues and ovarian tumor-initiating cells (TICs) have reduced iron efflux pump ferritin (FPN) and increased TFR1 levels. Iron promotes cancer cell invasion through the expression of matrix metalloproteinase and the synthesis of interleukin 6 (IL-6), thereby increasing metastasis and diffusion (57). Anticancer therapies target iron inside cells through many ways. When erastin and/or the iron compound ferlixit were used to induce ferroptosis in HEY, COV318, PEO4 and A2780CP ovarian cancer cell lines, it was found that erastin treatment was accompanied by NCOA4-mediated ferritin phagocytosis and mitochondrial dysfunction in HEY cells with high intracellular unstable iron pools (58). Another study (59) found that increasing the amount of iron in ovarian cancer cells using ferric ammonium citrate (FAC) can improve ferroptosis and stop the growth of cancer cells. However, ferroptosis inducers cannot promote ferroptosis in all cancer cell lines, indicating that the genetic and metabolic susceptibility determinants limit the application of ferroptosis inducers *in vivo*.

Ferroptosis is regulated by multiple factors. However, These regulatory factors also play an important role in ovarian cancer. The p53 gene, as a typical tumor suppressor gene and a key regulator of cell metabolism, is closely related to the occurrence and development of ferroptosis (60). Overexpression of p53 can inhibit xCT and increase GSH consumption (61). The oncogene MEX3A (RNA-binding protein) destroys the stability of the p53 protein through ubiquitination, inhibits ferroptosis, and enhances tumorigenesis (62). Methylenetetrahydrofolate reductase (MTHFR) polymorphism is associated with an increased risk of gynecological cancers. Upregulation of MTHFR and heme oxygenase 1 (HMOX1) is associated with a poor prognosis in OC patients. HMOX1 is a rate-limiting enzyme that degrades heme to Fe^{2+}. MTHFR can inhibit ferroptosis by blocking the ubiquitination of HMOX1. Therefore, these ferroptosis-based oncogenes can be used for the development of new therapeutic drugs. Besides, they can be used as diagnostic and predictive indicators for OC patients (63). Another study aimed to find a long non-coding RNA (LncRNA) marker associated with ferroptosis in OC and assess how it affects prognosis and clinicopathological features. In that study, lncRNAs (different between ovarian tumor tissues and normal tissues) were associated with ferroptosis genes. Finally, a prognostic risk model containing 18 LncRNAs related to ferroptosis was obtained (64). Similar studies have also found that PRNP, a ferroptosis-related gene, is significantly associated with cancer stage, main treatment outcome, and age of OC patients by mining differential genes (DEGs) of OC through public datasets. *In vitro* experiments have shown that PRNP overexpression can inhibit the proliferation, migration, and invasion of OC cells (65). Nonetheless, a prospective and multi-center study with real clinical data should assess whether the cancer-related ferroptosis gene or the ovarian cancer gene can control ferroptosis to accelerate the transformation of treatment concepts into clinical trials and improve the effectiveness of ovarian cancer treatment.

4.4 Other ovarian diseases

Endometriosis begins with the ectopic deposition of endometrial matrix and epithelial cells and is characterized by aggressive benign diseases. Endometrial cells form a ' chocolate cyst ' on the ovary when they are ectopic to the ovary and have undergone periodic bleeding, damage, and repair (66). Repeated bleeding of ectopic lesions can increase the concentration of free iron in chocolate cysts by 100–1000 times compared with levels in peripheral blood or other benign cysts (67). Iron overload and transferrin deficiency occur in the follicular fluid of EMs infertility patients (68). GC secretions are essential for the follicular microenvironment that controls oocyte growth and development. Some scholars have found that ferritin phagocytosis mechanisms are involved in GC ferroptosis induced by iron overload in follicular fluid *in vitro* (9). High iron content in ovarian endometriotic lesions can adversely affect adjacent GC through the free iron-mediated Fenton reaction, thereby reducing the number and quality of oocytes. This may lead to impaired fertility and adverse pregnancy outcomes (69). However, ectopic endometrial cells can acquire ferroptosis-resistant properties by up-regulating GPX4 and promoting GSH production (70). Huda I. Atiya et al. showed that a subset of ectopic endometrial cell-derived mesenchymal stem cells (enMSC) (characterized by a lack of CD10 expression) can specifically support the growth of ovarian clear cell carcinoma (OCCC). OCCC is a fatal and drug-resistant cancer that occurs in the unique microenvironment of endometriosis (71). These phenomena suggest that ectopic endometrial cells are associated with ferroptosis resistance. However, GC are highly sensitive to ferroptosis. Therefore, new therapeutic strategies should be developed based on the researched mechanism to protect GC while effectively killing ectopic endometrial cells, thereby alleviating the suffering of patients.

5 Regulatory mechanisms of ferroptosis in ovarian diseases

The types of ovarian diseases described in this article only differ in their disease background and predisposing factors and ultimately affect the reproductive and endocrine functions of the ovary by acting on various types of germ cells. Mitochondrial dysfunction, oxidative stress and inflammatory response are the common upstream pathogenesis of various ovarian diseases. Ferroptosis is

a type of regulatory cell death that is closely related to the mitochondria, oxidative stress and inflammatory response. At present, there are several crosstalk mechanisms between classical regulatory genes of ferroptosis in ovarian diseases (Figure 2). Nrf2 is a key regulator of antioxidant response and a ferroptosis signaling pathway with Nrf2 as the core plays an important role in protecting cells from ferroptosis. Excessive androgen is one of the key pathogenic markers of PCOS. The impaired cell anti-ferroptosis activity and increased fetal loss rate observed in pregnant women with PCOS can be attributed to the interaction between over-activated androgen receptors and Nrf2. This interaction leads to lower levels of SLC7A11 and GPX4 proteins and higher levels of 4-HNE modified proteins in pregnant rats. These molecular changes contribute to the dysregulation of cell anti-ferroptosis mechanisms, ultimately impacting fetal development and survival in PCOS pregnancies (72). Estrogen has an antioxidant function, and estrogen deficiency can inhibit the Nrf2/GPX4 pathway to induce ferroptosis (73). Estrogen has also been found to reverse chemotherapy resistance of ovarian cancer by targeting the Nrf2/GPX4 signaling axis to induce ferroptosis in drug-resistant human epithelial ovarian cancer cells (74). In conclusion, activation of the Nrf2 signaling pathway plays a crucial role in protecting ovarian granulosa cells from oxidative damage and ferroptosis (72). This also provides a mechanism for exploring the application of other antioxidant drugs in ovarian diseases.

The Hippo signaling pathway is a highly conserved pathway across diverse species and plays a crucial role in regulating the proliferation and differentiation of various cell types (75). The

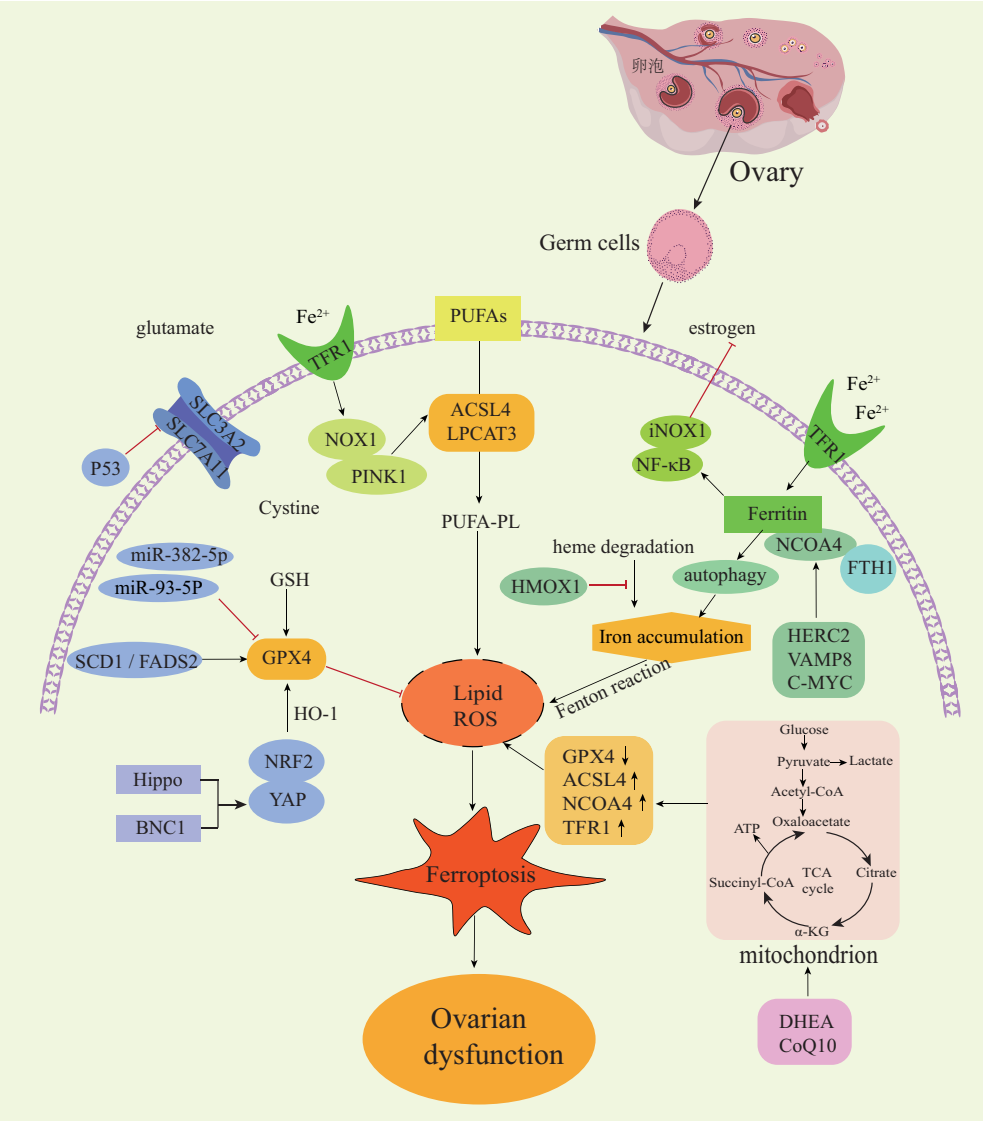

FIGURE 2
Regulatory mechanisms of ferroptosis in ovarian diseases. NOX1, NADPH oxidase 1; PINK1, PTEN induced kinase 1; NF-κB, nuclear factor kappa B; NCOA4, Nuclear receptor coactivator4; FTH1, ferritin heavy chain-1; HMOX1, heme oxygenase 1; HERC2, E3 ubiquitin ligase for NCOA4 and FBXL5; VAMP8, mediates autophagosome-lysosome fusion; SCD1, stearoyl-CoA desaturase-1; FADS2, acyl-CoA 6-desaturase; Nrf2, nuclear factor erythroid 2-related factor 2; YAP, yes-associated protein; BNC1, Basonuclin 1.

Hippo pathway is particularly important in follicular development because the activation of this pathway causes changes in the nuclear localization of YAP1 to perform different regulatory functions. The crosstalk between YAP1 and Nrf2 can change the sensitivity of cells to ferroptosis. BNC1 is involved in lipid metabolism and maintaining redox homeostasis in oocytes. The dysfunction of BNC1 activates ferroptosis through the Nrf2-Hippo pathway in oocytes, resulting in POI (44). NCOA4 is a selective receptor that binds to ferritin heavy chain-1 (FTH1) to form a ferritin complex, which targets lysosomes for 'ferritin phagocytosis' and promotes ferritin degradation. It has been reported that the low expression of NCOA4 in cells is accompanied by an increased Fe^{2+} and oxidative stress level, a decreased GSH level. Thus, NCOA4 is recognized as a facilitator of ferroptosis, while HERC2 (an E3 ubiquitin ligase for NCOA4 and FBXL5), VAMP8 (involved in autophagosome-lysosome fusion), and C-MYC have the potential to influence ferritin autophagy by modulating NCOA4 expression. Consequently, these factors participate in regulate ferroptosis and immune escape of ovarian cancer cells, highlighting new therapeutic targets that could alleviate chemotherapy resistance among ovarian cancer patients (76–78).

Germ cells require extremely high mitochondrial dynamics to maintain physiological characteristics, and a high-load operation of the mitochondrial respiratory chain is closely related to ROS production. Metabolic reprogramming mainly occurs in the mitochondria and cytoplasm, which refers to the metabolic changes made by cells in response to various stimulus pressures. To reveal the intricate interaction between cell energy metabolism and ferroptosis in senescent germ cells, Lin et al. included 75 patients with ovarian aging. Using multi-omics analysis combined with human ovarian pathology and clinical biopsy, they found that glucose metabolism and tricarboxylic acid cycle (TCA) cycles changed in the granulosa cells of aging patients. It has been verified that supplementary metabolic reprogramming nutrients [such as dehydroepiandrosterone (DHEA) and coenzyme Q10 (CoQ10)] can cause changes in glycolysis and enhance mitochondrial oxidative phosphorylation by regulating the expression of ferroptosis-related genes. Consequently, targeting and inhibiting the ferroptotic effect on germ cells holds promise for enhancing the success rate of *in vitro* fertilization (IVF) in elderly patients (79). In addition, the relationship between ferroptosis and inflammation is a research hotspot. NF-κB plays a key role in regulating the immune response to infection, and thus it has a chronic activity in some inflammatory diseases. A previous study found that abnormally up-regulated transferrin and ferritin in the ovaries of naturally aging rats can cause iron-accumulating oxidative stress and inflammatory aging through the NF-κB signaling pathway (43). Similarly, it was also found that activated NF-κB can reduce the expression of GPX4, SLC7A11 and Nrf2 and promote GC cell apoptosis and ferroptosis in PCOS disease, and thus it negatively impacts ovarian function (10). Inflammatory injury, repair and fibrosis are closely related. Although it has been reported that conventional chemotherapy drugs (such as cyclophosphamide (CTX) and paclitaxel) promoted the production of excessive superoxide in GC to trigger lipid peroxy-iron death, inducing decreased ovarian reserve and ovarian fibrosis in mice (80). To date, the presence of a ferroptosis-associated inflammatory regulatory mechanism in the advancement of ovarian aging and ovarian fibrosis associated with EMs has not been investigated (81).

6 Treatment based on ferroptosis

Ferroptosis is gradually being recognized as an adaptive process. The body can remove cells damaged by nutrient deficiency, infection or stress through ferroptosis. Therefore, ferroptosis has an inhibitory effect on tumor cells (82). Excessive ferroptosis is also closely related to autoimmune diseases, ovarian aging, polycystic ovary syndrome and other diseases (10, 42, 83). Existing studies have shown that turning on or turning off ferroptosis may help treat diseases (Table 1).

6.1 Role of ferroptosis in cancer therapy

At present, the first-line chemotherapy for ovarian cancer is platinum drugs combined with paclitaxel and targeted drugs bevacizumab and PARP inhibitors are often used for maintenance therapy. Because many people who receive chemotherapy have primary or secondary resistance to it, the treatment does not work as effectively as it should (92). Studies have shown that combining ferroptosis agonists with cisplatin (CDDP) or PARP inhibitors can inhibit ovarian cancer cell growth and metastasis. It is reasonable to ascertain the direction of the treatment of these drug-resistant tumors using ferroptosis (93, 94). With the continuous expansion of the treatment direction for ovarian cancer, new ferroptosis-based drugs, molecules and targets are constantly being developed.

6.1.1 Molecular targets

Peritoneal metastasis is the most common type of cancer cell growth in ovarian cancer patients, and it is strongly linked to a poor prognosis (95). Notably, the amount of fatty acid desaturation is critical in keeping most malignant tumors dry and aggressive (96). Lipidomics analysis showed that elevated unsaturated fatty acids (UFAs) were positively correlated with SCD1/FADS2 (two key fatty acid desaturases) levels and the carcinogenic ability of ovarian cancer cells (OvCa) (87). Genetic deletion of SCD1/FADS2 or direct blockage with a drug downregulates GPX4 and GSH/GSSG ratios. This destroys the cell/mitochondrial redox balance and accelerates cell death through iron-mediated lipid peroxidation, providing a promising chemotherapy strategy for peritoneal metastases of epithelial ovarian cancer. MiRNA interacts with target gene mRNA and regulates the translation of functional proteins and various biological processes during carcinogenesis. Some researchers have found that miR-382-5p expression is down-regulated and SLC7A11 expression is up-regulated in ovarian cancer tissues, and lidocaine targets the miR-382-5p/SLC7A11 axis (which up-regulates miR-382-5p expression and down-regulates SLC7A11 expression) to promote ferroptosis in ovarian cancer cells and exert anti-tumor activity (97). Lidocaine can also increase the expression of ACSL4 by directly knocking down miR-

TABLE 1 A brief description of the molecular target about ferroptosis in its related ovary diseases.

Disease	Model	Molecular target or key pathway	Trigger mechanism of Ferroptosis	medicine	References
ovarian aging	small white follicles of laying chickens	Nrf2/HO-1	oxidative damage	rutin	(84)
ovarian aging	Ovary of rats	ACSL4	Lipid Peroxidation	~	(42)
ovarian aging	Rat Ovaries and rat granulosa cells	Transferrin/Ferritin/NF-κb	Iron Accumulation and Oxidative Inflammaging	~	(43)
Primary ovarian insufficiency	Mice Ovary and Oocytes	BNC1/Nrf2-YAP	lipid metabolism and redox homeostasis	ferrostatin−1	(44)
PCOS	Mice Ovary Human ovarian granulosa cell tumor cells (KGN cells)	miR-93-5p/NF-kB	apoptosis and ferroptosis	~	(10)
PCOS	KGN cell	TET levels and DNA methylation/GPX4, SLC7A11, ASCL4 and DMT1.	oxidative stress	ferrostatin−1	(48)
PCOS	Mice Ovary KGN cells	TFRC/NOX1/PINK1/ ACSL4	Mitophagy and lipid peroxidation	~	(50)
PCOS	Rat Ovaries and Rat Ovarian Granulosa Cells	NFR1, GPX4, NF-κB and MAPK/ERK	oxidative stress, inflammation, and apoptosis	Cryptotanshinone (CRY)	(85)
PCOS	Mice Ovary	GPX4/SIRT3/AMPK/ mTOR	mitochondrial oxidative pathway	Metformin	(86)
ovarian cancer	ascites-derived ovarian cancer cells; the clinical samples (tumor, omentum, and ascites from OvCa patients)	SCD1/FADS2/GPX4/GSH/ GSSG	iron-mediated lipid peroxidation and mitochondrial dysfunction	~	(87)
ovarian cancer	Ovarian cancer cell line SKOV-3; Tumor tissues of ovarian cancer patients	MiR-382-5p/SLC7A11	accumulation of Fe^{2+}; iron and lipid reactive oxygen species (ROS)	Lidocaine	(19)
ovarian cancer	Tumor tissues of ovarian cancer patients; Human ovarian cancer cell lines HO8910 and SKOV3	miR-424-5p/ACSL4	Lipid peroxidation	erastin and RSL3	(88)
ovarian cancer	Human ovarian cancer cell lines TOV-21G/ES-2/RMG-2/RMG-V/OVCA432/OVCA429/ OVCA420	TAZ/ANGPTL4/NOX2	Lipid peroxidation; sensitivity to the erastin-induced ferroptosis	~	(89)
ovarian cancer	high-grade serous ovarian tumors (HGSOC) and associated malignant ascites; Platinum-Tolerant mice and SKOV3/OVCAR3 Cells	Frizzled-7/GPX4	redox homeostasis	~	(90)
ovarian cancer	Ovarian Cancer Xenograft Mouse; human ovarian cancer cells lines (SKOV3/ES2/ OVCAR3/OVCAR8)	glutathione peroxidase (GPx); cystine/glutamate antiporter system Xc (xCT)	ROS accumulation	Selenium-Chrysin Polyurea Dendrimer Nanoformulation/sodium selenite	(91)

424-5p to promote lipid peroxidation in ovarian cancer cells and increase their sensitivity to the ferroptosis activators erastin and RSL3 (88). Some marker genes can also be used to help choose tumors that are most likely to respond to ferroptosis induction therapy. Ovarian cancer with high expression of PDZ-binding motif (TAZ) and Angiopoietin-Like 4 (ANGPTL4), which is sensitive to ferroptosis, is a good example of a tumor that is likely to respond to this therapy. Chemotherapy resistance to such ovarian cancer can be eliminated using ferroptosis activators (89). In addition, Wang et al. (90) found that the expression of the Wnt receptor Frizzled-7 (FZD7) was increased in carboplatin-resistant cells and tumor tissues. Overexpression of FZD7 activates the carcinogenic factor

Tp63, drives the up-regulation of GPX4, and protects cells from chemotherapy-induced oxidative stress. This finding reveals that Frizzled-7-labeled platinum-resistant cancer cells have GSH metabolic changes and also provides a breakthrough for the treatment of ovarian cancer by inducing ferroptosis.

6.1.2 Drugs

Progressive drug development is essential for the treatment of clinical patients. Systematic studies of highly effective anticancer drugs provide valuable insights into the discovery of new anticancer drugs and have great potential for the expansion of the anticancer direction of existing drugs. Sorafenib — as a ferroptosis-related clinical drug — has been approved by the United States Food and Drug Administration for the treatment of ovarian cancer (98). A multicenter, double-blind, randomized, placebo-controlled phase 2 trial assessed the efficacy of sorafenib plus topotecan as a maintenance therapy for ovarian cancer that was resistant or unresponsive to platinum. Statistically and clinically, the results improved the progression-free survival of women with ovarian cancer who were resistant to platinum (99). Chen et al. (100) developed a hybrid compound called linoleic acid (LA)-glucosamine (GlcN) (LA-GlcN) as an effective treatment for high-grade serous ovarian cancer (HGSOC). The unique feature of this compound is that GlcN specifically targets and recognizes the overexpressed glucose transporter 1 (GLUT 1) in tumor cells, thereby enhancing the uptake of LA-GlcN. Since HGSOC cells contain approximately five times more iron than normal ovarian cells, the presence of unsaturated LA triggers ferroptosis, a process involving iron-dependent lipid peroxidation that leads to the breakdown of fats at a rapid pace. Norcantharidin (NCTD) is a demethylated form of cantharidin, which is widely used in clinical practice as an optional anticancer drug. *In vitro* studies showed that norcantharidin significantly raised the levels of MDA and Fe^{2+} and caused ferroptosis in ovarian cancer cells by stopping Nrf2/HO-1 signaling. Its use in ovarian cancer was initially expanded (101). Since cancer treatment using traditional Chinese medicine has gradually attracted attention, some experts have isolated the bioactive protein MAP30 from bitter melon seeds and administered it simultaneously with cisplatin. MAP30 has been shown to activate AMP-activated protein kinase (AMPK) signaling via CaMKK-, resulting in a synergistic effect on cisplatin-induced ovarian cancer cytotoxicity. Notably, blood tests showed that MAP30 did not impair liver or kidney function in MAP30-treated mice (102). Experts recently highlighted that sodium molybdate (Na2MoO4) is a molybdenum compound that is soluble and easily absorbed by organisms. Na2MoO4 can not only induce the increase in the unstable iron pool in ovarian cancer cells but also induce the depletion of GSH by mediating the production of nitric oxide (NO). Meanwhile, NO causes apoptosis in ovarian cancer cells by inhibiting mitochondrial aconitase activity and ATP production. Due to its multiple inhibitions of cell proliferation and activity, it is a top candidate drug for ovarian cancer (103).

With the increase in drug categories, some studies have focused on improving the safety, absorption efficiency and action time of drugs to strive for perfection. The enhanced permeability and retention (EPR) effect of nanotechnology shows the advantages of drug solubility, effective systemic circulation and tumor targeting. In their study, Gao et al. (104) developed nanoparticle micelles composed of arachidonic acid-conjugated amphiphilic copolymers to encapsulate RSL3. These micelles, when exposed to free radicals present in the tumor microenvironment, facilitate the swift release of RSL3, which targets the protein GPX4. *In vitro* and *in vivo* experiments demonstrated that drug-loaded micelles significantly enhanced the efficacy of RSL3 in inducing ferroptosis in drug-resistant cancer cells, thereby weakening the multidrug resistance (MDR) of anticancer drugs. Other studies investigated the two mechanisms of action of high-dose sodium selenite and selenium-containing chrysin (SeChry) in ovarian cancer (91, 105). As a competitive inhibitor of xCT, it promotes GSH consumption while inhibiting the expression of the antioxidant H2S-producing enzyme cystathionine-synthase (CBS) to achieve oxidative stress toxicity. As a vehicle to deliver SeChry to its target, it was inserted in folic acid-targeted polyurea dendrimer fourth-generation (PUREG4-FA) nanoparticles. The delivery of Sechry to ovarian cancer cells was more targeted when nanoparticles were used. The drug concentration in the tumor reached the therapeutic threshold without harming adjacent normal cells.

6.2 Inhibition of ferroptosis exerts a therapeutic effect

Inhibition of ferroptosis is undoubtedly an effective treatment option for functional disorders involving ferroptosis. Ferrostatin-1 (Fer-1) is the first aromatic amine found to effectively inhibit ferroptosis and lipid peroxidation accumulation and protect cells from multiple stresses and/or toxic chemicals. Recently, it was demonstrated that ferroptosis blockade significantly improved the estrous cycle disorder and prolonged the estrous cycle of primary ovarian aging by intraperitoneal injection of Fer-1 in Bnc1 mutant mice, and the ratio of oxidized to reduced lipids in the ovary was significantly reduced. One of the most important ways that ovaries age is through oxidative free radicals, and rutin has anti-inflammatory and antioxidant effects (44). Wu et al. (84) found that rutin activated the Nrf2/HO-1 signaling pathway to reduce oxidative stress caused by ferroptosis in the ovaries of naturally aging chickens. This suggests that rutin plays a protective role in ovarian function in elderly laying hens and prolongs the laying period. As a traditional Chinese medicine, electroacupuncture (EA) can inhibit oxidative stress and ferroptosis in the ovaries of premature ovarian failure mice by improving fibrosis and atresia follicles and increasing hormone levels in POF mice, thereby promoting follicular maturation, EA also offers the benefit of minimal side effects (106). Despite the contrasting follicle counts observed in PCOS and ovarian aging, both conditions are affected by oxidative stress and ferroptosis, leading to a significant decline in the quality of oocytes and granulosa cells. In the KGN cell model of PCOS, Fer-1 was found to inhibit the apoptosis, oxidative stress and ferroptosis of KGN cells. This protective effect may be achieved by enhancing the Tet enzyme (dioxygenase) and DNA methylation. This provides an experimental basis for the application of Fer-1 as a potential therapeutic drug in the clinical treatment of PCOS (48).

Cryptotanshinone is an extract of Danshen (*Salvia miltiorrhiza* Bunge). *Salvia miltiorrhiza* is a pleiotropic plant recognized in traditional Chinese medicine for the treatment of various diseases (107). Cryptotanshinone can inhibit oxidative stress, inflammation and ferroptosis by activating MAPK/ERK signaling to prevent ovarian tissue damage in PCOS (108). Adverse pregnancy outcomes caused by endocrine disorders in PCOS are also common clinical problems. Because metformin can improve insulin resistance and obesity, it is commonly used in the treatment of PCOS. It was recently reported that metformin improves PCOS in mice by inhibiting ovarian ferroptosis, which has expanded the new mechanism of this drug. This is the so-called new mechanism of old drugs (85). Other animal experiments have found that an antioxidant N-acetylcysteine can activate the SLC7A11-GSH-GPX4 axis and regulate iron metabolism, suggesting that antioxidants based on the mechanism of ferroptosis may be a good measure to prevent PCOS complicated with pregnancy loss (86).

7 Summary

Ferroptosis is a process involving abnormal metabolism of iron, glutathione and lipids and is regulated by various mechanisms. It is characterized by redox imbalance caused by abnormal metabolic processes, which ultimately leads to cell injury and death. The infinitely rapid proliferation of ovarian tumor cells and the high metabolic characteristics of germ cells require large amounts of energy from the mitochondria, which are the main sources of ROS. Once the imbalance between oxidation and antioxidation is established, it is easy to stimulate waterfall oxidative stress. The free radical theory that ROS cause DNA damage in germ cells is also one of the main pathogeneses of ovarian aging and dysfunction. The simultaneous development of multiple follicles in PCOS patients requires energy, and endocrine disorders (such as insulin resistance, elevated androgen hormones, etc.) are accompanied by abnormal glucose and lipid metabolism. The periodic damage and repair of the ovary in endometriosis are in a continuous inflammatory state. Therefore, numerous studies have been reasonably carried out on ferroptosis in female ovarian diseases. Ovarian tumor studies found that some molecules, such as SCD1/FADS2, miR-382-5p, Frizzled-7, etc., will be used as targets for future intervention in clinical treatment. It can also improve the chemoresistance of tumor cells by increasing the sensitivity of ovarian tumor cells to ferroptosis and guide clinical decision-making by analyzing the tumor risk prognostic model of ferroptosis-related genes in ovarian tumor tissues. Studies on benign ovarian diseases have found that the ferroptotic effect of ovarian granulosa cells affects the growth and development of oocytes, ultimately influencing ovarian function. The mechanism mainly involves Nrf2/GPX4, Hippo, NF-κB, NCOA4, ferritin autophagy, energy metabolism reprogramming, etc. Interestingly, some drugs based on the study of the regulatory mechanisms of ferroptosis in ovarian diseases, such as cryptotanshinone, N-acetylcysteine, rutin etc., has significantly improved ovarian function.

Although ferroptosis and its related regulatory drugs have great potential in ovarian diseases, current research on ferroptosis in ovarian diseases is still in its infancy. For example, some ferroptosis-related predictors, targets and models are still at the level of multi-omics sequencing and basic experimental verification. Besides, there is a huge need for prospective experimental big data to augment the application of ferroptosis and its related regulatory drugs in clinical practice. There are many types of ovarian cancer. Moreover, research should not only focus on the common types of high clinical incidence but should also be more comprehensive to explore the relationship between different subtypes of ovarian cancer and ferroptosis, to carry out mechanism-regulated therapeutic intervention more accurately. Since mitochondria are the main source of cell energy supply, the relationship between ferroptosis and metabolic reprogramming may also play a role in other highly metabolic ovarian diseases such as PCOS and ovarian tumors, in addition to ovarian aging. Furthermore, ferroptosis of granulosa cells in PCOS has different effects on ovarian function, which may be related to the severity of PCOS and individual heterogeneity. Notably, close attention should be paid to the methods that can improve ferroptosis resistance of ectopic endometrial cells in the ovary while reducing the iron damage to adjacent ovarian granulosa cells and oocytes. In recent studies, several transcription factors, including FoxO3a, Atf3, REST, and KLF11, have been suggested to play a regulatory role in ferroptosis. These studies have specifically investigated the involvement of these transcription factors in conditions such as cerebral ischemia-reperfusion injury, acute kidney injury, and lung adenocarcinoma (34–37). Hence, further research on these transcription factors in ovarian diseases may provide some new ideas for solving clinical problems. Despite considerable advancements in the investigation of ferroptosis in animal and cell models of ovarian diseases, there remain some unresolved issues that must be addressed before the findings from experimental studies can be effectively translated into clinical treatments for ovarian diseases.

Author contributions

YY and YL conceived the study and designed the contents. YY and BW drew patterns for the paper. YY and BW wrote the manuscript. YY and YL supervised the entire project. YJ and HG made a lot of contributions in the revision of the manuscript. All authors have read and agreed to the published version of the manuscript.

Funding

This work was supported by the Hospital Fund Projects of the First Hospital of Lanzhou University (No.lldyyyn2021-7).

Conflict of interest

The authors declare that the research was conducted in the absence of any commercial or financial relationships that could be construed as a potential conflict of interest.

Publisher's note

References

1. Georgieff MK, Krebs NF, Cusick SE. The benefits and risks of iron supplementation in pregnancy and childhood. *Annu Rev Nutr* (2019) 39:121–46. doi: 10.1146/annurev-nutr-082018-124213

2. Galaris D, Barbouti A, Pantopoulos K. Iron homeostasis and oxidative stress: an intimate relationship. *Biochim Biophys Acta Mol Cell Res* (2019) 1866:118535. doi: 10.1016/j.bbamcr.2019.118535

3. Seibt TM, Proneth B and Conrad M. Role of GPX4 in ferroptosis and its pharmacological implication. *Free Radic Biol Med* (2019) 133:144–52. doi: 10.1016/j.freeradbiomed.2018.09.014

4. Li J, Wang X, Zhou R, Cheng F, Tang X, Lao J, et al. Polygonatum cyrtonema hua polysaccharides protect BV2 microglia relief oxidative stress and ferroptosis by regulating NRF2/HO-1 pathway. *Molecules* (2022) 27(20):7088. doi: 10.3390/molecules27207088

5. Zeng C, Lin J, Zhang K, Ou H, Shen K, Liu Q, et al. SHARPIN promotes cell proliferation of cholangiocarcinoma and inhibits ferroptosis *via* p53/SLC7A11/GPX4 signaling. *Cancer Sci* (2022) 113:3766–75. doi: 10.1111/cas.15531

6. Shen Q, Liu Y, Li H and Zhang L. Effect of mitophagy in oocytes and granulosa cells on oocyte quality†. *Biol Reprod* (2021) 104:294–304. doi: 10.1093/biolre/ioaa194

7. Ra K, Park SC, Lee BC. Female reproductive aging and oxidative stress: mesenchymal stem cell conditioned medium as a promising antioxidant. *Int J Mol Sci* (2023) 24(5):5053. doi: 10.3390/ijms24055053

8. Dixon SJ, Lemberg KM, Lamprecht MR, Skouta R, Zaitsev EM, Gleason CE, et al. Ferroptosis: an iron-dependent form of nonapoptotic cell death. *Cell* (2012) 149:1060–72. doi: 10.1016/j.cell.2012.03.042

9. Ni Z, Li Y, Song D, Ding J, Mei S, Sun S, et al. Iron-overloaded follicular fluid increases the risk of endometriosis-related infertility by triggering granulosa cell ferroptosis and oocyte dysmaturity. *Cell Death Dis* (2022) 13:579. doi: 10.1038/s41419-022-05037-8

10. Tan W, Dai F, Yang D, Deng Z, Gu R, Zhao X, et al. MiR-93-5p promotes granulosa cell apoptosis and ferroptosis by the NF-kB signaling pathway in polycystic ovary syndrome. *Front Immunol* (2022) 13:967151. doi: 10.3389/fimmu.2022.967151

11. Dong L, Teh DBL, Kennedy BK, Huang Z. Unraveling female reproductive senescence to enhance healthy longevity. *Cell Res* (2023) 33:11–29. doi: 10.1038/s41422-022-00718-7

12. Yang WS, Stockwell BR. Synthetic lethal screening identifies compounds activating iron-dependent, nonapoptotic cell death in oncogenic-RAS-harboring cancer cells. *Chem Biol* (2008) 15:234–45. doi: 10.1016/j.chembiol.2008.02.010

13. Khare A, Samudre S and Arora A. Sneak-peek into iron deficiency anemia in India: the need for food-based interventions and enhancing iron bioavailability. *Food Res Int* (2022) 162:111927. doi: 10.1016/j.foodres.2022.111927

14. McKie AT, Marciani P, Rolfs A, Brennan K, Wehr K, Barrow D, et al. A novel duodenal iron-regulated transporter, IREG1, implicated in the basolateral transfer of iron to the circulation. *Mol Cell* (2000) 5:299–309. doi: 10.1016/s1097-2765(00)80425-6

15. Philpott CC, Jadhav S. The ins and outs of iron: escorting iron through the mammalian cytosol. *Free Radic Biol Med* (2019) 133:112–7. doi: 10.1016/j.freeradbiomed.2018.10.411

16. Liu MZ, Kong N, Zhang GY, Xu Q, Xu Y, Ke P, et al. The critical role of ferritinophagy in human disease. *Front Pharmacol* (2022) 13:933732. doi: 10.3389/fphar.2022.933732

17. Billesbølle CB, Azumaya CM, Kretsch RC, Powers AS, Gonen S, Schneider S, et al. Structure of hepcidin-bound ferroportin reveals iron homeostatic mechanisms. *Nature* (2020) 586:807–11. doi: 10.1038/s41586-020-2668-z

18. Wilkinson N, Pantopoulos K. The IRP/IRE system *in vivo*: insights from mouse models. *Front Pharmacol* (2014) 5:176. doi: 10.3389/fphar.2014.00176

19. Hirota K. An intimate crosstalk between iron homeostasis and oxygen metabolism regulated by the hypoxia-inducible factors (HIFs). *Free Radic Biol Med* (2019) 133:118–29. doi: 10.1016/j.freeradbiomed.2018.07.018

20. Ma LL, Sun L, Wang YX, Sun BH, Li YF, Jin YL. Association between HO–1 gene promoter polymorphisms and diseases (Review). *Mol Med Rep* (2022) 25(1):29. doi: 10.3892/mmr.2021.12545

21. Taleb M, Maillet I, Le Bert M and Mura C. Targeted autophagy disruption reveals the central role of macrophage iron metabolism in systemic iron homeostasis. *Blood* (2022) 140:374–87. doi: 10.1182/blood.2021014493

22. Gulec S, Anderson GJ, Collins JF. Mechanistic and regulatory aspects of intestinal iron absorption. *Am J Physiol Gastrointest Liver Physiol* (2014) 307:G397–409. doi: 10.1152/ajpgi.00348.2013

23. Conrad M, Sato H. The oxidative stress-inducible cystine/glutamate antiporter, system x (c) (-) : cystine supplier and beyond. *Amino Acids* (2012) 42:231–46. doi: 10.1007/s00726-011-0867-5

24. Cardoso BR, Hare DJ, Bush AI, Roberts BR. Glutathione peroxidase 4: a new player in neurodegeneration? *Mol Psychiatry* (2017) 22:328–35. doi: 10.1038/mp.2016.196

25. Chen JJ, Galluzzi L. Fighting resilient cancers with iron. *Trends Cell Biol* (2018) 28:77–8. doi: 10.1016/j.tcb.2017.11.007

26. Pallotti F, Bergamini C, Lamperti C and Fato R. The roles of coenzyme q in disease: direct and indirect involvement in cellular functions. *Int J Mol Sci* (2021) 23 (1):128. doi: 10.3390/ijms23010128

27. Hu Q, Wei W, Wu D, Huang F, Li M, Li W, et al. Blockade of GCH1/BH4 axis activates ferritinophagy to mitigate the resistance of colorectal cancer to erastin-induced ferroptosis. *Front Cell Dev Biol* (2022) 10:810327. doi: 10.3389/fcell.2022.810327

28. Friedmann Angeli JP, Xavier da Silva TN, Schilling B. CD8(+) T cells PUF(A)ing the flames of cancer ferroptotic cell death. *Cancer Cell* (2022) 40:346–8. doi: 10.1016/j.ccell.2022.03.003

29. Stockwell BR, Jiang X and Gu W. Emerging mechanisms and disease relevance of ferroptosis. *Trends Cell Biol* (2020) 30:478–90. doi: 10.1016/j.tcb.2020.02.009

30. Wu ZF, Liu XY, Deng NH, Ren Z and Jiang Z. Outlook of ferroptosis-targeted lipid peroxidation in cardiovascular disease. *Curr Med Chem* (2023) 30(31):3550–61. doi: 10.2174/0929867330666221111162905

31. Reed A, Ichu TA, Milosevich N, Melillo B, Schafroth MA, Otsuka Y, et al. LPCAT3 inhibitors remodel the polyunsaturated phospholipid content of human cells and protect from ferroptosis. *ACS Chem Biol* (2023) 17:1607–18. doi: 10.1021/acschembio.2c00317

32. Zhang F, Li Z, Gao P, Zou J, Cui Y, Qian Y, et al. HJ11 decoction restrains development of myocardial ischemia-reperfusion injury in rats by suppressing ACSL4-mediated ferroptosis. *Front Pharmacol* (2022) 13:1024292. doi: 10.3389/fphar.2022.1024292

33. Zhang J, Sheng S, Wang W, Dai J, Zhong Y, Ren J, et al. Molecular mechanisms of iron mediated programmed cell death and its roles in eye diseases. *Front Nutr* (2022) 9:844757. doi: 10.3389/fnut.2022.844757

34. Zhong S, Chen W, Wang B, Gao C, Liu X, Song Y, et al. Energy stress modulation of AMPK/FoxO3 signaling inhibits mitochondria-associated ferroptosis. *Redox Biol* (2023) 63:102760. doi: 10.1016/j.redox.2023.102760

35. Jin Z, Gao W, Guo F, Liao S, Hu M, Yu T, et al. Astragaloside IV alleviates neuronal ferroptosis in ischemic stroke by regulating fat mass and obesity-associated-N6-methyladenosine-acyl-CoA synthetase long-chain family member 4 axis. *J Neurochem* (2023). doi: 10.1111/jnc.15871

36. Gong S, Zhang A, Yao M, Xin W, Guan X, Qin S, et al. REST contributes to AKI-to-CKD transition through inducing ferroptosis in renal tubular epithelial cells. *JCI Insight* (2023) 8(11):e166001. doi: 10.1172/jci.insight.166001

37. Zhao G, Liang J, Shan G, Gu J, Xu F, Lu C, et al. KLF11 regulates lung adenocarcinoma ferroptosis and chemosensitivity by suppressing GPX4. *Commun Biol* (2023) 6:570. doi: 10.1038/s42003-023-04959-z

38. Ding M, Lu Y, Huang X, Xing C, Hou S, Wang D, et al. Acute hypoxia induced dysregulation of clock-controlled ovary functions. *Front Physiol* (2022) 13:1024038. doi: 10.3389/fphys.2022.1024038

39. Liu K, He X, Huang J, Yu S, Cui M, Gao M, et al. Short-chain fatty acid-butyric acid ameliorates granulosa cells inflammation through regulating METTL3-mediated N6-methyladenosine modification of FOSL2 in polycystic ovarian syndrome. *Clin Epigenet* (2023) 15:86. doi: 10.1186/s13148-023-01487-9

40. Xing J, Qiao G, Luo X, Liu S, Chen S, Ye G, et al. Ferredoxin 1 regulates granulosa cell apoptosis and autophagy in polycystic ovary syndrome. *Clin Sci (Lond)* (2023) 137:453–68. doi: 10.1042/cs20220408

41. Tesarik J, Galán-Lázaro M and Mendoza-Tesarik R. Ovarian aging: molecular mechanisms and medical management. *Int J Mol Sci* (2021) 22(3):1371. doi: 10.3390/ijms22031371

42. Zheng H, Jiang L, Tsuduki T, Conrad M and Toyokuni S. Embryonal erythropoiesis and aging exploit ferroptosis. *Redox Biol* (2021) 48:102175. doi: 10.1016/j.redox.2021.102175

43. Sze SCW, Zhang L, Zhang S, Lin K, Ng TB, Ng ML, et al. Aberrant transferrin and ferritin upregulation elicits iron accumulation and oxidative inflammaging causing ferroptosis and undermines estradiol biosynthesis in aging rat ovaries by upregulating NF-κb-Activated inducible nitric oxide synthase: first demonstration of an intricate mechanism. *Int J Mol Sci* (2022) 23(20):12689. doi: 10.3390/ijms232012689

44. Wang F, Liu Y, Ni F, Jin J, Wu Y, Huang Y, et al. BNC1 deficiency-triggered ferroptosis through the NF2-YAP pathway induces primary ovarian insufficiency. *Nat Commun* (2022) 13:5871. doi: 10.1038/s41467-022-33323-8

45. Zhou J, Lin L, Xia G and Wang C. The transcriptome reveals the molecular regulatory network of primordial follicle depletion in obese mice. *Fertil Steril* (2023) S0015-0282(23)00541-1. doi: 10.1016/j.fertnstert.2023.05.165

46. Azziz R, Carmina E, Chen Z, Dunaif A, Laven JS, Legro RS, et al. Polycystic ovary syndrome. *Nat Rev Dis Primers* (2016) 2:16057. doi: 10.1038/nrdp.2016.57

47. He M, Mao G, Xiang Y, Li P, Wu Y, Zhao D, et al. MicroRNA-664a-3p inhibits the proliferation of ovarian granulosa cells in polycystic ovary syndrome and promotes apoptosis by targeting BCL2A1. *Ann Transl Med* (2021) 9:852. doi: 10.21037/atm-21-1614

48. Shi Q, Liu R and Chen L. Ferroptosis inhibitor ferrostatin−1 alleviates homocysteine−induced ovarian granulosa cell injury by regulating TET activity and DNA methylation. *Mol Med Rep* (2022) 25(4):130. doi: 10.3892/mmr.2022.12645

49. Zhang Y, Hu M, Jia W, Liu G, Zhang J, Wang B, et al. Hyperandrogenism and insulin resistance modulate gravid uterine and placental ferroptosis in PCOS-like rats. *J Endocrinol* (2020) 246:247–63. doi: 10.1530/joe-20-0155

50. Zhang L, Wang F, Li D, Yan Y and Wang H. Transferrin receptor-mediated reactive oxygen species promotes ferroptosis of KGN cells via regulating NADPH oxidase 1/PTEN induced kinase 1/acyl-CoA synthetase long chain family member 4 signaling. *Bioengineered* (2021) 12:4983–94. doi: 10.1080/21655979.2021.1956403

51. Zhang P, Pan Y, Wu S, He Y, Wang J, Chen L, et al. N-3 PUFA promotes ferroptosis in PCOS GCs by inhibiting YAP1 through activation of the hippo pathway. *Nutrients* (2023) 15(8):1927. doi: 10.3390/nu15081927

52. Torre LA, Trabert B, DeSantis CE, Miller KD, Samimi G, Runowicz CD, et al. Ovarian cancer statistics, 2018. *CA Cancer J Clin* (2018) 68:284–96. doi: 10.3322/caac.21456

53. Lheureux S, Gourley C, Vergote I and Oza AM. Epithelial ovarian cancer. *Lancet* (2019) 393:1240–53. doi: 10.1016/s0140-6736(18)32552-2

54. Wang K, Jiang J, Lei Y, Zhou S, Wei Y and Huang C. Targeting metabolic-redox circuits for cancer therapy. *Trends Biochem Sci* (2019) 44:401–14. doi: 10.1016/j.tibs.2019.01.001

55. Zeng Q, Ma X, Song Y, Chen Q, Jiao Q and Zhou L. Targeting regulated cell death in tumor nanomedicines. *Theranostics* (2022) 12:817–41. doi: 10.7150/thno.67932

56. Torti SV, Manz DH, Paul BT. Blanchette-farra n and torti f m. *Iron Cancer Annu Rev Nutr* (2018) 38:97–125. doi: 10.1146/annurev-nutr-082117-051732

57. Basuli D, Tesfay L, Deng Z, Paul B, Yamamoto Y, Ning G, et al. Iron addiction: a novel therapeutic target in ovarian cancer. *Oncogene* (2017) 36:4089–99. doi: 10.1038/onc.2017.11

58. Battaglia AM, Sacco A, Perrotta ID, Faniello MC, Scalise M, Torella D, et al. Iron administration overcomes resistance to erastin-mediated ferroptosis in ovarian cancer cells. *Front Oncol* (2022) 12:868351. doi: 10.3389/fonc.2022.868351

59. Li D, Zhang M and Chao H. Significance of glutathione peroxidase 4 and intracellular iron level in ovarian cancer cells-"utilization" of ferroptosis mechanism. *Inflammation Res* (2021) 70:1177–89. doi: 10.1007/s00011-021-01495-6

60. Liu Y, Gu W. p53 in ferroptosis regulation: the new weapon for the old guardian. *Cell Death Differ* (2022) 29:895–910. doi: 10.1038/s41418-022-00943-y

61. Zhang Y, Xia M, Zhou Z, Hu X, Wang J, Zhang M, et al. p53 promoted ferroptosis in ovarian cancer cells treated with human serum incubated-superparamagnetic iron oxides. *Int J Nanomed* (2021) 16:283–96. doi: 10.2147/ijn.S282489

62. Wang CK, Chen TJ, Tan GYT, Chang FP, Sridharan S, Yu CA, et al. MEX3A mediates p53 degradation to suppress ferroptosis and facilitate ovarian cancer tumorigenesis. *Cancer Res* (2023) 83:251–63. doi: 10.1158/0008-5472.Can-22-1159

63. Wang X, Xu Z, Ren X, Chen X, Yi Q, Zeng S, et al. MTHFR inhibits TRC8-mediated HMOX1 ubiquitination and regulates ferroptosis in ovarian cancer. *Clin Transl Med* (2022) 12:e1013. doi: 10.1002/ctm2.1013

64. Gao J, Pang X, Ren F and Zhu L. Identification of a ferroptosis-related long non-coding RNA signature for prognosis prediction of ovarian cancer. *Carcinogenesis* (2022) 44(1):80–92. doi: 10.1093/carcin/bgac082

65. Hu K, Zhang X, Zhou L and Li J. Downregulated PRNP facilitates cell proliferation and invasion and has effect on the immune regulation in ovarian cancer. *J Immunol Res* (2022) 2022:3205040. doi: 10.1155/2022/3205040

66. Rossi AC, Prefumo F. The effects of surgery for endometriosis on pregnancy outcomes following *in vitro* fertilization and embryo transfer: a systematic review and meta-analysis. *Arch Gynecol Obstet* (2016) 294:647–55. doi: 10.1007/s00404-016-4136-4

67. Sanchez AM, Papaleo E, Corti L, Santambrogio P, Levi S, Viganò P, et al. Iron availability is increased in individual human ovarian follicles in close proximity to an endometrioma compared with distal ones. *Hum Reprod* (2014) 29:577–83. doi: 10.1093/humrep/det466

68. Li A, Ni Z, Zhang J, Cai Z, Kuang Y and Yu C. Transferrin insufficiency and iron overload in follicular fluid contribute to oocyte dysmaturity in infertile women with advanced endometriosis. *Front Endocrinol (Lausanne)* (2020) 11:391. doi: 10.3389/fendo.2020.00391

69. Kobayashi H, Yoshimoto C, Matsubara S, Shigetomi H and Imanaka S. Current understanding of and future directions for endometriosis-related infertility research with a focus on ferroptosis. *Diagn (Basel)* (2023) 13(11):1926. doi: 10.3390/diagnostics13111926

70. Ota H, Igarashi S, Kato N and Tanaka T. Aberrant expression of glutathione peroxidase in eutopic and ectopic endometrium in endometriosis and adenomyosis. *Fertil Steril* (2000) 74:313–8. doi: 10.1016/s0015-0282(00)00638-5

71. Atiya HI, Frisbie L, Goldfeld E, Orellana T, Donnellan N, Modugno F, et al. Endometriosis-associated mesenchymal stem cells support ovarian clear cell carcinoma through iron regulation. *Cancer Res* (2022) 82:4680–93. doi: 10.1158/0008-5472.Can-22-1294

72. Hu M, Zhang Y, Lu L, Zhou Y, Wu D, Brännström M, et al. Overactivation of the androgen receptor exacerbates gravid uterine ferroptosis via interaction with and suppression of the NRF2 defense signaling pathway. *FEBS Lett* (2022) 596:806–25. doi: 10.1002/1873-3468.14289

73. Lv Y, Zhang S, Weng X, Huang J, Zhao H, Dai X, et al. Estrogen deficiency accelerates postmenopausal atherosclerosis by inducing endothelial cell ferroptosis through inhibiting NRF2/GPX4 pathway. *FASEB J* (2023) 37:e22992. doi: 10.1096/fj.202300083R

74. Ma B, Zhong Y, Chen R, Zhan X, Huang G, Xiong Y, et al. Tripterygium glycosides reverse chemotherapy resistance in ovarian cancer by targeting the NRF2/GPX4 signal axis to induce ferroptosis of drug-resistant human epithelial ovarian cancer cells. *Biochem Biophys Res Commun* (2023) 665:178–86. doi: 10.1016/j.bbrc.2023.04.111

75. Maas K, Mirabal S, Penzias A, Sweetnam PM, Eggan KC, Sakkas D. Hippo signaling in the ovary and polycystic ovarian syndrome. *J Assist Reprod Genet* (2018) 35:1763–71. doi: 10.1007/s10815-018-1235-0

76. Jin Y, Qiu J, Lu X, Li G. C-MYC inhibited ferroptosis and promoted immune evasion in ovarian cancer cells through NCOA4 mediated ferritin autophagy. *Cells* (2022) 11(24):4127. doi: 10.3390/cells11244127

77. Anandhan A, Dodson M, Shakya A, Chen J, Liu P, Wei Y, et al. NRF2 controls iron homeostasis and ferroptosis through HERC2 and VAMP8. *Sci Adv* (2023) 9:eade9585. doi: 10.1126/sciadv.ade9585

78. Jin Y, Qiu J, Lu X, Ma Y and Li G. LncRNA CACNA1G-AS1 up-regulates FTH1 to inhibit ferroptosis and promote malignant phenotypes in ovarian cancer cells. *Oncol Res* (2023) 31:169–79. doi: 10.32604/or.2023.027815

79. Lin PH, Su WP, Li CJ, Lin LT, Sheu JJ, Wen ZH, et al. Investigating the role of ferroptosis-related genes in ovarian aging and the potential for nutritional intervention. *Nutrients* (2023) 15(11):2461. doi: 10.3390/nu15112461

80. Zhang S, Liu Q, Chang M, Pan Y, Yahaya BH, Liu Y, et al. Chemotherapy impairs ovarian function through excessive ROS-induced ferroptosis. *Cell Death Dis* (2023) 14:340. doi: 10.1038/s41419-023-05859-0

81. Sun WC, Wang NN, Li R, Sun XC, Liao JW, Yang G, et al. Ferritinophagy activation and sideroflexin1-dependent mitochondrial iron overload contribute to patulin-induced cardiac inflammation and fibrosis. *Sci Total Environ* (2023) 892:164472. doi: 10.1016/j.scitotenv.2023.164472

82. Zhang C, Liu N. Ferroptosis, necroptosis, and pyroptosis in the occurrence and development of ovarian cancer. *Front Immunol* (2022) 13:920059. doi: 10.3389/fimmu.2022.920059

83. Zhang J, Ding N, Xin W, Yang X and Wang F. Quantitative proteomics reveals that a prognostic signature of the endometrium of the polycystic ovary syndrome women based on ferroptosis proteins. *Front Endocrinol (Lausanne)* (2022) 13:871945. doi: 10.3389/fendo.2022.871945

84. Wu Y, Zhou S, Zhao A, Mi Y and Zhang C. Protective effect of rutin on ferroptosis-induced oxidative stress in aging laying hens through Nrf2/HO-1 signaling. *Cell Biol Int* (2023) 47:598–611. doi: 10.1002/cbin.11960

85. Peng Q, Chen X, Liang X, Ouyang J, Wang Q, Ren S, et al. Metformin improves polycystic ovary syndrome in mice by inhibiting ovarian ferroptosis. *Front Endocrinol (Lausanne)* (2023) 14:1070264. doi: 10.3389/fendo.2023.1070264

86. Hu M, Zhang Y, Ma S, Li J, Wang X, Liang M, et al. Suppression of uterine and placental ferroptosis by n-acetylcysteine in a rat model of polycystic ovary syndrome. *Mol Hum Reprod* (2021) 27(12):gaab067. doi: 10.1093/molehr/gaab067

87. Xuan Y, Wang H, Yung MM, Chen F, Chan WS, Chan YS, et al. SCD1/FADS2 fatty acid desaturases equipoise lipid metabolic activity and redox-driven ferroptosis in ascites-derived ovarian cancer cells. *Theranostics* (2022) 12:3534–52. doi: 10.7150/thno.70194

88. Ma LL, Liang L, Zhou D and Wang SW. Tumor suppressor miR-424-5p abrogates ferroptosis in ovarian cancer through targeting ACSL4. *Neoplasma* (2021) 68:165–73. doi: 10.4149/neo_2020_200707N705

89. Yang WH, Huang Z, Wu J, Ding CC, Murphy SK, Chi JT. A TAZ-ANGPTL4-NOX2 axis regulates ferroptotic cell death and chemoresistance in epithelial ovarian cancer. *Mol Cancer Res* (2020) 18:79–90. doi: 10.1158/1541-7786.Mcr-19-0691

90. Wang Y, Zhao G, Condello S, Huang H, Cardenas H, Tanner EJ, et al. Frizzled-7 identifies platinum-tolerant ovarian cancer cells susceptible to ferroptosis. *Cancer Res* (2021) 81:384–99. doi: 10.1158/0008-5472.Can-20-1488

91. Choi JA, Lee EH, Cho H and Kim JH. High-dose selenium induces ferroptotic cell death in ovarian cancer. *Int J Mol Sci* (2023) 24(3):1918. doi: 10.3390/ijms24031918

92. Chandra A, Pius C, Nabeel M, Nair M, Vishwanatha JK, Ahmad S, et al. Ovarian cancer: current status and strategies for improving therapeutic outcomes. *Cancer Med* (2019) 8:7018–31. doi: 10.1002/cam4.2560

93. Cheng Q, Bao L, Li M, Chang K and Yi X. Erastin synergizes with cisplatin via ferroptosis to inhibit ovarian cancer growth *in vitro* and *in vivo*. *J Obstet Gynaecol Res* (2021) 47:2481–91. doi: 10.1111/jog.14779

94. Hong T, Lei G, Chen X, Li H, Zhang X, Wu N, et al. PARP inhibition promotes ferroptosis via repressing SLC7A11 and synergizes with ferroptosis inducers in BRCA-proficient ovarian cancer. *Redox Biol* (2021) 42:101928. doi: 10.1016/j.redox.2021.101928

95. Ahmed N, Stenvers KL. Getting to know ovarian cancer ascites: opportunities for targeted therapy-based translational research. *Front Oncol* (2013) 3:256. doi: 10.3389/fonc.2013.00256

96. Vriens K, Christen S, Parik S, Broekaert D, Yoshinaga K, Talebi A, et al. Evidence for an alternative fatty acid desaturation pathway increasing cancer plasticity. *Nature* (2019) 566:403–6. doi: 10.1038/s41586-019-0904-1

97. Sun D, Li YC, Zhang XY. Lidocaine promoted ferroptosis by targeting miR-382-5p /SLC7A11 axis in ovarian and breast cancer. *Front Pharmacol* (2021) 12:681223. doi: 10.3389/fphar.2021.681223

98. Sun J, Wei Q, Zhou Y, Wang J, Liu Q and Xu H. A systematic analysis of FDA-approved anticancer drugs. *BMC Syst Biol* (2017) 11:87. doi: 10.1186/s12918-017-0464-7

99. Chekerov R, Hilpert F, Mahner S, El-Balat A, Harter P, De Gregorio N, et al. Sorafenib plus topotecan versus placebo plus topotecan for platinum-resistant ovarian cancer (TRIAS): a multicentre, randomised, double-blind, placebo-controlled, phase 2 trial. *Lancet Oncol* (2018) 19:1247–58. doi: 10.1016/s1470-2045(18)30372-3

100. Chen Y, Liao X, Jing P, Hu L, Yang Z, Yao Y, et al. Linoleic acid-glucosamine hybrid for endogenous iron-activated ferroptosis therapy in high-grade serous ovarian cancer. *Mol Pharm* (2022) 19:3187–98. doi: 10.1021/acs.molpharmaceut.2c00333

101. Zhu X, Chen X, Qiu L, Zhu J and Wang J. Norcantharidin induces ferroptosis via the suppression of NRF2/HO-1 signaling in ovarian cancer cells. *Oncol Lett* (2022) 24:359. doi: 10.3892/ol.2022.13479

102. Chan DW, Yung MM, Chan YS, Xuan Y, Yang H, Xu D, et al. MAP30 protein from momordica charantia is therapeutic and has synergic activity with cisplatin against ovarian cancer *in vivo* by altering metabolism and inducing ferroptosis. *Pharmacol Res* (2020) 161:105157. doi: 10.1016/j.phrs.2020.105157

103. Mao G, Xin D, Wang Q and Lai D. Sodium molybdate inhibits the growth of ovarian cancer cells via inducing both ferroptosis and apoptosis. *Free Radic Biol Med* (2022) 182:79–92. doi: 10.1016/j.freeradbiomed.2022.02.023

104. Gao M, Deng J, Liu F, Fan A, Wang Y, Wu H, et al. Triggered ferroptotic polymer micelles for reversing multidrug resistance to chemotherapy. *Biomaterials* (2019) 223:119486. doi: 10.1016/j.biomaterials.2019.119486

105. Santos I, Ramos C, Mendes C, Sequeira CO, Tomé CS, Fernandes DGH, et al. Targeting glutathione and cystathionine β-synthase in ovarian cancer treatment by selenium-chrysin polyurea dendrimer nanoformulation. *Nutrients* (2019) 11(10):2523. doi: 10.3390/nu11102523

106. Geng Z, Nie X, Ling L, Li B, Liu P, Yuan L, et al. Electroacupuncture may inhibit oxidative stress of premature ovarian failure mice by regulating intestinal microbiota. *Oxid Med Cell Longev* (2022) 2022:4362317. doi: 10.1155/2022/4362317

107. Wu YH, Wu YR, Li B and Yan ZY. Cryptotanshinone: a review of its pharmacology activities and molecular mechanisms. *Fitoterapia* (2020) 145:104633. doi: 10.1016/j.fitote.2020.104633

108. Liu H, Xie J, Fan L, Xia Y, Peng X, Zhou J, et al. Cryptotanshinone protects against PCOS-induced damage of ovarian tissue via regulating oxidative stress, mitochondrial membrane potential, inflammation, and apoptosis via regulating ferroptosis. *Oxid Med Cell Longev* (2022) 2022:8011850. doi: 10.1155/2022/8011850

frontiers | Frontiers in Endocrinology

TYPE Original Research
PUBLISHED 04 August 2023
DOI 10.3389/fendo.2023.1164186

OPEN ACCESS

EDITED BY
Changyin Zhou,
Guangdong Second Provincial General Hospital, China

REVIEWED BY
Oscar Lorenzo,
Health Research Institute Foundation Jimenez Diaz (IIS-FJD), Spain
Mianqun Zhang,
Anhui Agricultural University, China

*CORRESPONDENCE
Lishan Huang
mzslishan2019@163.com

RECEIVED 12 February 2023
ACCEPTED 12 April 2023
PUBLISHED 04 August 2023

CITATION
Liang Y, Zeng W, Hou T, Yang H, Wu B, Pan R and Huang L (2023) Gut microbiome and reproductive endocrine diseases: a Mendelian randomization study. *Front. Endocrinol.* 14:1164186. doi: 10.3389/fendo.2023.1164186

Gut microbiome and reproductive endocrine diseases: a Mendelian randomization study

Ye Liang, Weihong Zeng, Tao Hou, Haikun Yang, Boming Wu, Ru Pan and Lishan Huang*

Department of Gynecology, Meizhou People's Hospital, Meizhou, Guangdong, China

Background: Observation studies have confirmed the association between the gut microbiome and reproductive endocrine diseases (REDs), namely, polycystic ovary syndrome (PCOS), endometriosis, and female infertility. However, their association has never been confirmed by a two-sample Mendelian randomization (MR) analysis.

Methods: We conducted a two-sample MR analysis to evaluate the relationship between the gut microbiome and the three aforementioned REDs. In order to get more comprehensive results, two different thresholds were adopted to select instrumental variables (IVs): one was a locus-wide significance threshold (P <1.0×10^{-5}) and the other was a genome-wide significance level (P< 5×10^{-8}). Summary-level statistics for the gut microbiome and REDs were collected from public databases. Inverse-variance weighted (IVW) was the main method used to estimate causality, and sensitivity analyses were conducted to validate the MR results.

Results: At the locus-wide significance level, we identified that the genera Streptococcus (OR=1.52, 95%CI: 1.13-2.06, P=0.006) and RuminococcaceaeUCG005 (OR=1.39, 95%CI: 1.04-1.86, P=0.028) were associated with a high risk of PCOS, while Sellimonas (OR= 0.69, 95%CI: 0.58-0.83, P=0.0001) and RuminococcaceaeUCG011 (OR=0.76, 95%CI: 0.60-0.95, P=0.017) were linked to a low PCOS risk. The genus Coprococcus2 (OR=1.20, 95%CI: 1.01-1.43, P=0.039) was correlated with an increased risk of female infertility, while Ruminococcus torques (OR=0.69, 95%CI: 0.54-0.88, P=0.002) were negatively associated with the risk of female infertility. The genera Olsenella (OR= 1.11, 95%CI: 1.01-1.22, P=0.036), Anaerotruncus (OR= 1.25, 95%CI: 1.03-1.53, P=0.025), and Oscillospira (OR= 1.21, 95%CI: 1.01-1.46, P=0.035) were linked to a high risk of endometriosis. However, the results showed that the gut microbiome did not possess a causal link with REDs risk based on the genome-wide significance level. Sensitivity analyses further confirmed the robustness of the MR results.

Conclusion: Our study provides evidence that gut microbiome is closely related with REDs. Subsequent studies should be conducted to promote microbiome-orientated therapeutic strategies for managing REDs.

KEYWORDS

Mendelian randomization, polycystic ovary syndrome, gut microbiome, endometriosis, female infertility

1 Introduction

The homeostasis of sex hormones plays a significant role in the reproductive endocrine system throughout the lifetime of a female. Disturbance in sex hormones may lead to reproductive endocrine diseases (REDs) such as polycystic ovary syndrome (PCOS), endometriosis, and infertility that have bothered female people of reproductive age for many years. PCOS is one of the most prevalent endocrine and metabolic disorders in reproductive-aged female people. Female people presenting PCOS have a high prevalence of endocrine–metabolic dysfunction, including obesity, insulin resistance, hyperinsulinemia, and dyslipidemia, resulting in a significantly increased risk for mood disorders, type 2 diabetes mellitus, infertility, metabolic disorders, cardiovascular disorders, and the development of cancer (1–3). Infertility is defined as the failure to conceive after 12 months of regular unprotected sexual intercourse. The causes of infertility include male factors, female factors, and unknown factors. It has become a major public health problem affecting 8-12% of reproductive-aged couple (4). Endometriosis is a disease characterized by endometrial tissue outside the uterus, which affects 10% of reproductive-aged female people worldwide and leads to chronic painful symptoms and infertility in severe cases (5). Due to the health, economic, and social burdens caused by these diseases, it is urgent to understand the underlying mechanisms and obtain an adequate treatment for them.

Growing evidence has revealed the relationship between the gut microbiome and REDs. The gut microbiome is considered to be an endocrine organ and plays a major role in the reproductive endocrine system by affecting the fluctuation of sex hormones. The gut microbiome can affect estrogen levels by modulating the secretion of β-glucuronidase. The dysbiosis and reduction of gut microbiota diversity can decrease or increase β-glucuronidase activity and result in the fluctuation of circulating estrogens, which may lead to obesity, metabolic syndrome, cancer, endometrial hyperplasia, endometriosis, PCOS, and infertility (6, 7). The gut microbiome can also affect the level of circulating testosterone. The gut microbiota can synthesize and transform androgens by expressing the enzymes and are involved in the degradation of testosterone *via* microbial processes (8). For example, Proteobacteria can degrade androgen (9), and Clostridium scindens has a high potential to convert glucocorticoids into androgens (10). A combination of signs and symptoms of hyperandrogenism is a typical feature of PCOS. Previous studies found that the gut microbiome and its metabolites played an important role in the regulation of PCOS-associated ovarian dysfunction and insulin resistance (11). Obesity and PCOS also have a reverse effect on changing the gut microbiome composition, which may disrupt the ovarian function, damage oocyte quality, and cause chronic inflammation, hence further deteriorating fertility (12). Thus, the gut microbiome may have an impact on PCOS pathogenesis through a variety of mechanisms.

The majority of instances of female infertility can be explained in terms of ovulation disorders, uterine or cervical issues, tubal alterations, endometriosis, immune factors, and/or pelvic infections. However, approximately 30% of cases cannot be explained, and these are defined as "unexplained infertility" (13). Growing evidence has confirmed that gut microbiota dysbiosis has an indispensable impact on inflammatory conditions that affect male and female fertility (14, 15). An observational study found that female infertility showed a different bacterial richness and ratio, and an increasing level of inflammation comparing with the fertile group (15). A systematic review demonstrated that many autoantibodies, such as thyroid-related autoantibodies, anti-phospholipid antibodies, and anti-nuclear antibodies, impede the chances of a successful *in vitro* fertilization cycle (16). Therefore, we concluded that gut microbiome may have a close relationship with female infertility.

The understanding of the etiology of endometriosis is still lacking. Recently, studies have shown that the gut microbiome may be closely associated with the onset and progression of endometriosis due to its influence on the estrogen metabolism and inflammation. The increasing level of circulating estrogen derived by gut microbiome dysbiosis may stimulate the growth and cyclic bleeding of endometriotic lesions (8). Another reason is that dysbiosis in the gut microbiome disrupts the immune function, leading to the elevation of inflammatory cytokines and alteration of immune cell profiles. Over time, a chronic state of inflammation is developed to create an environment conducive to increased adhesion and angiogenesis, which may drive endometriosis onset and progression (17). The gut microbiome also contributes to the chronic pain of endometriosis by regulating microglia, astrocytes, and immune cells, and gut microbiome dysbiosis could lead to incorrect immune responses (18).

These above observations indicate there is a close link between the gut microbiome and the pathogenesis and progression of REDs; however, a Mendelian randomization (MR) analysis about their associations is still lacking. It is necessary to establish a causal relationship analysis to further understand the gut microbiome-derived mechanism and provide new insights into microbiome-orientated therapeutic strategies. Hence, we conducted a two-sample MR analysis to evaluate the relationship between gut microbiome composition and REDs. MR is an effective method to infer causality between exposures and outcomes by using genetic variations strongly associated with exposures as instrumental variables (IVs). MR can be regarded as a natural randomized controlled trial (RCT), which is not easily disturbed by confounding factors and has a high level of evidence.

2 Materials and methods

2.1 Data sources

Genome-wide association studies (GWAS) data sources for the gut microbiome and PCOS, pregnancy loss, female infertility, and endometriosis were compiled and made publicly available online (Table 1). Single-nucleotide polymorphisms (SNPs) associated with the composition of the human gut microbiome were selected as IVs.

TABLE 1 Summary of genome-wide association studies (GWAS) datasets in our study.

Phenotype	Type of trait	Source	Ethnicity	Sample Size	No.of cases	No. of SNPs	References
Gut Microbiome	Genus	MiBioGen	Multi-ancestry	18,473	–	122,110	(19)
PCOS	Binary	Day et al.	European	113,238	10,074	9,295,102	(20)
Female Infertility	Binary	FinnGen	European	104,225	9,831	16,381,204	(21)
Endometriosis	Binary	OpenGWAS	European	77,257	8,288	16,377,306	(22)

"-" The group of cases were not set in the GWAS study of gut microbiome.

Ethics approval was not required, since the data used were obtained from published studies or public databases.

2.1.1 Gut microbiome

GWAS summary statistics for the human gut microbiome were obtained from the MiBioGen study, which is a large-scale, multiethnic GWAS study recruiting 18, 473 individuals (24 cohorts) from various countries with 122,110 loci of variation (19). Most of the participants had European ancestry (n = 13, 266). A total of 211 taxa were categorized by five biological categories, including 9 phyla, 16 classes, 20 orders, 35 families, and 131 genera. As the genus was the smallest and most precise taxonomic level among all the category criteria, we performed subsequent analyses at the genus level only. Therefore, a total of 119 specific genera were included in the current analysis after removing 12 unknown genera out of 131 genera.

2.1.2 PCOS

GWAS data for PCOS were taken from Apollo (https://doi.org/10.17863/CAM.27720), which includes 10,074 PCOS cases and 103, 164 controls of European ancestry (20). Cases were either diagnosed according to the National Institutes of Health (NIH) or Rotterdam criteria or self-reported history of PCOS.

2.1.3 Female infertility

Summary-level data for female infertility were also derived from the FinnGen consortium (104,225 female participants recruited, including 9, 831cases and 94,394 controls) (21).

2.1.4 Endometriosis

The GWAS summary datasets for endometriosis were accessed through the OpenGWAS database (22). The diagnostic criterion of endometriosis based on the International Classification of Diseases 10th code and GWAS ID is finn-b-N14_ENDOMETRIOSIS, with 77, 257 female participants recruited, including 8,288 cases and 68, 969 controls.

2.2 Selection of IVs

In this study, several steps were conducted to select eligible SNPs as IVs from the exposure data. First, SNPs strongly associated with the gut microbiome were selected. In order to obtain more comprehensive results, two different thresholds were adopted to select IVs: (1) SNPs at the locus-wide significance threshold ($P < 1.0\times10^{-5}$) were selected as potential IVs; (2) SNPs at the genome-wide significance level ($P< 5 \times 10^{-8}$) were selected as potential IVs. Second, to ensure that IVs used for the gut microbiome were independent, we excluded SNPs that had the linkage disequilibrium (LD) effect ($r^2 < 0.001$, clumping window = 10,000kb). Third, SNPs related to confounders and risk factors for outcome were removed from the analysis by using the online database "PhenoScanner" (http://www.phenoscanner.medschl.cam.ac.uk/) with the filtration of $r^2 > 0.8$ and $p < 1 \times 10^{-5}$. The IVs of the gut microbiome identified above were extracted from each outcome dataset. Proxy SNPs were not sought by default when specific SNPs were absent in the outcome GWAS. Palindromic SNPs were also excluded. Afterwards, the exposure data and the outcome data were harmonized, which means that the effect of the SNP on the exposure was reconciled with the effect on the outcome in terms of the same allele. The strength of the included IVs was assessed with the F-statistics and R^2. R^2 reflects the degree to which the IV explains the exposure and is calculated as formula $R^2 = 2 \times EAF \times (1 - EAF) \times \beta^2/[2 \times EAF \times (1 - EAF) \times \beta^2 + 2 \times EAF \times (1 - EAF) \times N \times se^2]$ (EAF: effect allele frequency, se: the standard error for effect size, β: the effect size, N: the sample size) (23).The F-statistic was calculated by the formula $F = R2 \times (N - 2)/(1 - R2)$ (N:the sample size), where weak instrument bias is relatively low with an F-statistic over 10 (24).

2.3 MR analysis

An MR analysis was performed to determine if there is a causal relationship between the gut microbiome and the risk of REDs by using inverse-variance weighted (IVW) as the main method and other methods too, including MR-Egger, weighted median, and weighted mode. IVW was conducted to estimate the causality of each SNP with the assumption of no pleiotropy in these SNPs (25). Comparing with IVW, the MR-Egger not only allows the presence of pleiotropy in > 50% of IVs, but also detects horizontal pleiotropy in term of its intercept with a y-axis (26, 27). There is horizontal pleiotropy when the intercept is not zero. Point estimates from IVW MR are close to that of the MR-Egger when the intercept is close to zero. The weighted median was performed when the presence of pleiotropy was < 50% in IVs (28). The weighted mode method had less power to detect causal effects than the IVW and weighted median methods, but it was larger than that of MR-Egger and presented less bias than the above methods (29).

2.4 Sensitivity analysis

Cochran's Q test was used to access heterogeneity (30). The MR-Egger regression test was performed to detect pleiotropy. There was horizontal pleiotropy when the intercept was not zero (26). MR-PRESSO was performed to reduce horizontal pleiotropy by detecting and removing final outliers (31). The leave-one-out sensitivity analysis was implemented to validate the robustness of the results by removing a single SNP each time.

A reverse MR analysis was not performed due to the lack of SNPs (related to REDs). All statistical analyses were performed using the package "TwoSampleMR" and "MR-PRESSO" in the R software (Version 4.2.0). Considering multiple-testing correction, FDR correction (Q-value) was performed using the Benjamini–Hochberg method.

3 Results

3.1 Instrumental variables selection

Initially, a total of 7098 SNPs categorized by 119 genera were extracted under the threshold of the locus-wide statistical significance ($P< 1\times 10^{-5}$). There was no genus containing only one SNP for each outcome dataset. In the present study, the F-statistic of IVs were all over 10, indicating no evidence of weak instrument bias. Detailed information including effect allele, other allele, Beta, SE, *P*-value, and F-statistics in IVs is shown in Supplementary Tables 1A–C. We evaluated the causal effect of each genus on the outcome data.

A total of 396 SNPs were extracted under the threshold of genome-wide statistical significance ($P<5\times10^{-8}$). After a series of quality control steps, a total of 12 independent SNPs were identified as IVs for PCOS, 11 independent SNPs for female infertility, and 11 independent SNPs for endometriosis. There was no weak instrument bias, as the F-statistics of IVs were all greater than 10. Detailed information including effect allele, other allele, Beta, SE, and *P*-value on IVs is shown in Supplementary Table 4A. Due to the limited number of IVs that met the requirements and each IV representing different genera, we took them as a whole to identify the gut microbiome to estimate its causal effect on outcome data.

3.2 Two-sample MR analysis(locus-wide significance level, $P<1\times10^{-5}$)

We conducted an MR analysis to evaluate the causal relationship between each genus and PCOS, female infertility, and endometriosis. The comprehensive results are shown in Supplementary Tables 2A–C. Streptococcus, Sellimonas, RuminococcaceaeUCG011, and RuminococcaceaeUCG005 were found to be associated with PCOS when evaluated by IVW. The IVW estimate suggested that the genera Streptococcus (OR:1.52, 95% confidence interval (CI):1.13-2.06, *P*=0.006) and RuminococcaceaeUCG005(OR:1.39, 95%CI:1.04-1.86, *P*=0.028) are positively associated with PCOS risk, while Sellimonas (OR:0.69,95%CI: 0.58-0.83, *P*=0.0001) and Ruminococcaceae UCG011(OR:0.76, 95%CI: 0.60-0.95, *P*=0.017) are negatively associated with PCOS risk (Table 2). However, only Sellimonas was still significant after FDR correction (Q-value= 0.015) (Supplementary Table 3). Ruminococcus torques and Coprococcus2 were found to be associated with female infertility when evaluated by IVW. The IVW estimate suggests that the genus Coprococcus2 (OR:1.20, 95%CI:1.01-1.43, *P*=0.039) is associated with an increased risk of female infertility, while Ruminococcus torques (OR:0.69, 95%CI:0.54-0.88, *P*=0.002) is associated with a decreased risk of female infertility (Table 2). However, no causal association of these genera with female infertility was supported after FDR correction (Supplementary Table 3). Olsenella, Anaerotruncus, and Oscillospira were found to be associated with endometriosis when evaluated by IVW. The IVW estimate suggested that the genera Olsenella (OR:1.11, 95%CI: 1.01-1.22, *P*=0.036), Anaerotruncus (OR:1.25, 95%CI: 1.03-1.53, *P*=0.025), and Oscillospira (OR:1.21,95%CI: 1.01-1.46, *P*=0.035) are associated with an increased risk of endometriosis (Table 2), while these associations were no longer significant after FDR correction (Supplementary Table 3).

The results of Cochran's Q test evaluated by the IVW test and MR-Egger showed no significant heterogeneity between the gut microbiome and PCOS, female infertility, and endometriosis. There was no evidence of horizontal pleiotropy according to the results of the MR-Egger regression analysis. In addition, MR-PRESSO analysis did not find any significant outliers (Table 2). The leave-one-out results further validated data robustness (Figure 1).

3.3 Two-sample MR analysis(genome-wide significance level, $P<5\times10^{-8}$)

Considering the gut microbiome as a whole, the results of the MR analysis evaluated by IVW (OR = 1.06, 95% CI 0.87-1.30, *P* =0.58) did not show a significant causal relationship between the gut microbiome and PCOS. The other methods showed directionally consistent results (Supplementary Table 4B). We also could not find a causal link between the gut microbiome and female infertility (IVW: OR = 0.98, 95% CI 0.86-1.13, *P* =0.82) and endometriosis (IVW: OR = 0.96, 95% CI 0.86-1.09, *P* =0.56). Cochran's Q statistics of the IVW test and the MR-Egger regression, respectively, showed no significant heterogeneity between gut the microbiome and PCOS and endometriosis. However, there was heterogeneity between the gut microbiome and female infertility; in this case, we applied the result of the weighted median as main MR result to evaluate the causal association between the gut microbiome and female infertility (OR =1.06, 95% CI 0.93-1.22, *P*=0.36). The MR-Egger regression results showed that there was no horizontal pleiotropy between the gut microbiome and PCOS, female infertility, and endometriosis. The MR-PRESSO analysis showed that there were no outliers in the analysis (Supplementary Table 4B). Moreover, the leave-one-out results further validated the data robustness (Supplementary Figure 1).

10.3389/fendo.2023.1164186

TABLE 2 Causal links between gut microbiota and REDs in the MR analysis. (P<1×10-5).

Bacterial genera (exposure)	Outcomes	nSNPs	Methods	OR (95% CI)	Beta	Se	P value	Horizontal pleiotropy			Heterogeneity		MR-PRESSO
								Egger intercept	SE	P value	Cochran's Q	P value	P value
Streptococcus	PCOS	15	MR Egger	2.36 (0.80-6.96)	0.86	0.55	0.145	-0.03	0.04	0.43	6.61	0.92	0.97
			IVW	1.52 (1.13-2.06)	0.42	0.15	0.006				7.28	0.92	
			Weighted median	1.62 (1.07-2.46)	0.48	0.21	0.023						
			Weighted mode	1.70 (0.89-3.25)	0.53	0.34	0.128						
Sellimonas	PCOS	9	MR Egger	1.14 (0.38-3.43)	0.13	0.56	0.826	-0.07	0.08	0.41	3.93	0.79	0.50
			IVW	0.69 (0.58-0.83)	-0.36	0.09	0.0001				4.72	0.79	
			Weighted median	0.69 (0.54-0.88)	-0.37	0.13	0.003						
			Weighted mode	0.70 (0.47-1.05)	-0.35	0.21	0.123						
RuminococcaceaeUCG011	PCOS	8	MR Egger	0.32 (0.11-0.91)	-1.13	0.53	0.077	0.11	0.07	0.15	6.51	0.37	0.275
			IVW	0.76 (0.60-0.95)	-0.28	0.12	0.017				9.40	0.23	
			Weighted median	0.75 (0.57-0.95)	-0.28	0.14	0.049						
			Weighted mode	0.61 (0.37-1.02)	0.19	0.42	0.117						
RuminococcaceaeUCG005	PCOS	14	MR Egger	1.20 (0.53-2.72)	0.19	0.42	0.664	0.01	0.03	0.72	11.91	0.45	0.35
			IVW	1.39 (1.04-1.86)	0.33	0.15	0.028				12.04	0.52	
			Weighted median	1.33 (0.89-1.89)	0.28	0.20	0.164						
			Weighted mode	1.23 (0.65-2.31)	0.20	0.32	0.541						
Ruminococcustorques	Female infertily	7	MR Egger	1.15 (0.56-2.35)	0.14	0.36	0.716	-0.04	0.02	0.19	1.99	0.85	0.21
			IVW	0.69 (0.54-0.88)	-0.38	0.12	0.002				4.27	0.64	

(Continued)

10.3389/fendo.2023.1164186

TABLE 2 Continued

Bacterial genera (exposure)	Outcomes	nSNPs	Methods	OR (95% CI)	Beta	Se	*P* value	Horizontal pleiotropy			Heterogeneity		MR-PRESSO
								Egger intercept	SE	*P* value	Cochran's Q	*P* value	*P* value
			Weighted median	0.80 (0.59-1.10)	-0.22	0.16	0.168						
			Weighted mode	0.86 (0.54-1.36)	-0.15	0.24	0.542						
Coprococcus2	Female infertily	8	MR Egger	1.09 (0.28-4.27)	0.09	0.70	0.903	0.01	0.05	0.90	5.01	0.54	0.07
			IVW	1.20 (1.01-1.43)	0.18	0.09	0.039				5.03	0.66	
			Weighted median	1.15 (0.91-1.45)	0.14	0.12	0.222						
			Weighted mode	1.15 (0.79-1.68)	0.14	0.19	0.492						
Olsenella	Endometriosis	8	MR Egger	1.03 (0.75-1.40)	0.03	0.16	0.863	0.01	0.02	0.63	7.12	0.52	0.61
			IVW	1.11 (1.01-1.22)	0.10	0.05	0.036				7.37	0.60	
			Weighted median	1.11 (0.97-1.27)	0.10	0.07	0.146						
			Weighted mode	1.04 (0.85-1.26)	0.04	0.10	0.715						
Anaerotruncus	Endometriosis	13	MR Egger	0.85 (0.49-1.47)	-0.17	0.28	0.566	0.03	0.02	0.17	11.47	0.41	0.329
			IVW	1.25 (1.03-1.53)	0.23	0.10	0.025				13.76	0.32	
			Weighted median	1.24 (0.97-1.60)	0.22	0.13	0.091						
			Weighted mode	1.20 (0.86-1.67)	0.18	0.17	0.299						
Oscillospira	Endometriosis		MR Egger	0.96 (0.45-2.06)	-0.04	0.39	0.918	0.02	0.04	0.55	2.88	0.82	0.742
			IVW	1.21 (1.01-1.46)	0.19	0.09	0.035				3.27	0.86	
			Weighted median	1.17 (0.93-1.47)	0.15	0.12	0.188						
			Weighted mode	1.12 (0.78-1.60)	0.11	0.18	0.553						

nSNPs, the number of SNPs being used as IVs; OR, odds ratio; I VW, inverse-variance weighted; PCOS, polycystic ovary syndrome; REDs, reproductive endocrine diseases;

4 Discussion

In the current study, we conducted MR analyses to evaluate the potential causality between the gut microbiota and REDs. Based on the locus-wide significance level, we identified that the genera Streptococcus and RuminococcaceaeUCG005 were associated with a high risk of PCOS, while Sellimonas and RuminococcaceaeUCG011were linked to a low PCOS risk. The genus Coprococcus2 was associated with an increased risk of female infertility, while Ruminococcus torques was negatively associated with the risk of female infertility. Genus Olsenella, Anaerotruncus, and Oscillospira were linked to a high risk of endometriosis. However, the results showed that gut microbiome did not have a causal link with REDs risk based on the genome-wide statistical significance level.

There are many previous studies on the relationship between the gut microbiome and PCOS, with Ruminococcaceae among them (32, 33). RuminococcaceaeUCG005 is a member of the Ruminococcaceae family and is viewed as a harmful bacterium in high-fat diet (HFD)-fed rats, and it correlates with oxidative stress, metabolism genes, and body weight (34). Prior evidence indicated that increased oxidative stress and elevated inflammatory status contribute to the progression of PCOS (35, 36), and weight loss is an important part of PCOS treatment (37, 38), which might partly explain why RuminococcaceaeUCG005 is associated with a high risk of PCOS. Female people presenting PCOS characterized by a combination of signs and symptoms of androgen excess have a high prevalence of obesity, insulin resistance, and dyslipidemia. Streptococcus, considered "bad bacteria", was previously shown to be associated with obesity and significantly higher in obese and PCOS adults (39–42). Streptococcus was positively correlated with insulin resistance, testosterone, and BMI (33, 43–45). It was also found to be involved with carbohydrate metabolism and positively associated with insulin, connecting peptide, lipopolysaccharide, and pro-inflammatory indicators (42, 46, 47).However, it was negatively correlated with short-chain fatty acids (SCFAs) (42). SCFAs, the microbial fermentation end-products, may help suppress the levels of pro-inflammation cytokines, reduce inflammation in the intestine, and maintain the homeostasis of the intestinal environment (48).SCFAs are associated with insulin releasing and blood glucose levels by supporting the health of beta cells in the pancreas, and they stimulate the secretion of glucagon-like peptide-1 (GLP-1) (49, 50). Additionally, SCFA acetate may help people control weight and support healthy weight maintenance in terms of regulating hormones (such as GLP-1), increasing metabolism, and inhibiting appetite (51). Research showed that acetate could protect ovarian function by supporting normal follicles growth and enhancing circulating 17-β estradiol through the inhibition of histone deacetylase in the rat model of PCOS (52). Additionally, it has been found that probiotics and SCFAs administration, as part of anti-obesity and diabetes interventions, could involve the modification of microbiota, the upregulation of GLP-1 production and related SCFAs, such as acetate, and increasing fasting fat oxidation and resting energy expenditure (53–55). Zhang et al. found that probiotics impact the gut microbiota and sex hormones of PCOS patients by significantly decreasing the levels of luteinizing

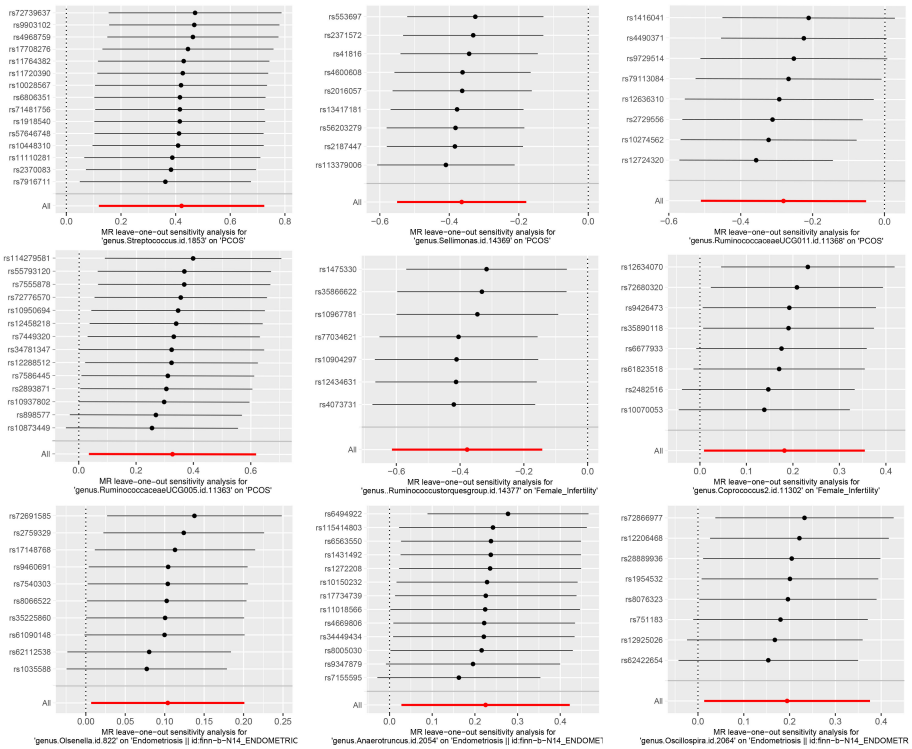

FIGURE 1
The leave-one-out sensitivity analysis assessed the associations between genera and REDs by removing a single SNP each time (P<1x10-5).

hormone (LH) and LH/follicle-stimulating hormone (LH/FSH) and markedly increasing SCFAs (56). The above evidence implies probiotics or SCFAs administration can be beneficial as part of the treatment of female disorders. Sellimonas was considered a potential biomarker of gut homeostasis recovery, as studies found that Sellimonas intestinalis was increased in patients with colorectal cancer who recovered their intestinal homeostasis following dysbiosis caused by radical surgery combined with chemotherapy (57)and in patients with liver cirrhosis who underwent therapeutic splenectomy (58). Studies on the association between Sellimonas and PCOS are limited. We speculated Sellimonas may contribute to the recovery of intestinal homeostasis in patients with PCOS. RuminococcaceaeUCG011 was negatively correlated with the serum and hepatic lipid profiles and was significantly increased after hypoglycemic and hypolipidemic intervention in type 2 diabetic mice (59). As Ruminococcaceae UCG011 was shown to be inversely correlated with the serum levels of triglyceride (TG), cholesterol (TC), low-density lipoprotein cholesterol (LDL-C), and the hepatic levels of TC, TG, non-esterified fatty acids (NEFA), and bile acids (BAs) (59), it may show a protective effect in PCOS, as in other metabolic diseases, which is consistent with our findings.

A great deal of evidence supports the role of the gut microbiome in female infertility. Coprococcus2, associated with an increased risk of female infertility in our study, was previously found to be the characteristic genus of obese patients with PCOS (60, 61). Coprococcus2 was also found to be indirectly associated with chronic low-grade systemic inflammation induced by diets and ectopic fat in the Multiethnic Cohort-Adiposity Phenotype Study (62). Increasing evidence suggests that infertility is related to chronic low-grade inflammation characterized by increased inflammatory markers, such as C-reactive protein (CRP), IL-18, TNF-α, and IL-6 (63, 64). Diets with a marked anti-inflammatory signature have been proposed in the nutritional management of infertile patients (65). For the first time, our finding has implied the relationship between Coprococcus2 and female infertility. This may provide new insights into improving fertility through diets that could decrease the abundance of Coprococcus2. Ruminococcus torques, negatively associated with the risk of female infertility in our study, was found to be negatively correlated with pre-pregnancy body weight in a previous study (66). Several studies have shown both underweight (BMI < 19 kg/m2) and overweight (BMI 25–29.9 kg/m2) affect infertility (67, 68). A cohort study with 9232 participants from Denmark found that overweight and obese mothers with a body mass index (BMI) >25 kg/m2 may harm the fertility of fetuses, and especially, sons born to overweight mothers have higher odds of infertility. However, the study did not find an association between maternal overweight and infertility in daughters (69). Tang et al. found that being underweight with BMI < 18.5 kg/m2 is linked to reduced implantation rates, clinical pregnancy rates, and ongoing pregnancy. Rates of miscarriage were markedly increased in the overweight group relative to the normal weight group (70). We speculated that Ruminococcus torques may affect fertility through its impact on pre-pregnancy body weight. Wen at el. found that Ruminococcus torques was generated after a high-cellulose diet in a mouse model of asthma. They speculated Ruminococcus torques is closely correlated with lipid metabolism *in vivo* (71).Wang et al. discovered that the abundance of Ruminococcus torques was relatively higher after mitigation treatment of colonic inflammation in colitis. Previous studies have revealed the protective role of Ruminococcus torques in other diseases, but further studies need to reveal their protective role in female infertility.

In previous studies, many researchers have revealed the relationship between the gut microbiome and endometriosis. As we know, endometriosis development is influenced by estrogen metabolism and inflammation. The abundance of Olsenella has been found to be associated with the exacerbation of inflammation. The low-abundance and pathogenic bacterium Olsenella proliferates when inflammatory hyperthermia causes host gut microbiota disorders, which further exacerbates the inflammatory response (72), whereas the downregulation of Olsenella can reduce the possibility of inflammation in the rumen epithelium and the organism (73). The abundance of Olsenella is positively correlated with the IL-10 levels (74). IL-10 family proteins, as the main members of Th2 anti-inflammatory cytokines, have been considered a critical factor for the development of endometriosis. Accumulating evidence has demonstrated that IL-10 is sharply increased in the ectopic endometrium and peritoneal fluid of female people with endometriosis, particularly in cases of advanced endometriosis (75–78). Previous research demonstrated that IL-10 from infiltrated plasmacytoid dendritic cells may suppress immunity against endometrial implants to contribute to the development of endometriosis (78) and promote angiogenesis in the early stage of endometriosis (79). Therefore, Olsenella may be involved in the development of endometriosis by modulating the level of IL-10. Moreover, N-acetylserotonin (NAS), an endogenous metabolite, was significantly negatively correlated with Olsenella (72). It has been proposed that the NAS/melatonin ratio is linked to endometriosis pathophysiology. Endometriosis, as an estrogen-dependent condition, is usually mitigated by lowering the estrogen effects. Melatonin inhibits the ERα (80), which modulates the stage transition in endometriosis (81), suggesting that melatonin inhibits ERα-driven pathophysiology in endometriosis. Endometriosis risk is also correlated with CYP1B1 SNPs (82), which increases the backward conversion of melatonin to NAS (83). Further analysis is needed to evaluate the relationships between the NAS/melatonin ratio, Olsenella, and endometriosis. The second genus we found to have a positive association with endometriosis is Oscillospira. Oscillospira was found to associated with adiposity and metabolic dysfunction and gut inflammation and serum triglycerides in mice and humans, respectively (84).Chen et al. discovered that Oscillospira is closely related to human health, because its abundance is positively correlated with high-density lipoprotein, microbial diversity, and sleep time and is inversely correlated with blood pressure, fasting blood glucose, uric acid, triglyceride, and Bristol stool type (85). Jae-Kwon Jo found that Oscillospira was significantly higher in the HFD mice than that those in the control group, producing SCFAs such as acetate, propionate, and butyrate (86). SCFAs butyrate supplement was found to alleviate the symptoms caused by low estrogen, such as excessive osteoclastogenesis and bone loss in estrogen-deficient mice due to ovariectomy (OVX) (87, 88).The association between Oscillospira and host health, SCFAs production, and the estrogen level needs further comprehensive exploration. We speculate that Oscillospira may be involved in endometriosis etiology

when gut dysbiosis and estrogen imbalance occur. Anaerotruncus was the last genus we found to positively relate to endometriosis, and it was found to associated with inflammation and obesity in previous studies (89). Li et al. confirmed that the relative abundance of Anaerotruncus decreased when anti-inflammation treatment reduced psoriasis-like inflammation in mice (90). Kong et al. found that Anaerotruncus, as a conditional pathogenic bacterium, increased in a mouse model fed by HFD and high-sucrose diets (HCDs) (91). Anaerotruncus has been positively associated with glucose intolerance and gut permeability and is involved in the pathogenesis of diabetes (92). However, the studies about the mechanism of Anaerotruncus in endometriosis etiology still lack.

Our study has several advantages. To our knowledge, this is the first MR analysis to evaluate the causal relationship between the gut microbiome and REDs. The MR design has the advantage of preventing disturbance from residual confounding and might be more convincing than observational studies. However, as the exact biological function of many genetic variants is still unknown, we cannot completely avoid the impact of horizontal pleiotropy. Thus, the results should be interpreted with caution. Moreover, we analyzed the causal effect of each taxon on REDs primarily from the genus level. This provides new insights for understanding the gut microbiome-derived mechanisms and microbiome-orientated therapeutic strategies. Several limitations should be mentioned. First, our study was unable to count the participants overlapping between the exposure and outcome GWAS, which may lead to an overestimation of the results. We were also unable to identify a reverse causal relationship between them due to the lack of an adequate number of IVs for REDs. Second, our study used gut microbiome data, including multiethnic male and female participants, whereas studies about REDs were conducted on female Europeans, which may have also influenced our results. However, we were unable to avoid this bias by conducting the sex or race subgroup analysis due to the lack of demographic data in the original research. Third, the sample size of each genus from the gut microbiome GWAS was relatively small compared with that for the REDs. Therefore, not enough IVs were identified for certain bacterial features at the genus level. Fourth, multiple statistical corrections are too rigorous and conservative, which may neglect potential genera that have a causal relationship with REDs. Therefore, we did not take the multiple testing results into account. Future studies need to plan to address these limitations.

In conclusion, we comprehensively evaluated the potential association between the gut microbiome and REDs. These strains may provide candidate biomarkers and new insights into the treatment for subsequent studies.

Data availability statement

The original contributions presented in the study are included in the article/Supplementary Material. Further inquiries can be directed to the corresponding author.

Author contributions

YL and LH designed the study. WZ, BW, and TH performed data analysis. YL, RP, HY, and LH structured the manuscript and contributed to the tables, figures, and text editing. All authors contributed to the final manuscript and approved the submitted version.

Acknowledgments

We want to acknowledge the participants and investigators of FinnGen, the UK Biobank study (NealeLab) study, and the MiBioGen consortium for sharing the genetic data.

Conflict of interest

The authors declare that the research was conducted in the absence of any commercial or financial relationships that could be construed as a potential conflict of interest.

Publisher's note

Supplementary material

The Supplementary Material for this article can be found online at: https://www.frontiersin.org/articles/10.3389/fendo.2023.1164186/full#supplementary-material

References

1. Escobar-Morreale HF. Polycystic ovary syndrome: definition, aetiology, diagnosis and treatment. *Nat Rev Endocrinol* (2018) 14(5):270–84. doi: 10.1038/nrendo.2018.24

2. Yin W, Falconer H, Yin L, Xu L, Ye W. Association between polycystic ovary syndrome and cancer risk. *JAMA Oncol* (2019) 5(1):106–7. doi: 10.1001/jamaoncol.2018.5188

3. Thong EP, Codner E, Laven JSE, Teede H. Diabetes: a metabolic and reproductive disorder in women. *Lancet Diabetes Endocrinol* (2020) 8(2):134–49. doi: 10.1016/S2213-8587(19)30345-6

4. Mascarenhas MN, Flaxman SR, Boerma T, Vanderpoel S, Stevens GA. National, regional, and global trends in infertility prevalence since 1990: a systematic analysis of 277 health surveys. *PLoS Med* (2012) 9(12):e1001356. doi: 10.1371/journal.pmed.1001356

5. Horne AW, Missmer SA. Pathophysiology, diagnosis, and management of endometriosis. *BMJ* (2022) 379:e070750. doi: 10.1136/bmj-2022-070750

6. Baker JM, Al-Nakkash L, Herbst-Kralovetz MM. Estrogen-gut microbiome axis: physiological and clinical implications. *Maturitas* (2017) 103:45–53. doi: 10.1016/j.maturitas.2017.06.025

7. Chadchan SB, Singh V, Kommagani R. Female reproductive dysfunctions and the gut microbiota. *J Mol Endocrinol* (2022) 69(3):R81–94. doi: 10.1530/JME-21-0238

8. Qi X, Yun C, Pang Y, Qiao J. The impact of the gut microbiota on the reproductive and metabolic endocrine system. *Gut Microbes* (2021) 13(1):1–21. doi: 10.1080/19490976.2021.1894070

9. Yang YY, Pereyra LP, Young RB, Reardon KF, Borch T. Testosterone-mineralizing culture enriched from swine manure: characterization of degradation pathways and microbial community composition. *Environ Sci Technol* (2011) 45 (16):6879–86. doi: 10.1021/es2013648

10. Ridlon JM, Ikegawa S, Alves JM, Zhou B, Kobayashi A, Iida T, et al. Clostridium scindens: a human gut microbe with a high potential to convert glucocorticoids into androgens. *J Lipid Res* (2013) 54(9):2437–49. doi: 10.1194/jlr.M038869

11. Qi X, Yun C, Sun L, Xia J, Wu Q, Wang X, et al. Gut microbiota-bile acid-interleukin-22 axis orchestrates polycystic ovary syndrome. *Nat Med* (2019) 25 (8):1225–33. doi: 10.1038/s41591-019-0509-0

12. Snider AP, Wood JR. Obesity induces ovarian inflammation and reduces oocyte quality. *Reproduction* (2019) 158(3):R79–r90. doi: 10.1530/REP-18-0583

13. Vander Borght M, Wyns C. Fertility and infertility: definition and epidemiology. *Clin Biochem* (2018) 62:2–10. doi: 10.1016/j.clinbiochem.2018.03.012

14. Lundy SD, Sangwan N, Parekh NV, Selvam MK, Gupta S, McCaffrey P, et al. Functional and taxonomic dysbiosis of the gut, urine, and semen microbiomes in Male infertility. *Eur Urol* (2021) 79(6):826–36. doi: 10.1016/j.eururo.2021.01.014

15. Azpiroz MA, Orguilia L, Palacio MI, Malpartida A, Mayol S, Mor G, et al. Potential biomarkers of infertility associated with microbiome imbalances. *Am J Reprod Immunol* (2021) 86(4):e13438. doi: 10.1111/aji.13438

16. Simopoulou M, Sfakianoudis K, Maziotis E, Grigoriadis S, Giannelou P, Rapani A, et al. The impact of autoantibodies on IVF treatment and outcome: a systematic review. *Int J Mol Sci* (2019) 20(4):892. doi: 10.3390/ijms20040892

17. Jiang I, Yong PJ, Allaire C, Bedaiwy MA. Intricate connections between the microbiota and endometriosis. *Int J Mol Sci* (2021) 22(11):5644. doi: 10.3390/ijms22115644

18. Ustianowska K, Ustianowski Ł, Machaj F, Gorący A, Rosik J, Szostak B, et al. The role of the human microbiome in the pathogenesis of pain. *Int J Mol Sci* (2022) 23 (21):13267. doi: 10.3390/ijms232113267

19. Kurilshikov A, Medina-Gomez C, Bacigalupe R, Radjabzadeh D, Wang J, Demirkan A, et al. Large-Scale association analyses identify host factors influencing human gut microbiome composition. *Nat Genet* (2021) 53(2):156–65. doi: 10.1038/s41588-020-00763-1

20. Day F, Karaderi T, Jones MR, Meun C, He C, Drong A, et al. Large-Scale genome-wide meta-analysis of polycystic ovary syndrome suggests shared genetic architecture for different diagnosis criteria. *PLoS Genet* (2018) 14(12):e1007813. doi: 10.1371/journal.pgen.1007813

21. Kurki MI, Karjalainen J, Palta P, Sipilä T, Kristiansson K, Donner K, et al. FinnGen: unique genetic insights from combining isolated population and national health register data. *medRxiv* (2022) 2022:2003. doi: 10.1101/2022.03.03.22271360

22. Elsworth B, Lyon M, Alexander T, Liu Y, Matthews P, Hallett J, et al. The MRC IEU OpenGWAS data infrastructure. *bioRxiv* (2020) 2020:2008. doi: 10.1101/2020.08.10.244293

23. Shim H, Chasman DI, Smith JD, Smith J, Mora S, Ridker PM, et al. A multivariate genome-wide association analysis of 10 LDL subfractions, and their response to statin treatment, in 1868 caucasians. *PLoS One* (2015) 10(4):e0120758. doi: 10.1371/journal.pone.0120758

24. Burgess S, Thompson SG. Avoiding bias from weak instruments in mendelian randomization studies. *Int J Epidemiol* (2011) 40(3):755–64. doi: 10.1093/ije/dyr036

25. Burgess S, Butterworth A, Thompson SG. Mendelian randomization analysis with multiple genetic variants using summarized data. *Genet Epidemiol* (2013) 37 (7):658–65. doi: 10.1002/gepi.21758

26. Burgess S, Thompson SG. Interpreting findings from mendelian randomization using the MR-egger method. *Eur J Epidemiol* (2017) 32(5):377–89. doi: 10.1007/s10654-017-0255-x

27. Bowden J, Davey Smith G, Burgess S. Mendelian randomization with invalid instruments: effect estimation and bias detection through egger regression. *Int J Epidemiol* (2015) 44(2):512–25. doi: 10.1093/ije/dyv080

28. Bowden J, Davey Smith G, Haycock PC, Burgess S. Consistent estimation in mendelian randomization with some invalid instruments using a weighted median estimator. *Genet Epidemiol* (2016) 40(4):304–14. doi: 10.1002/gepi.21965

29. Hartwig FP, Davey Smith G, Bowden J. Robust inference in summary data mendelian randomization *via* the zero modal pleiotropy assumption. *Int J Epidemiol* (2017) 46(6):1985–98. doi: 10.1093/ije/dyx102

30. Greco MF, Minelli C, Sheehan NA, Thompson JR. Detecting pleiotropy in mendelian randomisation studies with summary data and a continuous outcome. *Stat Med* (2015) 34(21):2926–40. doi: 10.1002/sim.6522

31. Verbanck M, Chen CY, Neale B, Do R. Detection of widespread horizontal pleiotropy in causal relationships inferred from mendelian randomization between complex traits and diseases. *Nat Genet* (2018) 50(5):693–8. doi: 10.1038/s41588-018-0099-7

32. Eyupoglu ND, Ergunay K, Acikgoz A, Akyon Y, Yilmaz E, Yildiz BO. Gut microbiota and oral contraceptive use in overweight and obese patients with polycystic ovary syndrome. *J Clin Endocrinol Metab* (2020) 105(12):dgaa600. doi: 10.1210/clinem/dgaa600

33. Liu R, Zhang C, Shi Y, Zhang F, Li L, Wang X, et al. Dysbiosis of gut microbiota associated with clinical parameters in polycystic ovary syndrome. *Front Microbiol* (2017) 8:324. doi: 10.3389/fmicb.2017.00324

34. Qin S, He Z, Wu Y, Zheng Z, Zhang H, Lv C, et al. Instant dark tea alleviates hyperlipidaemia in high-fat diet-fed rat: from molecular evidence to redox balance and beyond. *Front Nutr* (2022) 9:819980. doi: 10.3389/fnut.2022.819980

35. Artimani T, Karimi J, Mehdizadeh M, Yavangi M, Khanlarzadeh E, Ghorbani M, et al. Evaluation of pro-oxidant-antioxidant balance (PAB) and its association with inflammatory cytokines in polycystic ovary syndrome (PCOS). *Gynecol Endocrinol* (2018) 34(2):148–52. doi: 10.1080/09513590.2017.1371691

36. González F. Inflammation in polycystic ovary syndrome: underpinning of insulin resistance and ovarian dysfunction. *Steroids* (2012) 77(4):300–5. doi: 10.1016/j.steroids.2011.12.003

37. Paoli A, Mancin L, Giacona MC, Bianco A, Caprio M. Effects of a ketogenic diet in overweight women with polycystic ovary syndrome. *J Transl Med* (2020) 18(1):104. doi: 10.1186/s12967-020-02277-0

38. Li C, Xing C, Zhang J, Zhao H, Shi W, He B. Eight-hour time-restricted feeding improves endocrine and metabolic profiles in women with anovulatory polycystic ovary syndrome. *J Transl Med* (2021) 19(1):148. doi: 10.1186/s12967-021-02817-2

39. Langley G, Hao Y, Pondo T, Miller L, Petit S, Thomas A, et al. The impact of obesity and diabetes on the risk of disease and death due to invasive group a streptococcus infections in adults. *Clin Infect Dis* (2016) 62(7):845–52. doi: 10.1093/cid/civ1032

40. Pinart M, Dötsch A, Schlicht K, Laudes M, Bouwman J, Forslund S, et al. Gut microbiome composition in obese and non-obese persons: a systematic review and meta-analysis. *Nutrients* (2021) 14(1):12. doi: 10.3390/nu14010012

41. Gallè F, Valeriani F, Cattaruzza MS, Gianfranceschi G, Liguori R, Antinozzi M, et al. Mediterranean Diet, physical activity and gut microbiome composition: a cross-sectional study among healthy young Italian adults. *Nutrients* (2020) 12(7):2164. doi: 10.3390/nu12072164

42. Wang T, Sha L, Li Y, Zhu L, Wang Z, Li K, et al. Dietary α-linolenic acid-rich flaxseed oil exerts beneficial effects on polycystic ovary syndrome through sex steroid hormones-Microbiota-Inflammation axis in rats. *Front Endocrinol (Lausanne)* (2020) 11:284. doi: 10.3389/fendo.2020.00284

43. Ma M, Su J, Wang Y, Wang L, Li Y, Ding G, et al. Association of body mass index and intestinal (faecal) streptococcus in adults in xining city, China P.R. *Benef Microbes* (2022) 13(6):465–71. doi: 10.3920/BM2021.0046

44. Zhao F, Dong T, Yuan KY, Wang NJ, Xia FZ, Liu D, et al. Shifts in the bacterial community of supragingival plaque associated with metabolic-associated fatty liver disease. *Front Cell Infect Microbiol* (2020) 10:581888. doi: 10.3389/fcimb.2020.581888

45. Naderpoor N, Mousa A, Gomez-Arango LF, Barrett HL, Dekker Nitert M, de Courten B. Faecal microbiota are related to insulin sensitivity and secretion in overweight or obese adults. *J Clin Med* (2019) 8(4):452. doi: 10.3390/jcm8040452

46. Jones RB, Alderete TL, Kim JS, Millstein J, Gilliland FD, Goran MI. High intake of dietary fructose in overweight/obese teenagers associated with depletion of eubacterium and streptococcus in gut microbiome. *Gut Microbes* (2019) 10(6):712–9. doi: 10.1080/19490976.2019.1592420

47. Liu S, Cao R, Liu L, Lv Y, Qi X, Yuan Z, et al. Correlation between gut microbiota and testosterone in Male patients with type 2 diabetes mellitus. *Front Endocrinol (Lausanne)* (2022) 13:836485. doi: 10.3389/fendo.2022.836485

48. Gonçalves P, Araújo JR, Di Santo JP. A cross-talk between microbiota-derived short-chain fatty acids and the host mucosal immune system regulates intestinal homeostasis and inflammatory bowel disease. *Inflammatory Bowel Diseases* (2018) 24(3):558–72. doi: 10.1093/ibd/izx029

49. Pingitore A, Chambers ES, Hill T, Maldonado I, Liu B, Bewick G, et al. The diet-derived short chain fatty acid propionate improves beta-cell function in humans and stimulates insulin secretion from human islets in vitro. *Diabetes Obes Metab* (2017) 19 (2):257–65. doi: 10.1111/dom.12811

50. He J, Zhang P, Shen L, Niu L, Tan Y, Chen L, et al. Short-chain fatty acids and their association with signalling pathways in inflammation, glucose and lipid metabolism. *Int J Mol Sci* (2020) 21(17):6356. doi: 10.3390/ijms21176356

51. Hernández MAG, Canfora EE, Jocken JWE, Blaak EE. The short-chain fatty acid acetate in body weight control and insulin sensitivity. *Nutrients* (2019) 11(8):1943. doi: 10.3390/nu11081943

52. Olaniyi KS, Bashir AM, Areloegbe SE, Sabinari I, Akintayo C, Oniyide A, et al. Short chain fatty acid, acetate restores ovarian function in experimentally induced PCOS rat model. *PLoS One* (2022) 17(7):e0272124. doi: 10.1371/journal.pone.0272124

53. Wang Y, Dilidaxi D, Wu Y, Sailike J, Sun X, Nabi XH. Composite probiotics alleviate type 2 diabetes by regulating intestinal microbiota and inducing GLP-1 secretion in db/db mice. *BioMed Pharmacother* (2020) 125:109914. doi: 10.1016/j.biopha.2020.109914

54. Parascinet O, Mas S, Hang T, Llavero C, Lorenzo Ó. Ruiz-Tovar J. A pilot study: the reduction in fecal acetate in obese patients after probiotic administration and

percutaneous electrical neurostimulation. *Nutrients* (2023) 15(5):1067. doi: 10.3390/nu15051067

55. Canfora EE, van der Beek CM, Jocken JWE, Goossens GH, Holst JJ, Damink SW, et al. Colonic infusions of short-chain fatty acid mixtures promote energy metabolism in overweight/obese men: a randomized crossover trial. *Sci Rep* (2017) 7 (1):2360. doi: 10.1038/s41598-017-02546-x

56. Zhang J, Sun Z, Jiang S, Bai X, Ma C, Peng Q, et al. Probiotic bifidobacterium lactis V9 regulates the secretion of sex hormones in polycystic ovary syndrome patients through the gut-brain axis. *mSystems* (2019) 4(2):e00017-19. doi: 10.1128/mSystems.00017-19

57. Kong C, Gao R, Yan X, Huang L, He J, Li H, et al. Alterations in intestinal microbiota of colorectal cancer patients receiving radical surgery combined with adjuvant CapeOx therapy. *Sci China Life Sci* (2019) 62(9):1178–93. doi: 10.1007/s11427-018-9456-x

58. Liu Y, Li J, Jin Y, Zhao L, Zhao F, Feng J, et al. Splenectomy leads to amelioration of altered gut microbiota and metabolome in liver cirrhosis patients. *Front Microbiol* (2018) 9:963. doi: 10.3389/fmicb.2018.00963

59. Guo WL, Chen M, Pan WL, Zhang Q, Xu J, Lin Y, et al. Hypoglycemic and hypolipidemic mechanism of organic chromium derived from chelation of grifola frondosa polysaccharide-chromium (III) and its modulation of intestinal microflora in high fat-diet and STZ-induced diabetic mice. *Int J Biol Macromol* (2020) 145:1208–18. doi: 10.1016/j.ijbiomac.2019.09.206

60. Zhou L, Ni Z, Yu J, Cheng W, Cai Z, Yu C. Correlation between fecal metabolomics and gut microbiota in obesity and polycystic ovary syndrome. *Front Endocrinol (Lausanne)* (2020) 11:628. doi: 10.3389/fendo.2020.00628

61. Zhou L, Ni Z, Cheng W, Yu J, Sun S, Zha D, et al. Characteristic gut microbiota and predicted metabolic functions in women with PCOS. *Endocr Connect* (2020) 9 (1):63–73. doi: 10.1530/EC-19-0522

62. Lozano CP, Wilkens LR, Shvetsov YB, Maskarinec G, Park SY, Shepherd JA, et al. Associations of the dietary inflammatory index with total adiposity and ectopic fat through the gut microbiota, LPS, and c-reactive protein in the multiethnic cohort-adiposity phenotype study. *Am J Clin Nutr* (2022) 115(5):1344–56. doi: 10.1093/ajcn/nqab398

63. Dull AM, Moga MA, Dimienescu OG, Sechel G, Burtea V, Anastasiu CV. Therapeutic approaches of resveratrol on endometriosis *via* anti-inflammatory and anti-angiogenic pathways. *Molecules* (2019) 24(4):667. doi: 10.3390/molecules24040667

64. Rostamtabar M, Esmaeilzadeh S, Tourani M, Rahmani A, Baee M, Shirafkan F, et al. Pathophysiological roles of chronic low-grade inflammation mediators in polycystic ovary syndrome. *J Cell Physiol* (2021) 236(2):824–38. doi: 10.1002/jcp.29912

65. Fabozzi G, Verdone G, Allori M, Cimadomo D, Tatone C, Stuppia L, et al. Personalized nutrition in the management of female infertility: new insights on chronic low-grade inflammation. *Nutrients* (2022) 14(9):1918. doi: 10.3390/nu14091918

66. Liang YY, Liu LY, Jia Y, Li Y, Cai JN, Shu Y, et al. Correlation between gut microbiota and glucagon-like peptide-1 in patients with gestational diabetes mellitus. *World J Diabetes* (2022) 13(10):861–76. doi: 10.4239/wjd.v13.i10.861

67. Mintziori G, Nigdelis MP, Mathew H, Mousiolis A, Goulis DG, Mantzoros CS. The effect of excess body fat on female and male reproduction. *Metabolism* (2020) 107:154193. doi: 10.1016/j.metabol.2020.154193

68. Boutari C, Pappas PD, Mintziori G, Nigdelis MP, Athanasiadis L, Goulis DG, et al. The effect of underweight on female and male reproduction. *Metabolism* (2020) 107:154229. doi: 10.1016/j.metabol.2020.154229

69. Arendt LH, Høyer BB, Kreilgaard AF, Bech BH, Toft G, Hougaard KS, et al. Maternal pre-pregnancy overweight and infertility in sons and daughters: a cohort study. *Acta Obstet Gynecol Scand* (2021) 100(5):843–9. doi: 10.1111/aogs.14045

70. Tang S, Huang J, Lin J, Kuang Y. Adverse effects of pre-pregnancy maternal underweight on pregnancy and perinatal outcomes in a freeze-all policy. *BMC Pregnancy Childbirth* (2021) 21(1):32. doi: 10.1186/s12884-020-03509-3

71. Wen S, Yuan G, Li C, Xiong Y, Zhong X, Li X. High cellulose dietary intake relieves asthma inflammation through the intestinal microbiome in a mouse model. *PloS One* (2022) 17(3):e0263762. doi: 10.1371/journal.pone.0263762

72. Gao Y, Liu L, Li C, Liang Y, Lv J, Yang L, et al. Study on the antipyretic and anti-inflammatory mechanism of shuanghuanglian oral liquid based on gut microbiota-host metabolism. *Front Pharmacol* (2022) 13:843877. doi: 10.3389/fphar.2022.843877

73. Mocanu V, Rajaruban S, Dang J, Kung JY, Deehan EC, Madsen KL. Repeated fecal microbial transplantations and antibiotic pre-treatment are linked to improved clinical response and remission in inflammatory bowel disease: a systematic review and pooled proportion meta-analysis. *J Clin Med* (2021) 10(5):959. doi: 10.3390/jcm10050959

74. Chen Q, Yin Q, Xie Q, Jiang C, Zhou L, Liu J, et al. 2'-fucosyllactose promotes the production of short-chain fatty acids and improves immune function in human-Microbiota-Associated mice by regulating gut microbiota. *J Agric Food Chem* (2022) 70 (42):13615–25. doi: 10.1021/acs.jafc.2c04410

75. Antsiferova YS, Sotnikova NY, Posiseeva LV, Shor AL. Changes in the T-helper cytokine profile and in lymphocyte activation at the systemic and local levels in women with endometriosis. *Fertility Sterility* (2005) 84(6):1705–11. doi: 10.1016/j.fertnstert.2005.05.066

76. Podgaec S, Abrao MS, Dias JAJr., Rizzo LV, de Oliveira RM, Baracat EC. Endometriosis: an inflammatory disease with a Th2 immune response component. *Hum Reproduction* (2007) 22(5):1373–9. doi: 10.1093/humrep/del516

77. Zhou WJ, Yang HL, Shao J, Mei J, Chang K, Zhu R, et al. Anti-inflammatory cytokines in endometriosis. *Cell Mol Life Sci* (2019) 76(11):2111–32. doi: 10.1007/s00018-019-03056-x

78. Suen J-L, Chang Y, Chiu P-R, Hsieh T-H, Hsi E, Chen Y-C, et al. Serum level of IL-10 is increased in patients with endometriosis, and IL-10 promotes the growth of lesions in a murine model. *Am J Pathol* (2014) 184(2):464–71. doi: 10.1016/j.ajpath.2013.10.023

79. Suen JL, Chang Y, Shiu YS, Hsu C-Y, Sharma P, Chiu C-C, et al. IL-10 from plasmacytoid dendritic cells promotes angiogenesis in the early stage of endometriosis. *J Pathol* (2019) 249(4):485–97. doi: 10.1002/path.5339

80. Chuffa LG, Seiva FR, Fávaro WJ, Teixeira GR, Amorim JP, Mendes LO, et al. Melatonin reduces 17 LH. beta-estradiol and induces differential regulation of sex steroid receptors in reproductive tissues during rat ovulation. *Reprod Biol Endocrinol* (2011) 9:108. doi: 10.1186/1477-7827-9-108

81. Zhao L, Gu C, Huang K, Fan W, Li L, Ye M, et al. Association between oestrogen receptor alpha (ESR1) gene polymorphisms and endometriosis: a meta-analysis of 24 case-control studies. *Reprod BioMed Online* (2016) 33(3):335–49. doi: 10.1016/j.rbmo.2016.06.003

82. Tong X, Li Z, Wu Y, Fu X, Zhang Y, Fan H. COMT 158G/A and CYP1B1 432C/G polymorphisms increase the risk of endometriosis and adenomyosis: a meta-analysis. *Eur J Obstet Gynecol Reprod Biol* (2014) 179:17–21. doi: 10.1016/j.ejogrb.2014.04.039

83. Yu Z, Tian X, Peng Y, Sun Z, Wang C, Tang N, et al. Mitochondrial cytochrome P450 (CYP) 1B1 is responsible for melatonin-induced apoptosis in neural cancer cells. *J Pineal Res* (2018) 65(1):e12478. doi: 10.1111/jpi.12478

84. Guadagnini D, Rocha GZ, Santos A, Assalin H, Hirabara SM, Curi R, et al. Microbiota determines insulin sensitivity in TLR2-KO mice. *Life Sci* (2019) 234:116793. doi: 10.1016/j.lfs.2019.116793

85. Chen YR, Zheng HM, Zhang GX, Chen FL, Chen LD, Yang ZC. High oscillospira abundance indicates constipation and low BMI in the guangdong gut microbiome project. *Sci Rep* (2020) 10(1):9364. doi: 10.1038/s41598-020-66369-z

86. Jo JK, Seo SH, Park SE, Kim HW, Kim EJ, Kim ZS, et al. Gut microbiome and metabolome profiles associated with high-fat diet in mice. *Metabolites* (2021) 11(8):482. doi: 10.3390/metabo11080482

87. Liu L, Fu Q, Li T, Shao K, Zhu X, Cong Y, et al. Gut microbiota and butyrate contribute to nonalcoholic fatty liver disease in premenopause due to estrogen deficiency. *PloS One* (2022) 17(2):e0262855. doi: 10.1371/journal.pone.0262855

88. Zhang YW, Cao MM, Li YJ, Lu PP, Dai GC, Zhang M, et al. Fecal microbiota transplantation ameliorates bone loss in mice with ovariectomy-induced osteoporosis *via* modulating gut microbiota and metabolic function. *J Orthop Translat* (2022) 37:46–60. doi: 10.1016/j.jot.2022.08.003

89. Valido E, Bertolo A, Fränkl GP, Itodo O, Pinheiro T, Pannek J, et al. Systematic review of the changes in the microbiome following spinal cord injury: animal and human evidence. *Spinal Cord* (2022) 60(4):288–300. doi: 10.1038/s41393-021-00737-y

90. Li XQ, Chen Y, Dai GC, Zhou BB, Yan XN, Tan RX. Abietic acid ameliorates psoriasis-like inflammation and modulates gut microbiota in mice. *J Ethnopharmacol* (2021) 272:113934. doi: 10.1016/j.jep.2021.113934

91. Kong C, Gao R, Yan X, Huang L, Qin H. Probiotics improve gut microbiota dysbiosis in obese mice fed a high-fat or high-sucrose diet. *Nutrition* (2019) 60:175–84. doi: 10.1016/j.nut.2018.10.002

92. Everard A, Lazaveric V, Derrien M, Girard M, Muccioli GG, Neyrinck AM, et al. Responses of gut microbiota and glucose and lipid metabolism to prebiotics in genetic obese and diet-induced leptin-resistant mice. *Diabetes* (2011) 60(11):2775–2786. doi: 10.2337/db11-0227

frontiers | Frontiers in Endocrinology

TYPE Original Research
PUBLISHED 11 August 2023
DOI 10.3389/fendo.2023.1244507

OPEN ACCESS

EDITED BY
Shunfeng Cheng,
Qingdao Agricultural University, China

REVIEWED BY
Mohd Faizal Ahmad,
National University of Malaysia, Malaysia
Marziyeh Tavalaee,
Royan Institute, Iran

*CORRESPONDENCE
Zhi Qin Chen
ptchen1@51mch.com
Xiao Ming Teng
tengxiaoming@hotmail.com

RECEIVED 22 June 2023
ACCEPTED 27 July 2023
PUBLISHED 11 August 2023

CITATION
Ruan JL, Liang SS, Pan JP, Chen ZQ and Teng XM (2023) Artificial oocyte activation with Ca^{2+} ionophore improves reproductive outcomes in patients with fertilization failure and poor embryo development in previous ICSI cycles. *Front. Endocrinol.* 14:1244507. doi: 10.3389/fendo.2023.1244507

Artificial oocyte activation with Ca^{2+} ionophore improves reproductive outcomes in patients with fertilization failure and poor embryo development in previous ICSI cycles

Jing Ling Ruan[1,2], Shan Shan Liang[1,2], Jia Ping Pan[1,2], Zhi Qin Chen[1*] and Xiao Ming Teng[1*]

[1]Reproductive Medicine Center of Shanghai First Maternity and Infant Hospital, School of Life Sciences and Technology, Tongji University, Shanghai, China, [2]Shanghai Institute of Maternal-Fetal Medicine and Gynecologic Oncology, Shanghai First Maternity and Infant Hospital, School of Medicine, Tongji University, Shanghai, China

Research question: Does artificial oocyte activation (AOA) by a calcium ionophore (ionomycin) improve the previous fertilization failure or poor embryo development of intracytoplasmic sperm injection (ICSI) account for male factor infertility or other infertility causes?

Design: This retrospective study involved 114 patients receiving ICSI-AOA in Shanghai First Maternity and Infant Hospital with previous ICSI fertilization failure or poor embryo development. The previous ICSI cycles of the same patients without AOA served as the control group. The fertilization rates, cleavage rates, transferable embryo rates and blastocyst formation rates of the two groups were compared. Additionally, the clinical pregnancy, implantation rate and live birth rates were also compared to assess the efficiency and safety of AOA. Furthermore, two subgroup analyses were performed in this study based on the cause of infertility and the reason for AOA. The fertilization rate, embryonic development potential and clinical outcome were compared among groups.

Results: Among 114 ICSI-AOA cycles, the fertilization rate, top-quality embryo rate, implantation rate, clinical pregnancy per patient and live birth rate per patient were improved significantly compared with previous ICSI cycles ($p<0.05$ to $P< 0.001$), and the miscarriage rate in the AOA group was significantly lower than that of the control group ($p<0.001$). In the AOA subgroups based on the cause of infertility, the fertilization rates of each subgroup were significantly improved compared with previous control cycles except for the mixed factor infertility subgroup ($p<0.05$ to $p<0.001$). In the AOA subgroups based on the reason for AOA, the fertilization rates of each subgroup were significantly increased compared with those in their previous ICSI cycle without AOA ($p<0.001$); however, there was no significant difference in the top-quality embryo rate. No significant improvement was found in the implantation rates and the clinical pregnancy rate in each subgroup except for the poor embryo

development subgroup. In the 114 AOA cycles, 35 healthy infants (21 singletons and 7 twins) were delivered without major congenital birth defects or malformations.

Conclusion: This study showed that AOA with the calcium ionophore ionomycin can improve the reproductive outcomes of patients with previous fertilization failure and poor embryo development after ICSI.

KEYWORDS

artificial oocyte activation, ionomycin, intracytoplasmic sperm injection, fertilization failure, embryo development

Introduction

Intracytoplasmic sperm injection (ICSI) is mainly used for male factor infertility. The average fertilization rate after ICSI is approximately 70% to 80% (1). However, 1%~5% of ICSI cycles occurring still result in total fertilization failure (TFF) or almost complete fertilization failure, defined as a fertilization rate of less than 30% (2). Oocyte activation deficiency (OAD) is the main cause of ICSI fertilization failure, which may be related to sperm or oocyte factors leading to responsiveness of gamete interaction (3, 4).

In the past decade, an increasing number of studies have shown that sperm-specific phospholipase Cζ (phospholipase C zeta, PLCζ) is strongly associated with sperm-specific oocyte activation failure (OAF) (5). The low expression of PLCζ is one of the main reasons for fertilization failure (6–8). ICSI combined with artificial oocyte activation could mimic physiological calcium changes that occur during fertilization (9). During normal fertilization, sperm-specific PLCζ is released into the oocyte cytoplasm, triggering calcium shock and promoting the release of Ca^{2+} in the endoplasmic reticulum. The temporary increase of Ca^{2+} concentration in oocytes generates Ca^{2+} oscillations to activate oocytes and induces a cortical granular response. Oocytes recover and complete meiosis, extrude the second polar body and form two pronuclei (8). The endoplasmic reticulum is the main source of intracellular Ca^{2+} increase, which is mainly triggered by the successful induction of IP3 pathway by sperm-specific phospholipase C-ζ (PLC-ζ) around the sperm nucleus. The failure of oocyte activation leading to non-fertilization may be mainly caused by the failure of PLC-induced IP3 pathway (10). However, the molecular mechanism of OAD induced by oocyte-borne oocyte activation factors is unclear. According to previous reports, human oocytes with ICSI-TFF often carry with specific problems, such as abnormal cell structure, abnormal gene expression, abnormal chromosomes, immature oocytes and abnormal spindles (11). All of these problems may cause oocyte activation failure after ICSI.

AOA is the most commonly used technology to solve sperm-related OAF at present, and healthy live births have been delivered after using various activation methods. Abnormalities in the oocyte activating signal pathway may lead to the occurrence of OAF (12). To date, AOA is the most effective method to solve ICSI-TFF, low fertilization and OAF caused by sperm factors (13). However, large-scale clinical studies are still lacking, and there are also disputes regarding the efficiency of AOA and the safety of offspring. Therefore, this study analysed the clinical pregnancy outcomes and neonatal health of AOA patients who received the Ca^{2+} ionophore ionomycin during ICSI and evaluated the efficacy and safety of ionomycin on the fertilization rate and embryo development.

Materials and methods

Patients

This retrospective analysis was performed on the clinical data of couples receiving ICSI-AOA due to poor fertilization or poor embryo development after a previous ICSI cycle from January 2019 to December 2020 in Shanghai First Maternity and Infant Hospital affiliated with Tongji University. The indications for ICSI-AOA are as follows: previous ICSI fertilization failure (TFF or fertilization rate ≤ 30%) and poor embryo development (complete embryo development arrest, reduced blastocyst formation on day 5 (≤15%)). Controlled ovarian stimulation and oocyte retrieval were carried out according to standard protocols (14). A total of 114 couples were enrolled in this retrospective analysis (Figure 1). Most patients started ICSI with ovarian stimulation using either the long agonist or antagonist protocols. Ovulation was triggered by intradermal injection of 5000~10,000 IU HCG. Patients with AOA cycles in the previous cycle and half-AOA cycles were excluded from this study. The previous cycles without AOA were considered as a control group. The interval between the two stimulation cycles was no more than six months.

In addition, two subgroup analyses were performed in this study. According to the cause of infertility, patients were further divided into six subgroups: (i) oligoasthenoteratozoospermia (OAT), including oligozoospermia (low number of sperm), asthenozoospermia (poor sperm movement), and teratozoospermia (abnormal sperm shape); (ii) advanced age (age>35 years); (iii) primary ovarian insufficiency (POI, patients with primary ovarian insufficiency); (iv) unexplained

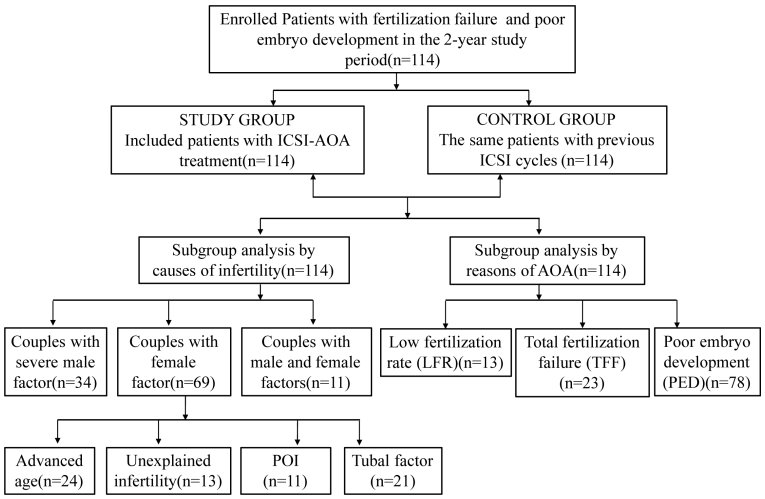

FIGURE 1
Flowchart of patients. ICSI, intracytoplasmic sperm injection; AOA, artificial oocyte activation; POI, patients with primary ovarian insufficiency.

infertility; (v) tubal factor; and (vi) mixed factor infertility (M+F). Based on the reason for AOA, patients were divided into three subgroups for analysis: total fertilization failure (TFF); low fertilization rate (LFR, fertilization rate <30%); and poor embryo development (PED). Similarly, the oocyte activation cycle was compared with the previous ICSI cycle of the same patients. The fertilization rate, embryonic development potential and clinical outcome were compared among groups.

This study was approved by the institutional review board of Shanghai First Maternity and Infant Hospital affiliated with Tongji University. All the enrolled patients in this study signed written informed consent and were informed of the potential risks of using AOA technology.

ICSI and calcium ionophore AOA procedure

The oocytes collected from each cycle were cultured at 37°C in a humidified triple-gas incubator with 6% CO_2 and 5% oxygen (Thermo Fisher Scientific, USA) for at least 2 h before removing cumulus cells. Subsequently, all metaphase II oocytes were treated according to the standard ICSI procedure (15). Oocyte activation with ionomycin was performed according to previous reports (16, 17). Briefly, thirty minutes after ICSI, the oocytes were immediately exposed to activated liquid droplets (G-mops, Vitrolife, Sweden) containing 10 μmol/l ionomycin (Sigma Aldrich, USA) for 10 minutes, rinsed with medium (G-mops, Vitrolife, Sweden) 3 times, and transferred to embryo culture medium (G1, Vitrolife, Sweden).

Fertilization check, embryo grading and embryo transfer

Fertilization observations were carried out 18-19 h after ICSI under an inverted microscope. Only oocytes with two clear pronuclei (2PN) and two polar bodies (2PB) were considered to be fertilized normally. Quality assessment of embryos was carried out according to routine guidelines described previously (18). Embryos were cultured *in vitro* to the third day (D3), and only embryos with 7-9 cells from normal fertilized oocytes and a fragment ratio <10% were defined as top-quality embryos. Then, top-quality embryos were transferred under transvaginal ultrasound guidance. The remaining top-quality embryos were cryopreserved for the next cycle. Additionally, all the remaining cleavage-stage embryos were cultured up to the blastocyst stage, the blastocysts were scored morphologically according to the Gardner scale (2), and the available blastocysts were cryopreserved for later transfer. According to provincial guidelines, up to two embryos can be transferred in any transfer cycle.

Study outcome assessment and clinical pregnancy

The following parameters were used to compare previous routine ICSI cycles with ICSI-AOA cycles of the same patient. The primary outcome measure was the 2PN fertilization rate, defined as the number of normal fertilized oocytes divided by the number of injected MII oocytes. Secondary outcome measures included the cleavage rate (number of cleaved zygotes/number of fertilized oocytes), top-quality embryo rate (number of high-quality embryos/number of cleaved zygotes), blastocyst formation rate (number of blastocysts formed/number of blastocysts cultured), and implantation rate (number of gestational sacs seen on scanning divided by the number of embryos replaced). Clinical pregnancy was defined as the presence of at least one gestational sac on ultrasound at 6 weeks. A baby born alive after 20 gestation weeks was classified as a live birth. The miscarriage rate was defined as the number of miscarriages before 20 weeks divided by the number of women with a positive pregnancy test. Additionally, information on the patient's pregnancy outcomes was followed up until March 2021 by telephone survey, including gestation weeks, gender of babies,

birth weight and body length, as well as major birth defects. There were still 40 and 103 frozen embryos remaining in the previous ICSI cycles and the AOA cycles, respectively, by the end of the study.

Statistical analysis

The one-sample Kolmogorov–Smirnov test was used to test the normal distribution of continuous variables. Continuous variables were given as the mean ± SD if normally distributed. Comparisons between groups were performed with paired t tests for continuous variables and chi-square tests for categorical variables, where appropriate. Statistical analysis was performed using the Statistical Program for Social Sciences (SPSS Inc., Version 14.0, Chicago, IL, USA). A two-tailed value of $P < 0.05$ was considered statistically significant.

Results

Patients' baseline clinical characteristics

Between January 2019 and December 2020, 114 patients who underwent ICSI-AOA were enrolled in this study with a history of poor fertilization or embryo development in the first ICSI cycles. The flow chart of the subjects is shown in Figure 1.

The average age of the women was 33.86 ± 4.981 years, and they had suffered infertility for 4.09 ± 2.991 years before ART treatment (Table 1). The other baseline characteristics of the patients are shown in Table 1, including infertility types, infertility years, infertility factors, female body mass index (BMI), antral follicle counts (AFC), and basal FSH. All couples received routine ICSI and AOA (Table 1). The stimulation protocol used in each group was similar between the two groups (P >0.05) (Table 2).

TABLE 1 General characteristics of the enrolled patients (mean ± SD).

Item	Value
No. of patients	114
Female age (y), mean ± SD	33.86 ± 4.981
Male age (y), mean ± SD	35.71 ± 5.799
Type of infertility, n (%)	
Primary infertility	72 (63.16%)
Secondary infertility	42 (36.84%)
Duration of infertility (y)	4.09 ± 2.991
Indication, n (%)	
Female factors	68(59.65%)
Male factors	35(30.70%)
Mixed	11(9.65%)
BMI for women (kg/m^2)	22.29 ± 3.291
AFC	9.99 ± 7.378
Basal FSH(IU/L)	7.24 ± 3.923

Values are shown as the mean ± SD or number. BMI, female body mass index; AFC, antral follicle count.

Embryological characteristics in previous standard ICSI cycles and AOA cycles

The stimulation protocols adopted in both groups were comparable. No significant differences were found in the number of oocytes obtained between the two groups. However, the numbers of oocytes fertilized, cleavage embryos, top-quality embryos, transferred embryos and frozen embryos were significantly higher in the AOA group than in the control group. Furthermore, the cycle cancellation rate, overall fertilization rate and top-quality embryo rate in the AOA group were significantly higher than those in the control group (P< 0.001). However, the cleavage rate, the transferable embryo rate, and blastocyst formation rate were comparable between the two groups (P>0.05) (Table 2).

Pregnancy outcomes in previous standard ICSI cycles and AOA cycles

During the study period, women in the AOA group and women in the control group had undergone 84 and 60 embryo transfer cycles, respectively. The proportions of fresh transfer and FET were similar between the two groups (p>0.05). The clinical pregnancy rate per transfer (41.67% versus 8.33%, P < 0.001), clinical pregnancy rate per patient (30.7% versus 4.39%, P < 0.001) and implantation rate (34.59% versus 6.02%, P < 0.001) were significantly higher in the AOA group than in the control group, whereas the miscarriage rate in the AOA group was significantly lower than that in the control group (17.14% versus 100%, p< 0.001). Furthermore, the live birth rate per transfer (30.95%) and live birth rate per patient (28.95%) were greatly improved after AOA treatment compared to those in the control group (Table 3).

Subgroup analysis based on the cause of infertility

Subgroup analysis was performed into six categories according to the cause of infertility. The fertilization rates of each subgroup were significantly increased compared with those in their corresponding previous ICSI cycles without AOA except for patients in the M+F group. However, there was no significant difference in the top-quality embryo rate among all the subgroups except for the M+F group. The implantation rates were significantly increased in the OAT and unexplained infertility subgroups. The pregnancy rate was significantly improved in the OAT patients. For the OAT patients, the fertilization rate, implantation rate and clinical pregnancy rate were significantly increased, but no improvement was found in the top-quality embryo rate. In the unexplained infertility group, the fertilization rate and implantation rate were significantly increased after AOA, but no significant difference was found in the top-quality embryo rate and clinical pregnancy rate. For the M+F patients, the top-

10.3389/fendo.2023.1244507

TABLE 2 Comparison of clinical outcomes previous standard ICSI cycles and AOA cycles.

	Control group (before)	AOA group (after)	$t/\chi^2/Z$ value	*P* value
No. of patients	114	114		
COS protocols				0.648
long protocol (%)	59(51.75)	66(57.89)	0.868	
Antagonist protocol (%)	40(35.09)	35(30.70)	0.497	
Other protocol (%)	15(13.16)	13(11.40)	0.163	
No. of oocytes obtained	6.89 ± 4.450	7.75 ± 5.048	1.830	0.070
No. of MII oocytes	5.33 ± 3.571	6.16 ± 4.153	-2.079	0.040
No. of oocytes fertilized	2.81 ± 2.844	4.78 ± 3.643	-5.317	0.000
Fertilization rate, %	52.63(320/608)	77.64(545/702)	90.813	0.000
No. of cleavage embryos	2.55 ± 2.677	4.50 ± 3.605	-5.625	0.000
Cleavage rate, %	90.94(291/320)	94.13(513/545)	3.312	0.077
No. of top-quality embryos	0.48 ± 0.790	1.24 ± 1.626	-4.984	0.000
Top-quality embryos rate, %	18.90(55/291)	27.49(141/513)	7.423	0.006
No. of transferable embryos	1.08 ± 1.390	2.07 ± 2.315	-5.13	0.000
Transferable embryos rate, %	42.27(123/291)	46.00(236/513)	1.049	0.306
No. of embryos frozen	0.76 ± 1.046	1.54 ± 1.838	-5.114	0.000
Blastocyst formation rate, %	23.53(28/119)	23.87(53/222)	0.005	0.943
Cancellation rate per cycle, %	45.61(52/114)	28.95(33/114)	6.772	0.009

COS, controlled ovarian stimulation; MII, metaphase II; ICSI, intracytoplasmic sperm injection; 2PN, two pronuclei; AOA, artificial oocyte activation; positive number/total number in brackets.

quality embryo rate was significantly increased after AOA, but no significant improvement was found in the top-quality embryo rate, implantation rate or clinical pregnancy rate. For the advanced age, POI and tubal factor patients, the fertilization rate was also significantly increased, but no significant increases were found in the top-quality embryo rate, implantation rate, and clinical pregnancy rate per patient after AOA treatment compared with their previous ICSI cycle (Figure 2).

Subgroup analysis based on the reason for AOA

Subgroup analysis was performed in three groups based on the reason for AOA. The fertilization rates of each subgroup were significantly increased compared with those in their previous ICSI cycle without AOA; however, there was no significant difference in the top-quality embryo rate. In the PED group, the fertilization rate,

TABLE 3 Comparison of pregnancy outcomes between previous standard ICSI cycles and AOA cycles.

	Control group	AOA group	$t/\chi^2/Z$ value	*P* value
Total number of transfer cycles	60	84		
Fresh transfer (%)	25(15/60)	26.19(22/84)	0.026	0.872
FET (%)	75(45/60)	73.81(62/84)	0.026	0.872
No. of embryos transferred	0.73 ± 1.071	1.18 ± 1.151	-3.538	0.001
Clinical pregnancy rate per transfer (%)	8.33(5/60)	41.67(35/84)	19.385	0.000
Clinical pregnancy rate per patients (%)	4.39(5/114)	30.70(35/114)	27.287	0.000
Implantation rate (%)	6.02(5/83)	34.59(46/133)	32.985	0.000
Miscarriage rate (%)	100(5/5)	17.14(6/35)	15.065	0.000
Live birth rate per transfer (%)	0	34.52(29/84)		
Live birth rate per patients (%)	0	25.44(29/114)		

FET, frozen-thawed embryo transfer; positive number/total number in brackets.

10.3389/fendo.2023.1244507

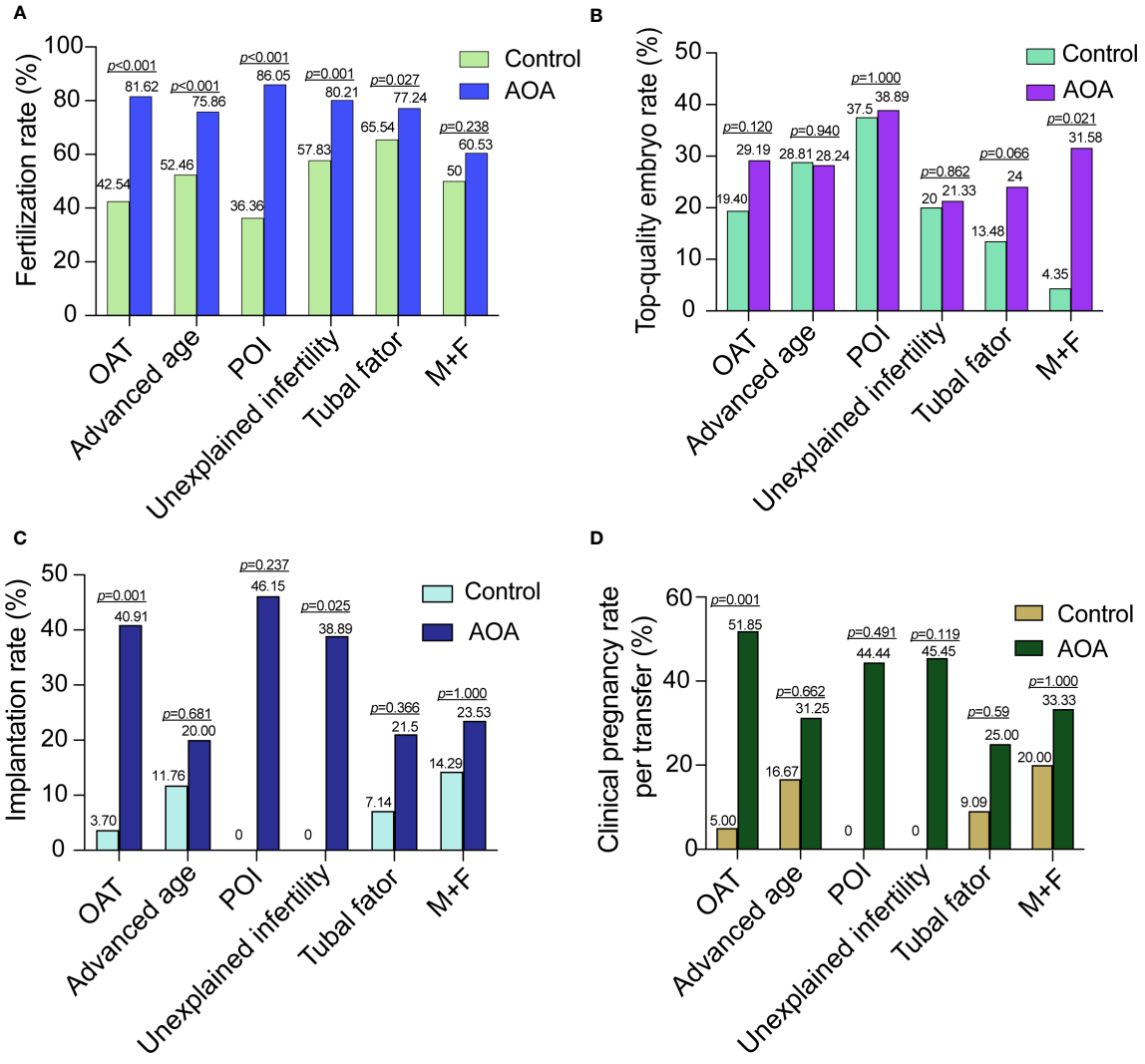

FIGURE 2
Comparison of activation effects in AOA subgroups based on the cause of infertility. **(A)** Comparison of fertilization rates between AOA subgroups and control groups. **(B)** Comparison of the top-quality embryo rate between AOA subgroups and control groups. **(C)** Comparison of the implantation rate between AOA subgroups and control groups. **(D)** Comparison of the clinical pregnancy rate between AOA subgroups and control groups. Control, previous ICSI cycles; *AOA*, artificial oocyte activation; *OAT*, oligoasthenoteratozoospermia; *POI* patients with primary ovarian insufficiency; *M+F* patients with male and female factors.

implantation rate and clinical pregnancy rate were highly increased after AOA, and the top-quality embryo rate was increased slightly after AOA treatment compared with their previous ICSI cycle without AOA but did not reach statistical significance. In the TFF and LFR groups, the fertilization rate was greatly improved, but no data on implantation rates and the clinical pregnancy rate were shown in the control group because no embryos could be transferred in these two groups (Figure 3).

The neonatal outcomes in the AOA group

In the AOA group, 21 singletons and 7 twins among 35 babies were born. All newborns, including 15 boys and 20 girls, had no major birth defects or congenital malformations. Only one baby was born with an atrial septal defect in preterm with gestational weeks of 28 w+4 d. The other neonatal characteristics in the AOA group are shown in Table 4 in terms of gestational weeks, body length, birth weight, low birth weight and preterm birth rate.

Discussion

In this study, we demonstrated that AOA with ionomycin can improve the reproductive outcome of patients with previous total ICSI fertilization failure and poor embryo development.

Our results indicated that AOA treatment significantly improved the fertilization rate, implantation rate, clinical pregnancy and live birth rates per patient compared with previous ICSI cycles, which is in accordance with previous reports (19–21). The evidence suggested that AOA can improve the fertilization rate and the developmental ability of embryos and

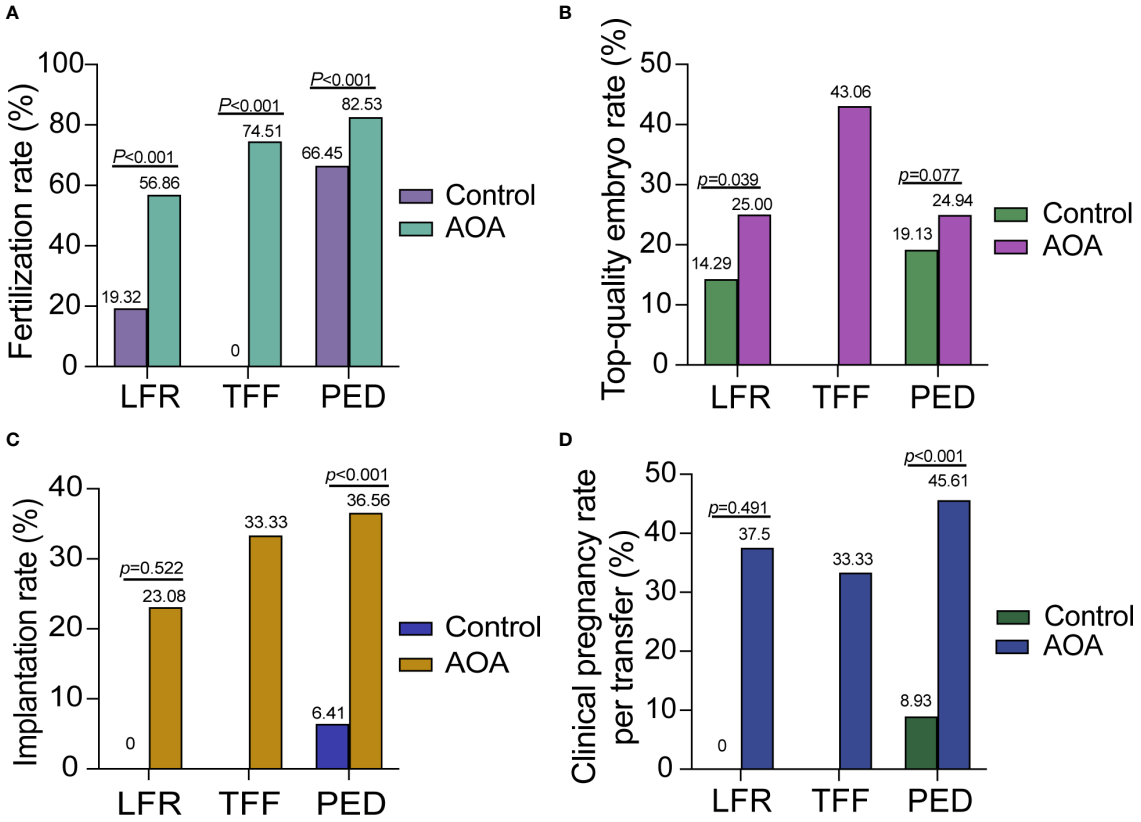

FIGURE 3
Comparison of activation effects in AOA subgroups based on the reason for AOA. **(A)** Comparison of fertilization rates between AOA subgroups and control groups. **(B)** Comparison of the top-quality embryo rate between AOA subgroups and control groups. **(C)** Comparison of the implantation rate between AOA subgroups and control groups. **(D)** Comparison of the clinical pregnancy rate between AOA subgroups and control groups. *Control* previous ICSI cycles; *AOA* artificial oocyte activation; *LFR* low fertilization; *TFF* total fertilization failure; *PED* poor embryo development.

potentially provide more good-quality embryos. Additionally, some studies have also demonstrated that AOA leads to better cumulative pregnancy and live birth rates. However, one study (22) indicated that although AOA can improve the fertilization rate, it might not improve the developmental ability of embryos and pregnancy outcomes. This discrepancy might be derived from the different activation methods used. In that study, double ionophores were applied in cases with previous failed/low fertilization or poor embryo development, and patients with a previous single ionophore were used as the control group.

TABLE 4 Neonatal characteristics in the AOA group.

Item	Value
Birth babies	35
Baby's gender	
Male, n	15
Female, n	20
Singletons, n	21
Twins, n	7
Gestational weeks (wk)	37.42 ± 3.200
Body length (cm)	48.26 ± 3.883
Birth weight (g)	2894.57 ± 773.143
Low birth weight rate (%) (<2,500 g)	28.57(10/35)
Preterm birth rate (%) (<37 wk)	25.71(9/35)
Birth defect rate (%)	2.86(1/35)

ICSI is the most effective method to treat male infertility, but complete fertilization failure will still occur occasionally in a few patients. Abnormal calcium oscillations after fertilization may be the principal mechanism for poor prognosis in patients with TFF. In this study, we found that the fertilization rate, implantation rate and clinical pregnancy rate were significantly increased in patients with TFF and LFR compared with previous ICSI cycles. AOA treatment with ionomycin can change the calcium oscillation pattern and improve the fertilization rate and clinical outcome of these patients. In the past 20 years, the application of AOA has successfully solved many infertility cases due to OAF caused by sperm factors, and Ca^{2+} ionophores have been successfully applied in cases of complete globozoospermia (23) or severe male factor infertility (24). Those results are consistent with our study, couples with OAT can benefit from ICSI-AOA in terms of higher fertilization rate, which in turn increases the number of available embryos and may improve the implantation and pregnancy rates. Recent researches found novel sperm-related oocyte activators, which showed that the ACTL7A/PLCZ1 mutation and DPY19

deletion decreased the expression of functional PLCζ, resulting in acrosomal detachment and oocyte activation failure associated with male infertility, and ICSI-AOA could rescue TFF in individuals with the ACTL7A/PLCZ1/DPY19 pathogenic variants (9, 25, 26). However, ICSI-AOA is not always beneficial for patients with previous LFR and a suspected oocyte-related activation deficiency (27), except Vanden Meerschaut F et al. reported that ICSI-AOA was very efficient in patients with a suspected oocyte-related activation deficiency and previous TFF after conventional ICSI. Our data demonstrated that the implantation rate, top-quality embryo rate and clinical pregnancy rate were not significantly different in the LFR group compared with previous ICSI cycles. AOA can cause calcium oscillation in oocytes, thereby improving fertilization rates in patients with LFR but may not improve embryo development and pregnancy outcomes in these patients.

Based on our study, we found that AOA treatment can improve the embryo development and reproductive outcome of patients with poor embryo development. This result is consistent with other studies, which demonstrated that AOA treatment can overcome the developmental incompetence of embryos and is an additional indication for ionophore treatment (14, 28). It was reported that the different frequencies and patterns of calcium oscillations could affect the induction of oocyte activation and embryo development (29). The calcium-binding proteins and intracellular calcium channels in the human endoplasmic reticulum that regulate inositol 1,4,5-trisphosphate receptors (IP3Rs) play an important role in the regulation of calcium signalling during oocyte maturation, fertilization, and early embryo development, and calcium signalling is a key factor in early embryo development (30). Therefore, AOA with calcium ionophores enhances calcium oscillations and may have beneficial effects on embryo development. However, one study on sibling oocytes showed that AOA using ionomycin 1 h after ICSI did not benefit the early or late development of embryos derived from patients with a history of embryo developmental problems (31). Admittedly, oocyte activation deficiencies are not the only reason for poor embryo development. Sperm DNA damage, oocyte abnormalities in structural proteins and mitochondria, or transcription factors may also contribute to poor prognosis of embryos (32), and none of them can be rescued by AOA.

We also observed that there was no significant difference in the top-quality embryo rate, embryo implantation rate or clinical pregnancy rate per patient in the advanced age and POI groups compared with the control group. These findings indicated that OAF might not be the main factor that affects infertility in advanced age and POI women. Problems with oocyte-derived and deficiencies in downstream signalling pathways may be the main cause of infertility in women of advanced age and POI (33). Furthermore, age-related defects may lead to mitochondrial DNA alignment, accompanied by mitochondrial dysfunction and changes in the gene expression profile (34). However, these studies suggested that AOA may not improve embryo development with advanced age and POI patients but may improve fertilization rates and thus potentially provide more transferable embryos (20). Vanden Meerschaut et al. also reported some cases of oocyte-related OAD, which could be overcome by AOA (27). In our study, the implantation rate was improved in patients with unexplained infertility, and the top-quality rate was also increased in patients with M+F.

We also found that the miscarriage rate in the AOA group was significantly lower than that in the control group. A prospective study demonstrated that the miscarriage rate was decreased in OAT, PCOS and unexplained infertility patients, which was in line with our study (35). Calcium oscillation is a landmark initial event in oocyte activation, and AOA can generate a single transient calcium oscillation, which may alter the activities of specific proteins and enzymes downstream of the Ca^{2+}-regulated pathway and may also have a profound impact on gene expression and development at the later stage of embryos.

Although AOA can improve the treatment outcome of patients with fertilization failure, as a new technology in the assisted reproduction field, its safety still needs more in-depth study. At present, most reports believe that AOA technology will not increase the probability of embryo chromosome abnormalities or the risk of foetal birth defects. Miller et al. compared 83 offspring born with AOA and 595 offspring born after ICSI and demonstrated that there was no significant difference between the two groups in the rate and type of birth defects, birth weight, gestational age, and foetal sex of the offspring (36). A meta-analysis also confirmed that there was no significant difference in congenital defects or types of congenital defects between ICSI-AOA and traditional ICSI (37). These reports were consistent with our study, which showed no statistically significant differences in the birth defect rate, birth weight, gestational age, preterm birth rate, early-neonatal death rate, and foetal sex ratio between the activation and control groups. However, most current studies all have small sample sizes, and we only followed up on early foetal health. Moreover, another study revealed that the application of high concentrations of ionomycin after mouse sperm ICSI increased the frequency and amplitude of Ca^{2+} release, affecting mitochondrial energy metabolism, increasing reactive oxygen species (ROS) and decreasing ATP, and blastocyst formation (38). Furthermore, the impact of AOA on the gene expression and epigenetics of early human embryos is still lacking large amounts of research, and thus, further studies are needed to evaluate the long-term effect of AOA on offspring.

There are still some limitations in our study. First, we performed a retrospective self-controlled study. The previous ICSI cycles of patients served as the control group, and ICSI-AOA was performed in the second cycle based on the previous condition of patients. Patients may not use the same regimen twice. The health status of patients may be improved by medications in the second cycles, and the number and quality of oocytes retrieved may be improved by adjusting the ovulation stimulation protocol. Undoubtedly, the best control group would comprise patients undergoing ICSI-AOA versus patients undergoing ICSI only, and the reproductive outcomes can be compared between the two groups. The reason why we did not undergo a second cycle without AOA was that once the patients had already failed in the first ICSI cycle and exhibited fertilization failure or poor embryo development, they usually asked for something to change in the

second cycle, and the physicians may probably recommend undergoing ICSI-AOA; thus, we lack a control group who are in a second cycle without AOA. Second, there may be some potential bias and confounders that cannot be excluded, and the POI, unexplained infertility and mixed factor infertility subgroups only had a small number of patients in each group; thus, the results should be interpreted with caution. Although the existing evidence was probably at a low level, this study might shed light on further research on AOA treatment, and another prospective, multicentre study with a larger sample size and parallel control would be needed in the future to provide a clearer answer.

In conclusion, our study demonstrated that AOA treated with ionomycin can obtain better reproductive outcomes in infertile couples with previous fertilization failure and poor embryo development. Subgroup analysis showed that couples with male/female factors and unexplained infertility may also benefit from AOA treatment in terms of improving fertilization rate and embryo development potential. However, before such procedures can be widely used in clinical practice, it is necessary to determine more physical agents and protocols that better mimic physiological Ca^{2+} release and conduct further research to evaluate the efficiency and safety of such treatments. At present, AOA should still be limited to application in patients with appropriate indications.

Data availability statement

The raw data supporting the conclusions of this article will be made available by the authors, without undue reservation.

Ethics statement

The studies involving humans were approved by Medical Ethics Committee of Shanghai First Maternal and Infant hospital (KS23210). The studies were conducted in accordance with the local legislation and institutional requirements. The participants provided their written informed consent to participate in this study.

Author contributions

JR was involved in study design, execution, data analysis, project administration, roles/writing-original manuscript. JP and SL were involved in data collection and management ZC was involved in methodology, review and editing, critical discussion. XT was involved in review and editing, supervision critical discussion, and final approval of the manuscript. All authors read and approved the final manuscript. All authors contributed to the article and approved the submitted version.

Acknowledgments

The authors thank all members of the ICSI and AOA teams for their contributions.

Conflict of interest

The authors declare that the research was conducted in the absence of any commercial or financial relationships that could be construed as a potential conflict of interest.

Publisher's note

References

1. Sun B, Yeh J. Calcium oscillatory patterns and oocyte activation during fertilization: a possible mechanism for total fertilization failure (TFF) in human. *In Vitro Fertilization? Reprod Sci* (2021) 28:639–48. doi: 10.1007/s43032-020-00293-5

2. ESHRE Special Interest Group of Embryology and Alpha Scientists in Reproductive Medicine. Electronic address: coticchio.biogenesi@grupposandonato.it. The Vienna consensus: report of an expert meeting on the development of ART laboratory performance indicators. *Reprod BioMed Online* (2017) 35:494–510. doi: 10.1016/j.rbmo.2017.06.015

3. Montag M, Köster M, van der Ven K, Bohlen U, van der Ven H. The benefit of artificial oocyte activation is dependent on the fertilization rate in a previous treatment cycle. *Reprod BioMed Online* (2012) 24:521–6. doi: 10.1016/j.rbmo.2012.02.002

4. Jones C, Meng X, Coward K. SPERM FACTORS AND EGG ACTIVATION: Phospholipase C zeta (PLCZ1) and the clinical diagnosis of oocyte activation deficiency. *Reproduction* (2022) 164:F53–66. doi: 10.1530/REP-21-0458

5. Dai J, Dai C, Guo J, Zheng W, Zhang T, Li Y, et al. Novel homozygous variations in *PLCZ1* lead to poor or failed fertilization characterized by abnormal localization patterns of PLCζ in sperm. *Clin Genet* (2020) 97:347–51. doi: 10.1111/cge.13636

6. Nomikos M, Yu Y, Elgmati K, Theodoridou M, Campbell K, Vassilakopoulou V, et al. Phospholipase Cζ rescues failed oocyte activation in a prototype of male factor infertility. *Fertil Steril* (2013) 99:76–85. doi: 10.1016/j.fertnstert.2012.08.035

7. Kashir J, Heindryckx B, Jones C, De Sutter P, Parrington J, Coward K. Oocyte activation, phospholipase C zeta and human infertility. *Hum Reprod Update* (2010) 16:690–703. doi: 10.1093/humupd/dmq018

8. Meng X, Melo P, Jones C, Ross C, Mounce G, Turner K, et al. Use of phospholipase C zeta analysis to identify candidates for artificial oocyte activation: a case series of clinical pregnancies and a proposed algorithm for patient management. *Fertility Sterility* (2020) 114:163–74. doi: 10.1016/j.fertnstert.2020.02.113

9. Tavalaee M, Nasr-Esfahani MH. Expression profile of *PLC ζ*, *PAWP*, and *TR-KIT* in association with fertilization potential, embryo development, and pregnancy outcomes in globozoospermic candidates for intra-cytoplasmic sperm injection and artificial oocyte activation. *Andrology* (2016) 4:850–6. doi: 10.1111/andr.12179

10. Vanden Meerschaut F, Nikiforaki D, Heindryckx B, De Sutter P. Assisted oocyte activation following ICSI fertilization failure. *Reprod BioMedicine Online* (2014) 28:560–71. doi: 10.1016/j.rbmo.2014.01.008

11. Kilani S, Chapman MG. Meiotic spindle norMality predicts live birth in patients with recurrent in *vitro* fertilization failure. *Fertil Steril* (2014) 101:403–6. doi: 10.1016/j.fertnstert.2013.10.045

12. Yu Y, Nomikos M, Theodoridou M, Nounesis G, Lai FA, Swann K. PLCζ causes Ca(2+) oscillations in mouse eggs by targeting intracellular and not plasma membrane PI(4,5)P(2). *Mol Biol Cell* (2012) 23:371–80. doi: 10.1091/mbc.E11-08-0687

13. Yan Z, Fan Y, Wang F, Yan Z, Li M, Ouyang J, et al. Novel mutations in PLCZ1 cause male infertility due to fertilization failure or poor fertilization. *Hum Reprod* (2020) 35:472–81. doi: 10.1093/humrep/dez282

14. Chen ZQ, Wang Y, Ng EHY, Zhao M, Pan JP, Wu HX, et al. A randomized triple blind controlled trial comparing the live birth rate of IVF following brief inCubation versus standard inCubation of gametes. *Hum Reprod* (2019) 34:100–8. doi: 10.1093/humrep/dey333

15. Kong P, Liu Y, Zhu Q, Yin M, Teng X. Effect of male age on pregnancy and neonatal outcomes in the first frozen-thawed embryo transfer cycles of IVF/ICSI treatment. *Andrology* (2021) 9:1540–8. doi: 10.1111/andr.13031

16. Nasr-Esfahani MH, Razavi S, Javdan Z, Tavalaee M. Artificial oocyte activation in severe teratozoospermia undergoing intracytoplasmic sperm injection. *Fertil Steril* (2008) 90:2231–7. doi: 10.1016/j.fertnstert.2007.10.047

17. Jia L, Chen P, Su W, He S, Guo Y, Zheng L, et al. Artificial oocyte activation with ionomycin compared with A23187 among patients at risk of failed or impaired fertilization. *Reprod BioMed Online* (2023) 46:35–45. doi: 10.1016/j.rbmo.2022.08.105

18. Jia L, Chen P-Y, Guo Y-C, Zhang Z-Q, Gong X, Chen J-B, et al. Prediction of cumulative live birth rate in women aged 40 years and over undergoing *in vitro* fertilization/intracytoplasmic sperm injection. *Reprod Dev Med* (2020) 4:233–8. doi: 10.4103/2096-2924.305931

19. Ebner T, Montag MOocyte Activation Study Group, , Montag M, van der Ven K, van der Ven H, et al. Live birth after artificial oocyte activation using a ready-to-use ionophore: a prospective multicentre study. *Reprod BioMed Online* (2015) 30:359–65. doi: 10.1016/j.rbmo.2014.11.012

20. Li J, Zheng X, Lian Y, Li M, Lin S, Zhuang X, et al. Artificial oocyte activation improves cycles with prospects of ICSI fertilization failure: a sibling oocyte control study. *Reprod BioMed Online* (2019) 39:199–204. doi: 10.1016/j.rbmo.2019.03.216

21. Shebl O, Trautner PS, Enengl S, Reiter E, Allerstorfer C, Rechberger T, et al. Ionophore application for artificial oocyte activation and its potential effect on morphokinetics: a sibling oocyte study. *J Assist Reprod Genet* (2021) 38:3125–33. doi: 10.1007/s10815-021-02338-3

22. Shebl O, Reiter E, Enengl S, Allerstorfer C, Schappacher-Tilp G, Trautner PS, et al. Double ionophore application in cases with previous failed/low fertilization or poor embryo development. *Reprod BioMed Online* (2022) 44:829–37. doi: 10.1016/j.rbmo.2021.11.008

23. Taylor SL, Yoon SY, Morshedi MS, Lacey DR, Jellerette T, Fissore RA, et al. Complete globozoospermia associated with PLCζ deficiency treated with calcium ionophore and ICSI results in pregnancy. *Reprod BioMed Online* (2010) 20:559–64. doi: 10.1016/j.rbmo.2009.12.024

24. Ebner T, Köster M, Shebl O, Moser M, van der Ven H, Tews G, et al. Application of a ready-to-use calcium ionophore increases rates of fertilization and pregnancy in severe male factor infertility. *Fertil Steril* (2012) 98:1432–7. doi: 10.1016/j.fertnstert.2012.07.1134

25. Zhao S, Cui Y, Guo S, Liu B, Bian Y, Zhao S, et al. Novel variants in *ACTL7A* AND *PLCZ1* are associated with male infertility and total fertilization failure. *Clin Genet* (2023) 103:603–8. doi: 10.1111/cge.14293

26. Tavalaee M, Nomikos M, Lai FA, Nasr-Esfahani MH. Expression of sperm PLCζ and clinical outcomes of ICSI-AOA in men affected by globozoospermia due to DPY19L2 deletion. *Reprod BioMedicine Online* (2018) 36:348–55. doi: 10.1016/j.rbmo.2017.12.013

27. Vanden Meerschaut F, Nikiforaki D, De Gheselle S, Dullaerts V, Van den Abbeel E, Gerris J, et al. Assisted oocyte activation is not beneficial for all patients with a suspected oocyte-related activation deficiency. *Hum Reprod* (2012) 27:1977–84. doi: 10.1093/humrep/des097

28. Tsai T-E, Lin P-H, Lian P-F, Li C-J, Vitale SG, Mikuš M, et al. Artificial oocyte activation may improve embryo quality in older patients with diminished ovarian reserve undergoing IVF-ICSI cycles. *J Ovarian Res* (2022) 15:102. doi: 10.1186/s13048-022-01036-7

29. Cooney MA, Malcuit C, Cheon B, Holland MK, Fissore RA, D'Cruz NT. Species-specific differences in the activity and nuclear localization of murine and bovine phospholipase C zeta 1. *Biol Reprod* (2010) 83:92–101. doi: 10.1095/biolreprod.109.079814

30. Yang YR, Follo MY, Cocco L, Suh P-G. The physiological roles of primary phospholipase C. *Adv Biol Regul* (2013) 53:232–41. doi: 10.1016/j.jbior.2013.08.003

31. Yin M, Li M, Li W, Wu L, Yan Z, Zhao J, et al. Efficacy of artificial oocyte activation in patients with embryo developmental problems: a sibling oocyte control study. *Arch Gynecol Obstet* (2022) 305:1225–31. doi: 10.1007/s00404-021-06329-8

32. Bashiri Z, Amidi F, Amiri I, Zandieh Z, Maki CB, Mohammadi F, et al. Male factors: the role of sperm in preimplantation embryo quality. *Reprod Sci* (2021) 28:1788–811. doi: 10.1007/s43032-020-00334-z

33. Jones KT, Lane SIR. Molecular causes of aneuploidy in mamMalian eggs. *Development* (2013) 140:3719–30. doi: 10.1242/dev.090589

34. Yin M, Yu W, Li W, Zhu Q, Long H, Kong P, et al. DNA methylation and gene expression changes in mouse pre- and post-implantation embryos generated by intracytoplasmic sperm injection with artificial oocyte activation. *Reprod Biol Endocrinol* (2021) 19:163. doi: 10.1186/s12958-021-00845-7

35. Lv M, Zhang D, He X, Chen B, Li Q, Ding D, et al. Artificial oocyte activation to improve reproductive outcomes in couples with various causes of infertility: a retrospective cohort study. *Reprod BioMed Online* (2020) 40:501–9. doi: 10.1016/j.rbmo.2020.01.001

36. Miller N, Biron-Shental T, Sukenik-Halevy R, Klement AH, Sharony R, Berkovitz A. Oocyte activation by calcium ionophore and congenital birth defects: a retrospective cohort study. *Fertil Steril* (2016) 106:590–6. doi: 10.1016/j.fertnstert.2016.04.025

37. Long R, Wang M, Yang QY, Hu SQ, Zhu LX, Jin L. Risk of birth defects in children conceived by artificial oocyte activation and intracytoplasmic sperm injection: a meta-analysis. *Reprod Biol Endocrinol* (2020) 18:123. doi: 10.1186/s12958-020-00680-2

38. Chen C, Sun T, Yin M, Yan Z, Yu W, Long H, et al. Ionomycin-induced mouse oocyte activation can disrupt preimplantation embryo development through increased reactive oxygen species reaction and DNA damage. *Mol Hum Reprod* (2020) 26:773–83. doi: 10.1093/molehr/gaaa056

frontiers | Frontiers in Endocrinology

TYPE Clinical Trial
PUBLISHED 29 August 2023
DOI 10.3389/fendo.2023.1237260

OPEN ACCESS

EDITED BY
Changyin Zhou,
Guangdong Second Provincial General Hospital, China

REVIEWED BY
Yumei Zhou,
Beijing University of Chinese Medicine, China
Zirui Dong,
The Chinese University of Hong Kong, China

*CORRESPONDENCE
Xiaoke Wu
xiaokewu2002@vip.sina.com

RECEIVED 09 June 2023
ACCEPTED 08 August 2023
PUBLISHED 29 August 2023

CITATION
Chang H, Shi B, Ge H, Liu C, Wang L, Ma C, Liu L, Zhang W, Zhang D, Wang Y, Wang CC and Wu X (2023) Acupuncture improves the emotion domain and lipid profiles in women with polycystic ovarian syndrome: a secondary analysis of a randomized clinical trial. *Front. Endocrinol.* 14:1237260. doi: 10.3389/fendo.2023.1237260

Acupuncture improves the emotion domain and lipid profiles in women with polycystic ovarian syndrome: a secondary analysis of a randomized clinical trial

Hui Chang[1,2], Baichao Shi[1], Hang Ge[1], Chengdong Liu[3], Lirong Wang[1], Chengcheng Ma[1], Lifeng Liu[1], Wanyu Zhang[1], Duojia Zhang[2], Yong Wang[4], Chi Chiu Wang[5] and Xiaoke Wu[2,6]*

[1]Heilongjiang University of Chinese Medicine, Harbin, China, [2]First Affiliated Hospital, Heilongjiang University of Chinese Medicine, Harbin, China, [3]Affiliated Hospital of Jiangsu University, Zhenjiang, China, [4]Nanjing Universityg, Nanjin, China, [5]The Chinese University of Hong Kong, Hong Kong, Hong Kong, SAR, China, [6]Heilongjiang Provincial Hospital, Harbin, China

Objective: This study aims to evaluate the effect of acupuncture on the emotion domain and metabolic parameters of Chinese women with polycystic ovarian syndrome (PCOS) by secondary analysis of a randomized clinical trial, conducted from 6 July 2012 to 7 October 2015.

Method: In this study, we investigated the effects of acupuncture (458 patients) and sham acupuncture (468 patients) on metabolic parameters, serum ions, and all quality-of-life scale scores related to PCOS. The quality of life of patients was evaluated using five relevant scales, operated by the research assistant, namely, PCOSQ, SF-36, and ChiQOL, as well as Zung-SAS and Zung-SDS. Metabolic parameters and serum ions were measured.

Results: A reduction in acne score, AN, Hcy, and LDL-C, and an increase in the level of lipoprotein α, Apo A1, and Apo A1/Apo B were observed in the acupuncture group after 4 months' intervention after adjusting clomiphene and reproductive outcome ($p< 0.05$). An increase in SF-36 total scores, RP and RE scores, ChiQOL total scores, and emotion domain scores was observed in the acupuncture group after 4 months' intervention, while PF and HT scores were decreased (adjusted $p< 0.05$). Those same changes were observed in sham acupuncture. Meanwhile, the serum levels of Ca, K, and Cl were elevated in the acupuncture group after the interventions (adjusted $p< 0.005$). There were no significant differences in HOMA-IR, MetS, FPG, FINS, HDL-C, TG, Apo B, and level of serum P, Mg, and Na. Also, no changes in BP, GH, VT, SF, physical form domain, and spirit domain were observed after treatment.

Conclusion: Acupuncture can improve not only the emotional changes in SF-36 scores and ChiQOL scores, but also lipid metabolism, implying that it may have a correlation between emotional change and lipid metabolism. Furthermore, acupuncture can also regulate the changes of serum Ca, K, and Cl.

Clinical trial registration: ClinicalTrials.gov, identifier NCT01573858.

KEYWORDS

polycystic ovarian syndrome, acupuncture, emotion, metabolism, ions

1 Introduction

Polycystic ovarian syndrome (PCOS) is the most common endocrine disease in women of reproductive age, affecting more than 15%–20% of the population (1). Women with PCOS are frequently associated with metabolic abnormalities, including hyperinsulinemia, chronic low-grade inflammation, insulin resistance (IR), dyslipidemia, and obesity, and even anovulatory infertility and type 2 diabetes, as well as the risk of cardiovascular disease (CVD) (2). PCOS is not a simple physical disease; it is associated with mental and psychological disorders. It affects not only the health-related quality of life (HRQoL) of women, but also their psychological function (3). In most cases following a diagnosis of PCOS, there is an increased prevalence of depression and anxiety symptoms; perceived stress; self-reported medical diagnoses of depression, anxiety, or other major mental illnesses; and treatment for psychological conditions or mental illness (4–6). Compared with normal women, women with PCOS have significantly increased personality defects and psychiatric disorders, including anxiety, somatoform disorder and bipolar disorder, depression, delusional disorder and thought disorder, reduction of coping abilities and social skills, perceptual distortion and cognitive slippage, constant alertness and worry, chronic stress, and post-traumatic stress disorder, as well as inferiority, negativity, and social loneliness (7–9). Moreover, there is an overlap of clinical symptoms between the emotion domain and PCOS. There is a possibility of common associations between emotional disorders and PCOS-associated abnormalities including lipid metabolism. A previous study has shown that emotion, especially comorbidity among anxiety and depression, is connected with the metabolic syndrome (MetS), and the improvement in emotion may play an inhibitory role in the development of the syndrome, resulting in a reduced risk of MetS via physiological regulation systems (10), but equally, it has indicated the effect of metabolism on limbic function and emotional regulation, which can disrupt emotion regulation in the context of metabolic dysfunction (11).

Acupuncture is an integral part of traditional Chinese medicine (TCM), which dates back more than 3,000 years. In recent years, the use of acupuncture to regulate the disorder of reproductive endocrinology and infertility has become more popular worldwide (12). As an alternative therapy, acupuncture can improve the internal regulation function of the human body to prevent or treat diseases by receiving stimulation of different acupoints (13); in particular, efficacy on regulating menstruation and hormones is similar to recently clinical trials, reporting that acupuncture can induce regular menstrual cycles and ovulation, as well as decrease high circulating levels of luteinizing hormone and testosterone in women with PCOS (14) by affecting more functional signaling pathways associated with metabolism and hypothalamic pituitary ovarian axes (15). However, no efficacy on live birth rates by acupuncture was reported in PCOSAct of Wu's study (16). Acupuncture had an effect of improving lipid profile, with an increase in levels of high-density lipoprotein cholesterol (HDL-C) and a decrease in other parameters including triglycerides (TG), total cholesterol (TC), and low-density lipoprotein cholesterol (LDL-C) (17). Previous clinical studies have demonstrated that acupuncture is effective for the improvement of quality of life and treatment of various diseases including anxiety disorders, fatigue, and depression (18, 19). Furthermore, acupuncture may alleviate anxiety during embryo transfer, and it has also been implied to have certain effects on perinatal depression (20). Although there are some studies on acupuncture treatment of glucose and lipid metabolism and emotional disorders in women with PCOS, the results have been conflicting.

The PCOSQ and SF-36 are most commonly used to assess the quality of life of women with PCOS. Among these, PCOSQ is a tool specifically designed and validated for evaluating HRQoL in PCOS, which together are able to capture different aspects of QoL in PCOS women and identify areas that can help improve QoL in these women (21). The Chinese QoL scale can provide effective information based on the universal QoL measures, and can also provide certain guidance for clinical applications (22). In addition, previous studies have demonstrated that acupuncture is effective in improving symptoms in PCOS with Self-assessed Anxiety Scale (SAS) and Self-assessed Depression Scale (SDS) scores (23). All the above scales have good applicability and reliability to evaluate the effectiveness of acupuncture in patients with PCOS. Therefore, this study, based on 1,000 patients with PCOS from the Acupuncture and Clomiphene in Polycystic Ovary Syndrome Trial (PCOSAct), is designed to explore the effects of acupuncture on metabolic parameters, serum ions, and the quality of life of PCOS.

2 Materials and methods

2.1 Design and target population

This is a *post-hoc* analysis of metabolic parameters, serum ions, and quality-of-life scales data from PCOSAct, a large-sample,

multicenter, two-by-two factorial randomized controlled clinical trial collected at sites (27 hospitals) in mainland China between 6 July 2012 and 7 October 2015. In total, 1,000 participants were diagnosed with PCOS according to the modified Rotterdam criteria (24, 25): oligomenorrhea (defined as an intermenstrual interval >35 days and<8 menstrual bleedings in the past year) or amenorrhea (defined as an intermenstrual interval >90 days), together with clinical or biochemical hyperandrogenism (hirsutism determined by modified Ferriman-Gallwey hirsutism score ≥5 in Chinese) (26, 27) and/or polycystic ovaries (≥12 antral follicles 2–9 mm or ovarian volume ≥10 cm^3). The study design, methods, and inclusion and exclusion criteria have been described in detail elsewhere (12), and the main results have been published (16). In brief, 926 women with PCOS were enrolled in the present study, and were assigned to the acupuncture group or the sham acupuncture group, with 458 patients and 468 patients per group, respectively.

The trial was registered on ClinicalTrials.gov (No. NCT01573858). The study was approved by the Regional Ethics Committee at The First Affiliated Hospital of Heilongjiang University of Traditional Chinese Medicine on 15 December 2011 (No. 2010HZYLL-010). All participants had signed informed consent before randomizing in the study.

2.2 Data collection

2.2.1 Blood sampling

At baseline on day 3 of a spontaneous menstrual period or a withdrawal, bleeding was induced by medroxyprogesterone acetate in patients with irregular cycles without recent menses, and upon pregnancy, it was monitored weekly by urinary human chorionic gonadotropin test, or at the end of the 16 weeks of treatment, fasting blood samples were collected for measurement of metabolic parameters, lipid profile, and serum ions in those patients who are not pregnant at that time.

The anthropometric, degree of hirsutism and acne were collected and body mass index (BMI) was calculated as weight in kilograms divided by height in meters squared. All biochemical assays were carried out in a core laboratory after an overnight fast. All fasting blood collected at baseline and after intervention was used for metabolic parameters and serum ion assays. These were measured in samples stored at −80°C using an ELISA assay with no pre-dilution.

2.2.2 Outcome measures

The biologic feature parameters of women with PCOS were obtained at baseline and at the follow-up visit, respectively, including age, male age, height, weight, BMI, waist, hip, waist–hip ratio (WHR), systolic pressure, diastolic pressure, respiration, pulse, Ferriman-Gallwey, acne scores, and acanthosis nigricans (AN).

In addition, metabolic parameters in blood test included homeostasis model assessment-insulin resistance (HOMA-IR), MetS, fasting plasma glucose (FPG), fasting plasma insulin (FINS), homocysteine (Hcy), HDL-C, LDL-C, lipoprotein α, TC, TG, Apolipoprotein A1 (Apo A1), Apolipoprotein B (Apo B), and Apo A1/Apo B, and serum ions including calcium (Ca), phosphorus (P), magnesium (Mg), potassium (K), sodium (Na), and chloride (Cl) were assayed.

Quality-of-life scales included Polycystic Ovary Syndrome Health-Related Quality of Life Questionnaire (PCOSQ, range of 1–7, with higher scores indicating better function) (28), Medical Outcomes Study 36-Item Short Form Health Survey (SF-36, range of 0–100, with higher scores indicating better function) (29), and Chinese Quality of Life Instrument (ChiQOL, range of 50–250, with higher scores indicating better function) (30), as well as the Zung-Self Rating Anxiety Scale (SAS, range of 25–100, with higher scores indicating worse anxiety) and Zung-Self Rating Depression Scale (SDS, range of 25–100, with higher scores indicating worse depression).

2.3 Statistical analyses

In the data description, categorical variables were summarized by frequencies. Continuous variables with normal distribution were presented as mean ± standard deviation ($\bar{x}$ ± s). The data of non-normal distribution were analyzed by Mann–Whitney *U* test. Paired samples *t*-test or Mann–Whitney *U* test was used to analyze the continuous indices. SPSS 22.0 was used for analysis and $p< 0.05$ was considered to be statistically significant.

3 Results

3.1 Baseline characteristics

A total of 4,645 women with PCOS were screened from 6 July 2012 to 7 October 2015. A total of 1,000 eligible women were randomized and only 926 participants were included in the analysis. A total of 458 participants were assigned to the acupuncture group and 468 participants were assigned to the sham acupuncture group. There were no significant differences in baseline biological characteristics, metabolic parameters, and serum ions between two groups (Table 1). Quality-of-life scales including SAS, SDS, PCOSL, SF-36, and ChiQOL scores were paralleled between two groups at baseline (Table 2).

3.2 Biological features

Acne scores and AN of biological features were decreased after acupuncture intervention in both groups after adjusting clomiphene and reproductive outcome ($p< 0.001$). Also, there was a significant decrease in acne scores in the acupuncture group after intervention, compared with the sham acupuncture group (adjusted $p = 0.0102$). By contrast, no significant difference in weight, BMI, waist, hip, WHR, systolic pressure, diastolic pressure, respiration, pulse, and Ferriman-Gallwey were found when comparing pre-treatment and post-treatment or between acupuncture and sham acupuncture (Table 3).

10.3389/fendo.2023.1237260

TABLE 1 Baseline characteristics of the subjects.

	Acupuncture group (*n* = 458)	Sham acupuncture group (*n* = 468)	Mean difference (95% CI)	*t*	*p*
Biological features					
Age	27.97 ± 3.33	27.87 ± 3.33	−0.11 (−0.52–0.31)	−0.51	0.6136
Male age	29.80 ± 4.03	29.81 ± 4.34	0.01 (−0.52–0.53)	0.02	0.9842
Height (cm)	161.24 ± 5.02	161.22 ± 5.16	−0.01 (−0.64–0.62)	−0.04	0.9695
Weight (kg)	62.53 ± 12.39	63.78 ± 12.45	1.25 (−0.29–2.79)	1.59	0.1115
BMI (kg/m^2)	23.99 ± 4.29	24.47 ± 4.23	0.48 (−0.05–1.01)	1.79	0.0734
Waist (cm)	85.10 ± 11.61	85.75 ± 11.35	0.65 (−0.78–2.07)	0.89	0.3722
Hip (cm)	98.25 ± 8.49	98.65 ± 8.76	0.40 (−0.67–1.48)	0.74	0.4598
WHR	0.86 ± 0.07	0.87 ± 0.07	0.00 (−0.01–0.01)	−0.84	0.4006
Systolic pressure (mmHg)	112.00 ± 9.33	112.61 ± 9.49	0.61 (−0.55–1.78)	1.03	0.3026
Diastolic pressure (mmHg)	74.80 ± 7.86	74.91 ± 7.93	0.11 (−0.87–1.09)	0.22	0.8233
Respiration (beats/min)	18.09 ± 1.69	18.01 ± 1.51	−0.08 (−0.28–0.12)	−0.83	0.409
Pulse (beats/min)	75.91 ± 6.33	76.22 ± 6.15	0.31 (−0.47–1.08)	0.78	0.4373
Ferriman-Gallwey	3.14 ± 2.85	2.93 ± 2.76	−0.22 (−0.57–0.13)	−1.23	0.2189
Acne sore	1.76 ± 0.73	1.71 ± 0.64	−0.05 (−0.14–0.04)	−1.1	0.2724
Acanthosis nigricans	1.73 ± 0.61	1.73 ± 0.68	−0.00 (−0.09–0.08)	−0.09	0.9274
Metabolic parameters					
HOMA-IR	23.82 ± 28.76	21.68 ± 21.29	−2.14 (−5.37–1.08)	−1.30	0.1926
Metabolic syndrome	71 (14.2)	83 (16.6)	-	-	0.2931
FPG (mmol/L)	5.07 ± 0.93	5.01 ± 1.04	−0.06 (−0.19–0.06)	−0.95	0.3408
FINS (pmol/L)	99.18 ± 96.88	92.97 ± 78.74	−6.21 (−17.41–4.99)	−1.09	0.277
Hcy (μmol/L)	8.39 ± 5.07	8.29 ± 4.64	−0.10 (−0.72–0.53)	−0.31	0.7574
HDL-C (mmol/L)	1.29 ± 0.36	1.26 ± 0.38	−0.03 (−0.08–0.02)	−1.32	0.1861
LDL-C (mmol/L)	3.00 ± 0.89	2.93 ± 0.86	−0.06 (−0.18–0.05)	−1.15	0.2511
Lipoprotein (mg/L)	132.65 ± 101.58	126.32 ± 97.97	−6.34 (−19.01–6.34)	−0.98	0.3268
Total cholesterol (mmol/L)	4.80 ± 1.10	4.68 ± 1.07	−0.11 (−0.25–0.02)	−1.62	0.105
Triglyceride (mmol/L)	1.59 ± 0.95	1.55 ± 0.87	−0.03 (−0.15–0.08)	−0.58	0.559
Apo A1(g/L)	1.53 ± 0.31	1.49 ± 0.32	−0.04 (−0.08 to −0.00)	−1.99	0.0474
Apo B (g/L)	0.91 ± 0.29	0.89 ± 0.28	−0.02 (−0.06–0.02)	−1.11	0.2669
Serum ion test					
Ca (mmol/L)	1.95 ± 0.43	1.96 ± 0.39	0.02 (−0.03–0.07)	0.68	0.4978
P (mmol/L)	1.13 ± 0.26	1.15 ± 0.34	0.02 (−0.02–0.06)	0.9	0.3666
Mg (mmol/L)	0.86 ± 0.18	0.87 ± 0.15	0.00 (−0.02–0.03)	0.44	0.6568
K (mmol/L)	4.14 ± 0.92	4.23 ± 0.88	0.09 (−0.03–0.20)	1.5	0.1329
Na (mmol/L)	135.66 ± 16.12	136.53 ± 14.21	0.87 (−1.08–2.81)	0.88	0.3815
Cl (mmol/L)	93.39 ± 12.24	94.08 ± 10.86	0.69 (−0.79–2.16)	0.91	0.3631

Data are median (IQR).
p-value represents comparison between acupuncture and sham acupuncture groups before treatment.

TABLE 2 The quality of life outcomes sore at baseline.

	Acupuncture group (*n* = 458)	Sham acupuncture group (*n* = 468)	Mean difference (95% CI)	*t*	P
SAS score	33.71 ± 6.93	33.86 ± 6.82	0.15 (−0.70–1.01)	0.35	0.7245
SDS score	35.24 ± 8.61	35.48 ± 8.21	0.24 (−0.81–1.29)	0.45	0.6525
PCOSQOL score	127.88 ± 28.38	127.09 ± 29.47	−0.79 (−4.38–2.81)	−0.43	0.6672
Emotions	4.27 ± 1.11	4.31 ± 1.14	0.04 (−0.10–0.18)	0.56	0.5777
Body hair	5.31 ± 1.52	5.25 ± 1.61	−0.06 (−0.26–0.13)	−0.63	0.5276
Weight	4.29 ± 1.72	4.20 ± 1.69	−0.08 (−0.29–0.13)	−0.75	0.4515
Infertility	3.65 ± 1.35	3.64 ± 1.41	−0.01 (−0.18–0.16)	−0.08	0.9368
Menstrual problems	4.41 ± 1.10	4.35 ± 1.14	−0.06 (−0.20–0.08)	−0.9	0.3666
SF-36 score	104.15 ± 4.52	104.06 ± 4.54	−0.09 (−0.65–0.47)	−0.32	0.7518
Physical functioning	93.36 ± 9.70	93.29 ± 9.53	−0.07 (−1.26–1.13)	−0.11	0.9126
Role-physical	23.35 ± 29.99	21.49 ± 30.55	−1.86 (−5.62–1.90)	−0.97	0.3321
Bodily pain	77.64 ± 12.96	76.75 ± 13.68	−0.89 (−2.54–0.77)	−1.05	0.2933
General health	52.91 ± 11.64	53.39 ± 12.20	0.48 (−1.01–1.96)	0.63	0.5288
Vitality	42.73 ± 11.92	42.20 ± 12.36	−0.53 (−2.04–0.98)	−0.69	0.4897
Social functioning	49.00 ± 13.09	48.95 ± 10.97	−0.05 (−1.55–1.45)	−0.07	0.9435
Role-emotional	26.40 ± 34.62	24.23 ± 34.90	−2.17 (−6.49–2.15)	−0.99	0.3244
Mental health	60.02 ± 10.46	60.84 ± 9.89	0.83 (−0.44–2.09)	1.28	0.1997
Health transition	48.55 ± 25.80	47.29 ± 25.62	−1.26 (−4.46–1.93)	−0.77	0.4388
ChiQOL score	148.20 ± 11.04	148.22 ± 11.28	0.03 (−1.36–1.42)	0.04	0.9674
Physical form domain	3.35 ± 0.80	3.25 ± 0.85	−0.10 (−0.20–0.00)	−1.93	0.0536
Spirit domain	95.53 ± 8.36	95.58 ± 8.21	0.05 (−0.98–1.08)	0.1	0.9176
Emotion domain	49.32 ± 7.04	49.39 ± 7.03	0.08 (−0.80–0.95)	0.17	0.8654

Data are median (IQR).
p-value represents comparison between acupuncture and sham acupuncture groups before treatment.

3.3 Metabolic parameters

The level of serum Hcy was significantly decreased after treatment in both groups (adjusted $p< 0.001$). Additionally, the levels of LDL-C and Apo A1 were significantly decreased, while the serum levels of lipoprotein α, Apo A1/Apo B, and TC were significantly increased after acupuncture treatment (adjusted $p< 0.05$). By contrast, no significant differences in HOMA-IR, MetS, FPG, FINS, Hcy, HDL-C, LDL-C, lipoprotein α, TC, Apo A1, and Apo B (except for TG) were found when comparing pre-treatment and post-treatment or between acupuncture and sham acupuncture (adjusted $p = 0.0476$) (Table 3).

3.4 Serum ions

The levels of serum Cl, serum Ca, and serum K were both significantly increased in the acupuncture group after intervention of 4 months compared with pre-treatment (adjusted $p< 0.05$). Also, the levels of Cl were increased in the sham acupuncture group. There were no significant differences in P, Mg, and Na when comparing pre-treatment and post-treatment or between acupuncture and sham acupuncture (Table 3).

3.5 The quality-of-life scales

The total scores, role-physical (RP) scores, and role-emotional (RE) scores of SF-36 were significantly increased after 4 months' acupuncture intervention (adjusted $p< 0.05$),but equally, the total score and emotion domain scores of ChiQOL scale were also significantly increased. By contrast, the scores on physical functioning (PF) and health transition (HT) of SF-36 were significantly decreased after intervention (adjusted $p< 0.05$). Those same changes were found in the sham acupuncture group.

There were no significant differences in bodily pain (BP), general health (GH), vitality (VT), social functioning (SF), RE, mental health (MH), and HT scores of SF-36 and total scores, emotion, body hair, weight, infertility problems of PCOSQOL, Physical Form Domain, and Spirit Domain of ChiQOL scores

10.3389/fendo.2023.1237260

TABLE 3 Metabolic parameters and serum ion after acupuncture and sham acupuncture.

	Acupuncture group				Sham acupuncture group					
	Pre-treatment (n = 458)	Post-treatment (n = 458)	p	p	Pre-treatment (n = 468)	Post-treatment (n = 468)	p	^{a}p	$p1$	$^{a}p1$
Biological features										
Weight (kg)	62.53 ± 12.39	62.26 ± 12.39	0.7382	0.7895	63.78 ± 12.45	63.52 ± 11.98	0.7410	0.7683	0.9118	0.9011
BMI (kg/m^2)	23.99 ± 4.29	23.90 ± 4.29	0.7424	0.7915	24.47 ± 4.23	24.39 ± 4.10	0.7488	0.7782	0.8839	0.8954
Waist (cm)	85.10 ± 11.61	84.85 ± 11.54	0.7391	0.7677	85.75 ± 11.35	85.39 ± 11.09	0.6134	0.6378	0.9752	0.9761
Hip (cm)	98.25 ± 8.49	98.15 ± 8.58	0.8607	0.8814	98.65 ± 8.76	98.45 ± 8.58	0.7115	0.7279	0.8975	0.8912
WHR	161.24 ± 5.02	161.24 ± 5.08	0.9887	0.7548	0.87 ± 0.07	0.87 ± 0.07	0.7101	0.7328	0.8666	0.8638
Systolic pressure (mmHg)	112.00 ± 9.33	112.07 ± 8.59	0.9024	0.8631	112.61 ± 9.49	112.48 ± 8.51	0.8248	0.8321	0.486	0.4861
Diastolic pressure (mmHg)	74.80 ± 7.86	74.95 ± 7.54	0.7725	0.7577	74.91 ± 7.93	75.48 ± 7.73	0.2598	0.2525	0.3863	0.3822
Respiration (beats/min)	18.09 ± 1.69	17.96 ± 1.72	0.2204	0.2308	18.01 ± 1.51	18.02 ± 1.76	0.8988	0.9181	0.109	0.1162
Pulse (beats/min)	75.91 ± 6.33	76.03 ± 6.39	0.7769	0.7647	76.22 ± 6.15	76.20 ± 5.94	0.9668	0.9624	0.8016	0.8114
Ferriman-Gallwey	3.14 ± 2.85	2.81 ± 2.70	0.0639	0.0670	2.93 ± 2.76	2.67 ± 2.66	0.1420	0.1465	0.5203	0.5105
Acne score	0.70 ± 0.46	0.24 ± 0.43	<0.0001	<0.0001	0.65 ± 0.48	0.27 ± 0.44	<0.0001	<0.0001	0.0096	0.0102
Acanthosis nigricans	1.21 ± 0.47	0.18 ± 0.44	<0.0001	<0.0001	1.21 ± 0.48	0.19 ± 0.44	<0.0001	<0.0001	0.81	0.8395
Metabolic parameters										
HOMA-IR	23.82 ± 28.76	26.24 ± 33.12	0.2381	0.2310	21.68 ± 21.29	23.28 ± 22.70	0.2706	0.2659	0.8554	0.8736
Metabolic syndrome	71(14.2)	57(11.4)	0.1851	0.1831	83(16.6)	68(13.6)	0.1852	0.1840	-	-
FPG (mmol/L)	5.07 ± 0.93	5.07 ± 1.27	0.9712	0.9980	5.01 ± 1.04	4.99 ± 1.19	0.7457	0.6999	0.5941	0.5654
FINS (pmol/L)	99.18 ± 96.88	107.25 ± 105.13	0.2243	0.2199	92.97 ± 78.74	100.59 ± 86.67	0.1609	0.1565	0.8581	0.8393
Hcy (μmol/L)	8.39 ± 5.07	6.76 ± 4.29	<0.0001	<0.0001	8.29 ± 4.64	6.26 ± 3.69	<0.0001	<0.0001	0.1128	0.0972
HDL-C (mmol/L)	1.29 ± 0.36	1.33 ± 0.41	0.1140	0.1175	1.26 ± 0.38	1.29 ± 0.39	0.2772	0.2872	0.6753	0.6600
LDL-C (mmol/L)	3.00 ± 0.89	2.86 ± 1.06	0.0346	0.0365	2.93 ± 0.86	2.75 ± 0.91	0.0012	0.0012	0.6249	0.5895
Lipoprotein α(mg/L)	132.65 ± 101.58	187.75 ± 111.97	<0.0001	<0.0001	126.32 ± 97.97	176.7 ± 113.90	<0.0001	<0.0001	0.4808	0.5429
Total cholesterol (mmol/L)	4.80 ± 1.10	4.65 ± 1.28	0.0610	0.0691	4.68 ± 1.07	4.51 ± 1.16	0.0213	0.0204	0.9273	0.8891
Triglyceride (mmol/L)	1.59 ± 0.95	1.49 ± 0.85	0.0969	0.1055	1.55 ± 0.87	1.56 ± 0.98	0.8853	0.8612	0.046	0.0476
Apolipoprotein A1 (g/L)	1.53 ± 0.31	1.57 ± 0.38	0.0382	0.0403	1.49 ± 0.32	1.54 ± 0.36	0.0202	0.0223	0.63	0.6351
Apolipoprotein B (g/L)	0.91 ± 0.29	0.88 ± 0.33	0.2024	0.2166	0.89 ± 0.28	0.86 ± 0.29	0.1231	0.1269	0.8685	0.8823
ApoA1/ApoB	1.84 ± 0.70	1.99 ± 0.77	0.0023	0.0024	1.80 ± 0.59	1.94 ± 0.66	0.0007	0.0008	-	-
Serum ion test										
Ca (mmol/L)	1.95 ± 0.43	2.04 ± 0.55	0.0026	0.0025	1.96 ± 0.39	2.02 ± 0.55	0.0703	0.0608	0.2101	0.1942
P (mmol/L)	1.13 ± 0.26	1.11 ± 0.30	0.4308	0.4418	1.15 ± 0.34	1.13 ± 0.38	0.5444	0.6009	0.8068	0.7768
Mg (mmol/L)	0.86 ± 0.18	0.88 ± 0.21	0.2758	0.2735	0.87 ± 0.15	0.87 ± 0.21	0.7689	0.7219	0.3738	0.3536
K (mmol/L)	4.14 ± 0.92	4.44 ± 1.97	0.0032	0.0032	4.23 ± 0.88	4.32 ± 1.73	0.3369	0.3435	0.0516	0.0502

(Continued)

TABLE 3 Continued

	Acupuncture group				Sham acupuncture group					
	Pre-treatment (n = 458)	Post-treatment (n = 458)	p	p	Pre-treatment (n = 468)	Post-treatment (n = 468)	p	^{a}p	$p1$	$^{a}p1$
Na (mmol/L)	135.66 ± 16.12	136.96 ± 22.03	0.3085	0.3129	136.53 ± 14.21	136.61 ± 22.21	0.9485	0.9258	0.233	0.2180
Cl (mmol/L)	93.39 ± 12.24	97.88 ± 17.92	<0.0001	<0.0001	94.08 ± 10.86	97.60 ± 18.04	0.0003	0.0003	0.2471	0.2324

Data are median (IQR).
p-values represent comparison before and after treatment within acupuncture and sham acupuncture groups.
[a]p-values represent comparison before and after treatment within acupuncture and sham acupuncture groups after adjusting clomiphene and reproductive outcome.
p1-values represent comparison of the difference value before and after treatment between acupuncture and sham acupuncture groups.
[a]p1-values represent comparison of the difference value before and after treatment between acupuncture and sham acupuncture groups after adjusting clomiphene and reproductive outcome.

when comparing pre-treatment and post-treatment or between acupuncture and sham acupuncture, as well as SAS and SDS scores (Table 4).

4 Discussion

Our results showed that total scores and RP and RE scores in the SF-36 scale after treatment in the two groups were significantly higher than before treatment, whereas PF, MH, and HT scores were significantly lower than those before treatment, after adjusting clomiphene and reproductive outcome. In the ChiQOL scale, the significant increase in total scores and emotion domain scores was observed in the two groups compared with pre-treatment. These findings indicated that acupuncture could improve the emotion domain of PCOS patients, and the same effects were found in sham acupuncture. The SF-36 questionnaire-a is a concise health survey that comprehensively summarizes the survival quality of respondents; it contains 36 items divided into nine areas of HRQoL. Our study revealed that acupuncture significantly improved the scores of RP and RE in SF-36 of patients with PCOS, which were decreased after acupuncture treatment in previous research (3). The ChiQOL questionnaire is a new universal scale based on TCM (30, 31). The total scores and emotion domain scores in the ChiQOL questionnaire were significantly increased after acupuncture intervention, which indicated that acupuncture could improve the quality of life of Chinese people; Dong et al.'s study had the same results (3). Some research reported that acupuncture played a significant improvement in the physical form domain and a significantly and continuously improved trend in the vitality domain (32), but in our study, the scores of PF, MH, and HT in SF-36 were decreased after acupuncture intervention, which may be related to the physical and mental health damage caused by long-term infertility of PCOS and could not be corrected by acupuncture. Moreover, sham acupuncture was not completely useless; the same effects were found in sham acupuncture group. The PCOSQ as the only validated disease-specific questionnaire has been used to evaluate the HRQoL of women with PCOS currently, which has been administered to understand women experiences of emotions, body hair, weight, infertility, and menstrual problems of PCOS symptomatology in detail (28, 33). It has been revealed that acupuncture plays a significant role in ameliorating negative emotion in PCOS patients, which was decreased in SAS and SDS scores and increased in PCOSQ scores (23), but no differences in PCOSQ, SAS, and SDS scores were observed in our study.

The level of serum Hcy was significantly decreased after treatment in both groups (adjusted $p< 0.001$). Additionally, the levels of LDL-C and Apo A1 were significantly decreased, while the serum levels of lipoprotein α, Apo A1/Apo B, and TC were significantly increased after acupuncture treatment (adjusted $p< 0.05$). It is a controversial issue whether acupuncture can improve lipid metabolism in patients with PCOS. A previous study indicated that acupuncture could improve TG levels in lipid metabolism of PCOS (34), whereas acupuncture had no effect on LDL-C, TG, and TC in lipid metabolism, as illustrated in another study (35). Our study found that the TG in lipid metabolism indicators was significantly different between two groups after treatment. Our findings showed that acupuncture was closely associated with a decrease in the level of LDL-C and an increase in the level of lipoprotein α and Apo A1, and slightly increased the ratio of Apo A1/Apo B in lipid profiles in patients with PCOS, while the sham acupuncture group could increase the TC level. Lai et al.'s clinical trials reported that the LDL-C level was reduced by acupuncture treatment (36); the same results have been found in our study. However, no significant change in HDL-C levels after acupuncture treatment was reported in our study, and the finding was not consistent with another study (37). Furthermore, acupuncture could significantly improve the acne symptoms of patients with PCOS, while other biological features such as BMI, WHR, and AN were not improved, compared with the sham acupuncture group. However, no significant differences in HOMA-IR, MetS, FPG, FINS, Hcy, HDL-C, LDL-C, lipoprotein α, TC, Apo A1, and Apo B (except for TG) were found when comparing pre-treatment and post-treatment or between acupuncture and sham acupuncture (adjusted $p = 0.0476$).

Our research found that acupuncture can regulate emotion and improve abnormal lipid metabolism and ion disorders, and these may have a certain relationship. Poor mental health was significantly associated with elevated levels of TG and LDL-C. A recent cross-sectional study demonstrated that female participants who experienced high stress showed higher levels of LDL-C compared with the low-stress participants, suggesting that higher levels of blood lipids and lipoprotein α were related with

10.3389/fendo.2023.1237260

TABLE 4 Quality of life outcomes score from pre-treatment to post-treatment.

	Acupuncture group				Sham acupuncture group					
	Pre-treatment (*n* = 458)	Post-treatment (*n* = 458)	*p*	[a]*p*	Pre-treatment (*n* = 468)	Post-treatment (*n* = 468)	*p*	[a]*p*	*p*1	[a]*p*1
SAS score	33.71 ± 6.93	34.50 ± 7.35	0.0840	0.0780	33.86 ± 6.82	34.20 ± 7.13	0.4532	0.4610	0.1727	0.1734
SDS score	35.24 ± 8.61	36.13 ± 8.61	0.1095	0.1023	35.48 ± 8.21	36.09 ± 8.40	0.2570	0.2620	0.3955	0.4055
PCOSQOL score	127.88 ± 28.38	128.71 ± 28.08	0.6488	0.6907	127.09 ± 29.47	127.05 ± 28.94	0.9834	0.9521	0.7371	0.7532
Emotions	4.27 ± 1.11	4.25 ± 1.10	0.8180	0.7721	4.31 ± 1.14	4.24 ± 1.08	0.3498	0.3255	0.4056	0.4030
Body hair	5.31 ± 1.52	5.27 ± 1.52	0.6960	0.7000	5.25 ± 1.61	5.21 ± 1.51	0.6924	0.6721	0.735	0.7378
Weight	4.29 ± 1.72	4.31 ± 1.64	0.8319	0.8780	4.20 ± 1.69	4.23 ± 1.66	0.8295	0.8744	0.588	0.5646
Infertility	3.65 ± 1.35	3.73 ± 1.30	0.3455	0.3746	3.64 ± 1.41	3.63 ± 1.43	0.9385	0.9116	0.1827	0.1866
Menstrual problems	4.41 ± 1.10	4.41 ± 1.12	0.9750	0.9552	4.35 ± 1.14	4.32 ± 1.15	0.7299	0.7449	0.7393	0.7563
SF-36 score	104.15 ± 4.52	106.89 ± 5.78	<0.0001	<0.0001	104.06 ± 4.54	106.78 ± 5.93	<0.0001	<0.0001	0.8016	0.7700
Physical functioning	93.36 ± 9.70	91.65 ± 11.53	0.0125	0.0129	93.29 ± 9.53	91.31 ± 11.43	0.0034	0.0034	0.9231	0.9268
Role-physical	23.35 ± 29.99	71.48 ± 32.39	<0.0001	<0.0001	21.49 ± 30.55	74.04 ± 32.23	<0.0001	<0.0001	0.1552	0.1594
Bodily pain	77.64 ± 12.96	76.78 ± 13.21	0.3105	0.2987	76.75 ± 13.68	75.80 ± 13.80	0.2821	0.3107	0.95	0.9026
General health	52.91 ± 11.64	53.60 ± 11.56	0.3558	0.3726	53.39 ± 12.20	54.00 ± 11.86	0.4276	0.4243	0.8012	0.8245
Vitality	42.73 ± 11.92	43.93 ± 11.97	0.1203	0.1213	42.20 ± 12.36	42.91 ± 12.21	0.3652	0.3451	0.5652	0.5629
Social functioning	49.00 ± 13.09	49.49 ± 11.79	0.5464	0.5464	48.95 ± 10.97	49.41 ± 12.15	0.5280	0.4826	0.8944	0.8264
Role-emotional	26.40 ± 34.62	71.43 ± 36.43	<0.0001	<0.0001	24.23 ± 34.90	73.40 ± 36.16	<0.0001	<0.0001	0.2813	0.2930
Mental health	60.02 ± 10.46	58.87 ± 10.56	0.0902	0.0875	60.84 ± 9.89	59.35 ± 10.83	0.0255	0.0247	0.8506	0.8769
Health transition	48.55 ± 25.80	42.48 ± 26.33	0.0003	0.0003	47.29 ± 25.62	39.89 ± 26.15	<0.0001	<0.0001	0.7356	0.7150
ChiQOL score	148.20 ± 11.04	149.80 ± 11.12	0.0254	0.0268	148.22 ± 11.28	149.78 ± 12.32	0.0410	0.0391	0.6637	0.6693
Physical form domain	3.35 ± 0.80	3.34 ± 0.82	0.9104	0.8837	3.25 ± 0.85	3.27 ± 0.80	0.6912	0.7051	0.5796	0.5996
Spirit domain	95.53 ± 8.36	96.34 ± 8.48	0.1386	0.1435	95.58 ± 8.21	96.18 ± 8.86	0.2791	0.2620	0.3763	0.3953
Emotion domain	49.32 ± 7.04	51.12 ± 7.36	0.0350	0.0353	49.39 ± 7.03	50.33 ± 7.44	0.0445	0.0451	0.8141	0.8332

Data are median (IQR).
p-values represent comparison before and after treatment within acupuncture and sham acupuncture groups.
[a]p-values represent comparison before and after treatment within acupuncture and sham acupuncture groups after adjusting clomiphene and reproductive outcome.
p1-values represent comparison of the difference value before and after treatment between acupuncture and sham acupuncture groups.
[b]p1-values represent comparison of the difference value before and after treatment between acupuncture and sham acupuncture groups after adjusting clomiphene and reproductive outcome.

psychological stress and emotional disorders (38). The same was found in patients with non-alcoholic fatty liver disease (NAFLD). There were impaired health status in NAFLD patients, including physical, emotional, mental, and social wellbeing (39), which also presented a complex, bidirectional relationship with lipid metabolism (40). As acupuncture could reduce the accumulation of intra-abdominal fat, inhibit lipid absorption in the small intestine, and downregulate the level of blood lipid, acupuncture may have potentially variable beneficial effects on improving the lipid metabolism in the presence of abnormal liver metabolism (41). These studies have suggested that there is a relationship between lipid metabolism and emotional domain. Our findings indicated that the role of acupuncture in improving emotion domain seemed to be related to the improvement of metabolic disorders in women with PCOS. Acupuncture treatment was found to positively improve leptin sensitivity in brain, thereby altering hepatic lipid metabolism and reducing depression-like behavior in chronic restraint stress mice (42). Clinical studies and lines of evidence from laboratory indicated that acupuncture regulates the endocrine system and modulates relevant molecules of metabolism in patients of simple obesity (43). As for the detection of dyslipidemia in both PCOS-like and obese rats, representative indices such as TG, TC, LDL-C, and Apo E were increased, while HDL-C was decreased. Moreover, there was also a certain degree of liver dysfunction, and all these abnormal changes could be reverted or improved with electroacupuncture (44). Therefore, the improvement of PCOS may represent a positive step towards relieving mental symptoms and preventing mental complications

by improving lipid metabolism. Moreover, in the perspective of TCM theory, the liver governs emotions, while the main organ of lipid metabolism is the liver.

We found that the changes of emotion and lipid provided molecular biological evidence for the scientific connotation of the theory of liver governing emotion in TCM. A previous study also found that acupuncture could effectively modify hepatic lipid metabolism by increasing the sensitivity to leptin. This is consistent with the theory of liver master sentiment in TCM (45). We also found that the effect of acupuncture on emotion and lipid metabolism played a role in sham acupuncture, probably due to the physiological effects of shallow acupuncture by stimulating the skin and causing afferent nerve activity, which, in turn, affects the corresponding functional areas of the brain, producing a "limbic contact response" (46). In addition, the patient's cognition of the acupuncturist; the patient's knowledge, attitudes, and behaviors; the patient's relationship with acupuncturist; and the trial environment increased the non-specific effects of acupuncture and sham acupuncture by prompting patients to change their healthy lifestyle (47).

Additionally, we found that the levels of serum Cl, serum Ca, and serum K have been both significantly increased in the acupuncture group after an intervention of 4 months compared with pre-treatment (adjusted $p< 0.05$). Also, the level of Cl was increased in the sham acupuncture group. It was reported that acupuncture could change the concentration of Ca^{2+} on the meridian line, which was one of the key factors of acupuncture effect, and the relationship between Ca^{2+} and acupuncture effect implied that Ca^{2+} was closely related to the neuroendocrine–immune network at acupoint (48). Studies on the mechanism of acupuncture seemed to suggest that the direct consequence in connection to acupuncture was the necessity of increasing intracellular Ca^{2+} (49). Since acupuncture was capable of delivering the extra Ca^{2+}, the improvement of ions in patients with PCOS seems to coincide with its ability.

In our study, a decrease in Hcy levels after acupuncture intervention was of novel interest. Studies have illustrated that elevated concentration of Hcy can affect blood vessels, which may have contributed to the deterioration of atherosclerosis and endothelial dysfunction by damaging the blood vessel, thus increasing the risk of CVD (50). Hcy may play a role in the long-term complications of PCOS, especially the arterial stiffness of CVD (51), but it is not clear whether it is connected with the metabolism of PCOS. It is well known that the level of Hcy is elevated in women with PCOS. A meta-analysis has shown that the Hcy level in obese patients with PCOS is significantly higher than that in nonobese patients (52), which showed that Hcy seems to be related to fat metabolism. Additionally, hyperhomocysteinemia contributes to elevated pregnancy loss and reduced ovulation in PCOS, indicating that the higher Hcy level leads to reproductive defects (53). Our study also found that acupuncture could reduce Hcy levels, but unfortunately did not have an effect on the live birth rate (16), which was worthy of further study in the future. Nevertheless, no significant differences in HOMA-IR, MetS, FPG, and FINS were found when comparing pre-treatment and post-treatment or between acupuncture and sham acupuncture, which was consistent with Dong's report (35).

4.1 Strengths and limitations

This research is the first study to use the most comprehensive scale to evaluate the effect of acupuncture on women with PCOS, and it is found that acupuncture can regulate emotion and lipid metabolism disorder, which may have a correlation, based on 1,000 PCOS women from randomized controlled trials that include the factorial design, adequate power, similar withdrawal rates among groups, and high adherence to treatment. Furthermore, acupuncture had a positive effect on levels of serum Ca, serum K, and serum Cl, which may also be another mechanism of acupuncture regulating emotion.

However, there were some limitations in our study. Firstly, both acupuncture and sham acupuncture played a role in the present study, and it was not clear what the specific mechanism was. On the one hand, sham acupuncture may have a comforting needle effect, and on the other hand, the techniques of acupuncturists may be different, although our acupuncturists had undergone several rounds of standardized and uniform training. Secondly, there was subjectivity in the assessment of acupuncture scale by PCOS patients. Although our research assistants have undergone intensive training on a regular basis, the particular variations in individual indicators may be caused by the subjective reasons of the research assistants. Thirdly, the subgroup analysis was not carried out based on BMI, which may lead to the deviation of the research results. Finally, the article only determined the potential relationships, and the specific mechanisms of the regulatory effect of acupuncture on emotion and lipid metabolism need to be further investigated.

5 Conclusions

Acupuncture can improve not only the emotional changes in SF-36 scale scores and ChiQOL scale scores, but also lipid metabolism. There is a correlation between emotional change and lipid metabolism. Meanwhile, acupuncture can regulate the changes of serum Ca, K, and Cl ions, which may be another mechanism of acupuncture in the treatment of PCOS. Moreover, sham acupuncture may not be completely ineffective, which may be related to the improvement in some aspects of patients with PCOS through the placebo effect.

Data availability statement

The original contributions presented in the study are included in the article/supplementary material, and further inquiries can be directed to the corresponding author/s.

Ethics statement

The studies involving humans were approved by The Regional Ethics Committee at The First Affiliated Hospital of Heilongjiang University of Traditional Chinese Medicine on December 15, 2011

(No: 2010HZYLL-010). The studies were conducted in accordance with the local legislation and institutional requirements. The participants provided their written informed consent to participate in this study. Inclusion of identifiable human data. Written informed consent was obtained from the individual(s) for the publication of any potentially identifiable images or data included in this article.

Author contributions

HC, CW, and XW initiated, designed, and supervised the study. HC, LW, CM, LL, WZ, and HG analyzed the data. HC, BS, and DZ drafted the manuscript. YW, CW, and XW revised the manuscript. All authors have read and approved the final version of the manuscript accepted for publication. All authors accept responsibility for the accuracy and integrity of all aspects of the study.

Funding

This work was supported by the National Natural Science Foundation of China (No. 82004404), the China Postdoctoral Science Foundation (Grant Nos. 2021T140188 and 2018M641886), the Academic Experience Inheritance Project of Famous TCM Experts, and the second batch of TCM clinical outstanding talents training program in Heilongjiang Province.

Acknowledgments

The authors would like to thank all the participants for their valuable contribution to this trial.

Conflict of interest

The authors declare that the research was conducted in the absence of any commercial or financial relationships that could be construed as a potential conflict of interest.

Publisher's note

References

1. Moulana M. Androgen-induced cardiovascular risk in polycystic ovary syndrome: the role of T lymphocytes. *Life* (2023) 13:1010. doi: 10.3390/life13041010

2. Dapas M, Dunaif A. Deconstructing a syndrome: genomic insights into PCOS causal mechanisms and classification. *Endocrine Rev* (2022) 43:927–65. doi: 10.1210/endrev/bnac001

3. Wang Z, Dong H, Wang Q, Zhang L, Wu X, Zhou Z, et al. Effects of electroacupuncture on anxiety and depression in unmarried patients with polycystic ovarian syndrome: secondary analysis of a pilot randomised controlled trial. *Acupuncture Med* (2019) 37:40–6. doi: 10.1136/acupmed-2017-011615

4. Karjula S, Morin-Papunen L, Auvinen J, Ruokonen A, Puukka K, Franks S, et al. Psychological distress is more prevalent in fertile age and premenopausal women with PCOS symptoms: 15-year follow-up. *J Clin Endocrinol Metab* (2017) 102:1861–9. doi: 10.1210/jc.2016-3863

5. Damone AL, Joham AE, Loxton D, Earnest A, Teede HJ, Moran LJ. Depression, anxiety and perceived stress in women with and without PCOS: a community-based study. *psychol Med* (2019) 49:1510–20. doi: 10.1017/S0033291718002076

6. Hasan M, Sultana S, Sohan M, Parvin S, Rahman MA, Hossain MJ, et al. Prevalence and associated risk factors for mental health problems among patients with polycystic ovary syndrome in Bangladesh: A nationwide cross—Sectional study. *PloS One* (2022) 17:e0270102. doi: 10.1371/journal.pone.0270102

7. Cooney LG, Lee I, Sammel MD, Dokras A. High prevalence of moderate and severe depressive and anxiety symptoms in polycystic ovary syndrome: a systematic review and meta-analysis. *Hum Reprod* (2017) 32:1075–91. doi: 10.1093/humrep/dex044

8. Santoro N. Polycystic ovary syndrome and mental health: a call to action. *Fertility Sterility* (2018) 109:799. doi: 10.1016/j.fertnstert.2018.02.121

9. Douglas KM, Fenton AJ, Eggleston K, Porter RJ. Rate of polycystic ovary syndrome in mental health disorders: a systematic review. *Arch Women's Ment Health* (2022) 25:9–19. doi: 10.1007/s00737-021-01179-4

10. Hoffmann MS, Brunoni AR, Stringaris A, Viana MC, Lotufo PA, Benseñor IM, et al. Common and specific aspects of anxiety and depression and the metabolic syndrome. *J Psychiatr Res* (2021) 137:117–25. doi: 10.1016/j.jpsychires.2021.02.052

11. Berent-Spillson A, Marsh C, Persad C, Randolph J, Zubieta J-K, Smith Y. Metabolic and hormone influences on emotion processing during menopause. *Psychoneuroendocrinology* (2017) 76:218–25. doi: 10.1016/j.psyneuen.2016.08.026

12. Kuang H, Li Y, Wu X, Hou L, Wu T, Liu J, et al. Acupuncture and clomiphene citrate for live birth in polycystic ovary syndrome: study design of a randomized controlled trial. *Evidence-Based Complementary Altern Med* (2013) 2013. doi: 10.1155/2013/527303

13. Wen J, Chen X, Yang Y, Liu J, Li E, Liu J, et al. Acupuncture medical therapy and its underlying mechanisms: a systematic review. *Am J Chin Med* (2021) 49:1–23. doi: 10.1142/S0192415X21500014

14. Cao Y, Chen H, Zhao D, Zhang L, Yu X, Zhou X, et al. The efficacy of Tung's acupuncture for sex hormones in polycystic ovary syndrome: A randomized controlled trial. *Complementary Therapies Med* (2019) 44:182–8. doi: 10.1016/j.ctim.2019.04.016

15. Johansson J, Redman L, Veldhuis PP, Sazonova A, Labrie F, Holm G, et al. Acupuncture for ovulation induction in polycystic ovary syndrome: a randomized controlled trial. *Am J Physiology-Endocrinology Metab* (2013) 304:E934–43. doi: 10.1152/ajpendo.00039.2013

16. Wu X-K, Stener-Victorin E, Kuang H-Y, Ma H-L, Gao J-S, Xie L-Z, et al. Effect of acupuncture and clomiphene in Chinese women with polycystic ovary syndrome: a randomized clinical trial. *JAMA* (2017) 317:2502–14. doi: 10.1001/jama.2017.7217

17. Abdi H, Abbasi-Parizad P, Zhao B, Ghayour-Mobarhan M, Tavallaie S, Rahsepar AA, et al. Effects of auricular acupuncture on anthropometric, lipid profile, inflammatory, and immunologic markers: a randomized controlled trial study. *J Altern Complementary Med* (2012) 18:668–77. doi: 10.1089/acm.2011.0244

18. Zhang X, Qiu H, Li C, Cai P, Qi F. The positive role of traditional Chinese medicine as an adjunctive therapy for cancer. *Bioscience Trends* (2021) 15:283–98. doi: 10.5582/bst.2021.01318

19. Zhang B, Shi H, Cao S, Xie L, Ren P, Wang J, et al. Revealing the magic of acupuncture based on biological mechanisms: A literature review. *BioScience Trends* (2022) 16:73–90. doi: 10.5582/bst.2022.01039

20. Wu L, Li Y, Yu P, Li H, Ma S, Liu S, et al. The application of acupuncture in obstetrics and gynecology: a bibliometric analysis based on Web of Science. *Ann Palliative Med* (2021) 10:3194–204. doi: 10.21037/apm-21-477

21. Behboodi Moghadam Z, Fereidooni B, Saffari M, Montazeri A. Measures of health-related quality of life in PCOS women: a systematic review. *Int J Womens Health* (2018) 10:397–408. doi: 10.2147/IJWH.S165794

22. Leung KF, Liu FB, Zhao L, Fang JQ, Chan K, Lin LZ. Development and validation of the chinese quality of life instrument. *Health Qual Life Outcomes* (2005) 3:26. doi: 10.1186/1477-7525-3-26

23. Zhang H-L, Huo Z-J, Wang H-N, Wang W, Chang C-Q, Shi L, et al. Acupuncture ameliorates negative emotion in PCOS patients: a randomized controlled trial. *Zhongguo Zhen jiu= Chinese Acupuncture & Moxibustion* (2020) 40:385–90. doi: 10.13703/j.0255-2930.20191231-k0005

24. Eshre TRA.-S.P.C.W. Group. Revised 2003 consensus on diagnostic criteria and long-term health risks related to polycystic ovary syndrome. *Fertility sterility* (2004) 81:19–25. doi: 10.1016/j.fertnstert.2003.10.004

25. Chen Z, Zhang Y, Liu J, Liang X, Yu Q, Qiao J. Diagnosis of polycystic ovary syndrome: standard and guideline of Ministry of Health of People's Republic of China. *Zhonghua Fu Chan Ke Za Zhi* (2012) 47:74–5.

26. Li R, Qiao J, Yang D, Li S, Lu S, Wu X, et al. Epidemiology of hirsutism among women of reproductive age in the community: a simplified scoring system. *Eur J Obstetrics Gynecology Reprod Biol* (2012) 163:165–9. doi: 10.1016/j.ejogrb.2012.03.023

27. Zhao X, Ni R, Li L, Mo Y, Huang J, Huang M, et al. Defining hirsutism in Chinese women: a cross-sectional study. *Fertility sterility* (2011) 96:792–6. doi: 10.1016/j.fertnstert.2011.06.040

28. Guyatt G, Weaver B, Cronin L, Dooley JA, Azziz R. Health-related quality of life in women with polycystic ovary syndrome, a self-administered questionnaire, was validated. *J Clin Epidemiol* (2004) 57:1279–87. doi: 10.1016/j.jclinepi.2003.10.018

29. Stewart M. The Medical Outcomes Study 36-item short-form health survey (SF-36). *Aust J Physiother* (2007) 53:208. doi: 10.1016/S0004-9514(07)70033-8

30. Leung K-f, Liu F-b, Zhao L, Fang J-q, Chan K, Lin L-z. Development and validation of the chinese quality of life instrument. *Health Qual Life Outcomes* (2005) 3:1–19. doi: 10.1186/1477-7525-3-26

31. Zhao L, Chan K, Leung K, Liu F, Fang J. Application of factor analysis in development and validation of a new questionnaire for quality of life. *Zhongguo Zhong xi yi jie he za zhi Zhongguo Zhongxiyi Jiehe Zazhi= Chin J Integrated Traditional Western Med* (2004) 24:965–8.

32. Chow YW, Dorcas A, Siu AM. The effects of qigong on reducing stress and anxiety and enhancing body–mind well-being. *Mindfulness* (2012) 3:51–9. doi: 10.1007/s12671-011-0080-3

33. Jones G, Benes K, Clark T, Denham R, Holder M, Haynes T, et al. The Polycystic Ovary Syndrome Health-Related Quality of life questionnaire (PCOSQ): a validation. *Hum Reprod (Oxford England)* (2004) 19:371–7. doi: 10.1093/humrep/deh048

34. Zheng R, Qing P, Han M, Song J, Hu M, Ma H, et al. The effect of acupuncture on glucose metabolism and lipid profiles in patients with PCOS: a systematic review and meta-analysis of randomized controlled trials. *Evidence-Based Complementary Altern Med* (2021) 2021. doi: 10.1155/2021/5555028

35. Dong H-x, Wang Q, Wang Z, Wu X-k, Cheng L, Zhou Z-m, et al. Impact of low frequency electro-acupuncture on glucose and lipid metabolism in unmarried PCOS women: a randomized controlled trial. *Chin J Integr Med* (2021) 27:737–43. doi: 10.1007/s11655-021-3482-z

36. Lai M-H, Ma H-X, Yao H, Liu H, Song X-H, Huang W-Y, et al. Effect of abdominal acupuncture therapy on the endocrine and metabolism in obesity-type polycystic ovarian syndrome patients. *Zhen ci yan jiu= Acupuncture Res* (2010) 35:298–302.

37. Chen J, Xing H, Li Q, Li M, Wang S. Regulative effects of the acupuncture on glucose and lipid metabolism disorder in the patients of metabolic syndrome. *Zhongguo Zhen jiu= Chin Acupuncture Moxibustion* (2017) 37:361–5. doi: 10.13703/j.0255-2930.2017.04.004

38. Yu J, Zhang Z, Li C, Zhang J, Ding Z, Zhu W, et al. Serum lipid concentrations are associated with negative mental health outcomes in healthy women aged 35–49 years. *Front Psychiatry* (2021) 12:773338. doi: 10.3389/fpsyt.2021.773338

39. Huang R, Fan J-G, Shi J-P, Mao Y-M, Wang B-Y, Zhao J-M, et al. Health-related quality of life in Chinese population with non-alcoholic fatty liver disease: a national multicenter survey. *Health Qual Life Outcomes* (2021) 19:1–8. doi: 10.1186/s12955-021-01778-w

40. Soto-Angona Ó., Anmella G, Valdés-Florido MJ, De Uribe-Viloria N, Carvalho AF, Penninx BW, et al. Non-alcoholic fatty liver disease (NAFLD) as a neglected metabolic companion of psychiatric disorders: common pathways and future approaches. *BMC Med* (2020) 18:1–14. doi: 10.1186/s12916-020-01713-8

41. Han J, Guo X, Meng X-J, Zhang J, Yamaguchi R, Motoo Y, et al. Acupuncture improved lipid metabolism by regulating intestinal absorption in mice. *World J Gastroenterol* (2020) 26:5118. doi: 10.3748/wjg.v26.i34.5118

42. Jung J, Lee SM, Lee M-J, Ryu J-S, Song J-H, Lee J-E, et al. Lipidomics reveals that acupuncture modulates the lipid metabolism and inflammatory interaction in a mouse model of depression. *Brain Behavior Immun* (2021) 94:424–36. doi: 10.1016/j.bbi.2021.02.003

43. Wang L-H, Huang W, Wei D, Ding D-G, Liu Y-R, Wang J-J, et al. Mechanisms of acupuncture therapy for simple obesity: an evidence-based review of clinical and animal studies on simple obesity. *Evidence-Based complementary Altern Med* (2019) 2019. doi: 10.1155/2019/5796381

44. Gao H, Tong X, Hu W, Wang Y, Lee K, Xu X, et al. Three-dimensional visualization of electroacupuncture-induced activation of brown adipose tissue via sympathetic innervation in PCOS rats. *Chin Med* (2022) 17:48. doi: 10.1186/s13020-022-00603-w

45. Jung J, Lee SM, Lee MJ, Ryu JS, Song JH, Lee JE, et al. Lipidomics reveals that acupuncture modulates the lipid metabolism and inflammatory interaction in a mouse model of depression. *Brain Behav Immun* (2021) 94:424–36. doi: 10.1016/j.bbi.2021.02.003

46. Gong Y, Chang H, Gao J-S, Liu C-D, Han B-W, Wu X-K. Progress of researches on non-specific effect of acupuncture. *Zhen ci yan jiu= Acupuncture Res* (2019) 44:693–7. doi: 10.13702/j.1000-0607.180909

47. Ho RS, Wong CH, Wu JC, Wong SY, Chung VC. Non-specific effects of acupuncture and sham acupuncture in clinical trials from the patient's perspective: a systematic review of qualitative evidence. *Acupuncture Med* (2021) 39:3–19. doi: 10.1177/0964528420920299

48. Yi G, Yanjun Z, Xiuyun W, Tangping X, Jinsheng C, Chunxu Z, et al. Study on the correlation between calcium ions and meridian acupoints. *World Chin Med* (2020) 15:970–5.

49. Yang ES, Li P-W, Nilius B, Li G. Ancient Chinese medicine and mechanistic evidence of acupuncture physiology. *Pflügers Archiv-European J Physiol* (2011) 462:645–53. doi: 10.1007/s00424-011-1017-3

50. Bajic Z, Sobot T, Skrbic R, Stojiljkovic MP, Ponorac N, Matavulj A, et al. Homocysteine, vitamins B6 and folic acid in experimental models of myocardial infarction and heart failure—How strong is that link? *Biomolecules* (2022) 12:536. doi: 10.3390/biom12040536

51. Wu X, Li Z, Sun W, Zheng H. Homocysteine is an indicator of arterial stiffness in Chinese women with polycystic ovary syndrome. *Endocrine connections* (2021) 10:1073. doi: 10.1530/EC-21-0224

52. Wang J, You D, Wang H, Yang Y, Zhang D, Lv J, et al. Association between homocysteine and obesity: a meta-analysis. *J Evidence-Based Med* (2021) 14:208–17. doi: 10.1111/jebm.12412

53. Chang H, Xie L, Ge H, Wu Q, Wen Y, Zhang D, et al. Effects of hyperhomocysteinaemia and metabolic syndrome on reproduction in women with polycystic ovary syndrome: a secondary analysis. *Reprod biomedicine Online* (2019) 38:990–8. doi: 10.1016/j.rbmo.2018.12.046

Frontiers in Endocrinology

Explores the endocrine system to find new therapies for key health issues

The second most-cited endocrinology and metabolism journal, which advances our understanding of the endocrine system. It uncovers new therapies for prevalent health issues such as obesity, diabetes, reproduction, and aging.

Discover the latest Research Topics

See more →

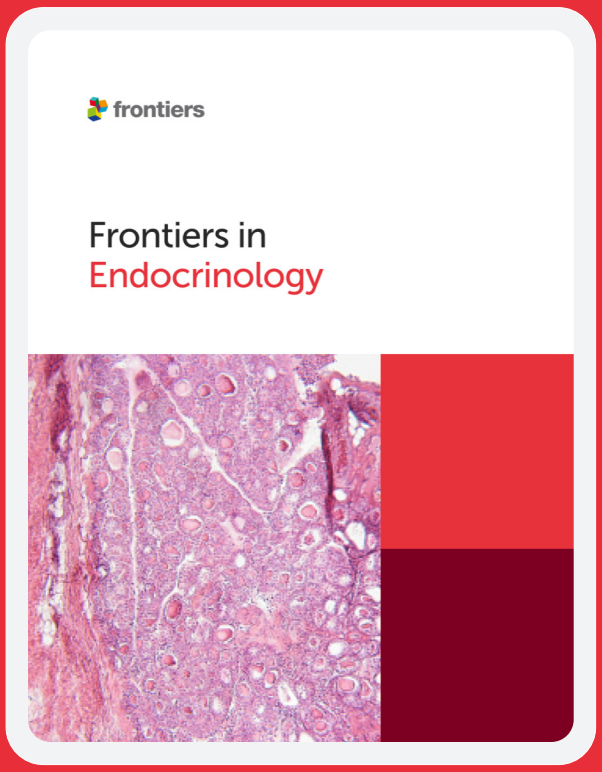

Frontiers

Avenue du Tribunal-Fédéral 34
1005 Lausanne, Switzerland
frontiersin.org

Contact us

+41 (0)21 510 17 00
frontiersin.org/about/contact